Staphylococcal Responses to Skin Surface Lipid Squalene

Xizhang Zhao

Thesis submitted in accordance with the requirements of the University of Liverpool for the degree of Doctor in Philosophy

September 2017

Acknowledgement

I would like to express my deepest appreciation to my supervisor Mal Horsburgh who was abundantly helpful and offered invaluable assistance, support and guidance. Without his knowledge and assistance this study would not have been complete.

I would like to thank all members in Horsburgh's lab for their unfailing support and assistance, but especially Josephine Moran who was never tired of training me in the world of bioinformatics.

I would like to expression my gratitude to all those who have helped me in the lab, with special thanks to lab manager Paul Loughnane who was always willing to help me and maintained this cracking place to work!

I would like to thank all my friends and family for the moral and emotional support in my life. Your encouragement is very important for me.

Abstract

The human skin surface is covered with a lipid film that represents the actual interface between the viable epidermal layers and outer environment and is crucial for our understanding of the colonisation of bacteria. The relationship between staphylococci and the abundant skin lipid squalene, which comprises about 12% of total skin surface lipids, remains poorly understood. This study therefore aimed to comparatively investigate the effects of the lipid squalene upon *S. aureus* and *S. epidermidis.*

Here, it was determined that culture of *S. aureus* with squalene dramatically reduced expression of staphyloxanthin, its eponymous golden pigment . Culture of cells with squalene lowered the survival of *S. aureus,* but not *S. epidermidis,* to both H_2O_2 and nisin, while squalene mediated enhanced survival of *S. epidermidis* to LL-37, but did not alter *S. aureus* survival. The transcriptional response of both species to squalene challenge was investigated using RNA-Seq and the proteome of *S. aureus* at late exponential phase of growth with squalene was studied using quantitative methods. While major similarities in the response of both species to squalene were observed with large changes to cellular pathway gene expression, reduced carotenoid (*crt*) operon expression was shown to be mediated at the level of transcription. Unexpectedly, challenge with squalene caused derepression of all the Fur-iron regulated uptake transporter genes in both *S. aureus* and *S. epidermidis*. This induction was accompanied by significantly decreased cellular iron. The means by which squalene causes iron starvation was not determined.

Similar to squalene, ethanol was found to reduce pigment expression in *S. aureus* and major similarities in the *crt* operon and overall transcriptional profiles of expression were revealed after challenge. The experimental evolution of *S. aureus* with a sub-bactericidal concentration of ethanol and selection for increased growth yield identified three SNPs, with one SNP potentially implicating altered cell wall meso-diaminopimelic acid biosynthesis in enhanced survival. This study revealed that squalene has potential to play a role in colonisation of staphylococci by decreasing pigment expression, modulating resistance to skin antimicrobials and through starvation for iron. The mechanistic basis for these phenomena requires further study.

Contents

List of Tables

List of Figures

Abbreviation

ACME:	arginine catabolic mobile element
AD:	atopic dermatitis
ADP:	adenosine diphosphate
AdsA:	adenosine synthase A
AFAs:	antimicrobial fatty acids
Agr:	accessory gene regulator
AIP:	autoinducing peptide
AMP:	antimicrobial peptide
ATP:	adenosine triphosphate
BHI:	Brain Heart Infusion
BWA:	Burrows-Wheeler aligner
CAMPs:	cathelicidin antimicrobial peptides
CA-MRSA:	community-associated MRSA
CDM:	chemical defined medium
CGR:	Centre for Genomic Research
CL:	cardiolipin
CoNS:	coagulase-negative staphylococci
DE:	differentially expressed
DEPC:	diethypyrocarbonate
DTT:	dithiothreitol
Ebh:	extracellular matrix-binding protein homologue

EPS: Exopolysaccharide

ESS: ESAT-6 like secretion system

FAME: fatty acid modifying enzyme

FarRE: fatty acid resistance regulator and effector

GAS: group A *Streptococcus*

GO: Gene ontology

HA-MRSA: hospital-acquired MRSA

hBD: human beta defensins

HNP: human neutrophil peptide

hSQS: human squalene synthase

ICP-OES: Inductively Coupled Plasma optical emission spectroscopy

LA-MRSA: livestock-associated MRSA

LB: Lysogeny Broth

McrA: myosin-cross reactive antigen

MRSA: methicillin-resistant *S. aureus*

MSCRAMMs: microbial surface components recognising adhesive matrix molecules

$NADP^+$: nicotinamide adenine dinucleotide phosphate, abbreviated

PBP: penicillin binding protein

PBS: phosphate buffered saline

PCR: polymerase chain reaction

PGA: poly-γ-glutamic acid

PIA: polysaccharide intracellular adhesin

PMF: proton motive force

PSMs: phenol-soluble modulins

qPCR: quantitative polymerase chain reaction

RH: relative humidity

RIN: RNA integrity number

ROS: reactive oxygen species

RPM: revolutions per minute

Sae: *S. aureus* exoprotein

SasF: *S. aureus* surface protein F

SCC*mec*: staphylococcal chromosome cassette *mec* element

SERAMs: secretable expanded repertoire adhesive molecules

SNP: single nucleotide polymorphism

SQ: squalene

SSLs: skin surface lipids

SssF: *S. saprophyticus* surface protein F

STX: staphyloxanthin

TAE: Tris base, acetic acid and EDTA

TCS: two-component system

TE: Tris base and EDTA

TFA: trifluoroacetic acid

THB: Todd Hewitt broth

WTA: wall teichoic acid

Chapter 1 Introduction

1.1 *Staphylococcus*

The genus *Staphylococcus* is comprised of over forty species of Gram-positive cocci and are one of the most abundant colonisers of mammalian skin and mucosa (Cogen *et al*., 2008; Costello *et al*., 2009; Taylor *et al*., 2003; Nagase *et al*., 2002). Due to the ubiquitous colonisation of several species on human skin and the wide spectrum of diseases they can cause, staphylococci have become the most investigated member of the skin microflora. The dominant staphylococcal species on skin is *Staphylococcus epidermidis*, which belongs to coagulase-negative staphylococci (CoNS) grouping, and is considered part of the normal skin microflora that is carried by 100 % of healthy individuals (Foster, 2009; Roth and James, 1988). Multiple CoNS can be found across different body sites including *S. epidermidis*, *S. capitis*, *S. cohnii*, *S. haemolyticus*, *S. hominis*, *S. saprophyticus*, *S. simulans, S. warneri* and *S. xylosus* (Kloos and Schleifer, 1975; Kloos and Musselwhite, 1975; Coates *et al*., 2014). While CoNS are not considered pathogenic, people with compromised immune systems, such as new-borns or patients after catheter or other surgical implant surgery are at risk of developing infection owing to the ability of several CoNS species to form biofilms that grow on these devices which can result in serious infections (Becker *et al*., 2014).

S. aureus, in contrast, is a coagulase-positive transient skin coloniser and skin pathogen, which only persistently colonises 25%–30% of the human population in the anterior nares (Peacock *et al*, 2001). This species is the most notorious member of the staphylococci due to the broad arsenal of virulence factors it possesses, which enable it to invade the human body and cause a diverse range of infections, from mild skin and soft tissue infections such as abscesses (Archer, 1998), to severe and life-threatening diseases such as pneumonia, bacteraemia and infective endocarditis (Lowy, 1998).

1.2 Methicillin-resistant *S. aureus* (MRSA)

Methicillin is a narrow-spectrum β-lactam antibiotic of the penicillin class, which was discovered in 1960 to replace penicillin to treat penicillin-resistant organisms that had evolved and spread (Lowy, 2003; Peacock and Paterson, 2015). However, it did not take long before reports of methicillin-resistance started to emerge. *S. aureus* was one of the first species to acquire resistance to methicillin, so the strains were named as methicillin-resistant *S. aureus* (MRSA) (Barber, 1961; Jevons, 1961). Horizontal gene transfer of an element, Staphylococcal Chromosome Cassette *mec* element (SCC*mec*) from a related staphylococcal species was proposed as the donor for this emergence (Peacock and Paterson, 2015; Wu *et al*., 1996). A penicillin binding protein (PBP2a/PBP2') that is encoded by *mecA* binds methicillin with extremely low affinity (Hartman and Tomasz, 1984), which results in PBP2a/PBP2' remaining functional even in presence of the methicillin. Therefore, possession of *mecA* significantly increased bacterial resistance to methicillin. The enzyme is a transglycosylase and transpeptidase involved in peptidoglycan biosynthesis which is the primary target for many antibiotics (Utsui and Yokota, 1985). To date, eleven SCC*mec* elements have been identified, of which four are commonly found in *S. aureus* from patients (Shore and Coleman, 2013).

HA-MRSA, the abbreviation for hospital-acquired MRSA, mainly infects immunocompromised people in hospitals such as patients with HIV, diabetes or after radiotherapy/ chemotherapy or those whose natural barriers are compromised by surgery (Enright *et al*., 2002). However, in the 1990s, there emerged MRSA strains in the community (community-associated MRSA; CA-MRSA) capable of infecting healthy individuals who had not been in contact with health care facilities. CA-MRSA was considered more virulent than HA-MRSA but researcher revealed that CA-MRSA did not evolve from the HA-MRSA (Calfee, 2011). In addition to HA-MRSA and CA-MRSA, livestock-associated MRSA (LA-MRSA) was observed in Korea, Brazil, Switzerland, Malaysia, India, Great Britain, Denmark, and China (Gopal and Divya, 2017).

1.3 Global regulators of *S. aureus*

The ability of *S. aureus* to adapt to different host environments is largely owing to a global regulatory network, including such loci as *sigB, sae, agr, sarA, rot, srrAB, arl*, and *svrA.* (Arvidson and Tegmark, 2001; Bronner *et al*., 2004; Yarwood and Schlievert, 2003; Liu *et al*., 2016). Each of these regulators is involved in stress responses and control expression of virulence factors (Goerke *et al*., 2005).

1.3.1 SigB

The alternative sigma factor gene *sigB* encoding SigB controls the transcription of genes involved in stress adaptation. SigB binds to the core (subunits ββ'α2ω) of RNA polymerase to form the holoenzyme that initiates the transcription by recognition and opening of promoters as well as the initial steps in RNA synthesis (Paget 2015). The role of SigB in stress responses of Gram-positive bacteria including *Bacillus subtilis*, *S. aureus* and *Listeria monocytogenes* has been studied for decades, with the best-investigated system being that in *B. subtilis* (Hecker *et al*., 2007) (Fig 1.1a). The activity of SigB is regulated by a post-translational mechanism. The *sigB* operon in *B. subtilis* comprises *rsbR, rsbS, rsbT, rsbU, rsbV, rsbW, sigB,* and *rsbX* (Pané-Farré *et al*., 2006). RsbW binds with SigB to form an inactive complex under normal growth conditions, but the affinity of RsbW for its antagonists, SigB and RsbV, can change due to a variety of stresses. This change in affinity promotes the binding of RsbV to RsbW, thus leaving SigB free, which is then able to proceed to form holoenzyme complexes with core RNA polymerase (Voelker *et al*., 1995). However, only non-phosphorylated RsbV is capable of competing with SigB for RsbW binding. The phosphorylation state of RsbV is regulated by the kinase activity of RsbW and the action of two phosphatases, RsbP and RsbU, under two different sources of stress. RsbU is active in response to physical and chemical stress, whereas RsbP phosphorylates RsbV under energy stress (Hecker *et al*., 1996; Vijay *et al*., 2000; Voelker *et al*., 1995).

With respect to *S. aureus*, however, only RsbU, RsbV, RsbW, and SigB are encoded in the staphylococcal genome (Fig 1.1a). Absence of the upstream *rsbR–rsbS–rsbT* genes and the downstream *rsbX* gene in *S. aureus* may link to failure of SigB activation by ethanol stress and energy uncouplers which are both strong inductors of SigB activity in *B. subtilis* (Pané-Farré *et al*., 2006). In *S. aureus*, SigB is activated under various conditions such as heat shock, addition of $MnCl_2$ or NaCl, alkaline shock, oxidation and infection, regulated by phosphatase RsbU, anti-anti-SigB factor RsbV and anti-SigB factor RsbW which apparently have the same functions as their homologues in *B. subtilis* (Hecker *et al*., 2007; Voelker *et al*., 1995; Pané-Farré *et al*., 2006).

1.3.2 SaeRS

The SaeRS two-component system, which is encoded by the *sae* (*S. aureus* exoprotein expression) locus, was identified during characterisation of a Tn*551* mutant for its defect in the production of exoproteins including α-hemolysin, β-hemolysin, nuclease, and coagulase (Giraudo *et al*., 1999). Like other typical TCS, the signalling cascade of the SaeRS TCS starts when SaeS, the sensor histidine kinase, senses cognate environmental signals and autophosphorylates at the conserved His131 residue. The phosphoryl group is then transferred to Asp51 of SaeR, and the resultant SaeR-P is capable of activating the transcription of the target genes (Novick and Jiang, 2003; Arya and Princy, 2016). The *sae* operon comprises four genes (*saeP, saeQ, saeR, and saeS*) and two promoters P1 and P3 (Fig 1.1b). The P3 promoter is located inside *saeQ* and only responsible for *saeR* and *saeS* transcription. The P3 promoter is weaker than P1, but the transcription of *saeRS* from P3 is sufficient for activation of the Sae-regulated genes. This was shown by deletion of the sequence upstream of P3 leading to no significant difference in exoprotein production (Jeong *et al*., 2011). The P1 promoter located in the front of the *saeP* directs transcription of all four genes. P1 is much stronger than P3 and is autoinduced by the SaeRS TCS (Novick and Jiang, 2003; Steinhuber *et al*., 2003). Induction of P1 will elevate the protein level of SaeRS, but the increase of SaeRS is not expected to further increase the

activity of the SaeRS TCS because overexpression of *saeRS* does not alter the expression pattern of the Sae-regulon (Mainiero *et al*., 2010). The functions of SaeP and SaeQ, whose encoding genes locate upstream of *saeRS,* are still not fully understood since neither shows significant homology to proteins of known functions. Although SaePQ are dispensable for the activation of the Sae system, they are essential to induce the phosphatase activity of SaeS by forming a SaePQS ternary complex to dephosphorylate SaeR-P facilitating resetting the activated systems to the pre-activation state (Jeong *et al*., 2012).

To date, there are three SaeS variants identified: $SaeS^{P}$, $SaeS^{SK}$, and $SaeS^{SKT}$ (Liu *et al*., 2016). $SaeS^{P}$ that has a L18P substitution mutation in the first transmembrane helix was firstly identified in the strain Newman (Steinhuber *et al*., 2003). This polymorphism results in increased activity of kinase SaeS, and leading to constant expression of the auxiliary proteins SaeP and SaeQ in Newman strain (Sun *et al*., 2010; Liu *et al*., 2016). $SaeS^{SK}$ is found in the strain MW2, Mu50 and USA600, but this variant does not show altered enzymatic activity of SaeS (Olson *et al*., 2013). $SaeS^{SKT}$ is a variant of $SaeS^{SK}$ with one more amino acid substitution at the C-terminus. This variant, however, alters the time of SaeRS being maximally expressed. The activity of the Sae system with $SaeS^{SKT}$ is highest in the exponential growth phase and reduced in the stationary growth phase, while the activity of normal SaeRS reaches maximum in post-exponential phase (Ramundo *et al*., 2016). The $SaeS^{SKT}$ was reported in ST30 and ST36 lineages of *S. aureus* (Ramundo *et al*., 2016).

Sae TCS can be activated by human neutrophil peptide 1, 2, and 3 (HNP1-3), calprotectin, which comprises approximately 50% of neutrophil cytoplasmic proteins and hydrogen peroxide, but also inhibited by: silkworm apolipophorin protein, which is known to reduce the transcription of the hemolysin genes; acidic conditions ($pH \leq 5.5$); and high NaCl concentrations ($\geq 1M$) (Geiger *et al*., 2008; Foell *et al*., 2006; Kehl-Fie *et al*., 2011; Hanada *et al*., 2011; Weinrick *et al*., 2004). Moreover, human skin fatty acid cis-6-hexadecenoic acid was reported to repress the Sae system in *S. aureus*, although the mechanism is not known (Neumann *et al*., 2015).

1.3.3 Agr

The quorum-sensing system in *S. aureus* is required for the ability to colonise various niches within the host and cause diverse infections. This system enables cell-to-cell communication and regulation of a large arsenal of virulence factors (Yarwood, 2003). The staphylococcal accessory gene regulator (*agr*) quorum-sensing system is one of the best characterised quorum-sensing systems, which down-regulates the expression of several surface proteins and up-regulates the expression of a large number of secreted virulence factors in the transition from late-exponential growth to stationary phase (Vuong *et al*., 2000; Novick, 2003). Inactivation of *agr* was found to impair staphylococcal pathogenesis in several infection models, including rabbit endocarditis (Cheung *et al*., 1994) and murine subcutaneous abscesses and arthritis (Bunce *et al*., 1992; Abdelnour *et al*., 1993).

RNAII and RNAIII are two primary transcripts expressed by the *agr* locus from the P2 and P3 promoters, respectively (Yarwood, 2003) (Fig 1.1c). AgrD is the precursor of the autoinducer in the agr system, processed into an octapeptide and secreted as the autoinducing peptide (AIP) signal by AgrB. AgrA and AgrC form a two-component system where the transmembrane component AgrC (histidine kinase), senses and binds the extracellular AIP, leading to AgrC autophosphorylation and activation of AgrA (the response regulator) (Novick and Geisinger, 2008). With increasing concentration of the AIP in the medium, AgrA induces increased P2 and P3 transcription, leading to up-regulation of down-stream genes including those encoding virulence factors such as protein A, α-hemolysin, adhesins, capsule, toxins, proteases, phenol soluble modulins and genes associated with biofilm formation (Novick and Geisinger, 2008).

The interactions between staphylococcal global regulators were revealed by many studies. For example, SigB was reported to down-regulate the transcription of the *sae* operon through the P1 promoter as well as other Sae regulon genes, such as *hla*, *hlgABC*, *nuc*, and *splABCDEF* (Bischoff *et al*., 2004). But this interaction was not observed in a study on device-related infection of *S. aureus* (Goerke *et al*., 2005). In addition, it was proposed that the Sae TCS is

downstream of Agr in the exoprotein production pathway, since the activity of *saeP1* promoter was decreased in *Δagr* strain, leading to a reduced expression level of saeSR (Novick and Jiang, 2003; Giraudo *et al*., 1999; Geiger *et al*., 2008). These effects, combined with the requirement of RNAIII for *sae* transcription from *saeP1* (Novick and Jiang, 2003), suggest a positive regulation Sae by Agr. However, other experiments suggest that Agr and Sae are independent of one another, because some target genes are regulated by Agr and Sae in an opposite pattern. For example, the Sae regulon genes, such as *hlgA, hlgB, hlgC*, and *lukA* were still highly expressed in an *agr* mutant during murine skin infection of the USA300 strain (Zurek *et al*., 2014).

(a)

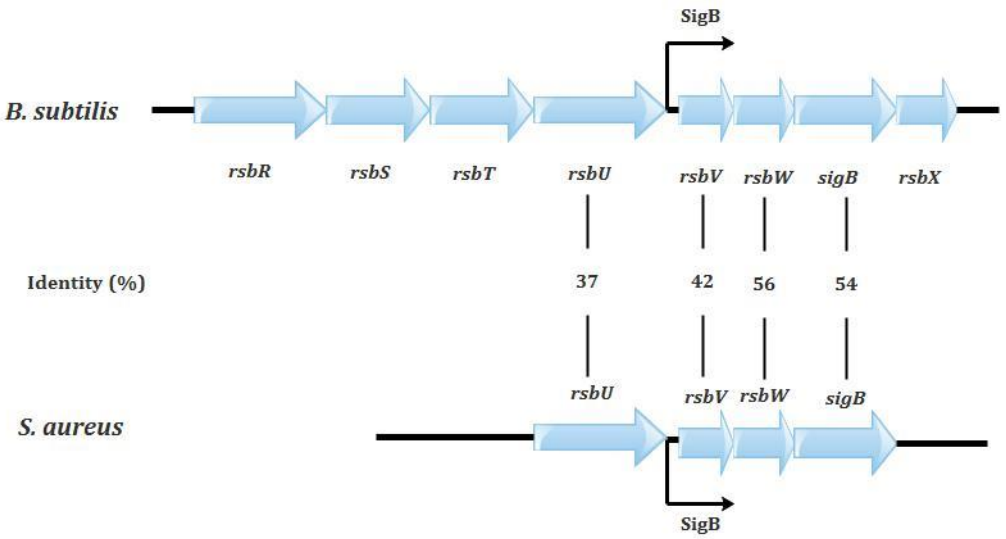

(b)

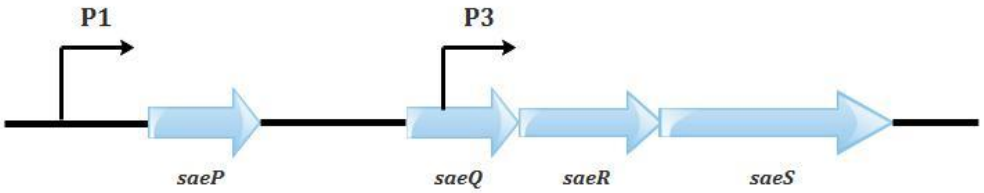

(c)

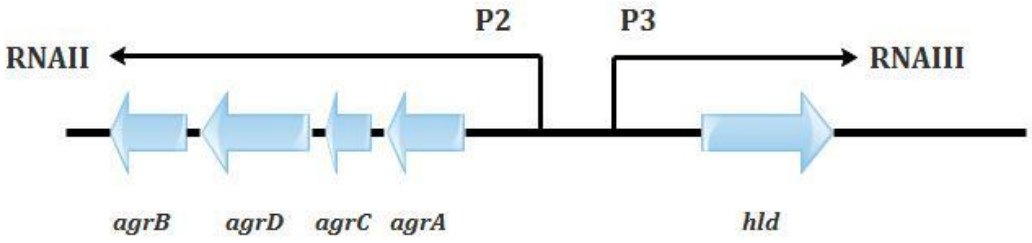

Figure 1.1 The *sigB* (a), *sae* (b) and *agr* operons (c) in *S. aureus*. (a) Comparison of *sigB* operon structures in *B. subtilis* and *S. aureus*. The level of amino acid conservation is shown for SigB and regulators present in both species. (b) Organization of the *sae* operon. Two angled arrows represent the P1 and P3 promoters, respectively. (c) The P2 operon encodes (via RNAII) the signalling mechanism, whereas the transcript of the P3 operon, RNAIII, acts as the riboregulator effector molecule of the *agr* locus.

1.4 The structure of human skin

Human skin is the largest organ of the integumentary system, which provides a variety of functions including maintenance of body temperature, prevention of excessive water loss, recognition of the outer environment, defence against microorganisms and protection from harmful materials in the external environment (Lee *et al*., 2006). The skin consists of layers of cells whose differentiation originates from migration towards the outermost layer. From innermost layer outwards, these layers are termed the basal (stratum basale), spinous (stratum spinosum), granular (stratum granulosum) and stratified (stratum corneum) (Candi *et al*., 2005; Proksch *et al*., 2008) (Fig 1.2). The keratinocyte cells in the basal layer are proliferative and function to generate new skin cells. In fact, every skin cell is completely replaced every 14 days that is more or less influenced by different metabolism rates of each individual (Candi *et al*., 2005; Roth and James, 1988). There are representative lamellar granules or Odland bodies in the granular layer keratinocytes. These small organelles consist of a collection of lipids including glucosylceramides, cholesterol, phospholipids and various enzymes such as acid hydrolases (Candi *et al*., 2005).

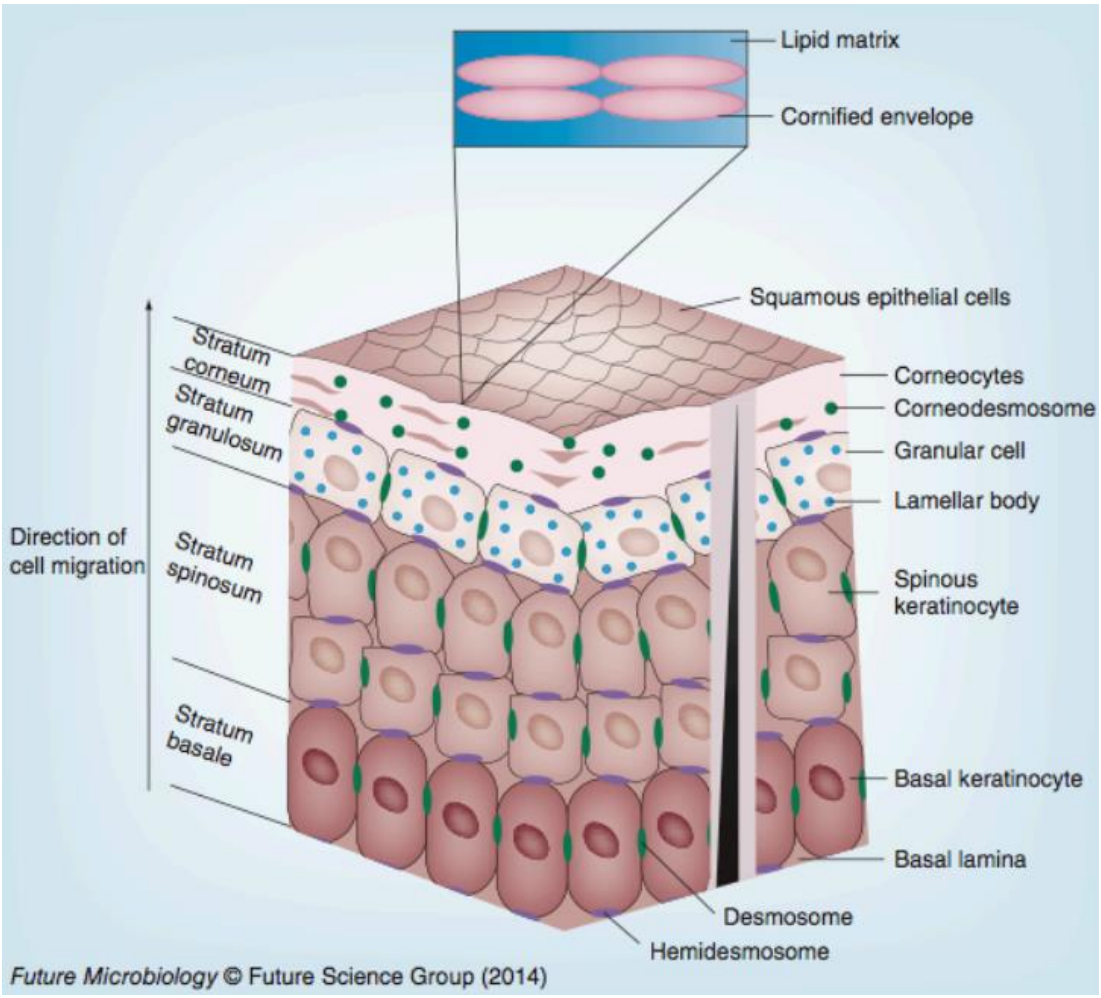

Figure 1.2 Structure of the skin
(Coates *et al*., 2014)

The major differentiation of keratinocytes occurs during cells immigrating from the granular layer to the stratum corneum and is accompanied with extrusion of the lamellar granules (Candi *et al*., 2005). As a result, considerable quantities of phospholipids and glucosylceramides are released from the lamellar granules followed by their hydrolysis into ceramides and free fatty acids (Madison, 2003; Drake *et al*., 2008). During this process, tight bundles are formed due to binding of keratin and fillagrin, leading to flattening of the keratinocytes (Candi *et al*., 2005). Cornified envelope is formed beneath the plasma membrane, which is a protein layer self-associated by isopeptide bonds. The bonds are so tight as to make this layer resistant to common proteolytic enzymes (Proksch *et al*., 2008). In addition, this cornified envelope is also linked to a lipid envelope, which

contains ω-hydroxyceramides, due to covalent bonds (Proksch *et al*., 2008; Candi *et al*., 2005; Madison, 2003). Finally, the plasma membrane is replaced by the lipid envelope and the cell's organelles are also lysed after apoptosis, leading to completion of differentiation, and these resultant cells are known as cornified cells or corneocytes (Candi *et al*., 2005).

1.5 Skin surface lipids (SSLs)

Corneocytes are covered with a lipid film that represents the actual interface between the viable epidermal layers and outer environment. This lipid layer plays a crucial role in our understanding of the colonisation of bacteria. Skin surface lipids (SSLs) are a mixture of mostly sebaceous lipids plus epidermal lipids, displaying a unique composition as compared with lipid fractions of other organs (Fig 1.3) (Pappas, 2009). This specificity originates from the unique contribution of sebum secreted from the sebaceous glands, unevenly distributed in all areas of the body with the exception of the palms and foot soles (De Luca & Valacchi, 2010). The major lipid components in human sebum include squalene, wax esters, and triglycerides (Nicolaides, 1974). Within this mixture there are multiple antimicrobial molecules including the fatty acid, sapienic acid and antimicrobial peptides (Pappas, 2009; Smith & Thiboutot, 2008).

The epidermal lipids (Fig 1.3a) mainly play a role as a barrier obstructing the movement of electrolytes and water. This blocking effect is achieved by the presence of three equal proportions of ceramides, cholesterol and free fatty acids, originating from the lamellar bodies (Pappas, 2009). Studies revealed that the biosynthesis of ceramides, fatty acids and cholesterol in epidermis is very active. Disruption of the skin barrier leads to a significant enhancement in cholesterol and fatty acids synthesis. This is further confirmed by inhibition of these pathways resulting in delayed recovery of the barrier function (Elias *et al*., 1992; Bouwstra *et al*., 1998).

(a) Epidermal lipids

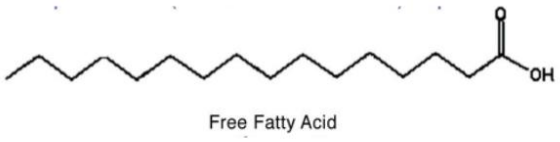

Free Fatty Acid — 33%

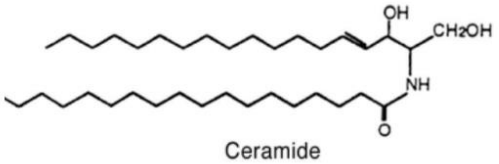

Ceramide — 33%

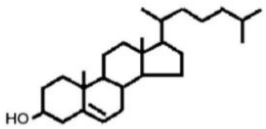

CHOLESTEROL — 33%

(b) Sebaceous lipids

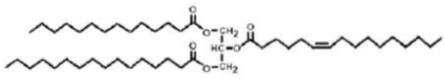

TRIGLYCERIDE — 45-50%

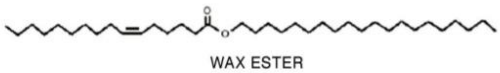

WAX ESTER — 25%

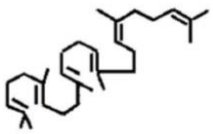

SQUALENE — 12%

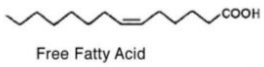

Free Fatty Acid — 10%

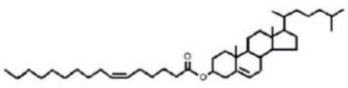

CHOLESTEROL ESTER — <5%

Figure 1.3 Representative structures and proportion of skin surface lipids.

Several unique ceramide species that are only found in the epidermal surface lipids but not at any other cell type were also identified and these molecules are believed to most importantly contribute to the skin barrier properties (Vasireddy *et al*., 2007). These lipids include the fatty acids esterified to the amide of the sphingosine head group, especially long chain fatty acids such as linoleic acid, palmitoleic acid, palmitic acid, stearic acid and oleic acid (Pappas, 2009; Kenny *et al*., 2009).

The sebaceous lipids are complex and unique (Fig 1.3b). The composition of human sebum is significantly different in quality and quantity from sebum of other species (Nicolaides and Ansari, 1968; Stewart and Downing, 1991). Although the reason for this distinction is not clear, it is believed to be associated with the unique texture of human skin. Formation of acne, for example, is potential evidence for that theory as acne is unique to humans. Elevated sebum level plays a major role in pathophysiology of acne, suggesting that the unique human sebaceous lipids are closely related to this specific disease (Ayer and Burrows, 2006; Thiboutot, 2004; Zouboulis, 2004).

Sapienic acid (16:1, Δ6) is the predominant fatty acid of human sebum. It consists of a double bond at the sixth position from the carboxyl end (Nicolaides, 1974). As a truly unique fatty acid in sebum, sapienic acid is not obtained from the diet and cannot be found anywhere else in the human body (Nicolaides, 1974). In addition, sapienic acid has high antimicrobial activity and can inhibit virulence determinant production (Neumann *et al*., 2014).

Wax esters account for approximately 25 % of the sebaceous gland lipids and are also only produced in sebaceous glands but not found in any other areas of the body (Pappas, 2009). Wax esters play an essential role in barrier function; they are more resistant to oxidisation and hydrolysis than triglycerides or phospholipids and have higher resistance to heat (Pappas, 2009). In addition to their barrier function, wax esters also serve as a lubricant, preventing the internal moisture of tissues from excessive hydration (Pappas, 2009).

1.6 Squalene

Squalene is an intriguing component of the skin surface lipids, being the precursor of cholesterol biosynthesis. Cholesterol is synthesised in most mammalian cells and is an essential molecule for membrane fluidity and structure (Pappas, 2009). Squalene is a unsaturated C30 hydrocarbon, which is quickly converted to lanosterol prior to cholesterol in most tissues. Intriguingly, as a component of the skin surface lipids, squalene produced in the sebaceous gland is not converted into lanosterol, which halts the biosynthesis of cholesterol (Picardo *et al*., 2009). The accumulation of this lipid is negligible in other organs of the human body and the reason for that is still unclear. In humans, the greatest accumulation of squalene is in skin, where in an adult it normally comprises about 12% of total skin surface lipids and reach up to 60 ug/cm^2 (Pappas, 2009). A variety of roles are proposed for squalene such as maintaining skin moisture and acting as antioxidant (Spanova & Daum, 2011). In humans, squalene is synthesised via squalene synthase (hSQS), and its further metabolism is catalysed by squalene epoxidase and squalene monooxygenase. It was proposed that the relative activity of these enzymes is responsible for the accumulation of squalene in sebaceous cells (Pappas, 2009).

Although significant efforts have been put into investigating the interaction between human skin surface components and staphylococci, especially antimicrobial peptides and the antimicrobial lipid sapienic acid, the effects of squalene on staphylococci remain poorly understood. In fact, there are very few studies investigating the relationship between squalene and microorganisms which likely correlates with squalene having no described antimicrobial properties.

1.7 Staphylococcal skin survival

Conditions on the human skin are extremely harsh for microbes with its low pH but high salt environment, along with the dry and nutrient-deficient surface, which all ensure that microbial reproduction is inhibited or at least largely restricted (Coates *et al*., 2014; Skaar, 2010). However, on the other hand, successful human skin colonisers, such as certain species of staphylococci, must have evolved essential mechanisms to conquer these barriers. This includes mechanisms for adhesion to the skin, evasion of components of the innate immune system, and gain of advantages during competition with other microbes (Cogen *et al*., 2008; Coates *et al*., 2014). Those factors are crucial for bacterial survival and persistence on human skin and are believed to be the causes for differential abilities for colonisation between *S. aureus* and *S. epidermidis* (McEwan *et al*., 2006; Cho *et al*., 2001; Melnik, 2006; Ong *et al*., 2002; Arikawa *et al*., 2002; Takigawa *et al*., 2005; Ishikawa *et al*., 2010).

1.7.1 Adhesion

Adhesion to the skin is the primary ability possessed by bacterial colonisers to attach so they are not pulled away by sheer forces and also ensures they can re-adhere to the new layers before the cells are lost through desquamation every 14 days (Candi *et al*., 2005). Bacteria produce adhesins that specifically target the receptors on the skin, resulting in a strong attachment to prevent loss. Although bacteria are found at both upper and lower layers of the stratum corneum, it is still unclear which method is better for bacterial long-term survival on the skin (Brooker and Fuller, 1984; Zeeuwen *et al*., 2012; Grice *et al*., 2009).

There are three groups of staphylococcal adhesins, microbial surface components recognising adhesive matrix molecules (MSCRAMMs), secretable expanded repertoire adhesive molecules (SERAMs), and non-proteinaceous adhesins (Heilmann, 2011). MSCRAMMs which are anchored to the staphylococcal cell wall are capable to recognise and bind to host skin factors.

Unlike MSCRAMMs which covalently bind to bacterial cell wall, SERAMs bind to the staphylococcal surface non-covalently. As well as having adhesive functions, SERAMs frequently have enzymatic functions such as Aae found in *S. epidermidis,* which is an autolysin with adhesive properties (Heilmann *et al*., 2003; Bowden *et al*., 2002). Non-proteinaceous adhesins comprise the polysaccharide PIA (polysaccharide intercellular adhesin) and wall teichoic acids plus lipoteichoic acids that are usually embedded in the membrane lipids and bind to target through non-covalent bonds (Heilmann, 2011). The staphylococcal adhesins with known receptors for human skin were summarised by Coates *el al* (2014).

MSCRAMMs are the best-studied group of staphylococcal adhesins. The genome of *S. aureus* encodes 20 MSCRAMMs that enable the bacteria to colonise multiple niches, from anterior nares to implanted medical devices and prostheses (Coates *et al*., 2014; Mulcahy *et al*., 2012). Contrastingly, coagulase-negative staphylococci are considered to have a reduced arsenal of adhesins in their genome, with 12 MSCRAMMs encoded by *S. epidermidis*. Besides *S. aureus* and *S. epidermidis*, however, the MSCRAMMs in other staphylococci is poorly understood. In the next best studied species, the genome of *S. saprophyticus* only has three genes (*sdrI, uafB* and *aas*) encoding adhesive functions (Sakinç *et al*., 2009; King *et al*., 2011; Hell *et al*., 1998). To date, the genomes of *S. caprae* and *S. lugdunensis* were also found to contain genes encoding adhesins (Coates *et al*., 2014).

1.7.2 Osmotic stress resistance

Osmotic stress is another limiting factor for bacterial growth and survival on skin. Differences in either the relative ionic concentration or relative humidity (RH) can cause osmotic stress (Potts, 1994). Environmental conditions of the skin are usually low RH but high ionic concentration, such that bacterial cells without specific coping solutions will easily lose their function due to dehydration. Moreover, skin bacteria also encounter hyperosmotic stress caused by sudden increases of water by increased sweating or washing.

The primary methods of *S. aureus* and *S. epidermidis* to survive low osmotic pressure when RH levels approach their growth limit are to thicken their cell walls, enlarge their cell size and form cuboidal packs of eight cells rather than typical grape-like clusters (de Goffau *et al*., 2009, 2011). These phenomena are proposed to be associated with autolysis, as similar changes were observed in staphylococcal autolysin mutants (de Goffau *et al*., 2011). As a consequence of alterations in morphology, the ratio of cell surface area to volume is reduced that may subsequently lead to reduction of water loss and maintenance of turgor pressure (de Goffau *et al*., 2011). In addition, staphylococci grown at low RH were found to be more hydrophilic, which may help water acquisition (de Goffau *et al*., 2011).

Exopolysaccharide (EPS) or polysaccharide intracellular adhesin (PIA) is a cell wall-located macromolecule implicated in osmotic stress tolerance in staphylococci (McKenney *et al*., 1998). Study of *Pseudomonas spp.* revealed that production of EPS mitigates desiccation by acting as a buffer to slow the drying rate of the bacteria thus offering more time to adjust to the changing environment (Roberson and Firestone, 1992). Intriguingly, EPS could also provide similar protection upon wetting, avoiding too rapid a rehydration occurring (Roberson and Firestone, 1992). Similar mechanisms may also apply with regard PIA of staphylococci on human skin as with EPS of *Pseudomonas* spp. isolated from soil.

A capsule of poly-γ-glutamic acid (PGA) plays an essential role in protection of *S. epidermidis* from high NaCl concentrations (2 M) (Kocianova *et al*., 2005). PGA biosynthesis genes and their homologues (*pgsBCAD/capBCAD*) are widely distributed in coagulase-negative staphylococci including *S. hominis, S. capitis, S. haemolyticus, S. caprae*, and *S. warneri*, but with exception of coagulase-positive *S. aureus* (Kocianova *et al*., 2005).

A factor observed in various bacteria that is associated with mediation of osmotic stress responses is the biosynthesis of cardiolipin (CL). Increased salinity is often accompanied by a decrease in the amount of membrane CL and other zwitterionic phospholipids in both Gram-positive and Gram-negative

bacteria (Romantsov *et al*., 2009). For example, the level of CL synthase was shown to elevate in response to ionic stress in *E. coli* (Romantsov *et al*., 2009). However, levels of CL were not observed to significantly increase in *S. aureus* with higher concentration of NaCl, though mutation of CL synthase genes resulted in reduced long-term survival in high salinity media (Tsai *et al*., 2011). CL is considered to improve membrane tightness, hence it may contribute to reducing membrane permeability (Nagamachi *et al.,* 1992).

Ebh (extracellular matrix-binding protein homologue) which is only found in *S. aureus* and *S. epidermidis* and absent from *S. haemolyticus* and *S. saprophyticus* is a cell wall and membrane-associated protein. Invaginated vacuoles along their septum were observed within 30 min when *ebh* mutants were exposed to high salt conditions, suggesting that this protein contributes to initial ionic stress resistance (Kuroda *et al*., 2008).

Importation of osmoprotectants is a common resistance mechanism employed by bacteria counteracting ionic stress (Potts, 1994). L-proline, proline betaine and glycine betaine all offered protection to *S. aureus* at 1 M NaCl where L-proline had lowest and proline betaine the highest effects in the majority of S. aureus strains tested (Amin *et al*., 1995). Proline betaine and glycine betaine also offered maximal protection in *S. saprophyticus* and *S. epidermidis* (Amin *et al*., 1995).

1.7.3 Acid resistance

The acid surface of the skin facilitates innate defence by preventing microbial colonisation, particularly against Gram-negative bacteria due to their relatively more rigid cell wall by the cross-linked peptidoglycan chains (Matousek and Campbell, 2002). There is a gradient of acidity across the skin layers, decreasing from the pH of 7.4 in the stratum granulosum to pH of 4-5 at the skin surface (Rippke *et al*., 2002; Matousek and Campbell, 2002; Schmid-Wendtner and Korting, 2006). In addition to the direct effect of acid against microbes, such as damaging proteins and DNA by denaturation, acid is also revealed to enhance the activity of cationic AMPs and antimicrobial fatty acids (Walkenhorst *et al*.,

2013; Cartron *et al*., 2014). The surface of human skin is more acidic than most other mammals. This feature is believed as an important reason for different microflora between human and animal skin (Matousek and Campbell, 2002).

As well as an antimicrobial role, the acid gradient is essential for the activity of skin enzymes, such as regulation of β-glucocerebrosidase and serine proteases (Rippke *et al*., 2002; Schmid-Wendtner and Korting, 2006). These two enzymes are regulated dependent on their location within the stratum corneum, dictated by the pH, and this regulation ensures timely differentiation and desquamation of keratinocytes (Matousek and Campbell, 2002; Schmid-Wendtner and Korting, 2006). Therefore, alteration of skin pH is usually a pathogenic factor causing irregular skin differentiation and desquamation, resulting in skin diseases such as atopic dermatitis and ichthyosis (Rippke *et al*., 2002; Matousek and Campbell, 2002; Schmid-Wendtner and Korting, 2006).

The acidic gradient in skin is developed by numerous components including free amino acids and lactic acid from sweat, free fatty acids from sebum, urocanic acid and pyrrolidone carboxylic acid produced by filaggrin degradation, and cholesterol sulphate (Rippke *et al*., 2002, Matousek and Campbell, 2002). The concentration of most of these components increase towards the skin surface, whilst the only exception is cholesterol sulphate, which presents in higher levels towards the stratum granulosum (Rippke *et al*., 2002). In order to stabilise the skin pH, alkaline molecules such as carbon dioxide, ammonia, and bicarbonate are also produced in the skin to act as buffer, preventing pH from rapid change (Matousek and Campbell, 2002).

Three mechanisms are usually employed by Gram-positive bacteria against acid stress: DNA and protein damage repair; increasing internal pH; and changing the cell envelope architecture (Cotter and Hill, 2003). F_1F_0-ATPase is a well-studied proton pump that mediates acid resistance by generating a proton motive force (PMF), leading to an increase in intracellular pH as protons are extruded in a ATP-fuelled process (Cotter and Hill, 2003). A similar mechanism is also conducted by glutamate decarboxylases, which can increase internal pH by exporting the proton combined with glutamate (Cotter and Hill, 2003). In *S.*

aureus, NADH dehydrogenase is believed to play a more important role than F_1F_0-ATPase in acid resistance, which moves $2H^+$ out of the cell, whilst converting NADH to NAD^+ (Bore *et al*., 2007). Moreover, the proteins encoded by the *dlt* operon were implicated in acid resistance as they were shown to reduce proton permeability in *Streptococcus mutans* (Cotter and Hill, 2003). However, no such effect of the *dlt* operon has been reported in *S. aureus* (Bore *et al*., 2007).

Ammonia production is also involved in acid resistance in Gram-positive bacteria whereby ammonia binds hydrogen ions to form NH_4^+, resulting in elevation of internal pH (Cotter and Hill, 2003). Ammonia is produced via the activity of ureases, which convert arginine to ornithine, ammonia and carbon dioxide (Cotter and Hill, 2003). During acid shock, the expression of urease genes but not arginine deiminase genes was observed to be up-regulated in *S. aureus*, suggesting an acid resistant function of ureases (Bore *et al*., 2007).

Osmotic stress resistance and acid stress resistance may link together as it was shown that osmoprotectant transporters were up-regulated following acid stress in *S. aureus* (Bore *et al*., 2007). The production of CL, which plays an important role in osmotic stress resistance, was altered under acid stress to support this theory (Ohniwa *et al*., 2013).

1.7.4 Antimicrobial peptides and proteins resistance

Human skin secretes a variety of antimicrobial peptides (AMPs) and antimicrobial proteins including cathelicidin, human beta defensins (hBD2, hBD3), psoriasin, dermcidin 1, RNase 7 and lysozyme (Cho *et al*., 2010; Niyonsaba and Ogawa, 2005). Cathelicidin LL-37 is expressed in the eccrine glands and stored in lamellar granules, with antimicrobial activity against Gram-positive and Gram-negative bacteria and is effective to kill the yeast *Candida albicans* (Schroder and Harder, 2006). So far, LL-37 is the only AMP produced by humans that belongs to the cathelicidin category. The mode of action of LL-37 is interference with biosynthesis of peptidoglycan, causing loss of turgor pressure and eventually inhibition of cell growth (Barns and Weisshaar, 2013).

The human beta defensins (hBD) hBD2 and hBD3 are produced by neutrophils and exhibit antimicrobial activity against Group A *Streptococcus* (GAS), *S. aureus* and certain viruses (Cho *et al*., 2010). Production of hBD2 is mainly performed in lamellar bodies, while hBD3 is found in tissues throughout the body (Schroder and Harder, 2006).

Psoriasin was found to be effective against *E. coli*, and may also be involved in wound healing due to its function of promoting host cell growth (Glaser *et al*., 2005, Shubbar *et al*., 2012; Anderson *et al*., 2009). However, overproduction of psoriasin is often considered as a risk factor as it may cause psoriasis and growth of certain cancers (Shubbar *et al*., 2012, Anderson *et al*., 2009).

RNase 7 is highly bactericidal to *E. coli, S. aureus* and enterococci (Simanski *et al*., 2012; Schroder and Harder, 2006). RNase7 binds to the bacterial membrane making it more permeable by action of clustered lysine residues, which can result in formation of pores and disruption of bacterial membrane (Huang *et al*., 2007).

Dermcidin 1 is produced by the eccrine glands and exhibits antimicrobial activity effects against *S. aureus*, *E. faecalis*, *E. coli* and *C. albicans* (Schroder and Harder, 2006). Dermcidin 1 inhibits bacterial biosynthesis of RNA and protein, which is proposed through ion channel formation (Song *et al*., 2013; Senyurek *et al*., 2009; Rieg *et al*., 2005).

Lysozyme that is secreted from apocrine glands is a peptidoglycan N-acetylmuramide glycanhydrolase (muramidase) that forms part of the innate immune system (Niyonsaba and Ogawa, 2005). The enzyme is active against Gram-positive cell walls by hydrolysis of 1,4-β-linkages between N-acetylmuramic acid and N-acetyl-D-glucosamine residues in peptidoglycan. Hydrolysis of peptidoglycan which is the main component of Gram-positive cell wall compromises cell wall integrity, eventually resulting in cell lysis (Niyonsaba and Ogawa, 2005).

MprF and DltABCD proteins were revealed to contribute to staphylococcal resistance to CAMPs, including cathelicidin LL-37 and defensins (Peschel *et al*.,

1999). These secreted proteins share a collective mechanism against CAMPs by increasing the net charge of the bacterial cell surface to mitigate electrostatic interactions with the CAMPs. Dlt proteins achieve this by mediating the addition of D-alanine to wall teichoic acid, while MprF modifies anionic phospholipids with L-lysine and translocates the resulting lysyl-phosphatidylglycerol to the outer membrane (Ernst and Peschel, 2011; Peschel *et al*., 2001). A similar protective surface effect was observed from PGA, where biosynthesis mutants had increased susceptibility to LL-37 and hBD3, which implicated the exopolysaccharide PGA biosynthesis in mitigating interaction of AMPs with the cell membrane (Kocianova *et al*., 2005).

GraRS plays a crucial role in staphylococcal resistance to CAMPs. The two-component system is activated when the bacteria sense intra-membrane presence of CAMPs (Yang *et al*., 2012). GraRS regulates over 200 genes including the *dlt* operon (Herbert *et al*., 2007). Gene mutation of *graRS* increased the susceptibility of staphylococci to CAMPs and attenuated *S. aureus* virulence in a mouse infection model (Kraus *et al*., 2008; Herbert *et al*., 2007; Yang *et al*., 2012). The *vraFG* genes which encode an ABC efflux pump, are co-transcribed with *graRS*. Mutation of *vraG* results in increased sensitivity to cationic peptides and VraG was also shown to facilitate AMP resistance (Yang *et al*., 2012).

Proteases are a widespread method to defend against AMPs in staphylococci (Lai *et al*., 2007). It was observed in *S. epidermidis* that production of proteases was induced by challenge with AMPs (Lai *et al*., 2007) and the protease SepA efficiently inactivates the anionic AMP dermcidin under the control of *sarA, agr* and *saeRS* (Lai *et al*., 2007). A similar induction of extracellular proteases was also characterised in *S. aureus*. It was revealed that *S. aureus* metalloprotease aureolysin disables the human LL-37, which contributes to skin persistence and causing infections by interfering phagocytosis due to complement inhibition (Coates *et al*., 2014).

Although lysozyme broadly exhibits activity against Gram-positive bacteria, the majority of staphylococci are lysozyme resistant. The counteracting activity is

primarily attributed to OatA, which modifies cell wall muramic acid residues by O-acetylation thus dramatically weakening the interaction between lysozyme and peptidoglycan (Bera *et al*., 2005). Similarly, TagO directs O-linkage to MurNAc of wall teichoic acid (WTA), which sterically interferes with the activity of lysozyme (Bera *et al*., 2007).

There is also a potent mechanism against CAMPs only equipped by *S. aureus* but not *S. epidermidis*. The polar carotenoid staphyloxanthin modulates the fluidity properties of the lipid membranes and such fluidity characteristics are critical to the interaction of membrane-targeting host defence CAMPs with *S. aureus* (Mishra *et al*., 2011).

1.7.5 Resistance to antimicrobial lipids

Antimicrobial lipids are an important antimicrobial component of skin surface lipids. These lipids include antimicrobial fatty acids (AFAs) and sphingoid bases such as sphingosine. They are produced from ceramides, phospholipids, and glucosylceramides and released from lamellar granules (Drake *et al*., 2008; van Smeden *et al*., 2014). In addition to lamellar granules, the hydrolysis of triglycerides and bi-glycerides in sebum also produces some AFAs (Kohler *et al*., 2009; Madison, 2003; Drake *et al*., 2008). AFAs more efficiently inhibit staphylococcal and micrococcal species, while sphingosines are widely active against not only bacteria but also fungi (Drake *et al*., 2008; Desbois and Smith, 2010). Besides their antimicrobial functions, AFAs and sphingosines also play barrier roles as discussed in section 1.4.

The primary resistance mechanism against antimicrobial lipids employed by staphylococci is the alternation of surface hydrophobicity, thus decreasing the ability of antimicrobial lipids to interact with the cell (Kohler *et al*., 2009). This can be achieved by production of WTA and IsdA that increase bacterial surface hydrophilicity, and also by thickening of the cell wall that further decreases the overall surface hydrophobicity, as indicated by gene expression profile in response to AFA challenge (Kenny *et al*., 2009).

Observation of the positive relationship between the level of pigmentation and the resistance to AFAs in *S. aureus* suggested carotenoid biosynthesis would be another mechanism for AFAs resistance. *S. aureus* strains with higher levels of carotenoid have greater resistance to AFAs, and carotenoid production is increased in response to AFAs (Chamberlain *et al*., 1991; Kenny *et al*., 2009). The proposed mechanism of carotenoids in AFAs resistance is the same with that in CAMPs resistance, which act as a membrane stiffener to reduce membrane fluidity (Chamberlain *et al*., 1991; Mishra *et al*., 2011). For those staphylococcal species that do not produce pigment, other factors such as cardiolipin and host-derived cholesterol are believed to have similar membrane reinforcement functions (Romantsov *et al*., 2009).

FAME (fatty acid modifying enzyme) is an enzyme specifically targeting AFAs to confer resistance upon *S. aureus* and *S. epidermidis* (Chamberlain and Brueggemann, 1997). This exoprotein esterifies lipids with cholesterol or primary alcohols. Those modifications usually lead to impairment of the toxicity of AFAs (Chamberlain and Brueggemann, 1997; Kapral *et al*., 1992). FAME is inhibited by diglycerides and triglycerides, and hydrolysis of triglycerides and diglycerides conducted by lipases produces free fatty acids that FAME can act upon, which may explain the reason for existing strong correlation between FAME and lipase production in staphylococci (Long *et al*., 1992, Lu *et al*., 2012). The gene encoding FAME remains unidentified.

Several cell wall anchored proteins in staphylococci were proposed to provide protection against AFAs, such as the *S. aureus* surface protein F (SasF), the *S. saprophyticus* surface protein F (SssF), and the homologues found in other staphylococcal species (King *et al*., 2012). These proteins all belong to the myosin-cross reactive antigen (McrA) family (King *et al*., 2012). Mutation in SasF was shown to confer reduced survival upon exposure to linoleic acid, and this defect was recovered by complementation of SasF and also SssF (Kenny *et al*., 2009, King *et al*., 2012). *S. saprophyticus* clinical strains with *sssF* gene exhibited greater resistance to linoleic acid than those without (King *et al*., 2012). These proteins are speculated to act as fatty acid hydratases, whose function is to saturate the fatty acid to form less-toxic derivatives such as

linoleic acid to oleic acid and stearic acid to mysteric acid (King *et al*., 2012; Campbell *et al*., 1983).

The arginine catabolic mobile element (ACME) was predicted to improve survival of *S. aureus* on the skin in CA-MRSA isolates (Diep *et al*., 2006), which was supported by observation of genes encoding arginine deaminase pathway enzymes (such as *arcABDC* operon) being up-regulated in response to AFAs (Kenny *et al*., 2013).

The ABC transporter permease VraE in *S. aureus* was also suggested to associate with staphylococcal AFAs resistance (Kenny *et al*., 2009). Mutation of *vraE* in *S. aureus* resulted in decreased survival in the presence of linoleic acid (Kenny *et al*., 2009). Export of AFAs from the bacterial cell was identified in meningococci, conducted by specific fatty acid efflux pumps (Schielke *et al*., 2010), which was also indicated to be present in staphylococci (Truong-Bolduc *et al*., 2014).

FarRE (fatty acid resistance regulator and effector), which belongs to the multidrug pumps superfamily was identified as the exporter pump facilitates resistance to linoleic acid and arachidonic acid (Alnaseri *et al*., 2015). Treatment with linoleic and arachidonic acid strongly induce expression of farE in an *farR*-dependent manner, and inactivation of *farE* resulted in significant increased susceptibility of *S. aureus* to linoleic and arachidonic acid (Alnaseri *et al*., 2015).

1.7.6 Competition on human skin

Many microbial colonisers share the same niches in the human body. For example, *S. aureus, S. epidermidis, S.haemolyticus*, *Finegoldia magna*, *Corynebacterium accolens*, *S. hominis,* and *Micrococcus* sp. all colonise the nasal cavity (Libberton *et al*., 2014; Wos-Oxley *et al*., 2010; Iwase *et al*., 2010). In these areas, competition usually occurs such as inhibition of staphylococci by corynebacteria (Frank *et al*., 2010; Libberton *et al*., 2014). Moreover, bacteriophages also participate in the competition, with some of these capable of infecting particular or multiple species on the skin, also increasing the survival stress of staphylococcal colonisers (Aswani *et al*., 2011).

There are three well-studied mechanisms of resistance to competition possessed by bacteria and yeasts: limiting other's colonisation via competitive interference by adhering to a range of receptors; developing resistance to competitor antimicrobials; and producing compounds to inhibit competitors' growth (Cogen *et al*., 2010). A range of bacteriocins are produced by staphylococci, which are effective against GAS, group B S*treptococcus, Lactobacillus* spp., *Enterococcus faecalis, Micrococcus luteus, Corynebacterium fimi* and other staphylococci (Cogen *et al*., 2010; Gamon *et al*., 1999; Potter *et al*., 2014). In addition, phenol-soluble modulins (PSMs) which are a group of amphipathic α-helical proteins, are produced by staphylococci to perform a range of tasks, from haemolysins (δ-toxin) to biofilm dissemination (Periasamy *et al*., 2012). The δ and γ PSMs of *S. epidermidis* also exhibit activity against *S. aureus* (Cogen *et al*., 2010).

S. epidermidis is able to stimulate production of human defensins from the host such as hBD2 and hBD3, that are not active against itself but efficient in killing of other species, including *S. aureus* (Lai *et al*., 2010; Iwase *et al*., 2010). Secretion of Esp by *S. epidermidis* is an example. Esp which is a serine protease can disrupt biofilm formation, and can also trigger hBD2 expression to act against *S. aureus* (Iwase *et al*., 2010; Park *et al*., 2011).

Overall, the conditions on the skin are very inhospitable for bacterial colonisers. Desiccation, low pH, desquamation, and presence of numerous antimicrobials all inhibit the growth of microbes. However, staphylococci in turn have evolved multiple defence mechanisms to counteract these barriers. The known mechanisms employed by *S. aureus* in order to colonise human skin are summarised by Coates *et al* (2014) in Fig 1.4.

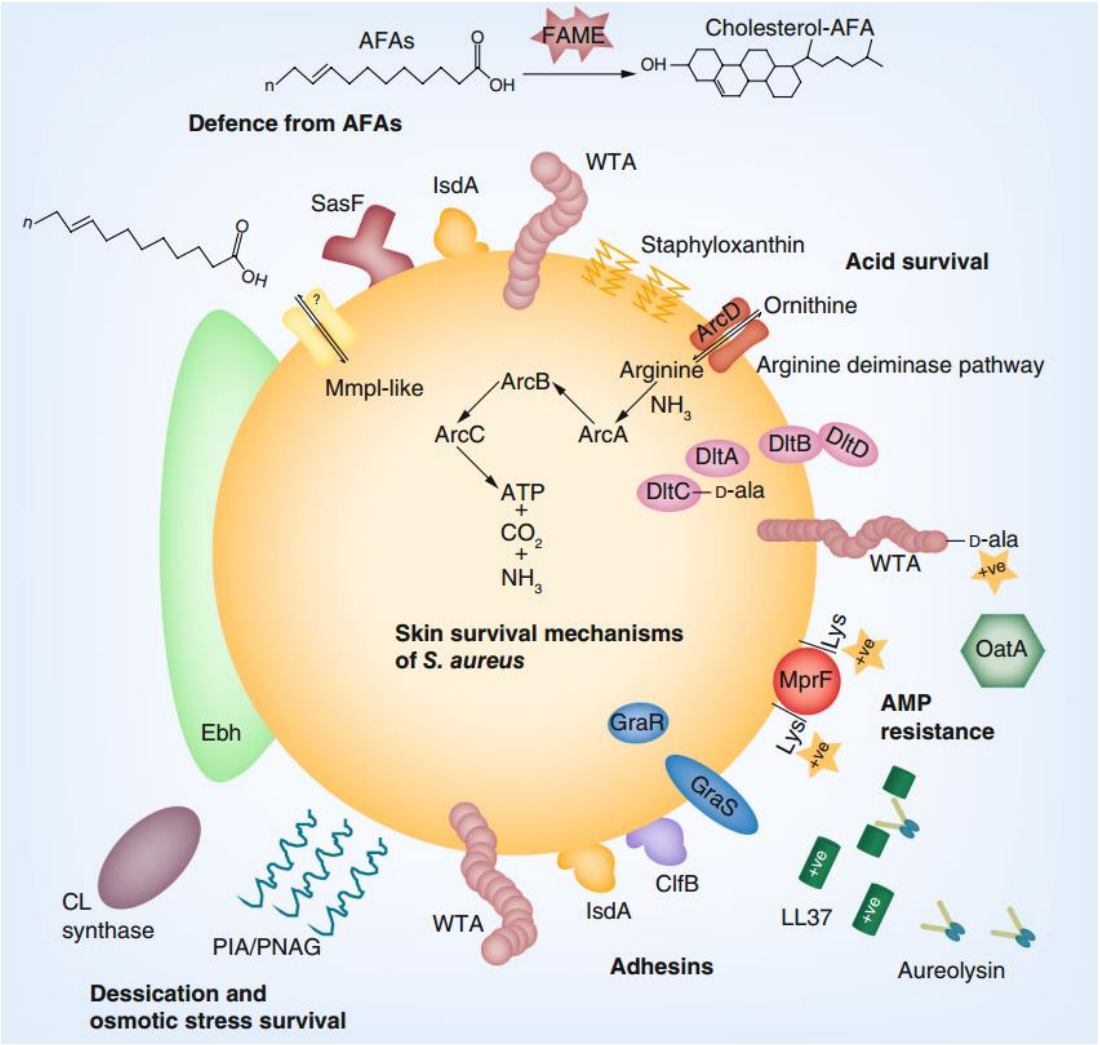

Fig 1.4 Human skin survival mechanisms of *S. aureus* (Coates *et al.*, 2014)**.**

1.8 Staphylococcal disease

1.8.1 Atopic dermatitis (AD)

Atopic dermatitis (AD) is an inflammatory disease of the skin, which has a high prevalence in a reported 97 countries across the world indicating that it is a significant problem in both developing and developed countries (Kong *et al*., 2012). Its symptoms include flaky lesions of the skin, infection and subsequent abscess formation. The disease Atopic dermatitis is associated with an increased production of the IgE antibody in response to environmental antigens usually otherwise well-tolerated. Patients with AD have high levels of *S. aureus* colonisation: up to 80% of the skin microflora may be comprised of *S. aureus*, with an associated reduction in overall microbiome diversity, in contrast with healthy skin where *S. epidermidis* comprises 90% of the resident microbiota (Baviera *et al*., 2014). It was proven that the severity of atopic dermatitis is linked to *S. aureus* abundance and the concomitant loss of microbiome diversity (Kong *et al*. 2012). Emergence of *S. aureus* on atopic dermatitis patients is believed due to dysregulation of the innate immune system, which reduced production of antimicrobial peptides, reduced recruitment of neutrophils to the skin and epidermal barrier dysfunction, resulting in alternation of the skin microbiome (Kong *et al*., 2012).

Specifically, the level of AMPs hBD2 and hBD3 are decreased in AD patients comparing with the healthy people and have therefore been linked with susceptibility to *S. aureus* colonisation (Cho *et al*., 2011). Expression of hBD2 and hBD3 are regulated by Th2 cytokines, where elevated level of Th2 cytokines leads to reduction of hBD2 and hBD3. Th2 cytokines are elevated in response to tissue damage and inflammation, which occurs in healthy skin when there is an overgrowth of *S. aureus* or there is an *S. aureus* infection (Cho *et al*., 2011); therefore, the reduced level of hBD2 and hBD3 could be a direct consequence of high *S. aureus* colonisation.

1.8.2 Abscess formation

Abscess formation is one of the most common presentations of staphylococcal diseases and exemplifies the comprehensive abilities of *S. aureus* to invade the human body. The abscess usually develops for several days or weeks and the disease forming bacteria are contained within a pseudo-membrane in the centre of a lesion. The pseudo-membrane is formed by immune cells which infiltrate the abscess. This process is usually accompanied by the accumulation of pus (mostly dead neutrophils) as well as severe inflammation of surrounding tissues (Lowy, 1998). Staphylococci in pus spread onto skin surfaces or enter circulating lymph and blood, which leads to the formation of abscesses at new sites. In patients lacking protective immunity, *S. aureus* is a frequent cause of bacteraemia, as a consequence of invasive disease originating from one or more abscesses (Cheng *et al*., 2011). The formation of staphylococcal abscess after subcutaneous invasion is separated into four stages, with each one characterised based on actions of a set of distinct surface proteins and virulence factors (Cheng *et al*., 2011).

The survival of *S. aureus* in the bloodstream is the first stage of disseminated staphylococcal abscess formation. Using a mouse model, researchers found 99.9% of the staphylococcal inoculum disappears from the blood within approximately six hours. Within three hours, however, the bacteria had reached the deep tissues where they could develop an abscess. Replication of these seed populations is measureable within 24 hours (Cheng *et al*., 2011). This means staphylococci are capable of survival in blood and circulating lymph fluids. Neutrophilic polymorphonuclear leukocytes, which account for 60-70 % of human white blood cells, are the host's main defence against *S. aureus* in blood (Voyich *et al*., 2005). The reactive oxygen species produced by leukocytes are toxic to many bacteria. *S. aureus* in turn produces the antioxidant staphyloxanthin, secretes catalase and regulates a range of other antioxidant defences through the repressor activity of PerR and Fur (Horsburgh *et al*., 2001, 2002; Pelz *et al*., 2005) to scavenge reactive oxygen species and protect *S. aureus* from neutrophil killing. In addition, PSMs are produced by *S. aureus*. These PSMs destroy human neutrophils by disrupting the cell membrane.

Further, *S. aureus* employs ClfA which binds to fibrin and fibrinogen, allowing agglutination of bacterial cells (McDevitt *et al*.,1994). This agglutination in turn, contributes to prolonged survival by inhibiting phagocytosis (Moreillon *et al*., 1995; Palmqvist *et al*., 2004). Finally, adenosine synthase A (AdsA) secreted during early staphylococcal infection converts AMP into adenosine, which is a key signal to the host to prevent excessive tissue damage. Large amounts of adenosine will repress the inflammatory response (Thiel *et al*., 2003).

Secondly, *S. aureus* will establish an infectious lesion when immune cells accumulate in an area at very high numbers. This process can be detected around 48 hours post intravenous challenge (Cheng *et al*., 2009). The recruitment of immune cells to lesions is achieved by released *S. aureus* lipoproteins that are recognised by Toll-like receptors, leading to improved pro-inflammatory signal levels that results in recruitment of immune cells (Bubeck Wardenburg *et al*., 2006). This process is believed to be facilitated by iron-acquisition (Skaar *et al*., 2004) where expression of the *isd* operon is required to fulfil the need for haem-iron but prevent the haem-toxicity (Mazmanian *et al*., 2003) (Torres *et al*., 2007).

At stage three, *S. aureus* cells are found tightly associated at the centre of an abscess lesion, covered with a pseudocapsule of fibrin deposits, which are produced from cleavage of fibrinogen by the action of coagulase (Cheng *et al*., 2009). This barrier keeps the immune cells away from *S. aureus* cells, and as a consequence *S. aureus* will replicate with less restriction. Based on mutation studies, two more genes play a crucial role at this stage. Staphylococcal protein A (SpA) prevents phagocytosis by binding a component of immunoglobulin (Forsgren & Sjöquist 1966) and Embp, which is expressed on the surface during cell growing, promotes biofilm-like growth (Cheng *et al*., 2009).

The last stage of staphylococcal abscess formation is persistence, accompanied by rupture and release, leading to new lesions. Expression of extracellular adhesion proteins Eap and Ess is required in this stage. Eap is a bi-functional protein which acts to induce cytokines IL-6 and IFN- α from monocytes, but can also inhibit T-cell activation and prevent adherence from neutrophils (Scriba *et*

al., 2008; Haggar *et al*., 2004). Ess (ESAT-6 like secretion system) is a non-canonical protein involved in a particular secretion pathway is reported to contribute to immune evasion by inhibiting phagocytosis (Davis and Ramakrishnan, 2009). Gene inactivation of *ess* results in normal abscess formation but failure of persistence (Burts *et al*., 2008) suggesting that Ess pathway is associated with prolonged staphylococcal survival within the abscess.

1.9 Thesis aims

Squalene is widely present in nature, and comprises about 12% of total skin surface lipids. Although significant efforts have been put into investigating the interaction between human skin surface components and staphylococci, especially the antimicrobial peptides and lipids, the effects of squalene on staphylococci remains poorly understood. The underlying hypothesis for this research was that squalene, as a major skin lipid, would have activity towards staphylococci that acts on the cells through direct antimicrobial action or by modulating the action of other skin antimicrobials.

This study therefore aimed to investigate the effects of the abundant skin lipid squalene upon *S. aureus* and *S. epidermidis*. The focus was on discovering the different impacts and responses between the two species to determine whether squalene may play a role in colonisation of staphylococci and thereby contribute to the differential skin survival and frequency of these two species.

Initial research will aim to determine if squalene has antimicrobial effects on *S. aureus* and *S. epidermidis*, and investigate whether squalene modulates the action of selected skin-related antimicrobials. Transcriptomics will be conducted by RNA-Seq as a discovery tool to identify DE genes in response to squalene and to compare the transcriptional profiles between *S. aureus* and *S. epidermidis*. This approach will identify whether differences in responses and possible resistance determinants can explain potential antimicrobial effects of squalene.

Chapter 2 Methods and Materials

2.1 Bacterial strains and growth conditions

The strains and plasmids used in this study and their relevant properties are shown in Table 2.1 and Table 2.2. Todd Hewitt broth (THB) was used for RNA preparation and proteomic work to match the experimental conditions with other lipid transcriptomic studies in the Horsburgh research group at Liverpool. Strains Newman and Tü3298 were selected for RNA-Seq analysis. Proteomics and experimental evolution work both used strain Newman. Iron-deficient chemically defined media was used for measurement of cell growth with different iron concentrations. Remaining experiments were all conducted in BHI media. Solid medium was made by adding agar (12 g L^{-1}) to broth.

Agar plates were grown at 37 °C for 12-18 h unless otherwise stated. Overnight broth cultures were grown for 18 h at 37 °C with shaking at speeds indicated. Optical density (600 nm) was measured during growth using a 1 cm path length. For *E. coli*, 10 ml of Lysogeny Broth (LB; Fisher Scientific) in a 50 ml polypropylene tube was inoculated with a single colony from LB agar plates (LB broth and 1.2 % w/v agar [Thermo Scientific]). Antibiotic was added when necessary at the following concentrations- ampicillin (Amp; 100 µg ml^{-1}), erythromycin (Ery/Erm; 10 µg ml^{-1}), chloramphenicol (Cm; 10 µg ml^{-1}), and tetracycline (Tet; 5 µg ml^{-1}). Two different concentrations of squalene (Sigma, CAS: 111-02-4), 2 mM (0.1%) and 20 mM (1% v/v) were used to challenge the culture in the experiments unless otherwise stated.

Table 2.1 Bacterial strains used in this study

Species	Strain Name	Reference or Source
Staphylococcus aureus	Newman	(Duthie and Lorenz, 1952)
Staphylococcus aureus	SH1000	(Horsburgh *et al*., 2002)
Staphylococcus aureus	BH1CC	(O'Neill *et al*., 2007)
Staphylococcus aureus	RN4220	(Nair *et al*., 2011)
Staphylococcus epidermidis	Tü3298	(Allgaier *et al*., 1986)
Staphylococcus capitis	G390	(Kloos and Schleifer, 1975)
Staphylococcus hominis	DM122	(Kloos and Schleifer, 1975)
Micrococcus luteus	ATCC4698	(Kocur *et al*., 1972)
Escherichia coli	Top10	Thermo Scientific

Table 2.2 Plasmids used in this study

Plasmids	Description	Reference
pMUTIN4	High copy number sub-cloning vector	(Vagner *et al*., 1998)
pSK5632	High copy number in *E. coli*, low copy number in *S .aureus* sub-cloning vector	(Grkovic *et al*., 2003)
pDG1514	tetracycline resistance cassette containing vector	(Guérout-Fleury *et al*., 1995)

2.2 Growth curves

Overnight cultures were adjusted to an OD_{600} of 0.5 using BHI; 2 ml of the diluted culture was used to inoculate 50 ml of media in 250 ml flasks. Flasks were incubated in a water bath with 125 rpm linear shaking at 37 ˚C. Samples were taken hourly between 0 and 8 h and diluted ten-fold in phosphate buffered saline (PBS) before recording the OD_{600}. This work also aimed to determine the concentration of *squalene* to be used for challenge conditions that would be used in future RNA-Seq work. If squalene has an antimicrobial effect, the ideal concentration should be the lowest concentration at which squalene could be added to the bacteria during the exponential phase (at OD_{600} 0.5) and be seen to reduce growth rate 20 min post challenge when results were displayed graphically.

2.3 H_2O_2, sapienic acid, nisin and LL-37 survival assays

S. aureus Newman and *S. epidermidis* Tü3298 were grown in BHI with different concentrations of squalene for 24 h. The cell culture was centrifuged and cell pellets were collected and washed twice with PBS. Cells were resuspended and diluted to OD_{600} 0.1 (~1.5 x 10^8 CFU ml^{-1}). Hydrogen peroxide, sapienic acid, nisin or LL-37 were added to the diluted cells with a final concentrations of 7.5 mM, 5 μg ml^{-1}, 250 μg ml^{-1} and 10 μg ml^{-1}, respectively. Cell suspensions were incubated at 37 ˚C statically. Samples were collected at time points 0 and 90 min into a 96-well plate and for the hydrogen peroxide treated cells catalase (10 mg ml^{-1}) was added immediately to the samples to neutralise the peroxide. Serial dilution and viable counts were performed to measure the survival rate.

Hydrogen peroxide, catalase, sapienic acid, nisin and LL-37 were all purchased from Sigma. Nisin was dissolved in 10 mM sodium citrate to a concentration of 5 mg ml^{-1} as a stock. Sapienic acid was dissolved in 100 % ethanol to a concentration of 5 mg ml^{-1} for stock. LL-37 was dissolved in water for a stock with the concentration of 100 μg ml^{-1}.

2.4 Staphyloxanthin expression and extraction

Staphyloxanthin was extracted with methanol and an absorbance spectrum was determined using a Fluostar Omega (BMG Labtech) plate reader. *S. aureus* Newman, SH1000 and BH1CC, *S. aureus* capitis G390, *S. aureus* hominis DM122 and *M. luteus* ATCC4698 were grown in BHI with different concentrations of squalene for 24 h. After growth, bacteria were centrifuged for 10 min at 4000 rpm, and cell pellets for each sample were collected. Pigment was extracted by adding 1 ml of methanol to cell pellet, with mixing and incubation for 15 min at 37 ˚C. Finally, the methanol extract was centrifuged again and 96-well polystyrene microtitre plates were loaded with 250 µl of extract in triplicate prior to absorbance measurement.

2.5 Agarose gel electrophoresis

Agarose gels were made to a concentration of 1 % or 2 % (w/v) agarose in TAE (Tris base, acetic acid and EDTA) buffer. The 1 % gels were used for gDNA integrity analysis whilst 2 % gels were
used for analysis of PCR products and small plasmids. Melted agarose was stored at 50 °C until required. Midori green DNA stain (Nippon Genetics) was mixed into molten agarose using either 4 µl or 2 µl per 100 ml of agarose, respectively. When necessary, loading dye (containing glycerol and bromophenol blue) was added to samples before loading samples into the gel. Samples were electrophoretically separated in TAE agarose/TAE buffer at 110 v for between 45 min and 2 h.

2.6 RNA sequencing

2.6.1 Notes

All work with RNA was done using RNase free plasticware and RNase free filter tips. Benches and pipettes were cleaned with RNase Zap (Ambion). Any water used was incubated at 37 °C with 0.1 % (v/v) diethypyrocarbonate overnight, prior to sterilisation by autoclaving (DEPC-treated water).

2.6.2 Growth and preparation of cells for RNA extraction

When bacteria reached an OD_{600} of 0.5, squalene was added. The final concentration of squalene for both *S. aureus* Newman and *S. epidermidis* Tü3298 was 1 % v/v. At 20 min after challenge with squalene, cells were harvested by pelleting for 5 min at 4,000 x g and 4 °C. Pellets were resuspended in 2 volumes of RNAlater (Qiagen) and incubated overnight at 4 °C.

2.6.3 Lysis of cells for RNA extraction

Per extraction, 1 ml of the bacterial preparation was used. The bacteria were pelleted at 6,000 x g for 5 min at 4 °C, and resuspended in 100 µl TE (Tris base and EDTA) containing 6 mg ml^{-1} lysostaphin and 400 U ml^{-1} mutanolysin.

This lysis mix was incubated at 37 °C for 15 min for *S. aureus,* and 30 min for *S. epidermidis*, mixing every 5 min. Bacteria were incubated for a further 30 min at 37 °C after the addition of 25 µl of Proteinase K (Qiagen).

2.6.4 RNA extraction

RNA was extracted using the RNeasy kit (Qiagen), with slight alterations to the manufacturer's protocol. Briefly the method was as follows: 350 µl buffer RLT containing 10 % (v/v) β-mercaptoethanol was added to the lysed cells and mixed before the addition of 250 ml ethanol. This suspension was centrifuged through the RNeasy column for 15 s at 10,000 x g. The column was then washed twice with 700 µl buffer RW1 for 15 s at 14,000 x g. The column was

then washed thrice with 500 µl buffer RPE for 15 s at 14,000 x g. Collection tubes were changed between buffers. The column was centrifuged in a clean collection tube for 1 min with the column lid off. The column was then air dried for 2-5 min. RNA was eluted twice with 30 µl water pre-warmed to 45 °C. RNasin (Promega) was added according to the manufacturer's instructions. A 2 µl aliquot of the sample was used for total RNA quantification using Qubit RNA assay kit (Invitrogen), according to manufacturer's protocol.

2.6.5 DNase treatment of RNA

Samples with > 3 µg total RNA were DNase-treated using turbo DNase (Ambion) according to manufacturer's instructions. DNase was removed using the RNeasy MinElute clean up kit (Qiagen) according to manufacturer's instructions, with the addition of 10 % beta-mercaptoethanol to the buffer RLT and elution was in 20 µl water. An aliquot of 4 µl was taken for quality control analysis, whilst the rest was frozen at -80 °C.

2.6.6 RNA quality control

Quality control analysis was conducted using a Qubit (Invitrogen) for quantification, 2100 Bioanalyser (Agilent technologies) to assess degradation levels and Nanodrop (Thermoscientific) to assess protein or solvent contamination. Tests were carried out according to manufacturer's instructions for bacterial RNA. Samples with a paired control and test condition sample with the following parameters were suitable for sequencing to ensure sufficient quantity, good integrity and low trace of contamination: Qubit reads indicating ≥ 3 µg RNA, Bioanalyser RIN ≥ 7.0, Nanodrop 260/280 and 260/230 ≥ 1.8.

2.6.7 RNA library preparation

Libraries preparation was performed by the Centre for Genome Research, University of Liverpool, UK. Total RNA samples were rRNA depleted using the Ribo-Zero magnetic kit for Gram-positive bacteria (Epicentre); this was repeated for samples with poor initial rRNA removal. Libraries were then

prepared using strand specific ScriptSeq kits (epicentre). Samples were sequenced using paired-end sequencing on the HiSeq platform (Illumina) and the analysis was done with single-end reads.

2.6.8 RNA sequencing differential expression analysis

Bowtie (Langmead *et al*., 2009) and Edge R (Robinson *et al*., 2010; Robinson and Oshlack, 2010) were used to map reads and determine the differentially expressed (DE) genes respectively. Genes with mapped transcripts that had a false discovery rate > 0.05, as determined by Benjamin and Hochberg analysis, and $\log_2$ fold change not ≥ ±1 were filtered out of the data set. The remaining gene set was considered differentially expressed between control and test conditions. This analysis was produced by the Centre for Genomic Research (CGR), Liverpool.

Changes in gene expression in biosynthetic pathways were assessed using DE gene sets with KEGG mapper-search and colour (Kanehisa *et al*., 2012, Kanehisa and Goto, 2000). Gene ontology (GO) terms were attached to DE genes using Uniprot (UniProt, 2014).

2.6.9 COG analysis

The sequences for all genes within the genomes of *S. aureus,* Newman and *S. epidermidis* Tü3298 were extracted into a fasta file using the Galaxy tool "Extract genomic DNA" (Goecks *et al*., 2010; Giardine *et al*., 2005). A bespoke perl script (DNA_fasta_to_protein_fasta.pl) was then used to convert these gene sequences into protein sequences. These protein sequences were then submitted to WebMGA function annotation (COG) (Wu *et al*., 2011), which assigns a COG ID to each gene.

Another bespoke Perl script was used to convert the names that had been assigned to the genes by the Galaxy extract genomic DNA tool back to their true gene names (replace_names.pl). The gene lists of DE genes were labelled with

their assigned COGs using a bespoke Perl script (label_cogs.pl). The numbers of genes in each COG class and the percentage of the genome accounted for by each COG class was then calculated using a further bespoke Perl script (counting_cogs.pl).

2.7 Experimental evolution

2.7.1 Evolution passaging

The wild-type *S. aureus* Newman strain was passaged under selective conditions, by continuous repeat incubation in broth containing 6 % (v/v) ethanol or 1 % (v/v) squalene for 14 days. From the second day and onwards, cells that had been cultured for 24 h at 37 °C with ethanol or squalene were diluted to OD_{600} 0.02 and added into fresh broth with the same concentration of ethanol or squalene. A control was also conducted by passage of the parental stain in broth, but without ethanol or squalene for 14 days using the same method. The passage was performed in duplicate.

2.7.2 DNA extraction

For genomic DNA extractions, 2 ml of overnight cultures of staphylococci were pelleted at 4,000 x g for 2 min in sterile Eppendorf tubes. The DNeasy Blood and tissue kit (Qiagen) was then used according to the manufacturer's instructions for Gram-positive bacteria, with the addition of lysostaphin at a final concentration of 25 μg ml^{-1}.

2.7.3 DNA Quality Control

Quality control analysis of purified DNA was conducted using the Qubit (Life Technologies) for quantification, agarose gel electrophoresis to assess overall DNA integrity and Nanodrop to assess protein or solvent contamination. Samples used for sequencing with the TruSeq DNA sample prep kit (Illumina)

had Qubit reads indicating ≥ 1 μg ml^{-1} DNA in ≤ 55 μl volume, plus an agarose gel result indicating minimal fragmentation of DNA and Nanodrop 260/230 and 260/280 ≥ 1.8 verifying purity. Samples for sequencing with Nextera DNA sample prep kit (Illumina) had the same requirements except that DNA concentration was ≥ 0.1 μg ml^{-1}.

2.7.4 Pooled DNA samples

The evolved clone DNA of *S. aureus* was pooled prior to library preparation. By the end of passage, 6 isolates (3 ethanol or squalene evolved and 3 broth evolved) from each duplicate were picked and their genomes were extracted and put into a pool for sequencing. DNA was pooled in equimolar concentrations based upon Qubit readings made using the same mastermix or using two internal control to normalise result when using a different mastermix.

2.7.5 DNA library preparation

DNA libraries for samples to be used as reference genomes for RNA sequencing were prepared using a Nextera DNA sample prep kit (Illumina) according to the manufacturer's instructions. DNA libraries for experimental evolution clones were prepared using TruSeq DNA sample prep kit (Illumina). All samples were sequenced on the MiSeq platform (Illumina) by the CGR, Liverpool.

2.7.6 Genome assembly

The NGS QC toolkit v2.3 (Patel and Jain, 2012) was used to filter out reads with less than 70 % of the read with quality scores over Q20 and to trim 3' ends with less than Q20 quality scores. VelvetOptimiser version 2.2.5 (Victorian Bioinformatics consortium), which utilises Velvet version 1.2.08 (Zerbino and Birney, 2008), was used to assemble genomes using k-mer lengths between 19 and 99 bp. This produced contigs that could be used as a reference for RNA-Seq data.

2.7.7 SNP analysis

Sequence reads were processed by the Centre for Genome Research, University of Liverpool (CGR) to remove adapter sequences and poor quality reads. Briefly, this meant trimming with cutadapt, version 1.2.1 (Martin, 2011), to remove adapter sequences from reads followed by a further trim with Sickle, version 1.200, to remove bases with lower than 20 base quality score. Reads shorter than 10 bp after trimming were filtered from the data files, if the paired read was not filtered out in this process it was moved to another file designated "R0". After this initial processing by the CGR, read quality was assessed using the NGS QC toolkit v2.3 (Patel and Jain, 2012). If filtered reads were assessed to be of good quality, reads were aligned to their reference genome using the Burrows-Wheeler aligner (BWA) aln and sampe packages (Li and Durbin, 2009, Li and Durbin, 2010) version 0.5.9-r16. Samtools (Li *et al*., 2009) version 0.1.18-r580 was used to process sam files to create a bcf file (binary varient call format) for SNP calling. SNPs were called using a bespoke Perl script (mpileup_SNPs_v2.pl) that utilises the SNPEFF package (Cingolani *et al*., 2012) version 3.4e to determine the effect of the SNP (e.g. synonymous, non-synonymous or truncation). Another bespoke Perl script was used to compare SNPs found in the evolved strains and parent or broth control strains (unique_SNPs_bwa.pl). Non-synonymous SNPs were further investigated.

2.8 qPCR

2.8.1 Primer design

Primers were taken from the literature where possible or designed using primer-BLAST (Ye *et al*., 2012). Primers with a length between 15 and 25 bp, predicted to have only one product, a Tm of 60 ±2 °C, low level of single base repeats and a GC clamp towards the 3' end were designed where possible.

Primers were confirmed to amplify a DNA product of the expected length without any secondary products using standard PCR with gDNA as a template.

The PCR mix was made using both BioMix Red (Bioline) which is a complete ready-to-use 2x reaction mix containing an ultra-stable Taq DNA polymerase and ACCUZYME DNA polymerase (Bioline) which is a proprietary proofreading enzyme that offers increased-fidelity and high PCR yield to minimise fidelity errors from the Taq polymerase, according to the manufacturer's instructions.

Primer efficiency was confirmed to be within 90-100 % using a dilution curve with gDNA as described previously (Nolan *et al*., 2006). Efficiency testing was done using the same conditions as for qPCR reactions (described below). The reaction mix in a total volume of 20 µl was set up with 0.5 µM of each primer, 10 µl SensiFAST and a dilution range of gDNA between $1x10^0$-$1x10^4$, with a starting concentration of 10 million copies. Negative controls without template were also implemented. Efficiency values were generated by the qPCR machine software, and an average of at least three resulting efficiency values was taken.

2.8.2 cDNA generation

The tetro cDNA synthesis kit (Bioline) was used for cDNA synthesis according to the manufacturer's instructions using random hexamer primers and approximately 2 µg RNA per reaction. Only RNA samples determined to have high integrity (described above) were used for these reactions.

2.8.3 qPCR conditions

All qPCR reactions were done using SensiFAST SYBR HiMROX kit (Bioline) with the ABI StepOnePlus (Life Technologies) machine. The reaction mix contained 10 µl SensiFAST, 0.5 µM of each primer, 80 µg cDNA and DEPC-treated water up to a total reaction size of 20 µl. The run cycle was 95 °C for 5 min, then 40 cycles of 95 °C for 10 s, 62 °C for 30 s. Data analysis was done using the ABI StepOnePlus software. At least two technical replicates and three biological replicates were used to determine fold change in gene expression between samples.

2.9 Proteomics

Overnight cultures of bacteria were diluted to OD_{600} 0.5, and 2 ml was used to inoculate 50 ml fresh THB in a 250 ml flask. Bacteria were incubated at 37 °C with linear shaking (250 RPM). Next, 1 % (v/v) of squalene was added OD_{600} at 0.5, while control cells were left untreated. Samples were grown for two more hours, followed by centrifuging 1ml of bacterial culture. The cell pellet was washed with PBS three times and diluted to OD_{600} 0.4. 1ml of diluted cells were centrifuged and the supernatant was discarded. The pellet was stored at -80 °C until analysis.

The following steps were performed by The Centre for Proteomics, University of Liverpool, Liverpool, UK. Washed pellets were suspended in 100 µl of 25 mM ammonium bicarbonate. To analyse for protein content, 0.05% RapiGest™ (Waters, Manchester) in 25 mM ammonium bicarbonate was added to the samples, and samples were incubated at 80 °C with 550 RPM for 10 min. The samples were then reduced by the addition of 10 µl 60 mM DTT (dithiothreitol) and incubation at 60 °C for 10 minutes, then alkylated by the addition of 10 µl of 180 mM iodoacetamide with incubation at room temperature for 30 minutes in the dark. Trypsin (Promega U.K. Ltd., Southampton, proteomics grade) was reconstituted in 50 mM acetic acid to a concentration of 0.2 µg μl^{-1} and 10 µl added to the samples followed by overnight incubation at 37 °C. The digestion was terminated and RapiGest™ removed by acidification using 1 µl of TFA (trifluoroacetic acid) and incubation at 37 °C for 45 min and centrifugation (15,000 x g for 15 min).

To check for complete digestion, each sample was analysed pre- and post-acidification by SDS-PAGE. For LC-MS/MS analysis, a 2 µl (1 µg) injection was analysed using an Ultimate 3000 RSLC™nano system (Thermo Scientific, Hemel Hempstead) coupled to a QExactiveHF™ mass spectrometer (Thermo Scientific).

The samples were loaded onto the trapping column (Thermo Scientific, PepMap100, C18, 300µm X 5 mm), using partial loop injection, for seven minutes at a flow rate of 4 µl min^{-1} with 0.1 % (v/v) FA. The samples were resolved on the analytical column (Easy-Spray C18 75 µm x 500 mm 2 µm

column) using a gradient of 97 % A (0.1% formic acid) 3% B (99.9% ACN 0.1% formic acid) to 70% A 30% B over 120 min at a flow rate of 300 ml min^{-1}.

The data-dependent program used for data acquisition consisted of a 60,000 resolution full-scan MS scan (AGC set to $3e^6$ ions with a maximum fill time of 100 ms). The 18 most abundant peaks were selected for MS/MS using a 30,000 resolution scan (AGC set to $1e^5$ ions with a maximum fill time of 45ms) with an ion selection window of 1.2 m/z and a normalised collision energy of 28. To avoid repeated selection of peptides for MS/MS the program used a 30 second dynamic exclusion window.

The data were used to search the *S. aureus* Newman protein sequence database using Mascot (Matrix Science, London, UK). A fixed carbamidomethyl modification for cysteine and variable oxidation modification for methionine were specified. A precursor mass tolerance of 10 ppm and a fragment ion mass tolerance of 0.01 Da were applied. The results were then filtered to obtain a peptide false discovery rate of 1 %.

2.10 Growth in iron deficient media

Iron-deficient chemical defined medium (CDM) was prepared by adding into one litre water: Na_2HPO_4 (7 g), KH_2PO_4 (300 mg), adenine sulfate (20 mg), guanine-HCl (20 mg), L-glutamic acid (2.22 g), L-aspartic acid (2.22 g), L-proline (2.22 g), glycine (2.22 g), L-threonine (2.22 g), L-serine (2.22 g), L-alanine (2.22 g), L-lysine-HCl (560 mg), L-isoleucine (560 mg), L-leucine (560 mg), L-histidine (440 mg), L-valine (440 mg), L-arginine (330 mg), L-cysteine (220 mg), L-phenylalanine (190 mg), L-tyrosine (170 mg), L-methionine (170 mg), L-tryptophan (60 mg), pyridoxal (0.8 mg), pyridoxamine-2HCl (0.8 mg), D-pantothenic acid (0.4 mg), riboflavin (0.4 mg), nicotinic acid (0.4 mg), thiamine-2HCl (0.4 mg), and biotin (0.02 mg). Iron limited conditions were achieved by adding 10 g L^{-1} Chlex-100 (Sigma) to the solution and mixing for 4 h, followed by filter sterilization. Finally, sterile glucose and $MgSO_4$ was added to obtain the final concentration of 10 g L^{-1} and 0.5 g L^{-1}, respectively.

Cell growth in iron-defined media was performed and measured using a 96-well plate using a Fluostar Omega (BMG Labtech) plate reader. Overnight culture was diluted to OD_{600} 0.02 and 200 µl aliquoted into 96 well plates. Cells were grown at 37 °C with double orbital shaking (200 rpm) for 12 h with the presence or absence of 1 % (v/v) squalene. Five concentrations of iron (0 uM, 0.02 uM, 0.2 uM, 2 uM) were tested. Cell density was determined by measurement of OD_{600}.

2.11 Cellular iron concentration analysis

Overnight cultures of bacteria were diluted to OD_{600} 0.5, and 4 ml used to inoculate 50 ml fresh THB in a 250 ml flask. Bacteria were incubated at 37 °C with linear shaking (250 RPM). When OD_{600} reached 0.5, cells were challenged with 1 % (v/v) squalene (squalene-treated cells), while control cells were left untreated. After 24 h, 5 ml of cell culture was harvested from each sample by centrifugation with washing three times with PBS. Viable counts were performed after washing. To lyse the cells, 0.1 mg ml^{-1} of lysostaphin (Sigma) was added and incubated for 2 h or until lysate was clear. HCl was added to the lysate to a final concentration of 0.1 M in 10 ml. The lysate was then filter sterilised prior to Inductively Coupled Plasma optical emission spectroscopy (ICP-OES) analysis.

ICP-OES analysis was performed by The Department of Chemistry, University of Liverpool, Liverpool, UK with an Agilent 5110 SVDV ICP-OES and the key parameters for the test are as follows: RF Power: 1.3kW; Wavelengths (nm): 261.187, 240.489, 238.204, 258.588; Read Time: 10 seconds; Viewing Mode: Axial; Neb Flow: 0.7L min^{-1}; Plasma Flow: 12L min^{-1}; AuxFlow: 1L min^{-1}.

Chapter 3 Influences of squalene on staphylococcal physiology and resistance to antimicrobials

3.1 Introduction

3.1.1 Squalene and its association with bacteria

Squalene (SQ) is widely present in nature, and large amounts are present in olive oil, palm oil, wheat-germ oil, amaranth oil, and rice bran oil. The richest source known of squalene is shark liver oil (60 wt.%), which has been traditionally used as source of this lipid (Xu *et al*., 2004). In humans, the highest accumulation of squalene is associated with skin, where it normally comprises about 12% of total skin surface lipids that in an adult corresponds to 60 μg/cm^2 (Pappas, 2009). Owing to its critical role in the biosynthesis of eukaryotic sterols and bacterial hopanoids, squalene is synthesised across types of cells and species. More specifically, squalene and its related compounds, oxidosqualene and bis-oxidosqualene, are precursors of nearly 200 different triterpenes. Several species of bacteria, metabolise SQ as a carbon source such as *Corynebacterium sp.*, *Rhodococcus sp.*, *Pseudomonas sp*., and *Arthrobacter sp*. (Spanova and Daum, 2011).

As an intriguing component of the skin surface lipids, squalene produced in the sebaceous gland mostly accumulates on the surface, not being converted into lanosterol, which as the next step halts the biosynthesis of cholesterol (Picardo *et al*., 2009). The accumulation of this lipid is negligible in other organs of the human body and the reason for that is still unclear. A variety of hypotheses have been proposed for squalene accumulation on the skin, such as maintaining skin moisture (Luca and Valacchi, 2010) and acting as an antioxidant for UV protection (Ohsawa *et al*., 1984), but there is no study reported describing any antimicrobial effect of squalene.

3.1.2 The effects of squalene on staphylococci pigmentation and antimicrobial resistance

S. aureus and many non-pathogenic species of staphylococci are able to produce staphyloxanthin (STX), which is an orange-red triterpenoid located in the membrane that is described to have a role in the environmental fitness of *S. aureus* (Clauditz *et al*, 2006). STX is encoded by genes of the *crtOPQMN* operon with a SigmaB-dependent promoter upstream of *crtO* and a terminator downstream of *crtN* (Pelz *et al*, 2005). In the first step of STX biosynthesis, two molecules of farnesyl diphosphate are condensed to form dehydrosqualene, catalysed by CrtM. Next the dehydrosqualene is dehydrogenated by CrtN to form the yellow intermediate 4,4-diaponeurosporene. Next, CrtP converts 4,4-diaponeurosporene into 4,4-diaponeurosporenic acid by oxidising the terminal methyl group. In the final steps, 4,4-diaponeurosporenic acid is firstly esterified by CrtQ and then acylated to form STX by CrtO.

Staphyloxanthin was revealed to have a role in antioxidation by detoxifying reactive oxygen species produced by phagocytes and neutrophils (Liu & Nizet, 2009). By comparative analysis of the wild type with a *crtM* mutant, Götz *et al* (2006) showed staphyloxanthin contributes to resistance from hydrogen peroxide, superoxide radical, hydroxyl radical, hypochlorite, and neutrophil killing. Several reports have proposed that STX also stabilises the membrane of *S. aureus* during infection and pathogenesis in a manner similar to that observed for cholesterol in eukaryotes (Rohmer *et al*, 1979 & Mishra *et al*, 2011).

Although squalene was not reported to have antimicrobial effects in previous studies, it remains possible that it modulates the action of skin antimicrobials produced by the host or other bacteria. As described in Chapter 1 general introduction, skin possesses a broad arsenal of antimicrobials that target potential colonisers. These effectors include a various types of reactive oxygen species (ROS), such as hydrogen peroxide, superoxide radical and hydroxyl radical; antimicrobial skin lipids such as sphingosine, antimicrobial fatty acids (AFAs) linoleic and sapienic acid; antimicrobial peptides (AMPs) such as LL-37, defensins and those produced by competing bacteria e.g. *S. epidermidis*

epidermin. Squalene, however, despite of its substantial amounts found on the skin, has not been reported to affect resistance to these antimicrobials in bacteria.

3. 2 Aims

Although significant efforts have been put into investigating the interaction between human skin surface components and staphylococci, especially the antimicrobial peptides, the effects of squalene on staphylococci remain poorly understood. Taking account of the considerable quantity of squalene presenting on human skin, it was deemed valuable to determine whether squalene has potential to play a role in colonisation of staphylococci and determine the nature of any role identified.

The main aims of this chapter were to first determine if squalene has antimicrobial effects on *Staphylococcus aureus* and *Staphylococcus epidermidis*. Additionally, investigations sought whether squalene modulates the action of selected antimicrobials. A minimum of two strains of each species were used to limit strain-specific effects. Tests based on growth rate assays and cell counts by Miles and Misra method were used to assess the antimicrobial activity of squalene. The described antimicrobials, H_2O_2, LL-37, nisin and sapienic acid were chosen to conduct antimicrobial tests to examine squalene influences. Overall these experiments should determine whether the role of squalene is more than just a precursor of cholesterol but influences the skin colonisation and persistence of bacteria.

3.3 Results

3.3.1 The effects of squalene on the growth of *Staphylococcus aureus* and *Staphylococcus epidermidis*

To determine whether squalene influenced the growth of *S. aureus* and *S. epidermidis,* and identify whether it had any antimicrobial properties, growth curves of the bacteria treated with different concentrations of squalene were measured by testing optical density every hour (Fig 3.1) over the first 8 hours and followed by viable counts determined 24 h after squalene addition (Fig 3.2). Briefly, bacteria were grown in fresh BHI broth for approximately 2.5 h until its OD_{600} reached 0.5. Two concentrations of squalene were added to obtain the final squalene concentrations from 0% to 1%. Two strains of each species (Newman and SH1000 for *S. aureus*, Tü3298 and RP62A for *S. epidermidis*) were used in these assays.

Both growth curves and viable counts results revealed that squalene does not influence cell growth and does not have obvious antimicrobial effects, under the conditions tested. A Pearson's correlation test supports that there was no significant relationship between the concentration of squalene in the medium and cell density ($p=0.84$). The results for SH1000 and RP62A were very similar as those obtained using strains Newman and Tü3298, which indicated the absence of a strain-specific effect by squalene on staphylococcal cell growth.

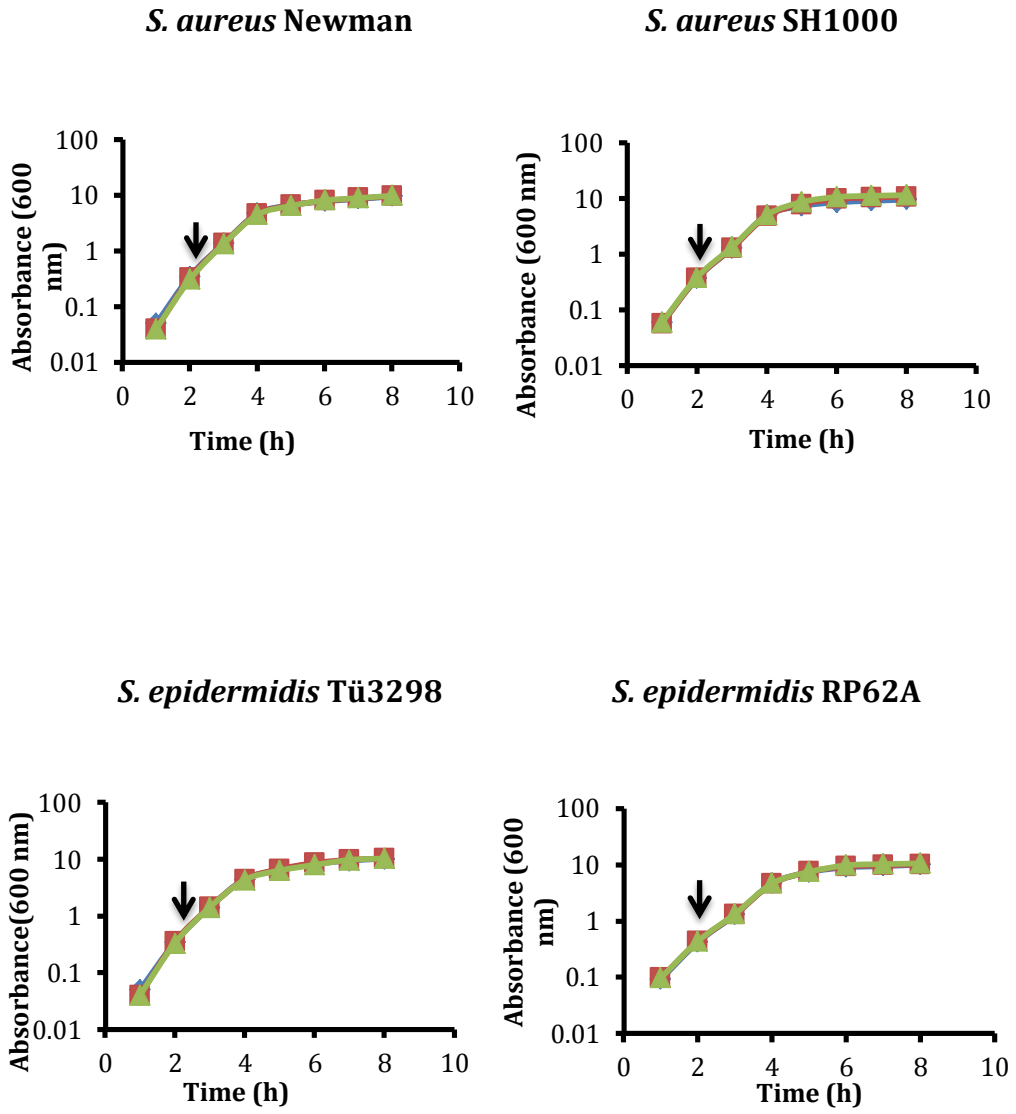

Figure 3.1 Growth curves of *S. aureus* and *S. epidermidis* strains challenged with different concentrations of squalene. Optical density was measured hourly. The arrow indicates squalene was added when OD_{600} reached 0.5. Squalene was added to a final concentration of 0.1% v/v (square), 1% v/v (triangle) or was absent (diamond).

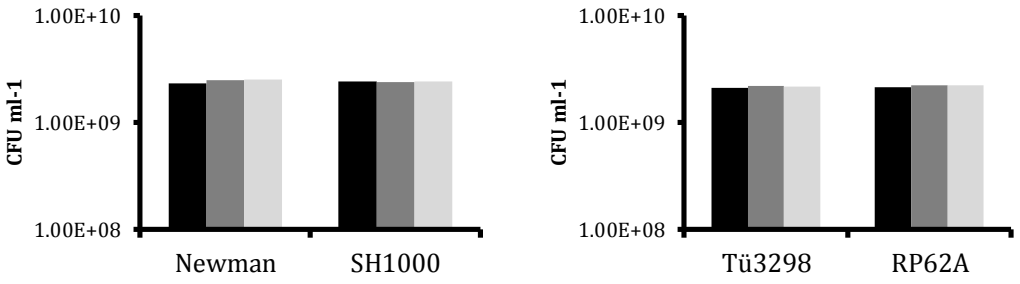

Figure 3.2 Viable cell counts of *S. aureus* and *S. epidermidis* strains after 24 h growth with different concentrations of squalene. Viable counts were measured using Miles and Misra technique after 24 h culture in BHI broth in the absence (black) or presence of squalene, 0.1 % v/v (deep grey), and 1% v/v (light grey).

3.3.2 The effects of squalene on staphylococcal pigmentation

Having established that squalene had no discernible antimicrobial activity, at least under the conditions tested, it was noted during viable count experiments that the eponymous golden colour of treated *S. aureus* cells dramatically reduced. This orange-red triterpenoid located in the membrane plays an important role in the environmental fitness of *S. aureus* as discussed (Clauditz *et al*, 2006). Therefore, to investigate this phenomenon, absorbance spectrum tests were conducted using methanol-extracted pigment from cell pellets.

The spectrum tests were performed using an optical spectrum analyser plate reader, which uses reflective techniques to separate out the wavelengths of light and measures the intensity of the light with an electro-optical detector. In the experiments, the pigment extracted from a wild-type pigmented *S. aureus* strain presents a spectrum with two peaks at 440 nm and 470 nm, which indicates the existence of staphyloxanthin (λmax=463 nm) and two biosynthetic precursors of staphyloxanthin, 4,4-diapolycopene (λmax=440,468 nm) and 4,4-diaponeurosporene (λmax=415, 439 nm) (Furubayashi *et al*., 2014). Corresponding with Beer's law (A=εcl), higher absorbance peak values indicate a greater quantity of carotenoids in the sample.

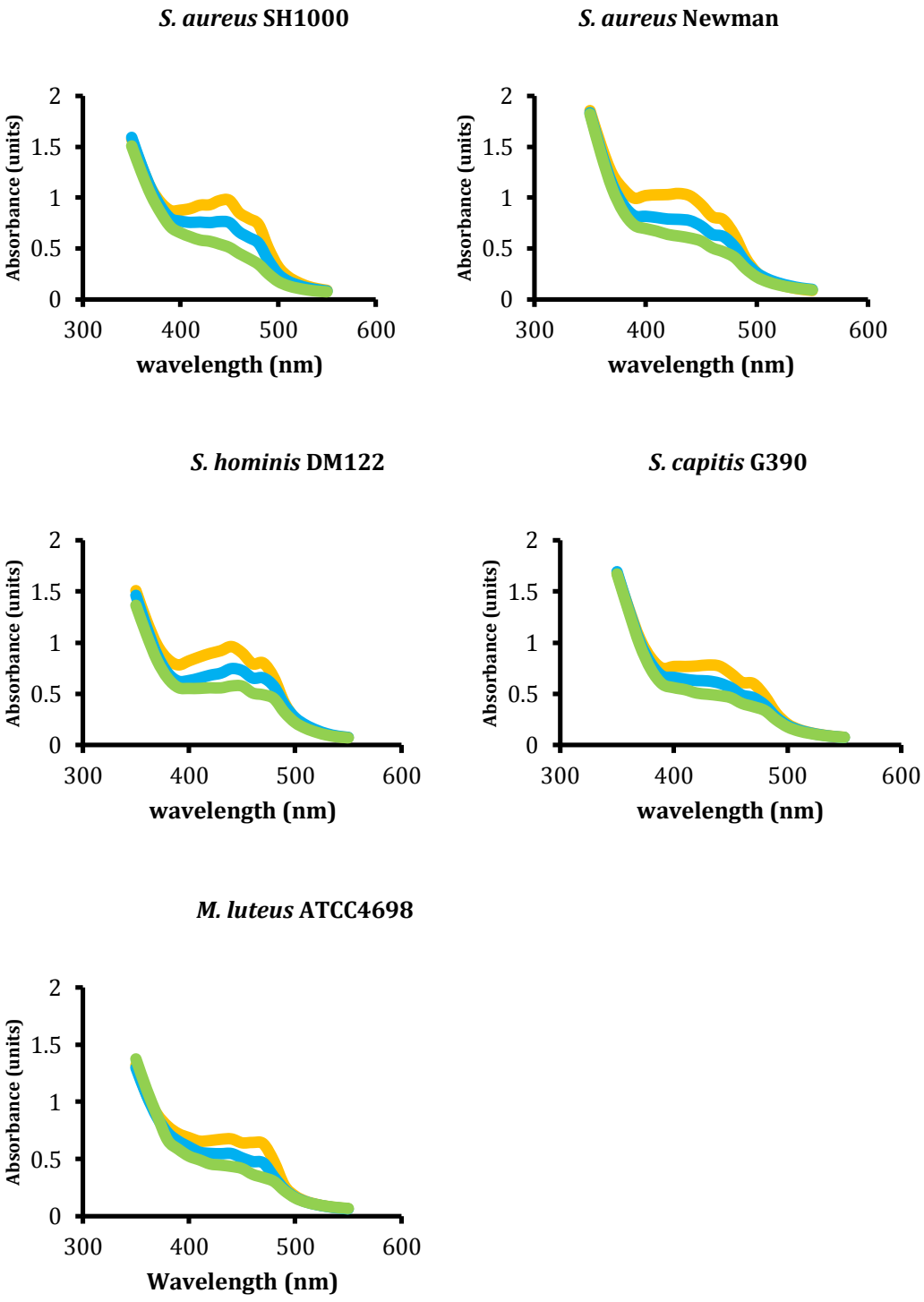

Figure 3.3 Absorbance spectra of MeOH-extracted pigment of squalene-treated cells. Strains *S. aureus* Newman and SH1000, *S. capitis* G390, *S. hominis* DM122 and *Micrococcus luteus* ATCC4698 were grown in BHI with different concentrations of squalene for 24 h. Orange: control; Blue: 0.1% v/v squalene; Green: 1% v/v squalene. The two peaks around a wavelength of 450 nm are the representative evidence for presence of the carotenoids. Readings were corrected based on cell amount such that a higher peak indicates a larger quantity of carotenoids in the sample.

Three pigmented staphylococci, *S. aureus* strains Newman and SH1000, *S. hominis*, and *S. capitis* G390 and a pigmented *M. luteus* ATCC4698 were assayed to determine if the effect of squalene applies more widely (Fig 3.3). *Micrococcus luteus* is a yellow-pigmented species that is part of the normal flora of mammalian skin and it shares similar niches with staphylococci. Although its pigment sarcinaxanthin differs from staphyloxanthin, the maximum absorption of *M. luteus* pigment is also around 470 nm (Netzer *et al*, 2010). From the spectral analysis, the characteristic peaks reduced indicating that levels of staphyloxanthin were lower with increased lipid indicating a concentration-dependent effect of squalene on staphylococcal pigmentation. Furthermore, together with the similar results obtained from *M. luteus*, it may propose a widespread existence of this effect on pigmented bacteria.

3.3.3 Influence of squalene on staphylococcal resistance to antimicrobials

As described, staphyloxanthin plays an important role in resistance to oxidative stressors, such as H_2O_2. Antioxidant properties derive from multiple conjugated bonds of STX that enable it to eliminate singlet oxygen. Therefore, it was hypothesised that reduced pigmentation by treatment with squalene would increase the cell's susceptibility to H_2O_2. In contrast, *S. epidermidis* lacks ability to produce any pigment, which theoretically would not be affected by treatment with squalene when applying the same test.

Susceptibility tests of *S. aureus* and *S. epidermidis* to H_2O_2 were performed. Cells of both species were cultured with 1% v/v of squalene for 24 h and the same quantity of washed cells for each sample were challenged with H_2O_2 for 90 min. The results support the hypothesis (Fig 3.4). For *S. aureus*, cells cultured with the highest concentration of squalene (1 % v/v) showed the lowest survival levels (~40 %), compared with 0.1 % (v/v) of squalene that caused 20 % loss of survival relative to untreated control cells. This difference was significant assessed by one-way ANOVA ($p<0.001$). Unlike *S. aureus*, the results showed that the overall susceptibility of *S. epidermidis* to H_2O_2 was much higher. Only 12 % of bacteria survived after 90 min compared with 68 % for *S. aureus*.

However, there was no significant difference in susceptibility across increasing concentrations of squalene (one-way ANOVA, p=0.98).

To determine whether preconditioning cells with squalene also changes the susceptibility of *S. aureus* or *S. epidermidis* to non-oxidative substances, nisin was used to challenge the cells cultured with squalene (Fig 3.4). Nisin is an antimicrobial peptide produced by bacteria including *Lactococcus lactis* that plays important role in the production of buttermilk and cheese. Nisin has relevance as a representative of one class of antimicrobial peptides i.e. type A lantibiotics targeting the cell membrane.

The results showed a similar pattern to the susceptibility tests to H_2O_2. For *S. aureus*, cells cultured with 0.1 % (v/v) squalene exhibited a decreased survival (~2-fold greater killing) compared with that of the control. Moreover, there was a dose-dependent effect since cell culture with 1 % (v/v) squalene further decreased survival (~3-fold more killing) relative to untreated cells. These results achieved statistical significance (one-way ANOVA, $p<0.005$). In contrast, *S. epidermidis* cells showed no clear trend of altered survival, with 0.1 % (v/v) squalene exhibited slightly reduced survival (~2 %) as culture with 1 % (v/v) squalene slightly increased cells' survival rate (~3 %). No statistical significance was achieved (one-way ANOVA, p=0.67) confirming the lack of any relationship between squalene concentration and survival of *S. epidermidis* from nisin.

The antibacterial activity of unsaturated fatty acids has been well known for several decades (Kabara *et al*. 1972; Knapp and Melly 1986; Shin *et al*. 2007; Neumann *et al*., 2015). The antimicrobial lipid sapienic acid, which shares the same site of origin with squalene, was also chosen to preform survival tests of squalene-treated cells. Sapienic acid was proven having effect against staphylococci including *S. aureus* and *S. epidermidis* as well as being capable of inhibiting virulence determinant production and the induction of antibiotic resistance mechanisms (Kenny *et al*., 2009; Neumann *et al*., 2015). However, survival assays of squalene-treated cells challenged with sapienic acid revealed that squalene did not significantly alter the resistance for either *S. aureus* or *S. epidermidis* (Fig 3.4), suggesting that there may not be direct causality between

susceptibility of staphylococci to sapienic acid and the decreased level of pigmentation.

Finally, a representative human antimicrobial peptide, LL-37, was chosen to perform survival tests of squalene-treated cells. The cathelicidin family member LL-37 is the a cationic antimicrobial peptide described in humans and is expressed by neutrophils and stimulated keratinocytes (Kim *et al*., 2005). LL-37 shows potent antimicrobial activity against Gram-positive and Gram-negative bacteria, fungi, and some viruses making the peptide an important component of the innate immune system (Gordon *et al*., 2005).

For cells cultured with increasing concentrations of squalene, the susceptibility of *S. epidermidis* to LL-37 was modestly increased (one-way ANOVA, $p<0.01$). LL-37 killed 7 % more *S. epidermidis* cells when they were grown with 0.1 % of squalene and 12 % more cells after treated with 1 % of squalene (Fig 3.4). But for *S. aureus*, no significant difference between survival from LL-37 of control and squalene-treated cells was observed (one-way ANOVA, $p=0.92$). These data indicate that squalene does not influence the resistance of *S. aureus* to LL-37.

Survival of H_2O_2

(a)

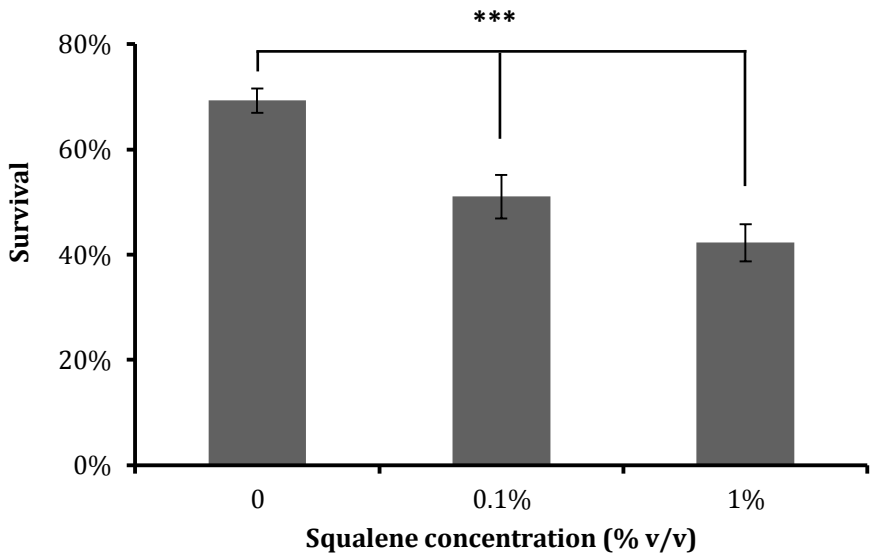

(b)

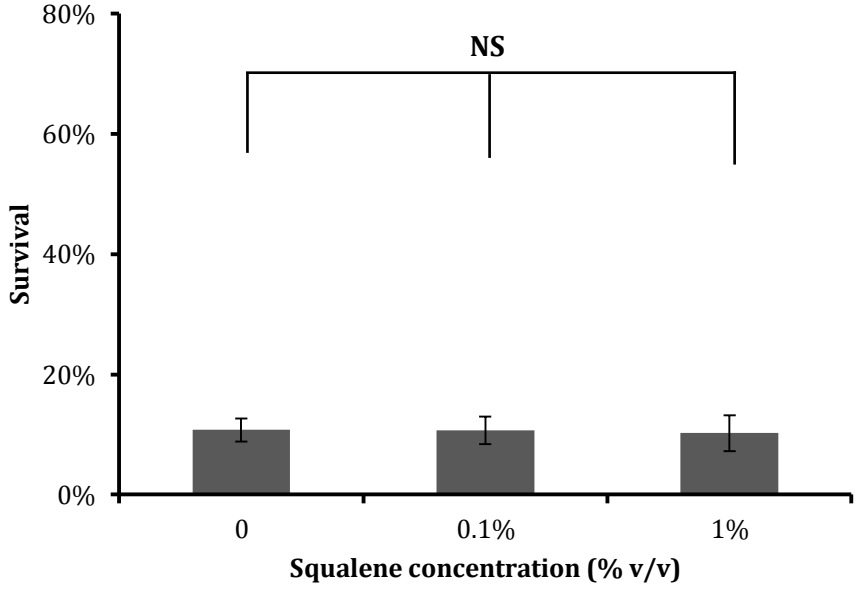

Survival of nisin

(a)

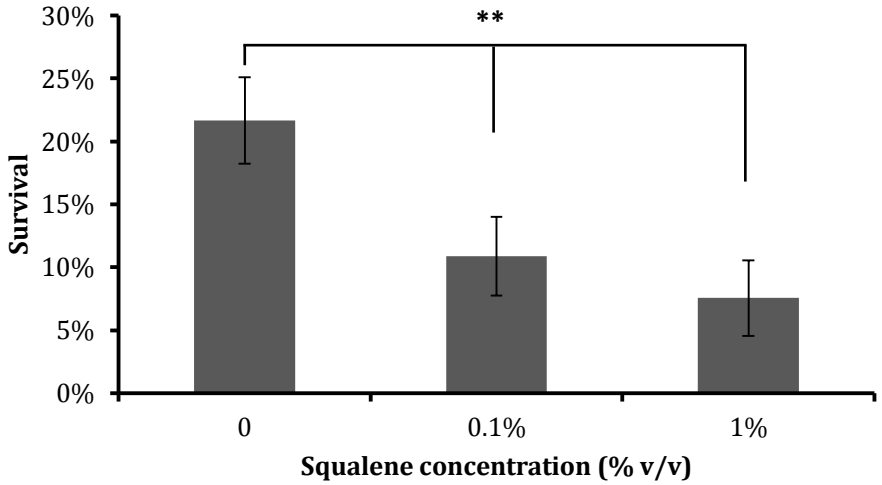

(b)

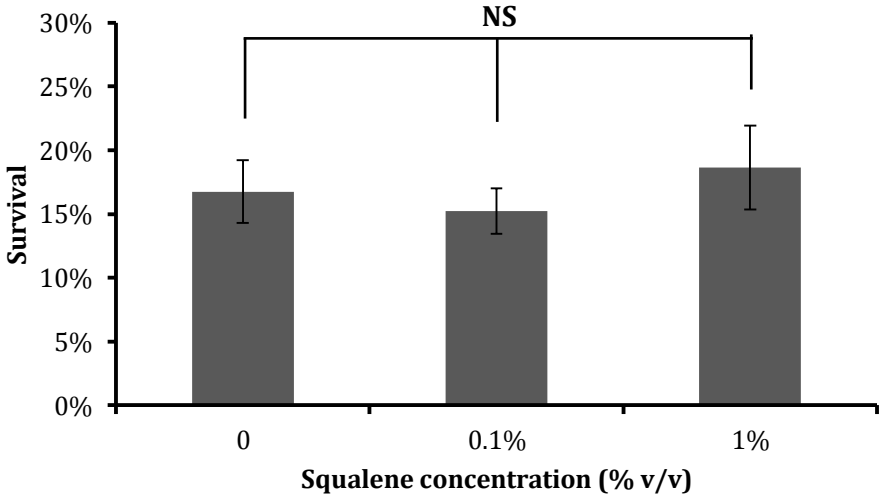

Survival of sapienic acid

(a)

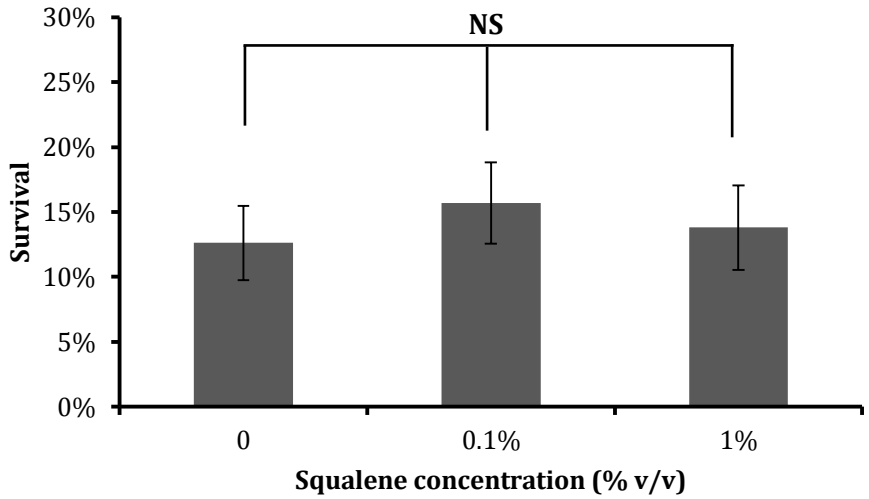

(b)

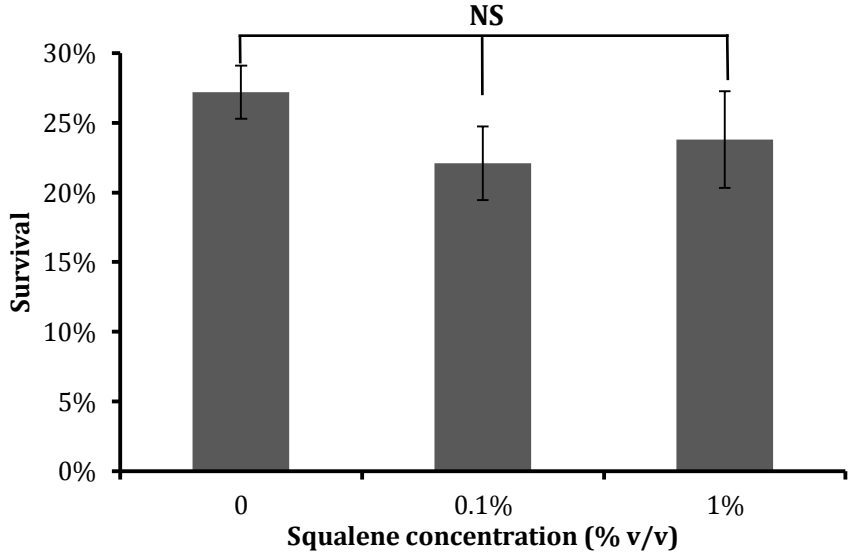

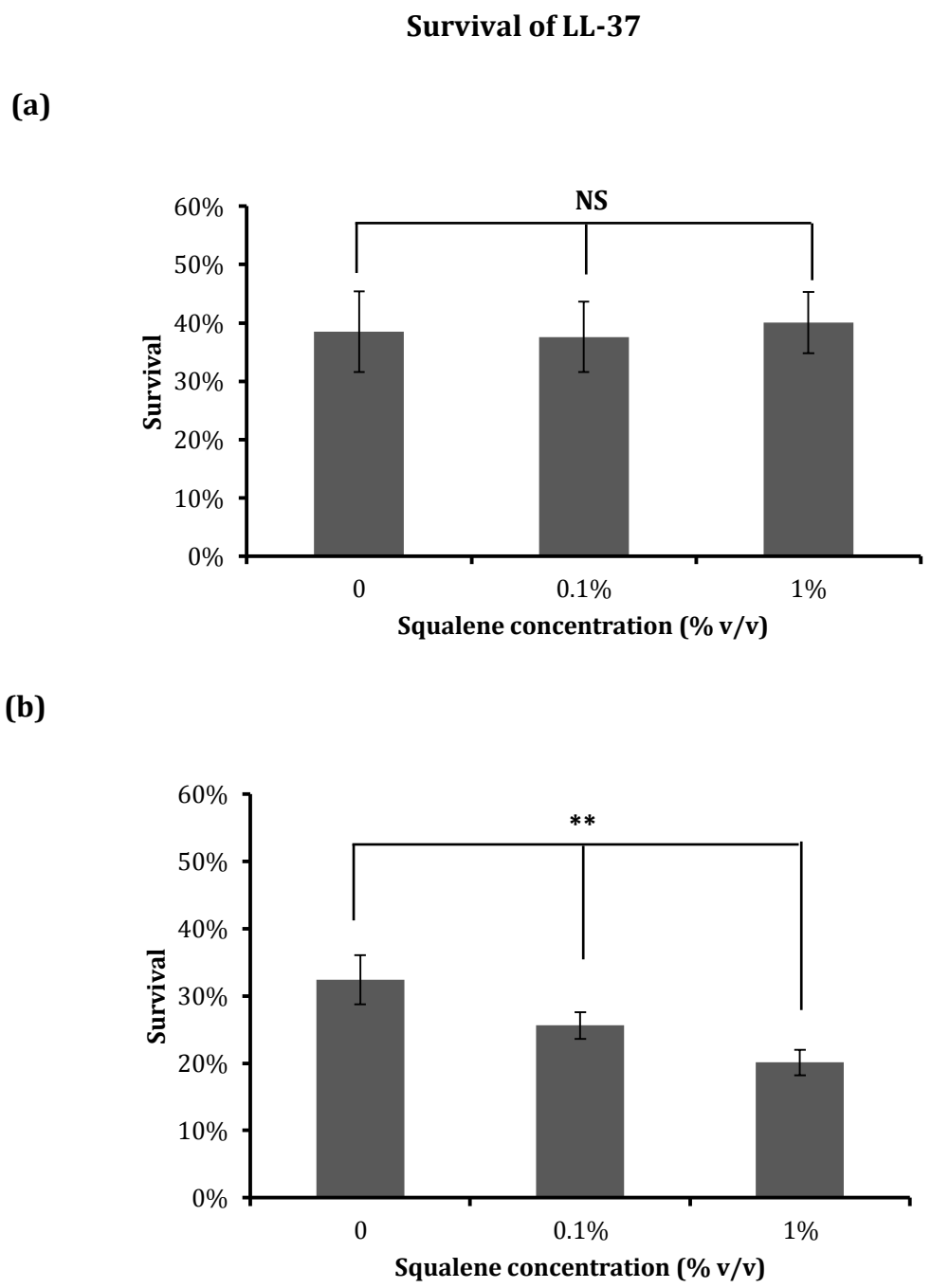

Figure 3.4 Survival of *S. aureus* Newman and *S. epidermidis* Tü3298 cells cultured with different concentration of squalene following challenge with H_2O_2, sapienic acid, nisin and LL-37. Cells were cultured with the indicated concentrations of squalene for 24 h. Cells were washed twice with PBS and diluted to an OD_{600} of 0.1. Viable Cell counts were performed at time zero and 90 min after challenge with antimicrobial peptides. The final concentration of H_2O_2, nisin, sapienic acid and LL-37 is 7.5 mM, 250 µg ml^{-1}, 5 µg ml^{-1}, and 10 µg ml^{-1} respectively. In each experiment, three replicates were conducted. In each survival test, *S. aureus* Newman is indicated as (a), while (b) represents *S. epidermidis* Tü3298. Asterisks show significance as measured by the one-way ANOVA (** $P \leq 0.01$; *** $P \leq 0.001$; NS: not significant).

3.4 Discussion

In this chapter, the antimicrobial properties of squalene were assessed across a range of squalene concentrations during bacterial growth using both growth curve measurement and viable counts. This study showed that at least under the conditions tested with rich growth medium, such as BHI, squalene does not have antimicrobial effects on *S. aureus* and *S. epidermidis*,. Squalene neither interfered with cell growth nor reduced the cell quantity after 24 hours treatment. The conclusion of its lack of toxicity was confirmed with three species and multiple strains of staphylococci. There are no previous studies that have reported in the literature an antimicrobial effect of squalene, despite numerous studies describing squalene's role as a major component of skin surface lipids (Pappas, 2009; Picardo *et al*., 2009; Spanova & Daum, 2011).

It was noted during culture in rich growth medium that the eponymous golden pigment of treated *S. aureus* cells was dramatically reduced. To investigate this phenomenon, pigment was extracted from the membranes of two strains of *S. aureus* (Newman and SH1000), two pigmented coagulase-negative *Staphylococcus* species (*S. capitis* G390 and *S. hominis* DM122) and a pigmented *Micrococcus luteus* strain ATCC4698. This experiment revealed that there was a negative relationship between squalene addition and bacterial pigmentation, and confirmed this correlation was concentration depended. Given the known relationships between pigmentation and defence from both antioxidants and certain antimicrobial peptides, the comparative effects of squalene treatment on *S. aureus* and *S. epidermidis* cells were studied with respect to four distinct types of antimicrobial: H_2O_2, nisin, sapienic acid and LL-37. The results revealed that pre-treatment of squalene has no effect on resistance to sapienic acid, but increased the susceptibility of *S. aureus* but not *S. epidermidis* to H_2O_2 and nisin. However, for LL-37, pre-treatment of squalene enhanced the resistance with *S. epidermidis* but did not alter the resistance of *S. aureus*.

Previous work by Bindu *et al* (2015) showed that squalene inhibits carotenoid biosynthesis in *S. aureus*. Their study was established after completion of the works shown in this chapter, but the results of two studies were highly

consistent. We confirmed that squalene inhibits carotenoid biosynthesis in *S. aureus*, and also in other pigmented skin colonisers *S. hominis*, *S. capitis* and *M. luteus*. The absorbance spectra of three pigmented staphylococci consistently demonstrated that the pigmentation levels inversely correlated with increasing concentrations of added squalene. From these data there is no clear explanation for a mechanism and further *in vitro* tests were deemed best after a broad approach to identify contributing determinants via a transcriptomic study presented in Chapter 4.

The staphyloxanthin biosynthesis genes are organised in an operon, *crtOPQMN*, with a *sigmaB*-dependent promoter upstream of *crtO* and a termination region downstream of *crtN* (Pelz *et al*., 2005). Therefore, as the only operon responsible for carotenoid biosynthesis, the decreased expression of the *crt* operon is expected in transcriptomic data of *S. aureus* cells challenged with squalene. In addition, *sigmaB* itself and the *rsb* operon that regulates the expression of the RNA polymerase accessory factor, sigmaB, may also have reduced transcription after squalene challenge.

It is known that the absence of *S. aureus* pigment in cells growing in anaerobic conditions repress production of staphyloxanthin (Hall *et al*., 2017). If squalene affects pigmentation via this pathway, then expression of contributing genes of anaerobic metabolism, such as *srrAB, ldh1, ldh2, adhE, adh, budA1, budB* and *nir* operon should be up-regulated (Fuchs *et al*., 2007).

Furthermore, it was reported that the cold shock protein CspA of *S. aureus* is required for maximal production of pigment (Katzif *et al*., 2005). Results from their transcriptional studies revealed that loss of CspA decreased expression of *crt* genes needed for the biosynthesis of 4,4'–diaponeurosporene, which is an intermediate of staphyloxanthin biosynthesis; expression of *sigmaB* was also decreased. Therefore, *cspA* might also show as reduced expression level in a transcriptomic study.

The observation that there was a similar effect of squalene on micrococcal pigmentation proposes that the action of squalene on bacterial carotenoids is more universal. The main carotenoid pigment in *M. luteus* is called

sarcinaxanthin, which shares several features with staphyloxanthin. Both pigments are C50 carotenoids that have multiple conjugated double bonds, and they contain at least one hydroxyl group; both these features contribute to strong antioxidative properties (Netzer *et al*., 2010). Like staphyloxanthin, biosynthesis of sarcinaxanthin also starts with converting C15 farnesyl pyrophosphate (FPP) into a longer carbon backbone. But the product from this step is C40 lycopene with sarcinaxanthin biosynthesis that is different from the C30 dehydrosqualene produced in staphyloxanthin biosynthesis. The biosynthetic pathways of both staphyloxanthin and sarcinaxanthin are shown in Fig 3.5. The proteins participant in sarcinaxanthin production are translated from the *crtEBIE2YgYh* operon (Netzer *et al*., 2010). Despite the different structures of staphyloxanthin and sarcinaxanthin, their biosynthetic pathways share similar enzymatic activities that might be the target for squalene to produce a transcriptional feedback via competitive inhibition, for example.

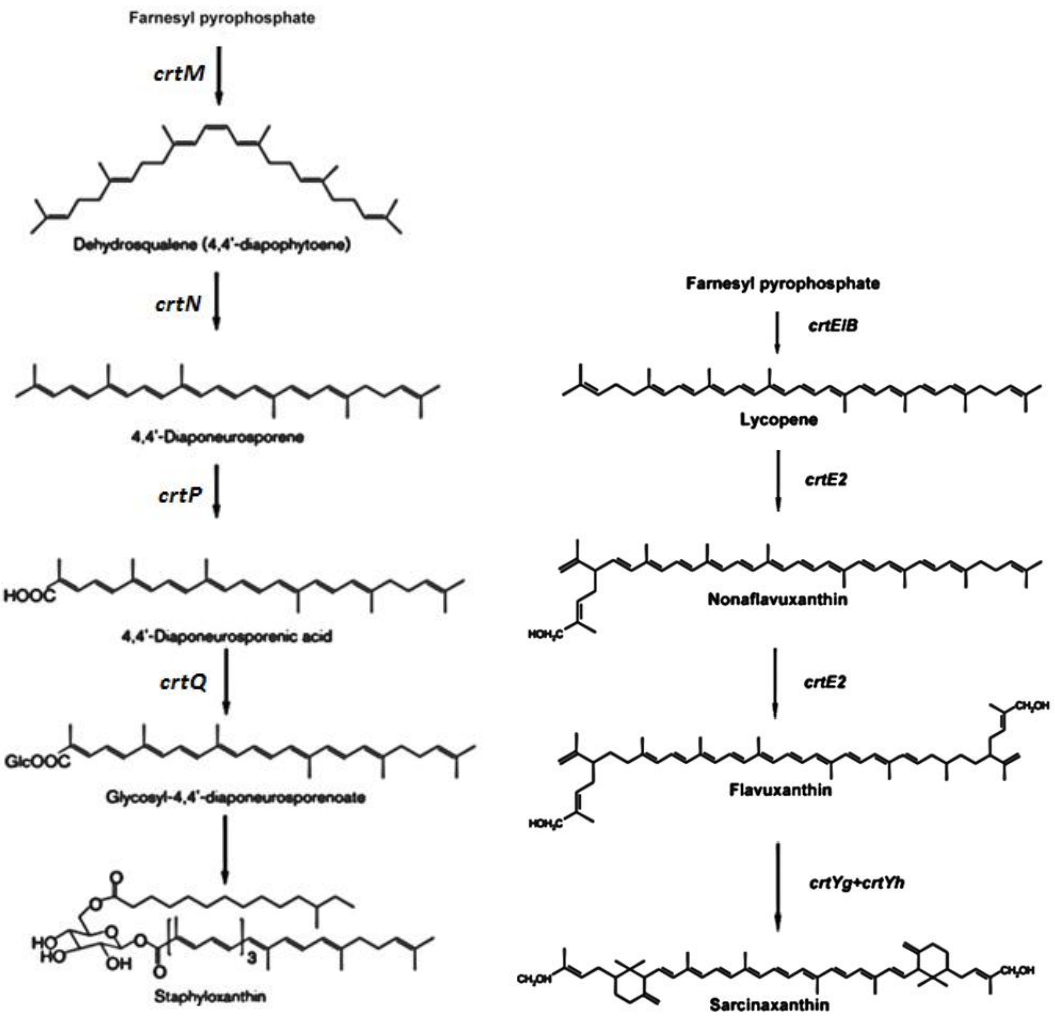

Figure 3.5 Comparison of the biosynthetic pathways of staphyloxanthin in staphylococci (left) and sarcinaxanthin in *M. luteus* (right). (Pelz *et al*., 2005; Netzer *et al*., 2010)

The susceptibility of *S. aureus* to H_2O_2 was increased after treatment of squalene, which fits with previous reports, because staphyloxanthin contributes to resistance to oxidative stress such as H_2O_2 by scavenging free radicals with its conjugated double bonds (Liu *et al*., 2009; Götz *et al*., 2006). In addition, staphylococci possess other mechanisms that contribute to defence against damage by ROS such as the activity of KatA that is transcriptionally regulated by SigmaB, PerR and Fur, thereby enhancing the survival of cells in response to oxidative stress (Horsburgh *et al*. 2001, 2002). Thus if down-regulated expression of *katA* or the regulator genes by treatment with squalene are observed, this could explain increased susceptibility of *S. aureus* to H_2O_2. Since

the H_2O_2 resistance of squalene-treated *S. epidermidis* cells was unchanged, despite expressing catalase, supports squalene having an effect on enzyme synthesis of carotenoids.

The results of nisin susceptibility tests of *S. aureus* and *S. epidermidis* are similar to the results to H_2O_2, where *S. aureus* but not *S. epidermidis* cells cultured with squalene had increased susceptibility. To interpret this result, it is necessary to first understand the mechanism of the antimicrobial action of nisin.

Nisin is a heat stable, cationic lantibiotic consisting of 34 amino acids that has antimicrobial activity against many species of Gram-positive bacteria, but not Gram-negative bacteria due to their outer membrane barrier. Nisin does not require a membrane receptor on its target cell. Instead, after passing through the target cell wall via hydrophobic or electrostatic interactions with anionic components in the cell wall, nisin binds to the cell wall precursor named lipid II which is essential for bacterial cell wall biosynthesis, thereby causing either lost function of lipid II or pore formation, both resulting in eventual cell death (Sahl *et al*., 1987).

It was reported that polar carotenoids modulate the fluidity properties of lipid membranes and such fluidity characteristics are critical to the interaction of membrane-targeting host defence cationic antimicrobial peptides (CAPs) with *S. aureus* (Mishra *et al*., 2011). Therefore, decreased fluidity of *S. aureus* cells arisen from reduced level of pigment by treatment with squalene can be a facile explanation. The result of the resistance of pigmentless *S. epidermidis* cells to nisin that were not influenced by squalene also supports this conclusion. However, there is another possible explanation, which should not be neglected. Hiron *et al* (2011) claimed that a two-component system of staphylococci, *braRS*, is involved in resistance to bacitracin and nisin. Should this be the contributing effector, different expression levels of *braRS* system between *S .aureus* and *S. epidermidis* might therefore be expected in transcriptomic data.

It was hypothesised that squalene treatment would decrease the resistance to LL-37 of *S. aureus* while having no effect on *S. epidermidis* on the basis of LL-37 sharing several properties with nisin. As the only cathelicidin produced by

humans, LL-37 is a cationic antimicrobial peptide (CAMP) expressed by neutrophils and keratinocytes. LL-37 contributes to human cutaneous immune defences against bacterial colonisers by formation of pores in the bacterial cell membrane (Dürr *et al*., 2006). Nevertheless, the susceptibility tests of *S. aureus* and *S. epidermidis* to LL-37 demonstrated the opposite outcome. The susceptibility of *S. aureus* to LL-37 was unaffected by squalene while that of *S. epidermidis* increased after treatment with squalene.

Staphylococci have a number of mechanisms to withstand the action of LL-37. At least four proteins have been proven to contribute to survival from LL-37 (Barns and Weisshaar, 2013): IsdA, a cell wall MSCRAMM adhesion and haem uptake protein, aureolysin protease, MprF and DltABCD that catalyse lysinylation of phospholipid and alanine transfer to teichoic acid, respectively. Therefore, if squalene differentially influences the expression of these genes in *S. aureus* and *S. epidermidis* this would account for the observed different effects of squalene on LL-37 susceptibility. Among these four proteins involved in defence against LL-37, IsdA is the one only present in *S. aureus* that is absent in in *S. epidermidis.* Thus if treatment of squalene triggers the increased expression of IsdA, this would enhance resistance to LL-37 to produce the observed outcome.

Chapter 4 The responses to squalene of *S. aureus* and *S. epidermidis*

4.1 Introduction

Understanding changes in gene expression is critical for improving our knowledge of the mechanisms between stimulation and response. The need for reliable assessment of transcript abundance in biological samples has driven scientists to develop more and more technologies to meet this demand. A decade ago, microarrays were employed for most transcriptomic analysis using nucleic acid probes, typically 60-mers, covalently bound to glass slides. Fluorescently-labelled target sequences are hybridised to the probes and scanned. The images are then converted to signal intensities and these data are processed using software specific to the application of the array (Mantione *et al*., 2014). Nowadays, the matured technique of high-throughput sequencing provides a more advanced method to capture all RNA transcripts. RNA-Seq has become the favoured technique as it has better quantitative accuracy of measurement and the ability to obtain absolute transcript abundance. The technique requires RNA fragmenting prior to reverse transcription and labelling with adapter sequences. The sequenced transcript fragments are typically 50–500 bp. The read sequences are then counted and assembled into full-length transcripts (Marguerat and Bahler, 2010).

One apparent difference between the capabilities of microarrays and RNA-Seq is whether target sequences go beyond known genomic sequences. Hybridisation-based techniques like microarray rely on and are limited to the transcripts bound to the array slides. Microarrays are only as good as the bioinformatic data available for the model organism's genome and transcriptome. RNA-Seq also detects annotated transcripts but is also able to detect novel sequences (Howard *et al*., 2013). Both RNA-Seq and microarrays can help characterise exon junctions, detect single nucleotide polymorphisms, and detect fusion genes. However, microarrays can only perform that with arrays designed for those

purposes. Finally, unlike RNA-Seq, microarray chips need to be updated to contain the most up to date sequence information.

The applications of RNA-Seq for other bioinformatic studies besides gene expression are far wider than that of a microarray. RNA-Seq is useful to distinguish host from parasite transcripts, study symbioses, and examine transcripts from non-model organisms (Howard *et al*., 2013; Croucher *et al*., 2010; Perkins *et al*., 2009). For example, RNA-Seq was employed to monitor temporal changes in transcript abundance of planktonic bacteria (Ottesen *et al*., 2013), which is impossible via a microarray-based approach.

RNA-Seq can achieve higher resolution of differentially expressed genes and has a much lower limit of detection than a standard whole genome microarray (Zhao *et al*. 2014). For detecting low abundance transcripts, microarrays must be customised to have denser probes, but there is an unlimited dynamic range of detection for RNA- Seq due to its digital nature (Mantione *et al*., 2014). However, the RNA-Seq method to determine differentially expressed genes does have an inherent bias towards longer transcripts (Oshlack and Wakefeld, 2009). The longer the transcript the more fragments available for sequencing, as samples need to be fragmented during processing. Microarrays do not have this length bias and expression levels are proportional to the degree of hybridisation to probes. The only bias that exists in microarray hybridisation would be due to the differences in the GC content of the probes used. Typically, validation of differentially expressed genes can be achieved by quantitative PCR or proteomic methods (Fu *et al*., 2009).

Statistical tests for RNA-Seq require evaluating the null hypothesis that a gene is not differentially expressed between two treatment groups after calculating *P* values (Marioni *et al*., 2008) using a Fisher Exact Test with a great resolution, which can accurately measure a 1.05 fold change. For RNA-Seq, there are many data analysis methods available, but not one standard protocol (Trapnell *et al*., 2012). Analysis of RNA-Seq data also requires extensive experience and the bioinformatics skills necessary to process the data files (Drewe *et al*., 2013).

A variety of transcriptional data sets from staphylococci are established so far. RNA-seq was used to determine the differentially-expressed (DE) genes between wild type and gene mutant cells (Truong-Bolduc *et al*.,2011), between treated and untreated cells (Campbell *et al*., 2012; Price-Whelan *et al*., 2013; Cuaron *et al*., 2013, Muthaiyan *et al*., 2012; Pietiainen *et al*., 2009) and between sensitive and resistant isolates (Song *et al*., 2013). Across all the transcriptome studies of staphylococci, investigation of DE genes between the control and cells treated with a given stimulant is the most common application. In this chapter, the DE genes were determined between control and squalene-treated cells of *S. aureus* and *S. epidermidis* using an RNA-Seq approach.

4.2 Aims

Squalene is an underestimated component of skin surface lipids with respect to staphylococci. In the previous chapter, it was determined that squalene plays a potentially important role in skin colonisation of staphylococci by reducing pigmentation of staphyloxanthin-expressing staphylococci, including *S. aureus, S. hominis* and *S. capitis*. In addition, squalene also modulated the action of several skin-relevant antimicrobials. Specifically, the decreased level of pigments when treated with squalene enhanced susceptibility of *S. aureus* to H_2O_2 and nisin. Decreased resistance to LL-37 of squalene-treated *S. epidermidis,* but not *S. aureus* was without explanation. Therefore, in this chapter the underlying genetic basis for these results will be investigated by determining the transcriptional response of *S. aureus* and *S. epidermidis* to a challenge with 1 % (v/v) of squalene. Further, the prolonged effects of squalene to *S. aureus* will be assessed by proteomic approach 2 hours after squalene treatment, at the end of exponential phase.

The main aim of this chapter is to identify DE genes in response to squalene and compare the transcriptional profiles between *S. aureus* and *S. epidermidis*. It is expected that this approach will find differences in responses and possible resistance determinants by bacteria, and explain potential antimicrobial effects of squalene that has the potential to influence the colonisation and persistence of staphylococci on human skin.

4.3 Results

To determine the transcriptional response of *S. aureus* and *S. epidermidis* to squalene, RNA-Seq was performed on squalene challenged and control cells of *S. aureus* Newman and *S. epidermidis* Tü3298. Cultures were challenged with 1% (v/v) squalene during the mid-logarithmic phase of growth (OD_{600}=0.5), as this squalene concentration caused distinct change in pigmentation level (Fig 3.4). After 20 min challenge, RNA was stabilised using RNAlater (Qiagen) and incubated overnight at 4 °C. Total RNA was then purified from cells the next day using the method described in chapter 2 (section 2.7).

4.3.1 RNA quality control

RNA samples for RNA-Seq have strict quality criteria and these were met for submission to the Centre for Genome Research (CGR), University of Liverpool. The purified RNA preparations must have low protein, salt and solvent contaminations, which was assessed by NanoDrop absorbance measurements to ensure 260/280 and 260/230 ratios over 1.8. In addition to quality, the required quantity of RNA samples must be above the minimum threshold concentration of 30 ng μl^{-1} and a yield of at least 3 µg is required. These parameters were determined by Qubit fluorometric quantitation reads (Table 4.1). Finally, and most importantly, because of the nature of easy degradation of RNA, it is critical that sufficient intact RNA is obtained. This was examined using an Agilent bioanalyser by verifying RNA integrity (RIN) scores >7.0 and low evidence of degradation on the output traces (Fig 4.1).

Table 4.1 RNA quality control assessment.

Purity of purified RNA samples was measured by NanoDrop and the concentration was assessed by Qubit. RNA integrity was tested using a bioanalyser. RIN=RNA integrity number, C=control condition, S=squalene challenge condition.

Species	Sample	Nanodrop 260/280	Nanodrop 260/230	Concentration ng µl-1	Sample volume (µl)	RIN
S. aureus	C1	2.2	2.2	794	5	7.4
	C2	2.1	2	421	10	7.8
	C3	2.2	1.8	810	5	7.8
	S1	2.2	2.2	376	10	7.1
	S2	2.1	2.2	399	10	9
	S3	2.2	2.3	547	6	9
S. epidermidis	C1	2.2	2.4	900	5	8.7
	C2	2.2	2.4	1200	5	9.3
	C3	2.2	2.4	1200	5	9.2
	S1	2.2	2	565	6	8.8
	S2	2.2	1.8	610	6	8.7
	S3	2.2	2.1	754	6	8.6

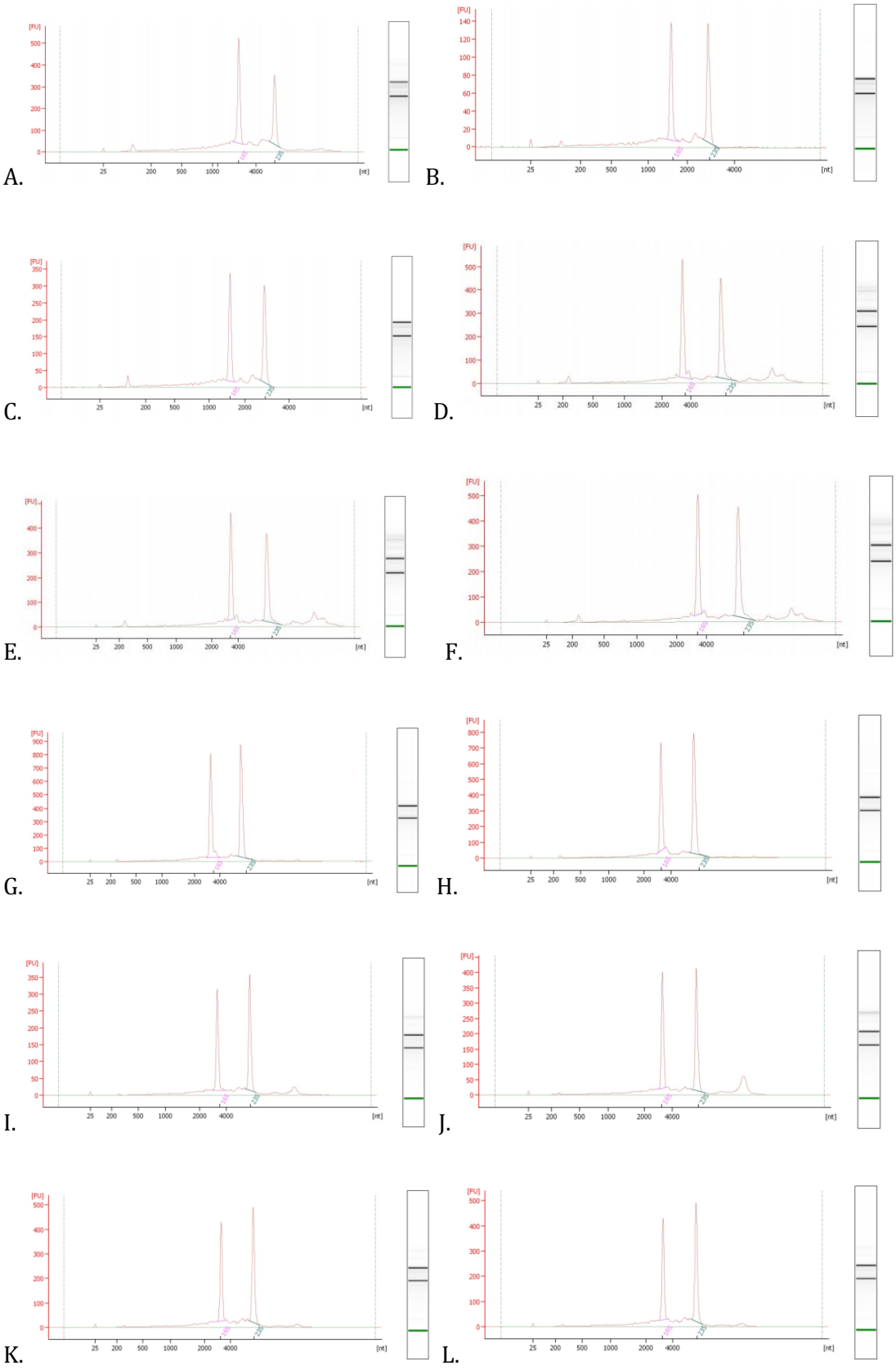

Figure 4.1 Bioanalyser traces of RNA samples submitted for sequencing. The visual output for the determined RNA integrity using the Agilent bioanalyser showed the characteristic profiles for purified, intact RNA with expected levels of particular sizes of RNA. The pronounced

two large peaks indicates the presence of 23S and 16S RNA and other small peaks suggest their degradation. The three bands in gel image on the right shown the presence of 23S RNA, 16S RNA and the assay marker. *S. aureus* control condition: A, B and C; *S. aureus* squalene challenge condition: D,E and F; *S. epidermidis* control condition: G, H and I and *S. epidermidis* squalene challenge condition: J, K and L.

4.3.2 Overall comparison of *S. aureus* Newman and *S. epidermidis* Tü3298 transcriptional response to squalene challenge

After sequencing, sequence reads were analysed and processed first by the CGR resulting in two output tables of statistically significantly DE genes of *S. aureus* Newman and *S. epidermidis* Tü3298 between the control and squalene-treated samples. The method was outlined in the Chapter 2 Methods section. The DE genes for each species were then compared with each other to distinguish homologous genes that are DE in both species, which contributes to determining the similarities as well as differences between *S. aureus* and *S. epidermidis* in response to squalene.

In response to squalene challenge, 414 genes of *S. aureus* Newman, which is 15.8 % of total protein coding genes across the genome, were significantly DE, compared with 1,415 DE genes of *S. epidermidis* Tü3298 which accounts for 60.7 % of total protein coding genes across its genome. While it would be tempting to suggest that *S. epidermidis* had a more pronounced response to squalene than *S. aureus*, the majority (1,127) of the *S. epidermidis* DE genes were altered by less than 1 $\log_2$ (2-fold), indicating that there was a greater breadth of response in the *S. epidermidis* data set. The degree of response to squalene between the species should therefore be considered as similar.

Of the 1,415 DE *S. epidermidis* genes, 1271 had a homolog in *S. aureus*, but only 181 genes were DE in both species, 83 were DE in *S. aureus* but not in *S. epidermidis*, and 1007 were DE in *S. epidermidis* but not in *S. aureus* (Fig 4.2a). Of the 181 genes that were DE in both species, 69 were similarly regulated in both species, of which 33 were up-regulated and 36 were down-regulated. This

means approximately 60% of the homologous genes were regulated in the opposite direction to their counterpart in the alternate species (Fig 4.2b).

(a)

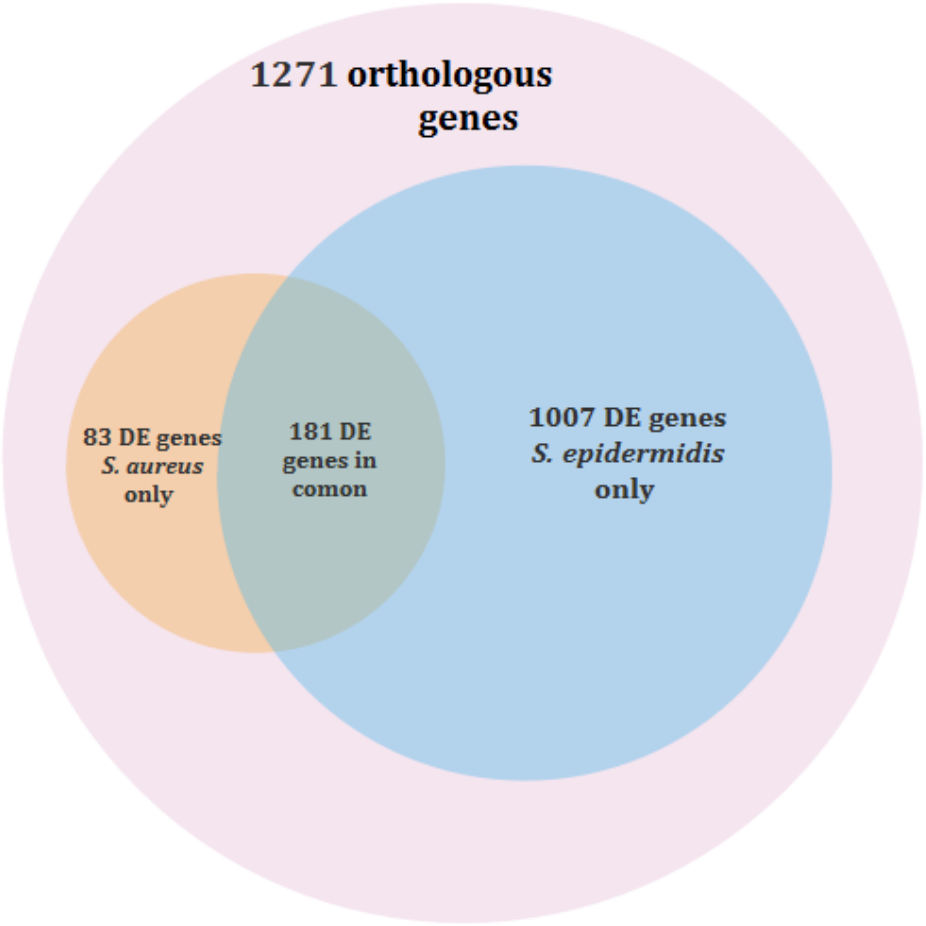

(b)

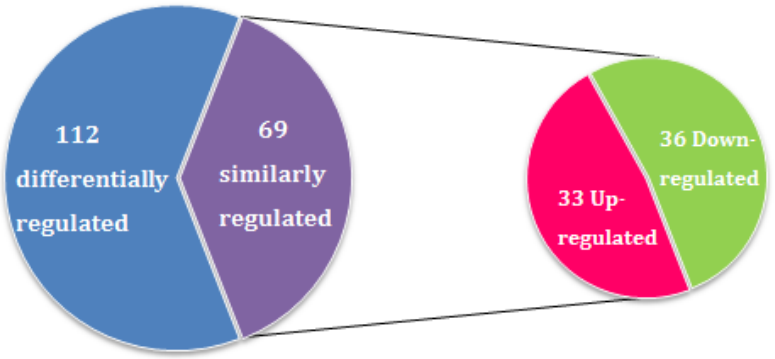

Figure 4.2 Comparison of differentially expression between *S. aureus* Newman and *S. epidermidis* Tü3298 homologous genes after challenge with squalene. (a). There are 1271 DE genes with a homolog in the alternate species, 181 genes were DE in both species, 83 were DE in *S. aureus* but not in *S. epidermidis*, 1007 were DE in S. *epidermidis* but not in *S. aureus*. (b). Among the 181 DE genes in both species, 112 were differently regulated and 69 were similarly regulated, of which the expression was increased for 33 genes and decreased for 36 genes.

Tabulated details of the DE genes from both data sets are provided in Appendix Table 1 & 2.

4.3.3 Comparison of DE COGs

Clusters of orthologous group (COG) enrichment analysis is frequently used to assess the cellular pathways that are most affected. This approach was used to further analyse the response to squalene challenge for *S. aureus* and *S. epidermidis*. The most frequent COG classes that DE genes were assigned to can be determined by using the WebMGA and bespoke perl scripts. The detailed method is described in chapter 2 (section 2.7.9). Furthermore, if it is assumed that DE genes are evenly distributed across the genome, the theoretical number of DE genes in each COG class could be calculated as they should be proportional to the number of genes encoded by the genome in that class. Thus COGs analysis will reveal whether the actual numbers of DE genes in these orthologous classes are higher or lower than the calculated number.

(a)

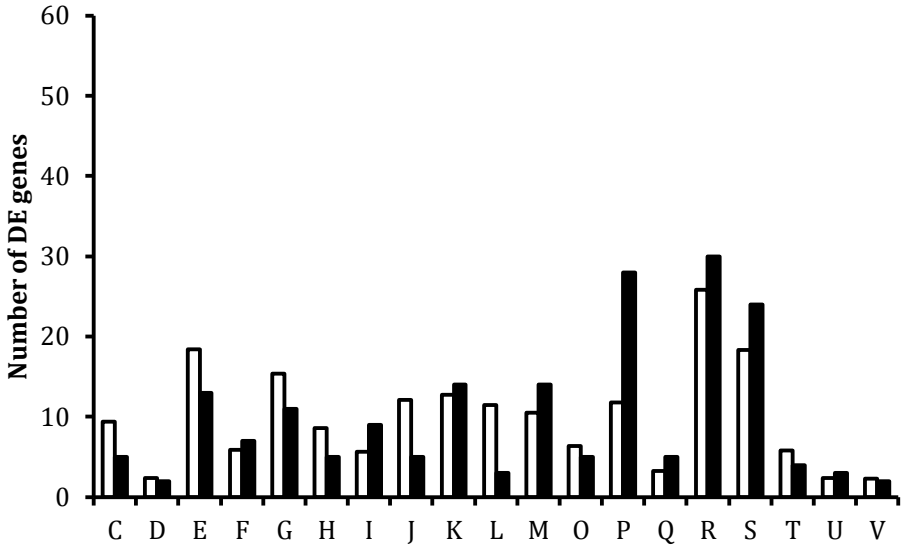

(b)

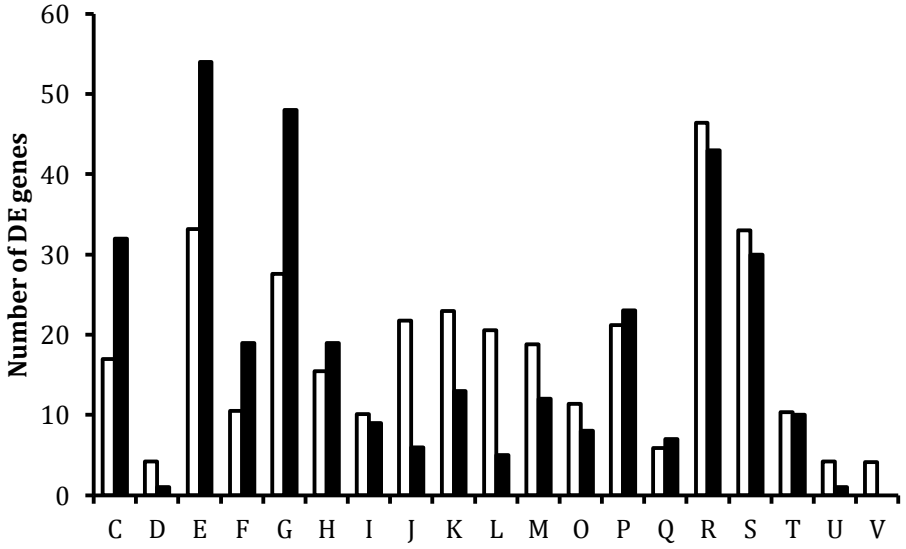

Figure 4.3 Numbers of *S. aureus* Newman DE genes per COG class in response to squalene challenge.

Comparison of numbers of DE genes between the theoretical (white bars) and the observed (black bars) per COG class for up-regulated DE genes (a) and down-regulated DE genes (b). The number of theoretical DE genes per class was calculated under the assumption that expression was uniform across the genome. Genes were assigned to a COG class using WebMGA, the number of DE genes in each class were then calculated using a bespoke Perl script. C: Energy

production and conversion; D: Cell cycle control, cell division, chromosome partitioning; E: Amino acid transport and metabolism; F: Nucleotide transport and metabolism; G: Carbohydrate transport and metabolism; H: Coenzyme transport and metabolism; I: Lipid transport and metabolism; J: Translation, ribosomal structure and biogenesis; K: Transcription; L: Replication, recombination and repair; M: Cell wall/membrane/envelope biogenesis; O: Posttranslational modification, protein turnover, chaperones; P: Inorganic ion transport and metabolism; Q: Secondary metabolites biosynthesis, transport and catabolism; R: General function prediction only; S: Function unknown; T: Signal transduction mechanisms; U: Intracellular trafficking, secretion, and vesicular transport; V: Defence mechanisms.

COG analysis revealed that challenge with squalene of *S. aureus* resulted in COG classes F (nucleotide transport and metabolism), I (lipid transport and metabolism), M (cell wall/membrane/envelope biogenesis), P (inorganic ion transport and metabolism), R (general function prediction only), and S (function unknown) having more up-regulated genes than the theoretical number (Fig 4.3). While COG classes C (energy production and conversion), E (amino acid transport and metabolism), G (carbohydrate transport and metabolism), H (coenzyme transport and metabolism), J (translation, ribosomal structure and biogenesis), and L (replication, recombination and repair) were found to have fewer up-regulated genes than the theoretical number. On the other hand, and as predicted for down-regulated genes, the ratio of the theoretical and observed DE genes for most of COG classes was opposite compared with that for up-regulated genes. In most cases, COG classes with more up-regulated genes than the theoretical number showed fewer down-regulated genes than the theoretical number (COG classes F, I, M, P, R, S, C, E, G, and H). However, two classes of COG, J (translation, ribosomal structure and biogenesis) and L (replication, recombination and repair), were found to have less DE genes than the theoretical number for both up and down regulated genes. This discrepancy suggests that treatment with squalene has limited influence upon the expression of genes involved in these two classes.

(a)

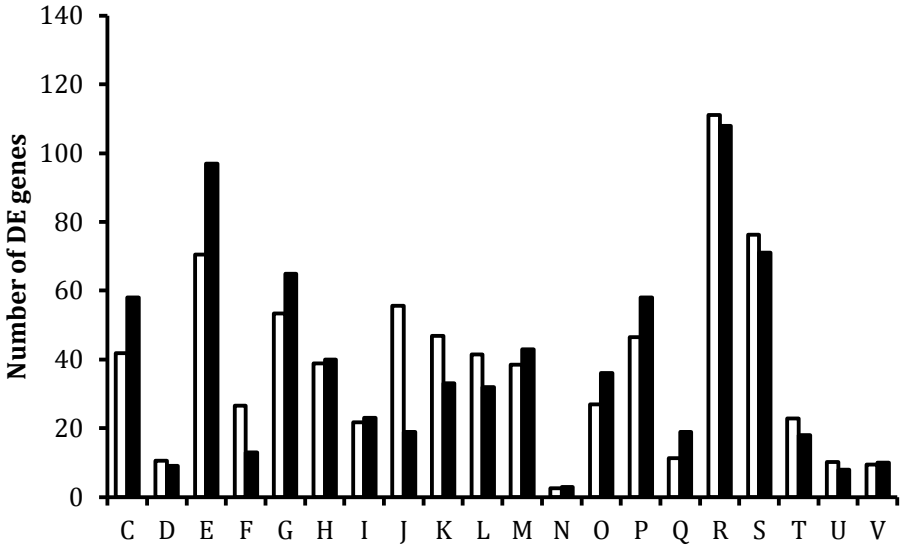

(b)

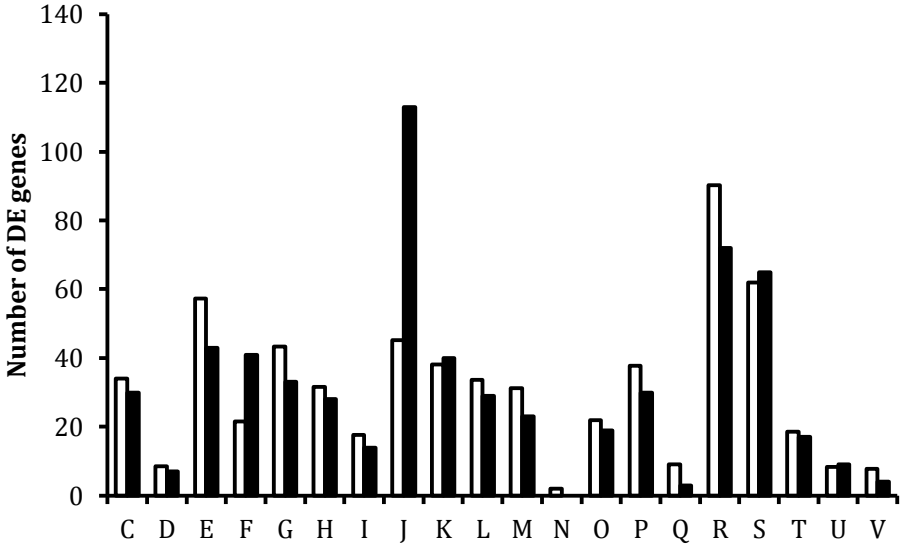

Figure 4.4 Numbers of *S. epidermidis* Tü3298 DE genes per COG class in response to squalene challenge.

The comparison of number of DE genes between the theoretical (white bars) and the observed (black bars) per COG class for up-regulated DE genes (a) and down-regulated DE genes (b). The number of theoretical DE genes per class was calculated under the assumption that expression was uniform across the genome. Genes were assigned to a COG class using WebMGA, the number of DE genes in each class were then calculated using a bespoke Perl script. C: Energy

production and conversion; D: Cell cycle control, cell division, chromosome partitioning; E: Amino acid transport and metabolism; F: Nucleotide transport and metabolism; G: Carbohydrate transport and metabolism; H: Coenzyme transport and metabolism; I: Lipid transport and metabolism; J: Translation, ribosomal structure and biogenesis; K: Transcription; L: Replication, recombination and repair; M: Cell wall/membrane/envelope biogenesis; O: Posttranslational modification, protein turnover, chaperones; P: Inorganic ion transport and metabolism; Q: Secondary metabolites biosynthesis, transport and catabolism; R: General function prediction only; S: Function unknown; T: Signal transduction mechanisms; U: Intracellular trafficking, secretion, and vesicular transport; V: Defence mechanisms.

COG analysis of squalene treated *S. epidermidis* DE genes showed that there were more up-regulated genes than the theoretical number in COG classes C (energy production and conversion), E (amino acid transport and metabolism), G (carbohydrate transport and metabolism), M (cell wall/membrane/envelope biogenesis), P (inorganic ion transport and metabolism) and Q (secondary metabolites biosynthesis, transport and catabolism)(Fig. 4.4). There were less up-regulated genes than the theoretical number in COG classes F (nucleotide transport and metabolism), J (translation, ribosomal structure and biogenesis), K (transcription), and L (replication, recombination and repair). For down-regulated DE genes, it showed a similar pattern as that of *S. aureus*, such that COG classes with greater (or fewer) up-regulated genes than the theoretical number were found to have fewer (or greater) numbers of down-regulated genes than the theoretical number (COG classes C, E, F, G, J, K, M, and Q) with the exception of COG class L (replication, recombination and repair) that had less DE genes than the theoretical number for both up and down regulations.

S. aureus and *S. epidermidis* both up-regulate a greater number of genes than the theoretical number in cell wall/membrane/envelope biogenesis (M) and inorganic ion transport and metabolism (P). This may suggest global effects of treatment of squalene on staphylococcal membrane homeostasis and function that are not reflected in a change of growth rate. Meanwhile the ion transportation and metabolism-associated discrepancy might reflect loss of or difficulty of obtaining inorganic ions following challenge. Moreover, in both

species squalene challenge has a smaller effect than expected on transcription of genes associated with replication recombination and repair (L).

There were differences between the numbers of *S. aureus* and *S. epidermidis* enriched COGs. After squalene challenge, *S. epidermidis* differentially expressed over 50 % more genes than *S. aureus* in energy production and conversion (C), amino acid transport and metabolism (E), and carbohydrate transport and metabolism (G). This may suggest that *S. epidermidis* has a greater need than *S. aureus* for energy after squalene treatment, or that *S. epidermidis* has a more rapid or effective adaptive response to squalene. Squalene could also act as a stimulus to which *S. epidermidis* has evolved to respond to as a competitive or adaptive strategy related to its niche. *S. epidermidis* showed overall down-regulation of translation, ribosomal structure and biogenesis genes, which would indicate a decrease in protein biosynthesis. This down-regulation would seem to be at odds with such large-scale changes in the transcriptional profile of the cell in these conditions.

4.3.4 Comparison of DE metabolic pathways

KEGG mapper (version 2.1) search & colour is an online program that highlights the proteins within KEGG pathways based upon the users gene list (Kanehisa *et, al*., 2012). This program was executed using the lists of DE genes produced by the CGR. The *S. epidermidis* Tü3298 genome is not available for the KEGG database, so *S. epidermidis* gene names were converted to homologous gene names from strain Rp62a prior to use in KEGG mapper. During the analysis, 305 DE genes (58.6 %) of *S. aureus* Newman and 313 DE genes (55.9 %) of *S. epidermidis* Tü3298 were not assigned into any pathways. This is due to incomplete pathway annotation for staphylococci to date together with unknown functions of genes. Analysis of these pathways contributes to detection of metabolic processes with DE genes and would help provide insight into the effect of squalene on metabolism.

Table 4.2 Squalene-regulated DE genes involved in energy production pathways in *S. aureus* Newman and *S. epidermidis* Tü3298.

DE genes highlighted by KEGG mapper analysis and the level of log_2 fold change in *S. aureus* Newman and *S. epidermidis* Tü3298 are listed. Genes that were not DE in one species are indicated by a dash in the relevant fold change column. Genes absent from one species are indicated with an "X" in both the relevant fold change column and gene name column. KEGG mapper output pathways relevant to this table were glycolysis/gluconeogenesis, pentose phosphate pathway, fructose and mannose metabolism, galactose metabolism, amino sugar and nucleotide sugar metabolism, pyruvate metabolism, propanoate metabolism, butanoate metabolism, and glutathione metabolism.

***S. aureus* Newman**		***S. epidermidis* Tü3298**
Gene name	**Fold change (log_2)**	**Gene name**
glcA	-1.35	-	*SETU_01969*
ptsG	-1.37	X	X
pgi	-	0.81	*pgi*
fbp	-	0.83	*SETU_01934*
fbaA	-	-1.13	*fbaA*
tpi	-1.07	-	*tpi*
gpmA	-1.83	0.52	*gpmA*
porA	0.91	-	*SETU_00859*
X	X	0.64	*SETU_02150*
X	X	0.59	*SETU_02151*
ldh	-2.2	1.13	*SETU_02009*
ald1	-1.09	1.23	*SETU_01943*
gntK	-1.53	-	*SETU_01917*
zwf	-	0.83	*SETU_01078*
NWMN_0534	-	0.51	*SETU_00194*

NWMN_0533	-	0.5	*SETU_00193*
NWMN_1672	-	0.76	*SETU_01333*
rbsK	-	0.63	*SETU_01955*
NWMN_0083	-1	0.57	*SETU_01614*
mtlA	-1.56	X	X
mtlD	-1.43	X	X
mtlF	-1.58	X	X
fruB	-2.2	0.82	*SETU_00319*
NWMN_0667	-1.7	1.05	*SETU_00320*
lacD	-2.02	0.67	*SETU_01668*
gltA	-	0.85	*SETU_01259*
mqo	-	0.68	*SETU_02229*
sdhA	-1.56	-0.66	*sdhA*
sdhB	-2.04	-0.72	*sdhB*
sucA	-1.57	1.00	*sucA*
sucB	-1.24	1.10	*SETU_00989*
sucC	-	1.12	*sucC*
malA	-1.33	1.43	*SETU_01080*
lacF	-	0.6	*SETU_01667*
lacE	-	0.52	*lacE*
lacG	-	0.74	*lacG*
lacC	-	0.55	*SETU_01669*
pckA	-1.41	-	*SETU_01340*

NWMN_2459	-	0.6	*SETU_01988*
pdhC	-	0.64	*SETU_02150*
NWMN_1315	-	1	*SETU_00980*
leuA	-	0.81	*SETU_01540*
X	X	1.19	*gldA*
alsD	-2.13	0.74	*SETU_02007*
alsS	-	1.03	*SETU_02008*
mvaS	-	0.75	*SETU_01977*
X	X	2.72	*SETU_02044*

DE genes associated with general energy production were mainly up-regulated in *S. epidermidis*, but were relatively down-regulated in *S. aureus* (Table 4.3). There appears to be a trend in regulation to increase energy production in *S. epidermidis*. Specifically, genes associated with glycolysis and sugar uptake (*pgi*, SETU_01934, *gpmA*, SETU_02150, SETU_02151, SETU_00319, and SETU_00320) were up-regulated in *S. epidermidis*. Up-regulation of these genes will reduce biosynthesis of glycerolipid and lipoteichoic acid in favour of glycolysis. Furthermore, genes that allow NADPH/NADP+ recycling (SETU_02009, SETU_02044, and SETU_01078) and those involved in pyruvate metabolism (SETU_02009, SETU_00980, SETU_01943, SETU_02150, SETU_02008 and SETU_02007) were all up-regulated in *S. epidermidis*. However, an exception was found that two genes associated with succinate metabolism, *sdhA* and *sdhB*, were down-regulated in both *S. aureus* and *S. epidermidis*. Since these two genes are critical in TCA cycle function, and other genes involved in this cycle are mainly up-regulated in *S. epidermidis* (therefore not a global down-regulation in TCA cycle), the reason for their reduced expression needs to be further studied.

Table 4.3 Squalene-regulated DE genes involved in ammonia production pathways in *S. aureus* Newman and *S. epidermidis* Tü3298.

DE genes highlighted by KEGG mapper analysis and the level of log_2 fold change in *S. aureus* Newman and *S. epidermidis* Tü3298 are listed. Genes that were not DE in one species are indicated by a dash in the relevant fold change column. Genes absent from one species are indicated with an "X" in both the relevant fold change column and gene name column. KEGG mapper output pathways relevant to this table were purine metabolism, arginine and proline metabolism, and nitrogen metabolism.

***S. aureus* Newman**		***S. epidermidis* Tü3298**
Gene name	**Fold change (log_2)**	**Gene name**
NWMN_0083	-1	0.57	*SETU_01614*
purF	-0.92	-0.79	*purF*
purD	-	-0.94	*purD*
purN	-0.55	-0.68	*SETU_00667*
purL	-0.94	-0.56	*SETU_00664*
purM	-	-0.94	*SETU_00666*
purB	-	-0.95	*SETU_01466*
purH	-0.4	-0.9	*purH*
guaC	-	-0.63	*SETU_00914*
pnp	-1.71	X	X
pnpA	-	-0.63	*SETU_00843*
guaB	0.83	-0.68	*guaB*
gmk	-	-0.58	*gmk*
guaA	-	-0.83	*guaA*
adk	-	-1.31	*adk*
NWMN_0378	1.13	-0.52	*SETU_00042*

NWMN_0519	-	-0.85	*SETU_00180*
NWMN_0518	-	-0.76	*SETU_00179*
glnA	-	-1.35	*glnA*
X	X	0.8	*gltD*
argH	-2.34	-0.32	*SETU_00508*
argG	-2.52	-0.51	*argG*

The expression of genes involved in ammonia production was down-regulated in both *S. aureus* and *S. epidermidis*, and this trend was more pronounced in *S. epidermidis*. In *S. epidermidis,* the entire *pur* operon, *guaA*, *guaB*, and SETU_00914 were down-regulated with each involved in purine biosynthesis. Down-regulation of these genes will result in decreased production of purine. In addition, genes associated with consumption of the ammonia pool were also generally down-regulated (SETU_00843, *gmk*, *adk*, SETU_00042, SETU_00180, SETU_00179, *glnA*, SETU_00508, and *argG*) which would indicate less consumption of the ammonia pool in the cell. The latter regulation may suggest a coordinated response due to reduced ammonia production.

Table 4.4 Squalene-regulated DE genes involved in amino acids production pathways in *S. aureus* Newman and *S. epidermidis* Tü3298.

DE genes highlighted by KEGG mapper analysis and the level of $\log_2$ fold change in *S. aureus* Newman and *S. epidermidis* Tü3298 are listed. Genes that were not DE in one species are indicated by a dash in the relevant fold change column. Genes absent from one species are indicated with an "X" in both the relevant fold change column and gene name column. KEGG mapper output pathways relevant to this table were histidine metabolism, glycine, serine and threonine metabolism, cysteine and methionine metabolism, lysine biosynthesis, valine, leucine and isoleucine biosynthesis and alanine, aspartate and glutamate metabolism.

***S. aureus* Newman**		***S. epidermidis* Tü3298**
Gene name	**Fold change ($\log_2$)**	**Gene name**
hisA	-	0.41	*SETU_02132*
hisB	-	1.04	*hisB*
hisC	1.4	0.59	*SETU_00345*
hisD	-	0.66	*SETU_02135*
hisF	-	0.38	*SETU_02131*
hisG	-	0.87	*hisG*
hisH	-	0.68	*hisH*
sdhA	-1.56	-0.66	*sdhA*
sdhB	-2.04	-0.72	*sdhB*
thrC	-0.88	1.66	*SETU_00906*
NWMN_1228	-	1.35	*SETU_00894*
thrB	-	0.98	*SETU_00907*
pyrB		-0.62	*pyrB*
pyrC	-2.49	-	*pyrC*
pyrR	-	-1.3	*SETU_00769*
pyrG	-	-1.34	*pyrG*

pyrAB	-1.86	-	*carA*
leuB	-	0.6	*SETU_01541*
leuD	-	0.92	*leuD*
ilvB	-0.99	0.61	*SETU_01537*
ilvC	-	1.01	*SETU_01539*
ilvE	-	0.91	*SETU_00172*
serA	-	0.6	*SETU_01286*
dapA	-0.85	1.27	*dapA*
dapB	-0.79	1.25	*SETU_00970*
dapD	-0.68	1.13	*SETU_00971*
metL	-	1.54	*SETU_00905*
metB	0.9	-	*SETU_00066*
cysM	1.64	-	*cysM*
cysK	-	1.28	*cysK*
asd	-1.01	0.94	*SETU_00968*
gltD	-	0.8	*gltD*

There was no consistent trend between two species with respect to DE genes involved in amino acids biosynthesis after squalene challenge. In *S. epidermidis*, genes for the production of histidine (SETU_02132, *hisB*, SETU_00345, SETU_02135, SETU_02131, *hisG*, and *hisH*), threonine (SETU_00906, SETU_00894, and SETU_00907), leucine (SETU_01541 and *leuD*), isoleucine & valine (SETU_01537, SETU_01539, and SETU_00172), lysine (*dapA*, SETU_00970, and SETU_00971), cysteine (*cysK*), and glutamate (*gltD*) were up-regulated. While genes responsible for catabolism of amino acids into energy (*sdhA*, *sdhB*, *pyrB*, SETU_00769, and *pyrG*) were all down-regulated. This might indicate accumulation of amino acids in the *S. epidermidis* cell or homeostasis to a new threshold, consistent with protein synthesis or proteome restructuring. In *S. aureus*, production of histidine and cysteine was increased as well, but biosynthesis of threonine, isoleucine and lysine was down-regulated. This suggests a different protein synthesis or restructuring mechanism or strategy towards homeostasis, which requires different amounts and types of amino acids.

Table 4.5 Squalene-regulated DE virulence factor genes in *S. aureus* Newman and *S. epidermidis* Tü3298.

DE genes highlighted by KEGG mapper analysis and the level of log_2 fold change in *S. aureus* Newman and *S. epidermidis* Tü3298 are listed. Genes that were not DE in one species are indicated by a dash in the relevant fold change column. Genes absent from one species are indicated with an "X" in both the relevant fold change column and gene name column. KEGG mapper output pathways relevant to this table was *S. aureus* infection.

***S. aureus* Newman**		***S. epidermidis* Tü3298**
Gene name	**Fold change (log_2)**	**Gene name**
aur	-	-1.08	*SETU_02085*
clfA	-1.17	X	X
sbi	1	X	X
sdrC	0.9	X	X
sdrD	1.51	X	X
lukS	1.82	X	X
lukF	1.54	X	X
hlgB	1.81	X	X
hlgC	1.74	X	X
NWMN_1503	1.44	X	X
vraF	-	-0.82	*SETU_00278*
vraG	-	-0.82	*SETU_00279*
fmtC	-	-1.14	*SETU_00936*
saeS	-	-2.09	*SETU_00325*
saeR	-	-2.1	*SETU_00326*
dltA	-	-2.75	*SETU_00479*
dltB	-	-2.44	*SETU_00480*
dltC	-	-2.72	*dltC*
dltD	-	-2.4	*SETU_00482*

dltX	-	-2.8	*dltX*
X	X	-2.6	*SETU_02365*
ssl2nm	1.52	X	X
ssl3nm	1.35	X	X
ssl4nm	1.35	X	X
ssl5nm	1.27	X	X
ssl9nm	1.25	X	X
ssl6	1.09	X	X
isdA	1.61	X	X
fnbB	1.91	X	X

The regulation of expression of a subset of virulence genes showed opposite patterns between *S. aureus* and *S. epidermidis*. In *S. aureus*, the majority of these virulence factors were up-regulated after challenge. This includes IsdA that has been described to increase cell hydrophobicity independent of its role in haem iron acquisition (Clarke *et al*., 2007). In addition, these up-regulated genes encode toxins that target leukocytes such as *lukS*, *lukF*, *hlgB*, and *hlgC*, genes predicted to play a role in tissue adhesion specificity including *sdrC* and *sdrD* and a series of genes encoding or predicted to encode immune evasion determinants including *NWMN_1503*, *ssl2nm, ssl3nm, ssl4nm, ssl5nm, ssl9nm, ssl6* (Omoe *et al*., 2004; Orwin *et al*., 2001; Niedergang *et al*., 1995).

Contrastingly, squalene repressed most of the DE virulence genes in *S. epidermidis*. This response includes down-regulation of SETU_02085 (*aur*) which encodes the aureolysin, the entire *dlt* operon whose products mediate cell surface charge, *fmtC* which catalyses lysinylation of phospholipid and *vraF* that co-regulates *dlt*. Collectively, the encoded proteins possess the ability to

alter cell surface hydrophobicity/charge. Moreover , the central virulence associated two-component regulator (TCR) in staphylococci, *saeRS*, was also repressed after squalene challenge. This TCR is proposed to have an overarching role in expression of virulence factors independent of the quorum-sensing *agr* system. Down-regulation of SaeRS TCR may explain the reduced expression of other virulence genes in *S. epidermidis*. Due to broadly enhanced expression of the observed suite of virulence genes in *S. aureus*, it is predicted the *saeRS*-encoded TCR is activated during squalene treatment. However, no significant changes in expression were observed in *S. aureus* data, which could merely reflect the known genetic signature of the *saeRS* locus *S. aureus* Newman. Alternatively, other mechanisms affected by squalene that regulate the virulence factors.

From the above analysis, it was revealed that *S. aureus* and *S. epidermidis* exhibit many discrete responses to squalene, despite sharing a high number of homologous genes. The overall trend of regulation was similar in some pathways, but not others. These variations of gene expression could result from the different lifecycles and frequency in host niches. *S. aureus* is a more virulent pathogen with a limited niche, while *S. epidermidis* is a ubiquitous skin coloniser.

4.3.5 Squalene transcriptome and *S. aureus* pigmentation

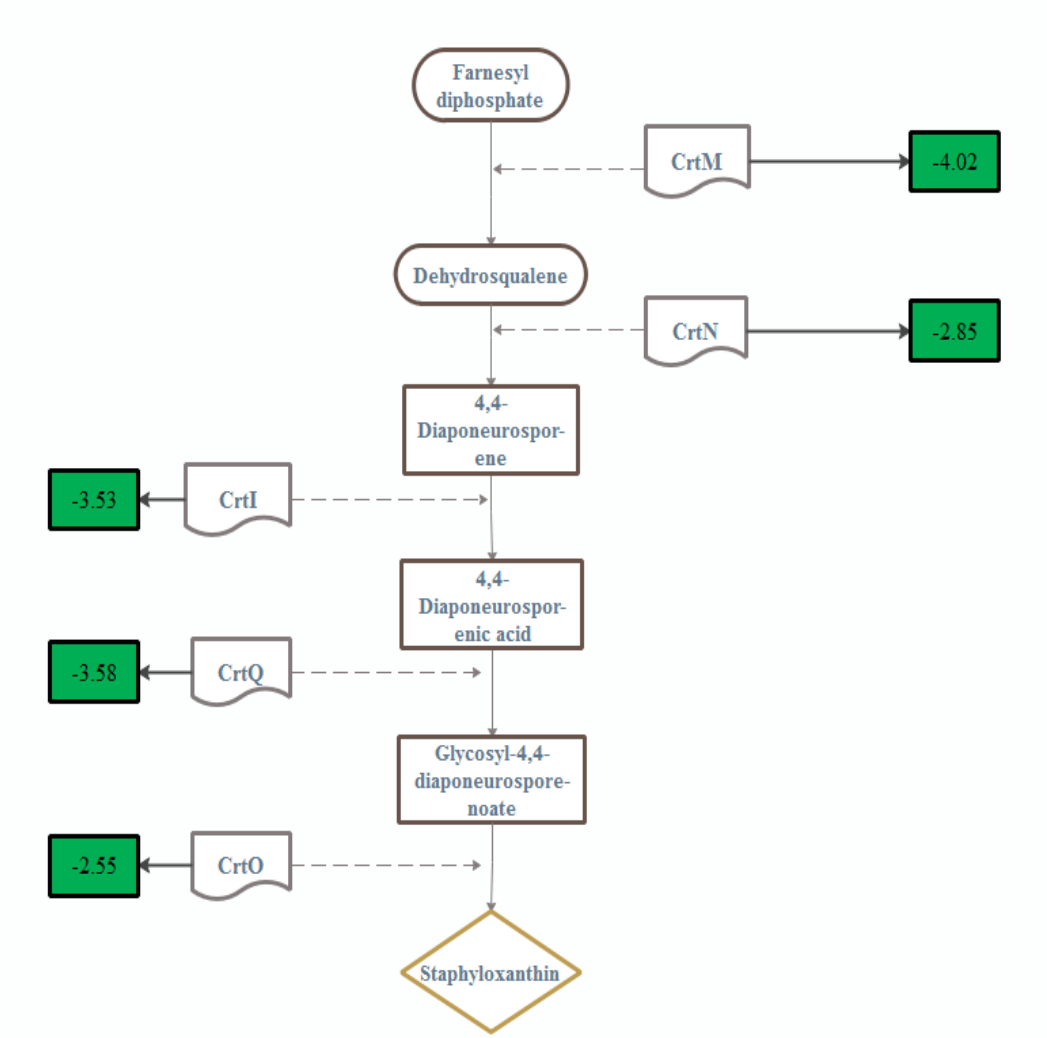

Figure 4.5 DE genes in response to squalene challenge in *S. aureus* Newman of the staphyloxanthin biosynthetic pathway .

In each box linked to the respective enzymes, the expression changes relative to the control are shown as fold number. Green colour indicates the respective transcript was significantly down-regulated. CrtO, NWMN_2465; CrtI, NWMN_2464; CrtQ, NWMN_2463; CrtM, NWMN_2462; CrtN, NWMN_2461.

The negative effects of squalene on bacterial pigmentation were reported in Chapter 3, where experiments with three pigmented staphylococcal species consistently demonstrated that their pigmentation was reduced with increasing

concentration of added squalene. As stated in Chapter 3, staphyloxanthin (STX) is produced via the *crt* operon in staphylococci. In the first step of STX biosynthesis, two molecules of farnesyl diphosphate are condensed to form dehydrosqualene, catalysed by CrtM. Next the dehydrosqualene is dehydrogenated by CrtN to form the yellow intermediate 4,4-diaponeurosporene. Next, CrtP converts 4,4-diaponeurosporene into 4,4-diaponeurosporenic acid by oxidising the terminal methyl group. In the final steps, 4,4-diaponeurosporenic acid is firstly esterified by CrtQ and then acylated to form STX by CrtO (Fig 3.5). From the experiments in Chapter 3, the decreased expression of *crt* operon was expected to be evident in the transcriptomic data of *S. aureus* cells challenged with squalene. It was considered that this reduction might occur via changes in the expression of SigmaB, which is the sole RNA polymerase accessory factor that regulates the *crt* operon via altered transcript levels (Katzif *et al*., 2005).

As expected, the five *crt* operon genes concerned with staphyloxanthin biosynthesis, *crtM, crtN, crtI, crtQ, and crtO* showed a decreased level of expression ranging from 2.5 to 4 fold (Fig 4.5). This decline of expression explains the reduced cell pigmentation, however *sigB* expression was unchanged. This may reflect changes to the activity of the rsbU, rsbV and rsbW modulators and anti-sigma factors that control SigmaB or it could indicate there is another regulatory pathway modulating *crt* expression.

Absence of pigment in *S. aureus* cells growing in anaerobic conditions is associated with anoxia and the consequent absence of ROS. The cold shock protein CspA of *S. aureus* is required for maximal production of pigment (Katzif *et al*., 2005). The expression of representative anaerobic metabolism genes and CspA could therefore participate in the phenotype and be modulated. Expression of the anaerobic respiration genes *srrA* (-2.41-fold), *ldh* (-2.2-fold), *nrdD* (-3.07-fold), and *narI* (-4.6-fold) were all down-regulated. The expression level of expression of *adhE*, *adh*, *budA*, *budB*, and *cspA* remained the same. Overall, these changes in gene expression rule out effects of respiration or CspA in the mechanism controlling squalene reduction of pigmentation.

4.3.6 Squalene effects on the transcriptome and iron uptake

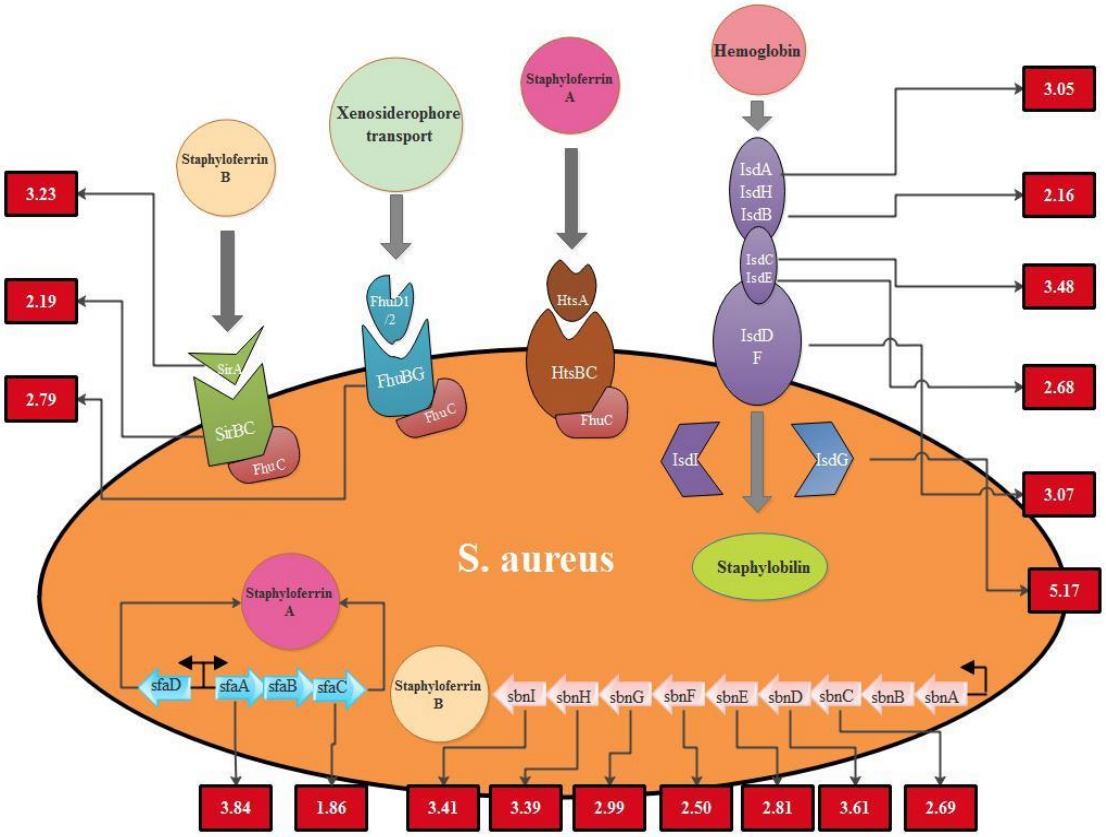

Figure 4.6 Assignment of DE genes of iron-uptake systems in response to squalene challenge in *S. aureus* Newman. For each box linked to a DE gene, the fold changes of squalene-challenged cells compared with untreated control are shown. Red colour indicates the respective transcript was significantly up-regulated. *sfaA*: NWMN_2081; *sfaB*: NWMN_2080; *sfaC*: NWMN_2079; *sfaD*: NWMN_2082.

One major correlation between the responses of both staphylococcal species is that genes encoding iron transport are up-regulated in both species, while the iron storage molecule ferritin gene is down-regulated. This, combined with the up-regulation of the haem-iron surface uptake system genes *isdA*, *isdB, isdC, isdE, isdG and isdF* in *S. aureus*, suggests squalene induces an iron limitation response in both species. There is also down-regulation of some enzymes that utilise iron,

such as *sdhA, sdhB*, SETU_01279 (*nifZ*), and *adhE*. Overall, there were 24 iron-uptake-related genes with increased differential expression in the 100 most up-regulated genes, in terms of fold-change, in the *S. aureus* DE transcriptome. *S. aureus* is remarkable for having the most numerous pathways for iron acquisition across those bacteria characterised to date, including production of siderophores (staphyloferrin A and staphyloferrin B) for extracellular iron and production of heme and haemoglobin receptors for heme uptake (Hammer and Skaar, 2011). With respect to siderophore biosynthesis, the data showed both genes which encode enzymes for staphyloferrin A production (*sfaA* and *sfaC*) and the entire *sbnABCDEFGHI* operon for staphyloferrin B were significantly up-regulated (Fig 4.6). Expression of the *sirABC* operon whose translational products control staphyloferrin B import and *fhuB* that mediates xenosiderophpre transport were also enhanced over 2-fold. To obtain haem-iron from its host, *S. aureus* has evolved the iron regulated surface determinant (*Isd*) system encoded by *isdA, isdB, isdCDEFsrtBisdG, isdH,* and *orfXisdI* for acquisition, transport and release of heme-iron. Within the transcriptome data, the expression of *isdA, isdB, isdC, isdD, isdE, isdF, isdG* and *srtB* were all elevated (Fig 4.6) indicating an activation of the Isd system after challenge with squalene.

In contrast with *S. aureus, S. epidermidis* possesses considerably fewer iron acquisition systems (Hammer and Skaar, 2011). The transcriptional data of *S. epidermidis* revealed that the expression of four genes annotated as iron ABC transporters were increased over 2-fold following squalene challenge, and their homologs (annotated as SstABCD ferrichrome transporter) were in the DE transcriptome data of *S. aureus* (Table 4.6). Collectively, these results are indicative of enhanced iron uptake as a common biological response of these skin colonisers under squalene challenge conditions.

Table 4.6 Changes in gene expression of a putative iron compound ABC transporter

S. aureus		*S. epidermidis*
Gene name	**Fold change (log_2)**	**Gene name**
NWMN_0703 (sstB)	1.5	1.11	*SETU_00357*
NWMN_0704 (sstC)	1.23	1.1	*SETU_00358*
NWMN_0705 (sstD)	0.92	1.09	*SETU_00359*
NWMN_0702 (sstA)	1.38	1.01	*SETU_00356*

4.3.7 Quantitative PCR validation

Validation of the RNA-Seq data was performed by quantification of selected DE genes in the squalene challenge RNA-Seq dataset using qPCR. The fold changes for each gene between control and squalene challenge samples were determined and then compared with RNA-Seq data. At least three biological and two technical qPCR replicates were used for each gene. RNA integrity was assessed by gel electrophoresis prior to conversion to cDNA for qPCR.

The *crtI*, *isdA*, and *fnbB* transcript levels and SETU_00479 (*dltA*), SETU_00325 (*saeS*), and SETU_00357 (*sstB* iron ABC transporter homolog) transcript levels were assessed for both *S. aureus* and *S. epidermidis* respectively. Collectively these genes are representative of carotenoid biosynthesis, iron acquisition, and virulence factor expression and regulation. All primers chosen had amplification efficiency values above 90 % and gave products of approximately 150 bp. The primers and their efficiency values are shown in Table 4.7.

Table 4.7 Primers for qPCR

Gene name	Primer sequences	Efficiency (%)	Reference
crtI	F- CCGGCAAGCTCAGGATATGT	92.2	This study
	R-TACTGGCGCTTGTGTGTGAT		
isdA	F- CAATCAAGCTGTAAGTG	94.6	This study
	R- CCTAAAAGGGCAAGTGTTGCG		
fnbB	F- CTCATGGTATCTCAACACTGC	90.4	This study
	R- TGCGTCACTGTTGTAGGATC		
SETU_00479	F- GGAACAGACAAATGCACAAG	90.6	This study
	R- ATACCATCCATTCTGCGA		
SETU_00325	F- GGATGGCGTCATTAGTGAT	91.0	This study
	R- CAAGTAATTGATCGAGCTG		
SETU_00357	F- GGTGAACAAGCAACTGTTG	90.5	This study
	R- CCTAATATTACACCAACTAGT		

The fold-level changes in expression that were determined from the qPCR data were consistent with RNA-Seq, where down-regulation of genes *crtI*, *SETU_00479*, and *SETU_00325*, as well as up-regulation of genes *isdA, fnbB*, and *SETU_00357* were also observed in qPCR results (Fig 4.7). All the fold-level changes showed broadly similar regulation that was in the same direction as the RNA-Seq data. However, results of qPCR data showed different absolute values compared with RNA-Seq data. The fold-level changes in the expression of genes *crtI, isdA, SETU_00479* and *SETU_00357* were lower. This phenomenon may be due to different methods of testing between two technologies. Overall, the data from qPCR supports the changes in the RNAseq dataset.

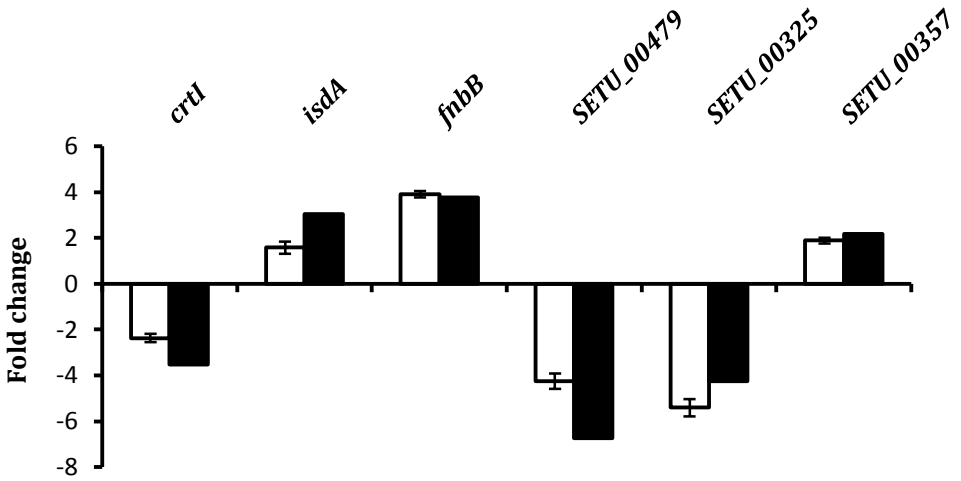

Fig 4.7 Differential expression of *crtI, isdA*, and *fnbB* in *S. aureus* and *SETU_00479, SETU_00325*, and *SETU_00357* in *S. epidermidis* after challenge with squalene, assessed by qPCR. Black bars indicate the fold change in gene expression from RNA-Seq data while white bars indicate those values from qPCR data.

4.3.8 Quantitative Proteomics analysis

While the bacterial responses to squalene was determined by transcriptomics after 20 min challenge, investigation of a prolonged exposure was also deemed to be valuable. Changes in protein expression during late exponential growth phase, due to the presence of squalene was investigated using quantitative methods. The aim was not to directly confirm transcriptional data from challenge at 20 min, but to glean insights into expression at another growth stage that might associate with the described squalene-associated phenomena. Therefore, protein expression differences between squalene-treated and untreated *S. aureus* were determined 2 h after squalene treatment, when cells were at the end of exponential phase.

In the proteomics experiment data, of the 1240 identified proteins identified with at least one peptide (47.3 % of the total proteins in *S. aureus*), there were 133 proteins with significantly changed abundance in squalene conditions. These proteins were further analysed based on the identified unique peptides. Proteins with less than 2 unique peptides were filtered out due to low validation of identification. Consequently, 21 proteins were selected from the proteomics experiment with > 1.5-fold change (Table 4.8).

Table 4.8 Differential protein expression compared with RNAseq expression data. *S. aureus* cells were challenged with 1% (v/v) squalene during the mid-logarithmic phase of growth (OD_{600}=0.5). Proteins were identified 2 h after squalene challenge, at the end of exponential growth phase. For comparison, corresponding transcripts 20 min after squalene challenge are shown. Expression of proteins listed was >1.5 fold changed relative to untreated control. A dash indicates that a protein or its cognate gene was not altered in expression.

Name	Description	Fold change in Proteomics	Fold change in Transcriptomics
Chp	Chemotaxis inhibitory protein	18.28	-
HlgB	Gamma hemolysin component B	4.25	3.51
HlgC	Gamma-hemolysin component C	4.24	3.47
NWMN_1076	Uncharacterised protein	3.5	4.29
FnbA	Fibronectin binding protein A	3.4	-
FnbB	Fibronectin binding protein B precursor	-	3.76
NWMN_2543	N-acetylmuramoyl-L-alanine amidase domain protein	3.2	-
LukF	Leukocidin/hemolysin toxin family F subunit	2.81	2.9
Coa	Coagulase	2.49	-
NWMN_0757	Secreted von Willebrand factor-binding protein	2.44	-
LukS	Leukocidin/hemolysin toxin family S subunit	2.37	3.53
HlgA	Gamma-hemolysin component A	2.22	-
CtpA	Carboxyl-terminal protease	2.17	-
NWMN_0429	N-acetylmuramoyl-L-alanine amidase aaa	1.88	-
NWMN_1831	Ferritin	-1.52	-2.53
PckA	Phosphoenolpyruvate carboxykinase	1.5	-
AldA	Aldehyde dehydrogenase homolog	1.5	-2.41

MsrA	Peptide methionine sulfoxide reductase MsrA	1.5	-
Fib	Fibrinogen-binding protein	1.5	-
SpxA	Regulatory protein Spx	-1.5	-
AdhE	Aldehyde-alcohol dehydrogenase	-1.68	-9.85

Although not intended as a direct comparison, there was agreement between most of the proteins with altered expression and their transcripts in the RNA-Seq data of squalene challenge. Six up-regulated proteins, that were also DE in squalene challenge transcriptome, included known virulence factors, such as gamma hemolysin components HlgB and HlgC, leukocidin proteins LukF and LukS, and fibronectin binding proteins FnbA (Table 4.8). Additional virulence factors were also up-regulated in the proteomics data such as the chemotaxis inhibitory protein CHIPS, γ-hemolysin component HlgA, and coagulase protein Coa. These data further support that squalene activates the SaeRS TCS and induces an invasive phenotype in *S. aureus*.

In further agreement with the RNA-Seq data, ferritin and the iron-containing alcohol dehydrogenase AdhE were both down-regulated. *S. aureus* uses ferritin to safely store iron intracellulary without risking inducing oxidative stress (Theil, 1987), and biosynthesis of AdhE requires iron. The down-regulation of ferritin and AdhE, combined with the up-regulation of iron-acquisition genes, strongly indicates that squalene induces iron limitation in staphylococci.

4.3.9 Experimental evolution of *S. aureus* with squalene selection

On the basis that squalene challenge triggered the derepression of iron acquisition mechanisms and reduced pigmentation of *S. aureus*, it was hypothesised that squalene might act as a selective pressure due to reduced iron levels and increased susceptibility to oxidative stress. Experimentally, the selection of mutations that confer adaptation of *S. aureus* to these phenotype-driving effects of squalene might identify genetic variation that enhances growth and determinants targeted by squalene. Therefore, experimental evolution of *S. aureus* with squalene as a selective agent was performed. Since squalene does not exhibit antimicrobial effects on *S. aureus* in rich medium (chapter 3), broth supplemented with squalene was used as growth medium in serial passages at a concentration that was consistent with previous RNA-Seq experiments. After passages, the purification and pooling DNA from end-point and untreated control isolates for sequencing, will enable more isolates to be sequenced without additional costs to reveal contributing Single Nucleotide Polymorphisms (SNPs) and Insertions and Deletions (INDELs). A high frequency of variance at a particular sequence might indicate the SNP contributes to improved growth fitness under selection. It was expected such variation compared with the parental strain would be a strategy to reveal the actions of squalene upon *S. aureus*.

The wild-type strain, *S. aureus* Newman was passaged by repeated incubations in broth containing 1 % (v/v) squalene in 24 h batch cultures for 14 d. From the second day forward, cells that were cultured for 24 h with squalene were diluted to OD_{600} reading of 0.02 and added into fresh broth with the same concentration of squalene. A control culture was also grown using the same method with passage of the parental stain for 14 days in broth without squalene. Any genetic variance in the control culture would help to filter out mutations selected during continuous culture in the broth over 14 d. The passages were performed in duplicate experiments. By the end of the 14 passages, 6 isolates (3 from squalene passage, 3 from broth passage) from each duplicate experiment were randomly picked and their genomic DNA was extracted and equal amounts of each clone was added to make a DNA pool for sequencing.

Prior to sequencing, DNA samples were assessed to ensure these were of sufficient quality and quantity for sequencing as judged by 260/280 & 260/230 ratios greater than 1.8 (Table 4.9) and suitable integrity (Fig 4.8), using procedures described in earlier chapters.

DNA from the chosen isolates was sequenced and the reads were aligned to the reference Newman genome using Burrows-Wheeler aligner (BWA) aln and sampe packages (Li and Durbin, 2009, Li and Durbin, 2010) version 0.5.9-r16. After alignment, SNPs and INDELs were called and filtered using a bespoke perl script, which utilised the SNPEff version 3.4e open source software. SNPs and INDELs that were synonymous or intergenic and more than 200 bp upstream of a transcriptional start site were filtered out. A second bespoke perl script was used to filter SNPs or INDELs identical to any found in either of the controls of the parental strain or the pool of no squalene passage isolates. After filtering twice, the remaining SNPs and INDELs were considered candidates for loci contributing to adaptation.

However, there were no non-synonymous SNPs identified from the evolution experiment. The most plausible reason for this outcome is a lack of selective pressure, thereby preventing increases in variants. The outcome also implies that although the expression of genes for iron acquisition was elevated, the cellular iron availability did not fall below the limit for survival and reproduction. The experimental evolution experiment was conducted in rich medium which was iron replete. Therefore, future experimental evolution could be performed in iron-limited CDM medium used in previous experiments to produce a growth selection due to additional iron limitation. In that case, genetic variants that overcome the effects of squalene might be selected successfully.

Table 4.9 Quality control analysis results for DNA samples of *S. aureus* Newman submitted for sequencing. Data of the quality checks performed prior to DNA sequencing. Concentrations and 260/280 and 260/230 absorbance reading were assessed by Qubit and Nanodrop, respectively. C0: parental *S. aureus* Newman strain without passage; C1: passage without squalene; S: passage with squalene. C1 and S were made as pools consisting of 6 genomes from selected isolates with the same amount of DNA.

Strain	Sample	Nanodrop 260/280	Nanodrop 260/230	Concentration ng µl-1	Sample volume (µl)
	C0	1.9	2.3	102.6	19.5
***S. aureus* Newman**	C1	2.0	2.2	95.7	21.0
	S	2.1	2.2	110.0	18.0

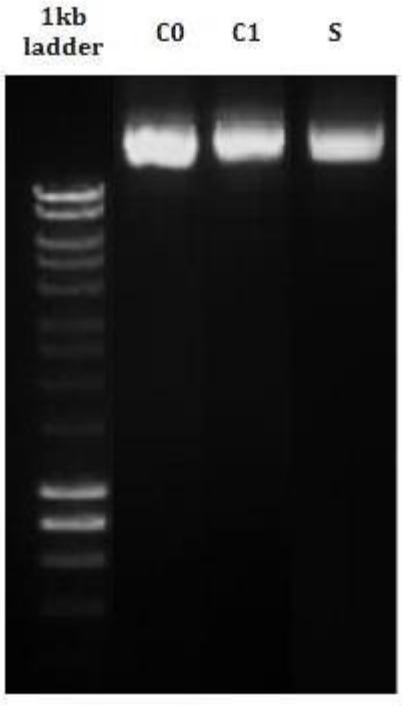

Figure 4.8 Gel electrophoresis of purified genomic DNA of pooled isolates. No apparent sign of degradation was observed, indicating the genomes of these isolates were intact. C0: parental *S. aureus* Newman strain without passage; C1: passage without squalene; S: passage with squalene. C1 and S were made as pools consisting of 6 genomes from selected isolates with the same amount of DNA.

4.4 Discussion

In Chapter 3, the experiments identified a concentration dependent negative relationship between squalene treatment and bacterial pigmentation. In addition, the comparative results of growth in the presence of squalene with *S. aureus* and *S. epidermidis* cells demonstrated that squalene modulates the function of three distinct antimicrobials, H_2O_2, nisin and LL-37. In this chapter, the transcriptional responses of *S. aureus* Newman and *S. epidermidis* Tü3298 to squalene were determined. The main aims in this chapter were to compare the DE genes of *S. aureus* and *S. epidermidis* challenged with squalene to find the potential for a transcriptional basis to this phenomenon observed in Chapter 3, and determine the extent to which squalene could impact upon staphylococcal skin colonisation.

Overall, it was revealed that there are considerable overlaps as well as significant differences between both species in their transcriptional responses to squalene. A greater number of DE genes were found for *S. epidermidis*, however the extent of the response to squalene between the species could be considered mostly similar because the majority of *S. epidermidis* DE genes had a <2 fold change.

The similarities of transcriptional response between *S. aureus* and *S. epidermidis* after squalene challenge were revealed by interrogation with COG and KEGG metabolic pathways. Both *S. aureus* and *S. epidermidis* transcriptomes revealed a greater number of up-regulated genes than the theoretical numbers for categories 'cell wall/membrane/envelope biogenesis' and 'inorganic ion transport and metabolism'. This discrepancy might indicate global effects of treatment of squalene on the staphylococcal cell surface which may also lead to loss of or difficulty of obtaining inorganic ions. It is coincident with the up-regulation of genes involved with iron acquisition in both species. Moreover, both species revealed less active genes than the theoretical number involved in DNA repair which may be suggestive of innocuousness of squalene towards bacterial genome integrity. The KEGG maps data indicates that the expression of

representative genes associated with this pathway, *ruvAB*, *rec* and *holAB*, were not significantly altered, which supports the COG result.

Another pathway sharing the same trend of regulation in response to squalene challenge between both species is the ammonia metabolic pathway. The overall expression of genes involved in ammonia production was down-regulated in both *S. aureus* and *S. epidermidis*. Down-regulation of the genes associated with consumption of ammonia pool including SETU_00843, *gmk*, *adk*, SETU_00042, SETU_00180, SETU_00179, *glnA*, SETU_00508, and *argG* may suggest a consequential compensation due to reduced ammonia production.

It was confirmed from the RNA-Seq data that the reduction in pigmentation level of *S. aureus* after culture with squalene was most likely due to decreased expression of the *crt* operon. Although the expression level of the *crt* operon was low during exponential growth as carotenoid is a secondary metabolite, the whole operon was over two-fold down-regulated. This finding rejected the hypothesis that the effect of squalene on staphylococcal pigmentation was due to competitive inhibition with dehydrosqualene in the CrtN catalysed dehydrogenation to form the yellow intermediate 4,4-diaponeurosporene . Instead, but equally complex, the data supports an effector through which squalene interferes with pigment production by reducing transcription. Nevertheless, the mechanism for that is still unclear and requires future experiments targeting such an effector.

At present, it is known that the *crt* operon is dependent on activation of the RNA polymerase alternative SigmaB factor. Notably *sigB* is not a DE gene in the RNA-Seq data which suggests the expression of *sigB* was not relevant. It brings two hypotheses that are not necessarily independent: there is an unknown regulatory pathway controlling expression of *crt* operon, or squalene somehow interferes with the activity of SigmaB, but not reduces its transcription. Examination of the first hypothesis could be straightforward. The suite of transcriptional regulators in *S. aureus* were broadly determined (Shaw *et al*., 2013) and the availability of an ordered gene inactivation library (The Nebraska

library) means that each regulator mutant could be targeted in a squalene-dependent pigment assay.

One candidate for a regulator is *rsbUVW-sigB* regulatory system where RsbU dephosphorylates the anti-anti-sigmaB factor RsbV and thus leads to the release of SigB from its inhibitory complex with RsbW (Pané-Farré *et al*., 2009). Inactivation of RsbU activity due to a 9 bp gene deletion in its gene renders *S. aureus* almost colourless and is a key phenotypic attribute of lab strain 8325/4 compared with the abundant pigment expression of strain SH1000 (Horsburgh *et al*., 2002). As the RsbUVW-mediated regulation of SigB is at the protein level, it was conceivable that the expression of *sigB* could remain unchanged and thereby was not indicated in RNA-Seq data. Notably, the transcriptional data showed that the expression level of *rsbV,* but not *rsbU* and *rsbW* slightly decreased (-1.8-fold) after squalene challenge. As the anti-anti-sigB factor, decreased level of RsbV leads to less release of SigB from SigB-RsbW complex, in turns resulting in impairing the overall SigB activity. However, this transcript difference might not be expression level since all the other genes on the same transcript were not DE, and how squalene challenge solely influences the transcriptional level of *rsbV* is unclear.

If SigB activity was abated by squalene challenge, then reduced expression of other genes coordinately regulated in the SigB regulon would also be expected. To investigate this regulation further, genes reported as members of the SigmaB regulon or impacted by *sigB* deletion (Bischoff *et al*., 2004) were compared with the DE genes in RNA-Seq data to determine if there was any overlap (Table 4.8 & Table 4.9).

Table 4.10 DE genes that are positively regulated by SigmaB in *S. aureus*

Gene name	Description	Up or down regulated after squalene challenge
clfA	clumping factor A	Down
crtM	squalene desaturase	Down
crtN	squalene synthase	Down
hutG	formimidoylglutamase	Down
mtlA	mannitol-specific IIA component	Down
mtlD	mannitol-1-phosphate 5-dehydrogenase	Down
rbsR	ribose transcriptional repressor RbsR	Down

Table 4.11 DE genes that are negatively regulated by SigmaB in *S. aureus*

Gene name	Description	Up or down regulated after squalene challenge
hlgB	gamma-hemolysin component B	Up
hlgC	gamma-hemolysin component C	Up
lip	lipase precursor	Down
lrgB	antiholin-like protein LrgB	Down
lukF	leukocidin/hemolysin toxin family F subunit	Up
ssa	secretory antigen precursor SsaA	Up

Seven genes positively regulated by *sigB* were DE in the RNA-Seq data (Table 4.10) and their expression was regulated in the same direction with that in the squalene challenge transcriptome. All seven DE genes were down-regulated, implicating that an impaired activity of SigB due to squalene challenge. Furthermore, six genes negatively regulated by *sigB* were DE in the RNA-Seq data (Table 4.11) with four of six shown the same direction of regulation but with only two exceptions. Overall, the results support the hypothesis that SigB activity was interrupted directly or indirectly by squalene challenge.

Decline of pigmentation level is one explanation for increased susceptibility of *S. aureus* to H_2O_2 after treatment of squalene, since staphyloxanthin contributes to oxidant resistance, including peroxide, by scavenging free radicals with its conjugated double bonds (Daum 2008; Liu *et al*., 2008; Götz *et al*., 2006). However, transcriptional data revealed that it maybe not the only case. Transcription of *katA*, which encodes the sole catalase was down-regulated in *S. aureus* but remains unchanged in *S. epidermidis*. The decrease in gene expression of *katA* in *S. aureus* potentially exacerbates the difference in susceptibility between two species. Catalase expression is regulated by several determinants (PerR, Fur; Horsburgh *et al*., 2001a,b) in *S. aureus*, in addition to SigmaB; regulation by the latter is owing to an upstream SigB promoter (Horsburgh *et al*., 2002)

As discussed in Chapter 3, polar carotenoids modulate the fluidity properties of lipid membranes and such fluidity characteristics are critical to the interaction of membrane-targeting host defence cationic antimicrobial peptides (CAPs) with *S. aureus* (Mishra *et al*., 2011). Therefore, decreased fluidity of the *S. aureus* cell membrane caused by reduced level of pigment due to treatment of squalene may lead to increased susceptibility of *S. aureus* cells to nisin. Moreover, it was reported that a two-component system of staphylococci, BraSR, is involved in resistance to bacitracin and nisin (Hiron *et al*., 2011). However, different expression levels of the BraSR between *S. aureus* and *S. epidermidis* was not observed in transcriptional data, thus whether BraSR plays a role in the observed nisin results cannot be confirmed .

In Chapter 3, it was noted that the susceptibility of *S. aureus* to LL-37 was unchanged while with *S. epidermidis* it increased after treatment of squalene. A hypothesis was proposed that differences in expression levels of *isdA*, *aur, mprF,* and the *dltABCD* operon between *S. aureus* and *S. epidermidis* may lead to this result as these genes were proven to contribute to defence against action of host LL-37 (Ryu *et al*., 2014). Expression of these genes was investigated in the current study to examine whether any differential expression might explain the observed phenotypes. Transcriptome data revealed *mprF* was not a DE gene in either species, while *isdA* was up-regulated in *S. aureus*, but does not have a homolog in *S. epidermidis*. Both *aur* and the entire *dlt* operon were down-regulated in *S. epidermidis* but were not DE loci in *S. aureus*.

The *dlt* operon in Gram-positive bacteria encodes proteins that catalyse the addition of D-alanine to wall-associated teichoic acid. The addition of this amino acid to the cell wall reduces negative charge on the bacterial cell surface and, as a consequence, reduces the interaction with cationic antimicrobial peptides (CAMPs) such as LL-37 (Neuhaus & Baddiley, 2003). The expression of *dlt* operon is regulated by the TCS GraRS that requires VraFG, whereby GraS senses CAMPs resulting in its autophosphorylation, which then phosphorylates GraR, driving *dlt* operon expression. VraFG affects expression of *dlt* via a positive feedback mechanism (Yang *et al*., 2011). Within the transcriptome data sets in this study, expression of the GraRS TCS was not altered in *S. epidermidis*, while *vraFG* was down-regulated (Table 4.5). This decrease in expression of *vraFG* could explain the reduced expression level of the *dlt* operon, and suggest that the expression of GraSR was unchanged. As a signal transduction system, the transcriptional level of GraSR does not have to decrease to reduce its downstream operon expression, instead, the switch from inactivation to activation or opposite is most critical. Therefore, absence of GraSR in transcriptional DE gene list does not mean the decrease in gene expression of *dlt* was not mediated by this system. Collectively, these gene expression data indicate that the resistance of *S. aureus* to LL-37 increased while that of *S. epidermidis* reduced, which explains the *in vitro* experimental results obtained in Chapter 3.

Overall, the reason remains unclear for the observed different regulation with respect to direction of virulence factor expression between *S. aureus* and *S. epidermidis*, as highlighted in KEGG pathway maps (Table 4.5) which was further confirmed in *S. aureus* proteomic data (Table 4.8). This difference could simply reflect distinct strategies possessed by the two species, particularly the aggressiveness of *S. aureus* and the relatively benign relationship that *S. epidermidis* has with its host. Both lifecycles are successful and enable the species to survive and spread but the less virulent species has greater advantages for persistence on its host (Massey *et al*., 2006). The *S. epidermidis* approach consists of a series of passive mechanisms to evade host defences, with production of protective matrix polymers instead of the production of aggressive toxins. This notion was recently supported with the increasing investigation of *S. epidermidis* virulence mechanisms (Otto, 2012). With respect to the study here, one possibility is that *S. epidermidis* has evolved to recognise squalene as a lipid that is a signature of its major niche, and thus decrease its virulence expression level for fitness purposes. In contrast, *S. aureus* may regard squalene as the sign of arrival upon host skin therefore up-regulates its virulence factors preparing for invasion. *S. aureus* is the major skin bacterial pathogen of humans and it was proposed that skin infection is a key to its transmission (Massey *et al*., 2006) that discriminates it from *S. epidermidis*.

Iron acquisition is a critical mechanism required for bacteria to colonise vertebrate hosts. This requirement is due to hosts are effectively devoid of free iron, with concentrations normally lower than 10^{-15}, that ensures that all bacteria encounter a barrier of iron starvation to impede its invasion. Therefore, bacterial pathogens have evolved powerful mechanisms to sense and acquire iron. *S. aureus* is renowned for its numerous and diverse pathways for iron acquisition, including production of siderophores (staphyloferrin A and staphyloferrin B), haem and haemoglobin receptors, combined its ability to lyse erythrocytes through the secretion of haemolysins (Hammer and Skaar, 2011). The expression profile of proteins involved in iron acquisition is regulated by the iron-dependent ferric uptake regulator (*fur*) (Xiong *et al*, 2000; Horsburgh *et al*, 2001). Fur binds a consensus DNA motif to repress the expression of

downstream genes in the presence of its iron corepressor. Fur binding is non-productive when iron limitation alters the intracellular iron corepressor concentration, which derepresses the expression of iron uptake genes (Hammer and Skaar, 2011). Inactivation of *fur* in *S. aureus* resulted in a growth defect due to oxidative stress caused by the unrestrained import of iron combined with alterations in reduced catalase expression (Horsburgh *et al*., 2001).

In this study, challenge with squalene triggered the derepression of the iron acquisition mechanisms in both *S. aureus* and *S. epidermidis* (Fig 5). And down-regulation of ferritin and iron-containing alcohol dehydrogenase AdhE was further confirmed in proteomic data of *S. aureus*. However, little can be stated at present as to why this would be an outcome pertaining to a long chain lipid with no functional side groups. The failure of selecting SNPs from experimental evolution of *S. aureus* indicates that the squalene treatment in rich medium cannot induce sufficient stress, at least under the conditions that were established. As the key and most intriguing finding of the transcriptomics work in this chapter, the effects of squalene on staphylococcal iron acquisition will be further investigated in Chapter 5.

Chapter 5 Squalene induced iron-starvation in *S. aureus* and *S. epidermidis*

5.1 Introduction

Numerous and diverse functions of iron have been studied in bacterial cells. Iron plays important roles in cell composition, intermediary metabolism, secondary metabolism, enzyme activity and host cell interactions associated with pathogenicity (Symeonidis and Marangos, 2012). Deficiency of iron can cause growth inhibition, decrease in RNA and DNA synthesis, inhibition of sporulation, and changes in morphology of cells (Symeonidis and Marangos, 2012). Iron contributes to intermediary metabolism processes including: tricarboxylic acid cycle; electron transport; oxidative phosphorylation; nitrogen fixation; and aromatic biosynthesis (Messenger and Barclay, 1983). Moreover, certain proteins and enzymes require iron such as peroxidase, superoxide dismutase, nitrogenase, hydrogenase, glutamate synthase, cytochromes, ferridoxins, and flavoproteins (Messenger and Barclay, 1983; Skaar, 2010; Schaible and Kaufmann, 2004; Symeonidis and Marangos, 2012).

Humans possess several defences against bacterial infection, where the very first line is the withholding of nutrients including iron to prevent bacterial outgrowth; a process termed nutritional immunity. Greater than 90 % of iron in the host is intracellular, sequestered by the iron storage protein ferritin or bound with the haem cofactor of haemoglobin or myoglobin. Moreover, neutral pH and the aerobic environment of serum ensures that extracellular iron is in its insoluble Fe^{3+} form and thereby more difficult to be sequestered by invading pathogens. A serum protein, transferrin, even enhances this difficulty by binding iron with an association constant of approximately 10^{36} (Skaar, 2010; Schaible and Kaufmann, 2004). Altogether, these factors ensure that the level of free iron available to invading bacteria is far lower than the minimal requirement for most with respect to bacterial replication and causing disease.

The arms race for nutrient iron never ends for both host and bacterial pathogens. Bacterial pathogens have evolved abilities to sense iron depletion and this may serve as a signal that they have arrived on host tissue (Skaar, 2010; Symeonidis and Marangos, 2012). This sensing typically involves transcriptional control mediated by the iron-dependent repressor known as Fur (ferric uptake regulator) (Hantke, 1981; Xiong *et al*, 2000; Horsburgh *et al*, 2001). Fur binds a consensus DNA sequence termed 'fur box' to repress the expression of down-stream Fur-regulated genes in the presence of iron cofactor. Fur releases from the DNA when iron is limited as cofactor and this derepresses the expression of iron uptake genes. The orthologs of Fur have been identified in a wide range of genera from both Gram-negative and Gram-positive bacteria and contributes to the virulence of both animal and plant pathogens (Ratledge and Dover, 2000).

In *S. aureus*, Fur also regulates the expression of staphylococcal virulence, including adhesins, biofilm formation, and manipulation of host wound healing (Athanasopoulos *et al*., 2006; Chavakis *et al*., 2002; Johnson *et al*., 2008). It was reported that Fur regulates the expression of secreted cytolytic and immunomodulatory toxins, which play critical roles in decreasing the host immune response that contributes to bacterial survival (Nizet, 2007). In addition to controlling iron acquisition mechanisms, Fur also positively regulates glycolytic and fermentative enzymes, indicating *S. aureus* modulates its metabolism in order to adapt to the iron-starved environment by increasing fermentative metabolism. Increased fermentative metabolism leads to elevated production of lactate, and secretion of lactate in turns lowers the pH of the microenvironment thus impairing the affinity of transferrin for iron (Friedman *et al*., 2006). Collectively, these studies suggest the ability possessed by *S. aureus* to alter the host environment in a way that promotes the release of iron from host proteins presumably increasing iron availability.

Production of siderophores is one of the key mechanisms for *S. aureus* to scavenge iron from host extracellular iron-binding proteins, such as transferrin and lactoferrin (Hammer and Skaar, 2011). Siderophores are small molecules secreted by bacteria and have an exceptionally high affinity for iron. Staphyloferrin A and staphyloferrin B are two distinct siderophores produced

by *S. aureus* that share many properties (Hammer and Skaar, 2011). The genes involved in the biosynthesis and import of both staphyloferrin A and B are regulated by Fur and are therefore maximally expressed in iron-limiting environments (Friedman *et al*., 2006; Lindsay and Riley, 1994). In addition to staphyloferrin A and B, the presence of a third *S. aureus* siderophore named aureochelin was suggested, but it is still not characterised (Courcol *et al*., 1997).

A further important mechanism possessed by *S. aureus* for iron acquisition is capture of host haem that represents the primary reservoir of iron within vertebrates (Drabkin, 1951). Studies revealed the utilisation of haem-iron is preferential when *S. aureus* grows in the presence of both transferrin and either haem or haemoglobin, suggesting that haem-iron is the preferred source of iron during infection (Torres *et al.*, 2006; Skaar *et al.*, 2004). Haemoglobin is obtained by lysis of erythrocytes by hemolysins, and subsequent trapping, transportation and lysis of haem is executed by proteins expressed from the iron regulated surface determinant (Isd) system encoded by *isdA, isdB, isdCDEFsrtBisdG, isdH,* and *orfXisdI* (Hammer and Skaar, 2011). Taken together, *S. aureus* utilises a remarkable arsenal of pathways to obtain iron during infection.

5.2 Aims

In the previous chapter, transcriptional data showed that *S. aureus* and *S. epidermidis* genes involved in iron acquisition were up-regulated, accompanied by the iron storage ferritin being down-regulated in both species. Overall, there were 24 iron-uptake-related genes with increased differential expression in the 100 most up-regulated genes in terms of fold-change in the *S. aureus* DE transcriptome. The transcriptional data of *S. epidermidis* also revealed that the expression of four genes annotated as iron ABC transporters were increased over 2-fold following squalene challenge.

Therefore, the primary aim of this chapter is to determine whether the transcriptional profile in response to iron limitation is driven by actual iron-deficiency or inactivation of Fur but independent to iron availability. To achieve this, a negative relationship between iron availability in medium and expression of the iron-uptake genes was assessed. In addition, growth of cells in iron-defined media was performed in the presence or absence of squalene to examine whether squalene could induce a further iron-limited situation thus inhibiting bacterial growth. Finally, intracellular iron concentration will be determined through ICP-OES for both squalene treated and control sample to provide direct evidence for whether squalene actually reduces the iron concentration in staphylococci.

5.3 Results

5.3.1 The transcriptional profile in response to iron-limitation were revealed by RNA-Seq data of squalene challenge for both *S. aureus* and *S. epidermidis*

As observed in chapter 4, both *S. aureus* and *S. epidermidis* significantly up-regulated the genes associated with iron acquisition as well as down-regulated several genes for iron storage and utilisation. These DE genes revealed by RNA-Seq data were summarised in Table 5.1.

Table 5.1 Genes associated with iron metabolism revealed by the transcriptional data in response to squalene challenge.

Gene name	Description	Fold change	Found in *S. aureus* or *S. epidermidis*
Genes involved in iron acquisition			
isdG	cytoplasmic heme-iron binding protein	4.08	*S. aureus*
NWMN_2081	biosynthesis of staphyloferrinA	3.81	*S. aureus*
sbnD	membrane transporter protein	3.58	*S. aureus*
isdC	iron-regulated cell surface protein	3.48	*S. aureus*
sbnI	SbnI protein	3.41	*S. aureus*
sbnH	diaminopimelate decarboxylase	3.36	*S. aureus*
sirA	siderophore compound ABC transporter	3.20	*S. aureus*
srtB	NPQTN-specific sortase B	3.12	*S. aureus*
isdF	iron/heme permease	3.07	*S. aureus*
isdA	iron-regulated heme-iron binding protein	3.05	*S. aureus*
NWMN_2076	FecCD iron compound ABC transporter	3.03	*S. aureus*
sbnG	2-dehydro-3-deoxyglucarate aldolase	2.97	*S. aureus*
NWMN_2185	iron compound ABC transporter	2.83	*S. aureus*
sstB	iron compound ABC transporter	2.81	*S. aureus*

sbnE	siderophore biosynthesis	2.81	*S. aureus*
fhuB	ferrichrome transport permease	2.77	*S. aureus*
sbnC	siderophore biosynthesis	2.69	*S. aureus*
isdE	iron compound ABC transporter	2.66	*S. aureus*
sstA	ferrichrome ABC transporter permease	2.58	*S. aureus*
NWMN_2078	ferrichrome ABC transporter lipoprotein	2.51	*S. aureus*
sbnF	siderophore biosynthesis	2.50	*S. aureus*
sstC	Iron ABC transporter ATP-binding protein	2.35	*S. aureus*
sirB	siderophore compound ABC transporter	2.17	*S. aureus*
isdB	iron-regulated heme-iron binding protein	2.14	*S. aureus*
fhuG	ferrichrome transport permease fhuG	1.96	*S. aureus*
sstD	ferrichrome ABC transporter lipoprotein	1.88	*S. aureus*
SETU_00357	iron compound ABC transporter *sstB* homolog	2.16	*S. epidermidis*
SETU_00358	iron compound ABC transporter *sstC* homolog	2.14	*S. epidermidis*
SETU_00359	iron compound ABC transporter *sstD* homolog	2.13	*S. epidermidis*
SETU_00356	iron compound ABC transporter *sstA* homolog	2.01	*S. epidermidis*
Genes involved in iron storage or utilisation			
NWMN_1831	ferritin	-2.54	*S. aureus*
SETU_01451	ferritin	-1.26	*S. epidermidis*
sdhA	succinate dehydrogenase flavoprotein	-2.93	*S. aureus*
sdhB	succinate dehydrogenase iron-sulfur	-4.08	*S. aureus*
SETU_01279	iron-sulfur cofactor synthesis protein nifZ	-1.49	*S. epidermidis*

5.3.2 Iron-concentration-dependent expression of iron-uptake genes, *sirA* & *sbnE*

It was known there is a negative relationship between iron availability in growth medium and expression level of the iron-uptake genes in *S. aureus* (Friedman *et al*., 2006). Confirmation of this relationship and establishment of a gene expression measure was achieved by quantifying the expression levels of two representative genes associated with siderophore production and transportation, *sbnE* and *sirA*, in chemically-defined medium (CDM) with different iron concentrations via qPCR. The primer sequences are listed in Table 5.2. RNA integrity was assessed by gel electrophoresis prior to conversion to cDNA for qPCR.

Table 5.2 Primers for qPCR

Gene name	Primer sequences	Efficiency (%)	Reference
sirA	F- GCCACTGACGTCGCTGTATC	95.2	This study
	R- GACGCGACAATTAAGTCCGG		
sbnE	F- CGATGCCTGATTCACCGATG	94.1	This study
	R- CATACGTCGGGTATGCCATC		

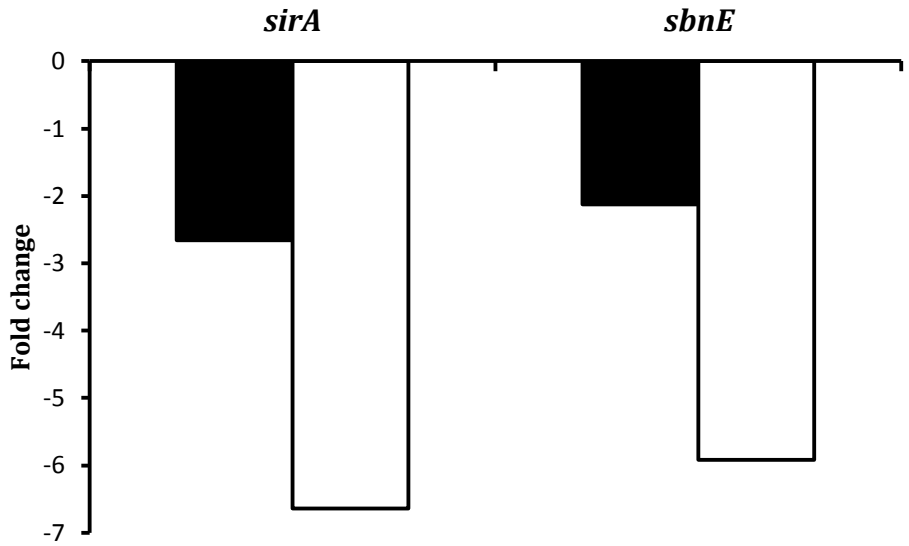

Figure 5.1 Decreased expression levels of *sirA* and *sbnE* in iron-depleted CDM with increasing added iron. Black bars indicate *S. aureus* cells cultured with 0.02 μM of iron, and white bars represent culture with 0.2 μM of iron. *S. aureus* cells were cultured in CDM with two iron concentrations (0.02 μM 0.2 μM). Cells were harvested 20 min later after OD_{600} reached 0.5 and cDNA was made for qPCR test. $Fe(NH_4)(SO_4)_2$ was added into iron-depleted CDM to obtain the desired iron concentration.

S. aureus cells were cultured in CDM with two iron concentrations, 0.02 μM, and 0.2 μM ($Fe(NH_4)(SO_4)_2$). The level of gene expression for samples cultured with 0.02 μM and 0.2 μM of iron were compared with samples grown in iron-deficient medium (0 μM) (Fig 5.1). The expectation was that the expression of *sirA* and *sbnE* would be at their maximum level in the iron-deficient condition, then the expression level would decrease with increasing iron concentration. As expected, the expression of both *sirA* and *sbnE* exhibited the same pattern that when iron concentration was elevated from 0 to 0.02 μM and 0.2 μM, the expression of both *sirA* and *sbnE* diminished. Collectively, these data confirmed the negative relationship between iron availability and the expression of *sirA* and *sbnE*. When less iron was available in broth, *S. aureus* cells express more SbnE and SirA to chelate and import iron. Since *sirA* and *sbnE* are two representative genes involved in staphylococcal iron acquisition and both of

them are regulated by Fur, this result should apply to the rest of the Fur regulon identified in the RNA-Seq data that also regulated by.

After confirmation of this inverse relationship, squalene challenge was performed on the basis of above experiment. In this case, squalene was added to a final concentration of 1 % (v/v) when OD_{600} reached 0.5, then the samples were cultured for a further 20 min, prior to cDNA preparation (Fig 5.2). Results revealed that the expression of both *sirA* and *sbnE* was increased after squalene challenge in each iron concentration. Although this increase was minor, the consistency of the change suggests squalene might further exacerbate the iron starvation of *S. aureus* cells.

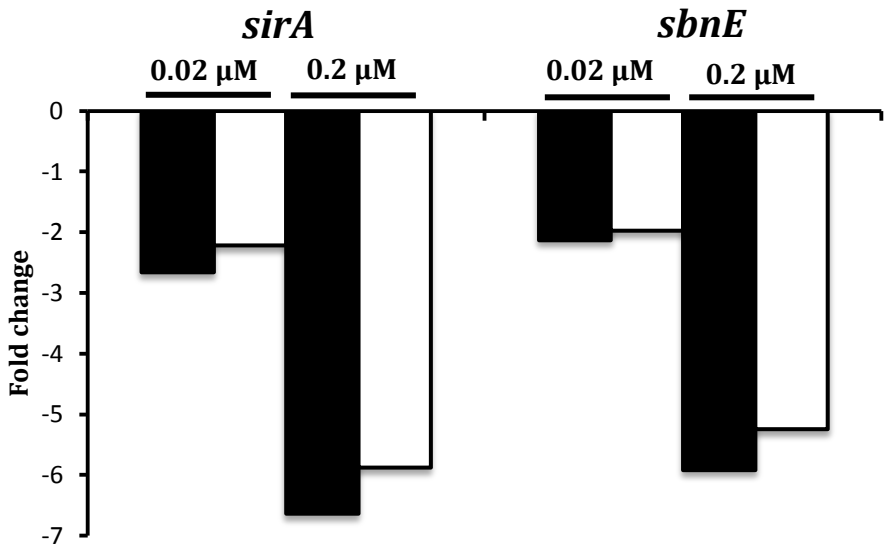

Figure 5.2 Comparative expression of *sirA* and *sbnE* in cells grown with increasing added iron, with or without 1 % (v/v) squalene challenge. Cells were cultured in iron deficient CDM with either none, 0.02 µM or 0. 2 µM supplemented iron in the absence (black bars) or presence (white bars) of 1 % (v/v) squalene. The level of gene expression for samples cultured with 0.02 µM and 0.2 µM of iron were compared with samples grown in iron-deficient medium (0 µM). Squalene challenge was conducted when OD_{600} reached 0.5 and grew the samples for further 20 min and cDNA was made after challenge for qPCR test. $Fe(NH_4)(SO_4)_2$ was added into no iron CDM to obtain desired iron concentration.

5.3.3 Squalene caused a growth defect in iron-limited media

Having established that the derepression of iron acquisition genes in staphylococci was induced by squalene challenge in iron replete conditions, it was hypothesized that staphylococci may be iron limited following squalene challenge, and that this would affect their growth in iron-limited conditions. Hence, *S. aureus* and *S. epidermidis* were grown in CDM with and without $Fe(NH_4)(SO4)_2$ supplementation to generate iron concentrations in the range 0–2 μM and also in an iron replete, rich medium control THB medium. Cells were cultured in the presence or absence of 1 % (v/v) squalene, and growth yield was measured by spectrophotometry after 12 hours (Fig 5.3).

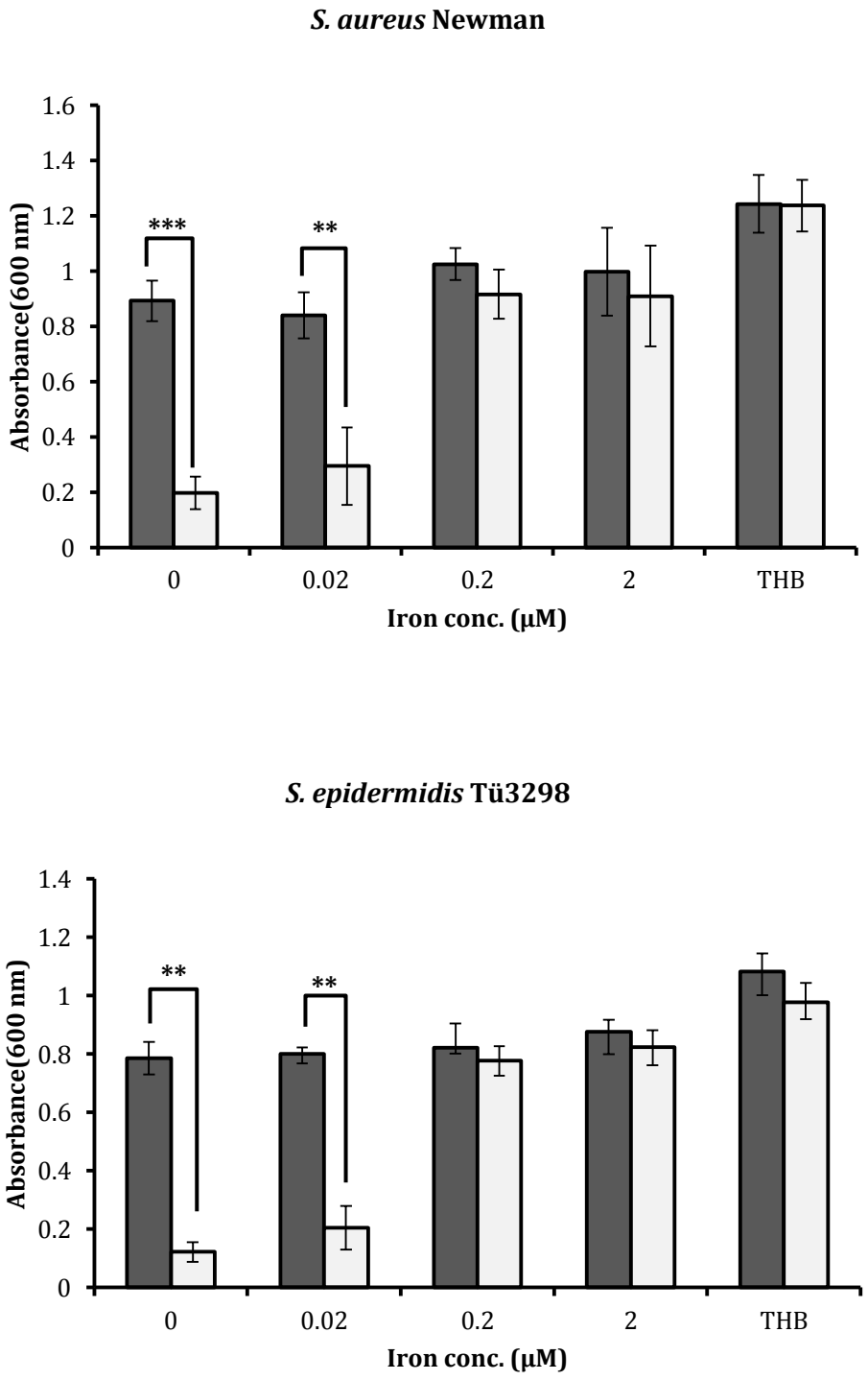

Figure 5.3 Growth yield of *S. aureus* and *S. epidermidis* after 12 h growth with or without 1 % (v/v) squalene in iron-deficient CDM with or without iron supplementation.

Overnight culture was diluted to an OD_{600} of 0.02, and grown at 37°C with shaking for 12 h in the presence or absence of 1% (v/v) squalene in iron deficient CDM supplemented with the indicated concentrations of iron. Growth yield was determined by measurement of OD_{600}. Shaded bars: untreated; grey: cultured with 1% (v/v) squalene. Asterisks show significance as measured by the Student's T-test (** $P \leq 0.01$; *** $P \leq 0.001$).

S. aureus and *S. epidermidis* growth yields in iron-deficient media were lower than cells cultured in iron-sufficient THB medium. In CDM that was iron-deficient supplementation with iron (0.02 μM and 0.2 μM) progressively improved yield with increasing concentrations. The yield of cells in iron-depleted media decreased in the presence of 1% (v/v) squalene, while there was no significant difference in yield when the medium was supplemented to an iron concentration at 0.2 μM and above .For *S. aureus* the difference in growth yield in the presence of squalene is statistically significant (paired t-test, p=0.001 and p=0.005) for cells cultured in CDM in the absence or presence of 0.02 μM iron, respectively, while there was no significant difference (paired t-test, p=0.27, p=0.71 and p=0.6) for cells cultured in CDM with 0.2 μM and 2 μM iron and in THB. Similar growth yield reductions caused by squalene were observed for *S. epidermidis* when cells were cultured in iron-depleted CDM in the absence of iron supplementation or with 0.02 μM iron added; paired t-test, p=0.002 and p=0.003, respectively. Growth yield was not different in the presence of squalene when cells were cultured in iron sufficient culture media (CDM with 0.2 μM, 2 μM iron, and THB), where differences were not statistically significant (paired t-test, p=0.3, p=0.41 and p=0.39). Altogether, these results revealed a growth defect of *S. aureus* and *S. epidermidis* in iron-limited media caused by squalene treatment, but this defect was iron concentration dependent, which supports the previous hypothesis that iron-limitation is induced by squalene challenge in both staphylococci.

5.3.4 Measurement of cellular iron concentration by ICP-OES

To determine whether squalene reduces the iron uptake of staphylococci, the cellular iron concentration of squalene-treated cells was compared with control cells. To achieve this, *S. aureus* Newman and *S. epidermidis* Tü3298 were grown in THB in the presence or absence of 1% (v/v) squalene for 24 h. Approximately 10^8 cells of each sample was lysed by treatment with lysostaphin for 2 h and then analysed by ICP-OES. For analysis of iron concentration, the bacterial lysates were diluted 1:10 in 0.1 M HCL. Lysates were compared with an equivalent sample of 0.1 M HCL to determine additional iron in HCL. Additionally, to determine whether cellular iron was depleted as a result of squalene chelating iron extracellularly, a broth only control with or without squalene treatment was also analysed by ICP-OES. The broth only sample was also treated with or without 1 % (v/v) squalene for 24 h, followed by centrifuging and only broth was extracted for analysis as squalene forms a layer away from the media. Values were corrected based on CFU counts and the results are shown in Figure 5.4.

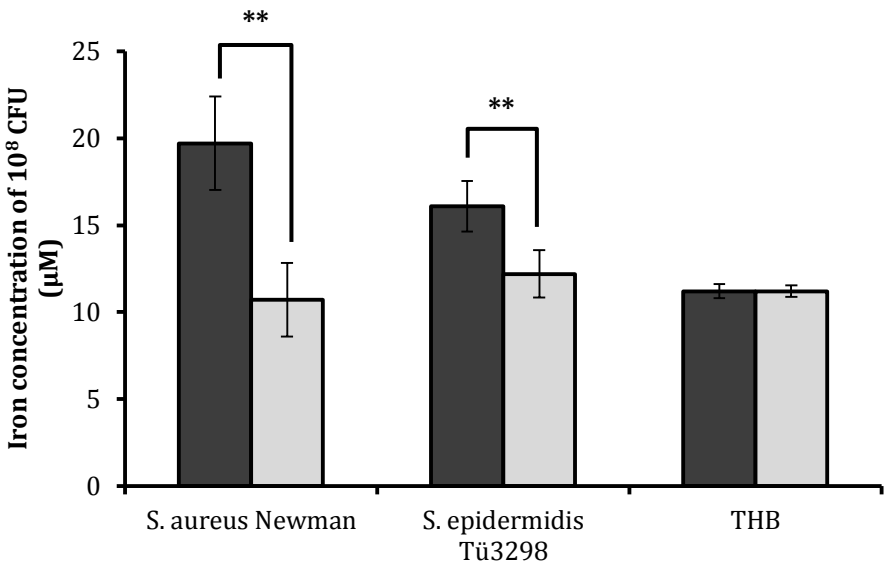

Figure 5.4 The cellular iron concentrations of *S. aureus* Newman and *S. epidermidis* Tü3298 with or without 1% (v/v) squalene treatment after 24 h. The cellular iron concentration of *S. aureus* and *S. epidermidis* in the absence (black bars) or presence of 1 % (v/v) squalene (grey bars). A broth only (THB) control was with the absence or presence or absence of 1% (v/v) squalene was assayed. Bacteria were lysed using lysostaphin and diluted in 0.1 M HCL prior to ICP-OES tests. The final iron concentration was corrected using viable cell counts. Asterisks show significance as measured by the Student's T-test (** $P \leq 0.01$).

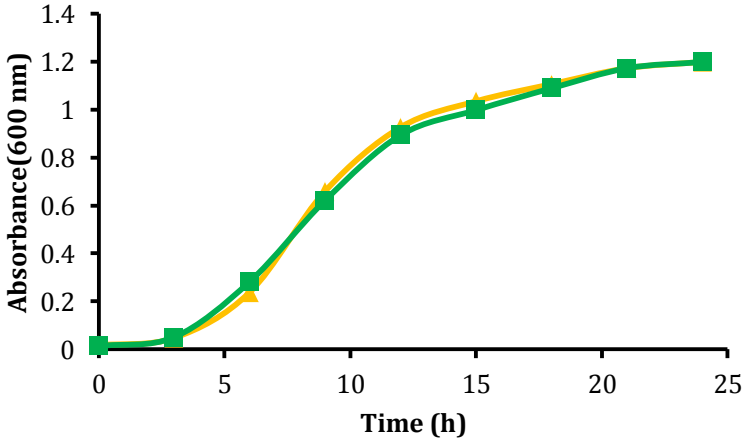

Figure 5.5 Growth of *S. aureus* Newman in THB or squalene-extracted THB. Squalene-extracted THB was prepared by adding 1% (v/v) squalene into fresh THB with vigorously shaking for 24 h, the mixture was then centrifuged and squalene was removed from the top layer. Yellow line: THB; green line: squalene extracted THB.

Staphylococcal cellular iron levels were significantly decreased in squalene-treated cells compared with those cultured in the absence of squalene (*S. aureus*: 46 % reduction, p = 0.005; *S. epidermidis*: 24 % reduction, p = 0.008). The THB control with or without squalene treatment had the same iron concentration (11.2 μM, p = 1). The results prove that squalene causes the decline of cellular iron levels and revealed that this effect was not brought about by a reduced iron concentration in the broth. In addition, to determine whether squalene might extract iron from the medium in a manner that restricts growth rate, THB extracted with squalene was used to culture *S. aureus* Newman in comparison with cells cultured in untreated THB (Fig 5.5). There was no evidence of growth differences indicating that squalene does not sufficiently influence THB to alter growth kinetics, at least under the conditions tested here.

5.4 Discussion

In the previous chapter, a typical bacterial response to iron-limitation was observed after squalene challenge as determined from transcriptomic data for both *S. aureus* and *S. epidermidis*. These data suggested that squalene may induce the iron-starvation response of staphylococci. Therefore, further experiments were performed in this chapter to determine if this iron limited response is caused by actual iron-deficiency or via an indirect route such as interference with Fur, but independent to iron availability. Confirmation of an inverse relationship between iron availability and the expression of genes associated with iron acquisition was conducted by using qPCR to measure the expression levels of two representative genes, *sirA* and *sbnE*, associated with siderophore transport and biosynthesis during culture in chemically-defined media with different iron concentrations. Squalene challenge was also studied using these qPCR tests. The expression of both *sirA* and *sbnE* was further increased after squalene challenge in each iron concentration tested that caused derepression of these Fur-regulated genes. This result combined with the finding that squalene caused a growth defect in iron-limited media for both *S. aureus* and *S. epidermidis*, was strongly suggestive that iron-limitation was direct consequence of squalene treatment for staphylococci. The cellular iron concentration was then quantified using ICP-OES, showing that the cellular iron levels for both species of staphylococci were significantly decreased in squalene-treated samples, but remained unchanged for the control squalene-treated THB. Assays using both ICP-OES and growth in squalene-extracted THB rule out the possibility that iron starvation in broth was brought about by reduced iron availability from sequestration by squalene. Collectively, the results in this chapter can be interpreted to propose that squalene induces iron limitation in staphylococci, which results in the differential expression of iron-related genes observed in the transcriptomic data.

However, the mechanism for how squalene treatment lowers intracellular iron concentration remains to be identified. Since expression of genes for iron acquisition were elevated in rich medium (THB) where iron is sufficient, it seems unlikely that squalene impedes iron-uptake pathways by reducing iron

affinity of siderophores or lowering the efficiency of siderophore transport, because very low levels of proteins for iron acquisition are required in an iron-sufficient environment. Squalene interfering with an iron efflux mechanism such that it leads to a net deficit of intracellular iron as a plausible explanation that requires interference with less cellular components. However, efflux pathways are not characterised.

Although it is clear that access to sufficient iron is crucial for successful microbial persistence within the host, during the course of infection, pathogens may encounter stress conditions that raise intracellular free iron levels and promote the Fenton reaction (shown below), presenting an entirely different challenge to survival. The Fenton reaction proceeds rapidly at physiological pH and temperature, and small alterations in the concentrations of H_2O_2 or free iron can have a dramatic impact on the amount of radical production and resulting damage (Park *et al*., 2005). DNA is the most critical target of hydroxyl radical damage, although proteins and lipids can be affected as well. It is therefore required that bacterial pathogens adapt to mediate iron uptake thus avoiding the oxidative damage caused by overload of iron.

$$Fe^{2+} + H_2O_2 \rightarrow Fe^{3+} + \bullet OH + OH^-$$

A mechanism for iron efflux is still uncharacterized in staphylococci, but has been well studied in other species such as *Streptococcus* and *Salmonella* (VanderWal *et al*., 2017; Frawley *et al*., 2014). In *Streptococcus*, the PerR-controlled metal transporter A (PmtA) which was previously implicated in antioxidant defences and suggested to protect against zinc toxicity was reported as a P_{1B4}-type ATPase that functions as an Fe(II) exporter and contributes to defences against iron intoxication and oxidative stress (VanderWal *et al*., 2017). An excess of intracellular iron directly derepresses expression of *pmtA* and this induction requires action of PerR. The inactivation of *pmtA* resulted in increased sensitivity to iron toxicity and oxidative stress due to an elevated intracellular

accumulation of iron. In *Salmonella*, two proteins were identified with the function of reducing levels of total intracellular iron. STM3944 and IceT are both expressed under stress conditions and appear to aid against reactive oxygen species (ROS) and reactive nitrogen species (RNS) (Frawley *et al*., 2014). Therefore, if iron efflux mechanisms were also employed by staphylococci, and squalene interferes with this process by enhancing its action, it could result in reduced intracellular iron that presents in transcriptomic data and *in vitro* experiments as iron starvation.

A separate study revealed a similar profile of up-regulated genes for iron acquisition in *E. coli* (Varghese *et al*., 2007). In that study, H_2O_2 was found to disrupt the activity of Fur protein, thus altering the free iron levels in *E. coli*. The mutants that cannot produce peroxidase and catalase exhibited an elevated expression level for genes normally repressed by Fur suggesting the repression function of Fur is impaired by oxidising the Fur:Fe2+ complex. However, the OxyR H_2O_2-response system restored Fur repression in iron-replete medium by up-regulating the synthesis of Fur protein. This co-regulation was also identified in *S. aureus*, where Fur and PerR, a functional ortholog to OxyR, was mutually regulated and co-regulate various genes involved in antioxidant, virulence factors and iron homeostasis (Horsburgh *et al*., 2001). As an unsaturated linear lipid, squalene can be partially oxidized into squalene-peroxide under culturing condition, which may induce the same alternation of gene expression as shown in the study of *E. coli*. But this still cannot explain why the actual total iron was reduced after squalene treatment. A discrete mechanism would be expected.

Fur was also shown to be capable of modulating the expression of a variety of virulence factors, especially those that target host neutrophils (Torres *et al*., 2010). The study reported that in an iron-deficient environment or Δ*fur* strain of *S. aureus*, α-hemolysin (Hla), γ-hemolysin (HlgC), and leukocidin ED (LukED) were up-regulated, while the expression of protein A (SpA), staphylococcal immunoglobulin G-binding protein (Sbi), Ssl proteins (Ssl 1, Ssl 2, Ssl 3, Ssl 4, Ssl 6, Ssl 7, Ssl 8, Ssl 9, Ssl 10, and Ssl 11), Coa, FLIPr, SCIN, extracellular fibrinogen-binding protein (Efb), SEA, and CHIP were down-regulated (Torres *et al*., 2010). These results share similarities with the transcriptional data obtained in this

study. In the RNA-Seq data, the expression of *hlgC, lukS*, and *lukF* was elevated as well, suggesting the regulation of the genes associated with leukocytes killing was not solely undertaken by the *saeRS* two-component system. Moreover, in their study (Torres *et al*., 2010), up-regulation of hemolysin genes and down-regulation of staphylococcal toxins were altogether interpreted as that when *S. aureus* becomes iron starved, it must acquire iron in order to survive, and thus Fur coordinates a gene expression profile that leads to significant host cell lysis and iron uptake using considerable energy, but this comes at the expense of decreased production of factors involved in escaping from cells of the immune system, which in turn results in increased susceptibility to immune cell clearance. But in the current study, genes involved in biosynthesis of hemolysin and toxin such as *hlg*, *luk*, *ssl* and *sbi* were all up-regulated by squalene challenge, which suggests the energy theory is less likely to be true. *S. aureus* is able to up-regulate both hemolysin genes and staphylococcal toxins in response to a single stimulant without regard to energy consumption.

In summary, challenge with squalene triggered derepressed transcription of the main iron acquisition mechanisms as well as decreased expression levels for genes involved in iron storage and utilisation in both *S. aureus* and *S. epidermidis*. These species showed growth defects in iron-limited media. ICP-OES analysis revealed decreased intracellular iron following squalene treatment. ICP-OES analysis of squalene extracted broth and growth of *S. aureus* in squalene treated broth ruled out the possibility that squalene altered the iron concentration of the medium by sequestration. Taken together, these data shows that squalene causes iron starvation in staphylococci.

Chapter 6 Transcriptional response and experimental evolution of *S. aureus* to ethanol

6.1 Introduction

Ethanol is one of the most common stabilisers, solvents, and disinfectants employed by numerous applications. A large variety of medicines, especially liquids for oral application, contain ethanol, such as cough suppressants, expectorants and oral tranquiliser suspensions. Most alcohol-based disinfectants contain ethanol, typically at a concentration of 70 to 85%. As an example, ethanol is utilised for disinfection of medical instruments and implantation materials and is widely applied. As a solvent, ethanol is used in biological experiments to dissolve organic compounds with intermediate polarity or non-polar nature, such as lipids, vitamins and various antimicrobials. For a general dissolution purpose, ethanol is usually the first choice if water is not suitable.

Ethanol possesses several bactericidal modes of action: disruption of membrane structure or function (Chatterjee *et al*., 2006; Barker and Park, 2001; Silveira *et al*., 2004); interference with cell division, affecting stationary phase growth (Fried and Novick, 1973); alteration of fatty acid composition and protein synthesis (Chiou *et al*., 2004); inhibition of nutrient transport via membrane-bound ATPases (Bowles and Ellefson, 1985); alteration of membrane pH and membrane potential (Terracciano and Kashket 1986); and a decrease in intracellular pH (Huang *et al*., 1986). In addition, ethanol influences bacterial morphology, growth, and viability even at a very low concentration (<0.1%) (Chatterjee *et al*., 2006). This latter study revealed that cells treated with 0. 1 % of ethanol displayed alterations of cell integrity in late-stationary phase growth, and a profound delay of post-stationary phase recovery (>48 h) was observed even if ethanol in the medium was completely metabolized during exponential phase (Chatterjee *et al*., 2006). These data suggest that a much lower than previously reported ethanol concentration is capable of altering bacterial

physiology thus leading to changes in gene expression profile (Fried and Novick, 1973; Bowles and Ellefson, 1985).

Although the effects of various ethanol concentrations on bacteria have been well-established (Fried and Novick, 1973; Bowles and Ellefson, 1985; Chatterjee *et al*., 2006; Barker and Park, 2001; Silveira *et al*., 2004), less is known about how different bacteria respond to ethanol at the transcriptional level. In this chapter, the transcriptional responses of *S. aureus* to challenge with a low ethanol concentration (1 % v/v) were recorded through RNA-Seq approach. In addition, a sub-bactericidal concentration (6 %) was used as a selection to experimentally evolve *S. aureus* cells. By analysing the transcriptional response and the single nucleotide polymorphisms (SNPs) from evolution, these data will facilitate our understanding of the underlying genetic basis for the responses of *S. aureus* to ethanol.

6.2 Aims

Previous work from our lab has revealed a reduction in pigmentation of *S. aureus* due to 1~5 % of ethanol treatment that is similar to the phenomenon identified with squalene. Thus, it was of interest to determine whether squalene and ethanol employ the same mechanism to affect carotenoid production. To investigate this further, the absorbance spectrum assay of pigmentation level of ethanol-treated *S. aureus* would firstly be confirmed. Next, characterisation of the transcriptional response to ethanol challenge would be obtained using RNA-Seq and these data would be compared with that for squalene challenge. In this way it will be possible to investigate if the responses to these organic compounds share similar genetic regulation. Finally, an experimental evolution approach would be used to investigate genetic selection of *S. aureus* to a sub-bactericidal concentration of ethanol. This research programme was expected to identify genes or alleles that contribute to ethanol resistance by analysis of SNPs and insertions and deletions (INDELs).

6.3 Results

6.3.1 The effects of ethanol on pigmentation of *S. aureus*

In preliminary work performed by others in the laboratory, it was noted that the golden colour of *S. aureus* cells was dramatically reduced when cells were treated with ethanol. The orange-red triterpenoid pigment, staphyloxanthin, located in the membrane has an important role in the environmental fitness of *S. aureus,* as discussed previously (Clauditz *et al*, 2006). Since this phenomenon was similar with that characterised for squalene treatment, it was decided to investigate this phenomenon, firstly with absorbance spectrum tests conducted using methanol-extracted pigment from cell pellets.

As covered in chapter 3, absorbance spectrum tests were performed using an optical spectrum analyser plate reader, which uses reflective techniques to separate the wavelengths of light and measures the intensity of the light with an electro-optical detector. In the experiments, the pigment extracted from a wild-type pigmented *S. aureus* strain presents a spectrum with two peaks at 440 nm and 470 nm, which indicates the existence of staphyloxanthin (λmax=463 nm) and two biosynthetic precursors of staphyloxanthin, 4,4-diapolycopene (λmax=440,468 nm) and 4,4-diaponeurosporene (λmax=415, 439 nm) (Furubayashi *et al*., 2014). Corresponding with Beer's law (A=εcl), higher absorbance peak values indicate a greater quantity of carotenoids in the sample.

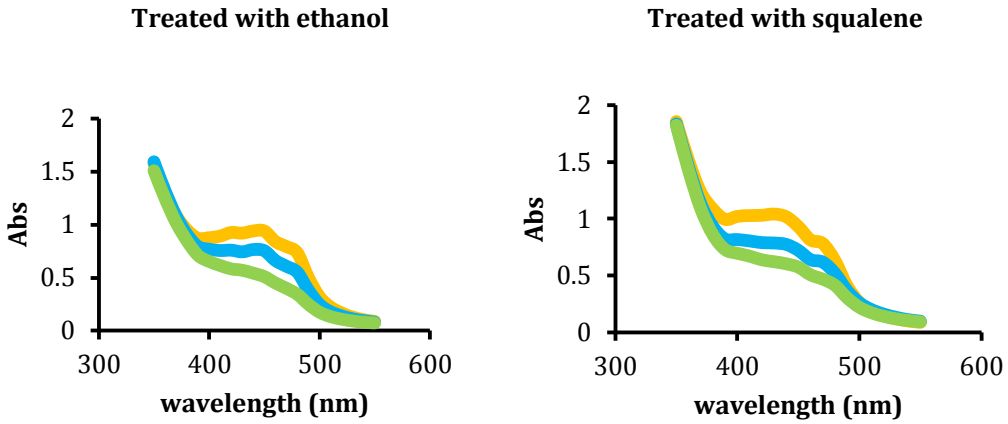

Figure 6.1 Absorbance spectra of extracted pigment of *S. aureus* Newman cells cultured with either ethanol or squalene. *S. aureus* Newman was grown in BHI with different concentrations of squalene or ethanol for 24 h. Orange: control; Blue: treated with 0.1% (v/v) of ethanol or squalene; Green: treated with 1% (v/v) of ethanol or squalene. The two peaks around wavelength of 450 nm are characteristic of the carotenoid staphyloxanthin. Readings were corrected based on viable cell numbers.

S. aureus Newman was used in the pigment extraction absorbance assay (Fig 6.1) to compare the relative effect of squalene and ethanol. From the spectral analysis, the characteristic peaks of absorbance due to staphyloxanthin reduced with increasing ethanol indicating a concentration-dependent effect of ethanol on staphylococcal pigmentation. The spectra for ethanol treatment was remarkably consistent with the spectra for squalene, suggesting they may share similar mechanisms to influence the pigment level of *S. aureus*, although the molar equivalents of each organic compound differed in the assay

As described, staphyloxanthin plays an important role in resistance to oxidative stressors, such as H_2O_2. Antioxidant properties derive from multiple conjugated bonds of STX that enable it to eliminate singlet oxygen. Therefore, it was hypothesised that reduced pigmentation by treatment with ethanol would increase the cell's susceptibility to H_2O_2. In contrast, *S. epidermidis* lacks the ability to produce any pigment, which would leave resistance unaffected by treatment with ethanol, when applying the same test.

(a)

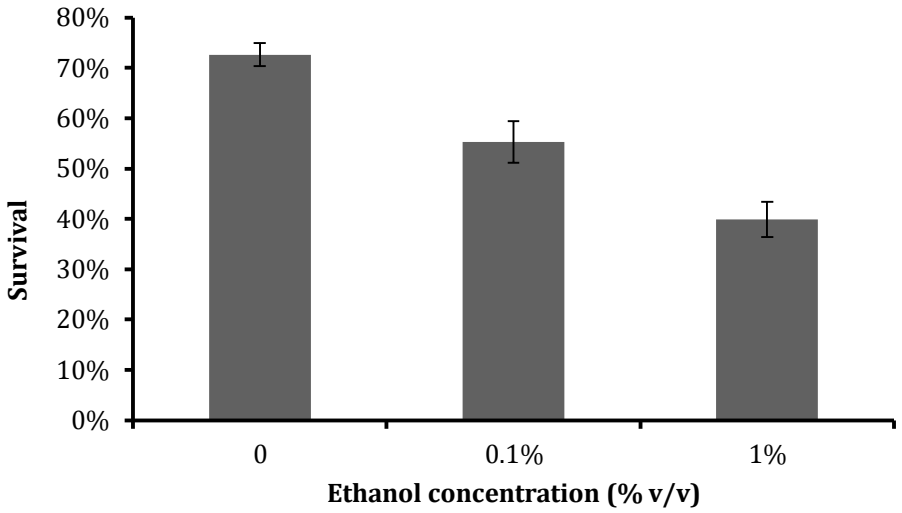

(b)

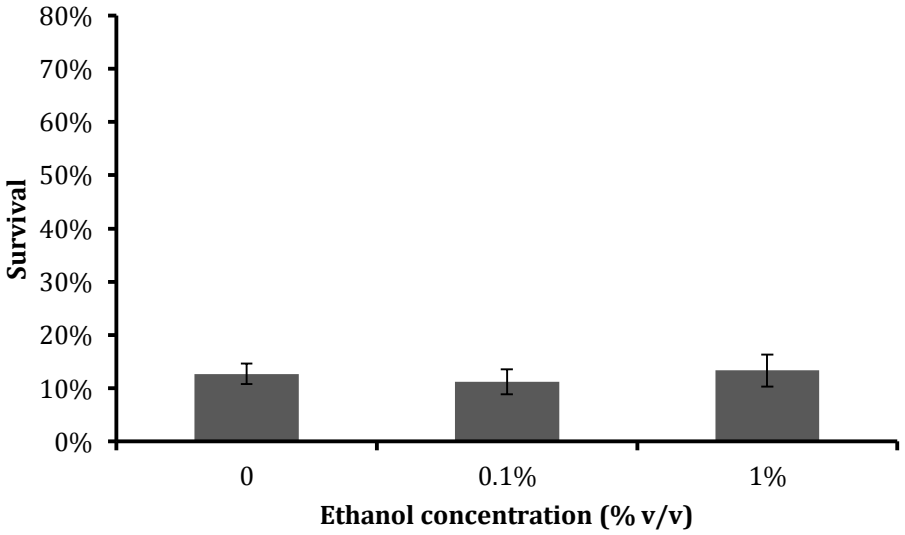

Figure 6.2 Survival of *S. aureus* Newman and *S. epidermidis* Tü3298 cells cultured with different concentrations of ethanol prior to challenge with H_2O_2. Cells were cultured with the indicated concentrations of ethanol for 24 h. Cells were washed twice with PBS and diluted to an OD_{600} of 0.1. Viable Cell counts were performed at time zero and 90 min after challenge with of 7.5 mM. H_2O_2. *S. aureus* Newman is indicated as (a), while (b) represents *S. epidermidis* Tü3298. Three replicate experiments were performed.

The susceptibility of *S. aureus* and *S. epidermidis* to challenge with H_2O_2 was assayed. Cells of both species were left untreated or treated with 0.1 or 1% v/v of ethanol for 24 h and equal numbers of washed cells for each sample were challenged with H_2O_2 for 90 min. The results support the hypothesis and were almost identical to the results gained from squalene survival limitation to peroxide in chapter 3 (Fig 6.2). For *S. aureus*, cells treated with the highest concentration of ethanol (1 % v/v) showed lowest survival levels (~40 %), compared with 0.1 % (v/v) of ethanol, which caused 20 % loss of survival relative to untreated control. This difference was significant assessed by student's t-test ($p<0.001$). However, there was no significant difference in susceptibility across increasing concentrations of ethanol of *S. epidermidis,* whose resistance to peroxide was unaffected by ethanol at either concentration (student's t-test, $p>0.5$).

6.3.2 RNA quality control

Having confirmed the ethanol induced reduction in *S. aureus* pigmentation, RNA-Seq was performed on ethanol challenged and control cultures of *S. aureus* Newman to determine the transcriptional response of *S. aureus* to ethanol. Cultures were challenged with 1% (v/v) ethanol during the mid-logarithmic phase of growth (OD_{600}=0.5), as this ethanol concentration caused distinct change in pigmentation level (Fig 6.1) but without inducing large survival pressure (Fried and Novick, 1973; Bowles and Ellefson, 1985; Chatterjee *et al*., 2006). After 20 min challenge, RNA was stabilised using RNAlater (Qiagen) and incubated overnight at 4 °C. Total RNA was then purified from cells the next day using the method described in chapter 2 (section 2.7).

RNA samples for RNA-Seq met the strict quality criteria for submission to the Centre for Genome Research (CGR), University of Liverpool. The required quality and quantity of the RNA samples were above the minimum threshold concentration of 30 ng μl^{-1} and the yields greater than the 3 µg required. These parameters were determined by Qubit fluorometric quantitation reads (Table 6.1). Sufficient intact RNA was confirmed using an Agilent bioanalyser by verifying RNA integrity (RIN) scores >7.0 and low evidence of degradation on the output traces (Fig 6.3).

Table 6.1 Quality control assessment.

Purity of samples was measured by NanoDrop and concentration was assessed by Qubit. RNA integrity was tested via bioanalyser. RIN=RNA integrity number, C=control condition, E=ethanol challenge condition.

Species	Sample	Nanodrop 260/280	Nanodrop 260/230	Concentration ng µl-1	Sample volume (µl)	RIN
S. aureus	C1	2.2	2.2	794.0	5.0	7.4
	C2	2.1	2.0	421.0	10.0	7.8
	C3	2.2	1.8	810.0	5.0	7.8
	E1	2.3	1.8	770.0	7.0	8.7
	E2	2.2	2.4	554.0	7.0	8.6
	E3	2.2	2.0	632.0	7.0	8.8

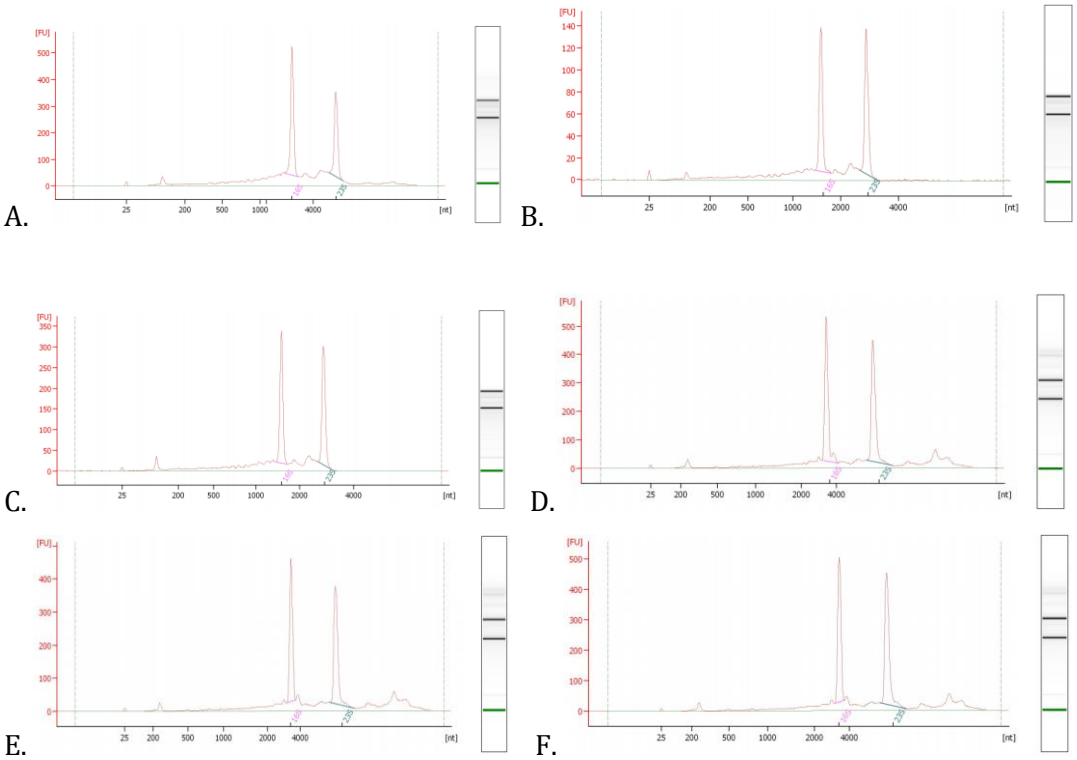

Figure 6.3 Bioanalyser traces of RNA samples submitted for sequencing. The visual output for the determined RNA integrity using the Agilent bioanalyser showed the characteristic profiles for purified, intact RNA with expected levels of particular sizes of RNA. The pronounced two large peaks indicates the presence of 23S and 16S RNA and other small peaks suggest their degradation. The three bands in the gel images on the right show the presence of 23S RNA, 16S RNA and the assay marker. *S. aureus* control condition: A, B and C; *S. aureus* ethanol challenge condition: D, E and F.

6.3.3 The transcriptional response to ethanol of *S. aureus* Newman and its comparison with the response to squalene

After RNA sequencing, sequence reads were analysed and processed first by the CGR resulting in an output table of statistically significantly DE genes of *S. aureus* Newman between the control and ethanol-treated samples. The method was outlined in Chapter 2. These DE genes for ethanol challenge were then compared with the DE genes identified in transcriptional data for squalene challenge, which enabled identification of the similarities and differences between the two treatments.

In response to ethanol challenge, 368 genes of *S. aureus* Newman were significantly DE, which is 14 % of total protein coding genes across the genome. The majority of the DE genes (303 genes) were altered by more than 1 $\log_2$ (2 fold), indicating that there was a major response to ethanol challenge. Of the 368 DE genes, 108 (29.3 %) were found up-regulated and 260 (70.7 %) were down-regulated.

When comparing these ethanol data with the transcriptional data for squalene challenge, there were 305 DE genes presented in both datasets (Fig 6.2). Surprisingly, of these 305 DE genes in both treatments, only 5 were regulated in the opposite direction (conserved hypothetical protein NWMN_2545, drug resistance transporter NWMN_2253, ferrichrome ABC transporter *sstD*, conserved hypothetical protein NWMN_2254 and conserved hypothetical protein NWMN_0048), which indicated the responses to squalene and ethanol of *S. aureus* shared spectacular consistency. Of note, this includes the genes for pigment biosynthesis, however it did exclude the up-regulation of genes associated with Fur-iron uptake regulon observed in the squalene challenge dataset.

Tabulated details of the DE genes are provided in Appendix Table 3.

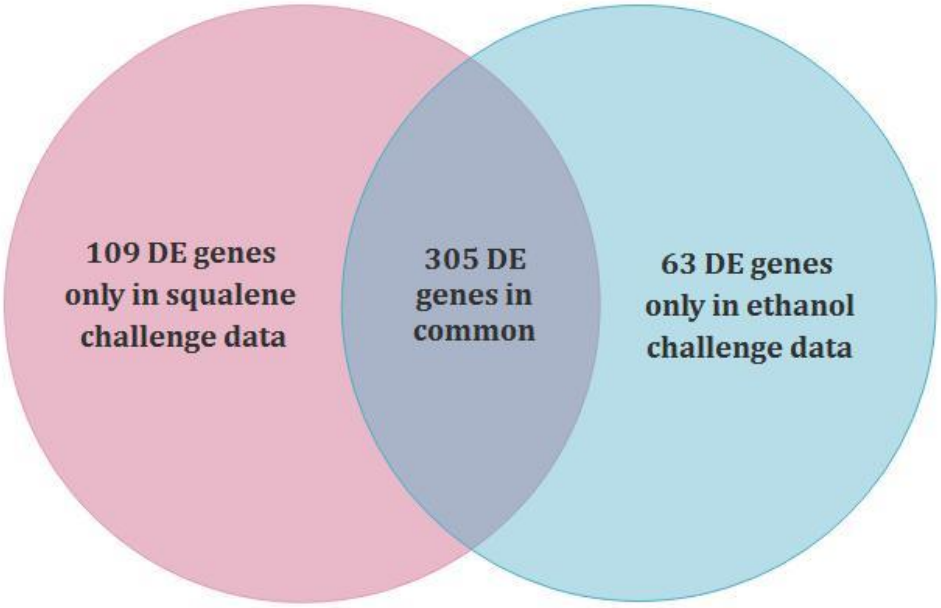

Figure 6.4 Comparison of DE genes in *S. aureus* Newman between squalene challenge and ethanol challenge.

There were 414 DE genes found in transcriptional data for squalene challenge, while 368 DE genes were found for ethanol challenge, and 305 genes shared DE in both treatments.

6.3.4 Comparison of DE COGs

Clusters of orthologous group (COG) enrichment analysis was performed to assess the cellular pathways that were most affected in response to ethanol challenge for *S. aureus*. The most frequent COG classes that DE genes were assigned to was determined by using the WebMGA, bespoke perl scripts and the IMG database as detailed in chapter 2 (section 2.7.9). if it is assumed that DE genes are evenly distributed across the genome, the theoretical number of DE genes in each COG class could be calculated as they should be proportional to the number of genes encoded by the genome in that class. Thus COGs analysis will reveal whether the actual numbers of DE genes in these orthologous classes are higher or lower than the calculated number.

(a)

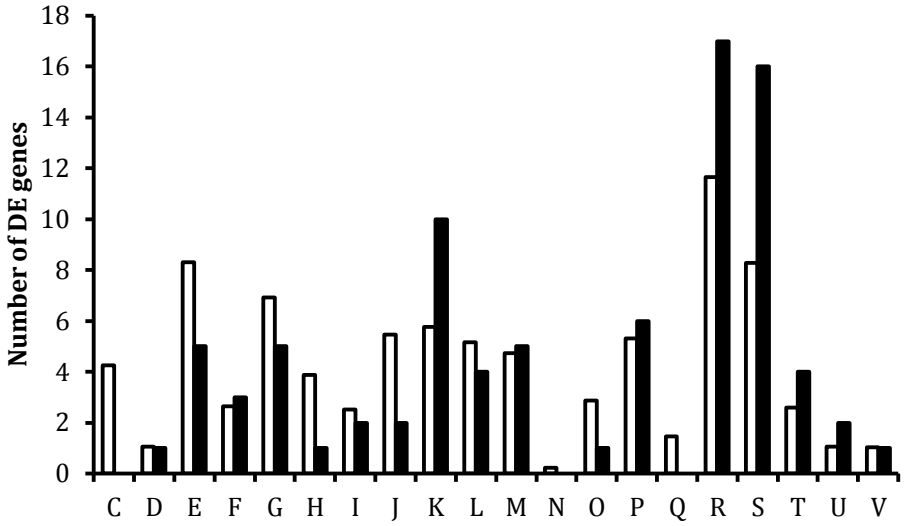

(b)

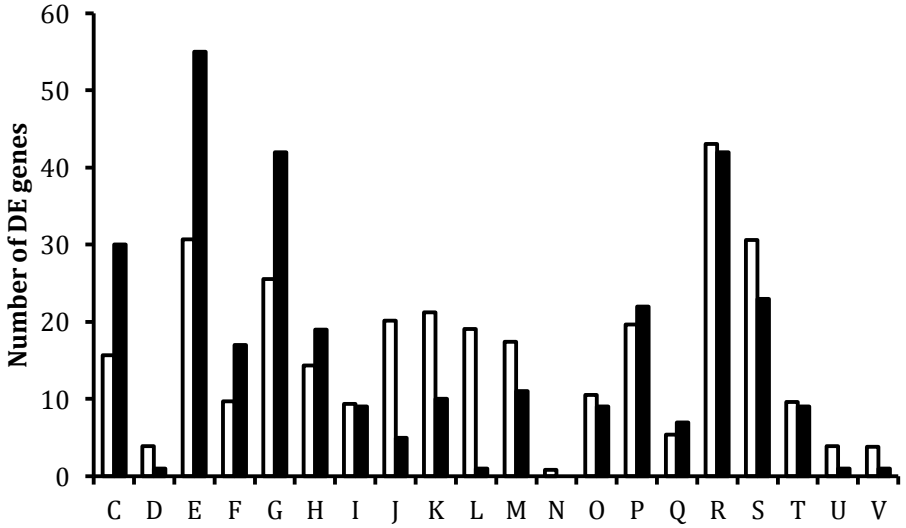

Figure 6.5 Numbers of *S. aureus* Newman DE genes in response to ethanol challenge per COG class. Comparison of numbers of DE genes between the theoretical (white bars) and the observed (black bars) per COG class for up-regulated DE genes (a) and down-regulated DE genes (b). The number of the theoretical DE genes per class was calculated with an assumption that expression was uniform across the genome. Genes were assigned to a COG class using WebMGA, the number of DE genes in each class were then calculated using a bespoke Perl script. C: Energy production and conversion; D: Cell cycle control, cell division, chromosome partitioning; E: Amino acid transport and metabolism; F: Nucleotide transport and metabolism; G: Carbohydrate transport and metabolism; H: Coenzyme transport and metabolism; I: Lipid transport and metabolism; J: Translation, ribosomal structure and biogenesis; K: Transcription;

L: Replication, recombination and repair; M: Cell wall/membrane/envelope biogenesis; O: Posttranslational modification, protein turnover, chaperones; P: Inorganic ion transport and metabolism; Q: Secondary metabolites biosynthesis, transport and catabolism; R: General function prediction only; S: Function unknown; T: Signal transduction mechanisms; U: Intracellular trafficking, secretion, and vesicular transport; V: Defence mechanisms.

COG analysis revealed that challenge with ethanol of *S. aureus* resulted in COG classes K (transcription), R (general function prediction only), S (function unknown), T (signal transduction mechanisms) and U (intracellular trafficking, secretion, and vesicular transport) with greater numbers of up-regulated genes than the theoretical number (Fig 6.5). While COG classes C (energy production and conversion), E (amino acid transport and metabolism), G (carbohydrate transport and metabolism), H (coenzyme transport and metabolism), J (translation, ribosomal structure and biogenesis), I (lipid transport and metabolism), L (replication, recombination and repair), O (posttranslational modification, protein turnover, chaperones), and Q (secondary metabolites biosynthesis, transport and catabolism) were found to have fewer up-regulated genes than the theoretical number. For down-regulated genes, COG classes C, E, F (nucleotide transport and metabolism), G, and H were found to have more down-regulated genes than expected, and COG classes D (cell cycle control, cell division, chromosome partitioning), J, K, L, M (cell wall/membrane/envelope biogenesis), O, and S exhibited fewer down-regulated genes than the theoretical number. In most cases, COG classes having more up-regulated genes than expected were shown to have less down-regulated genes than the theoretical number. However, COG classes J (translation, ribosomal structure and biogenesis) and L (replication, recombination and repair) revealed fewer DE genes than the theoretical number for both up- and down-regulated genes, which exhibited the same transcription pattern observed in DE COGs of the squalene challenge transcriptome. This suggests that treatment with both squalene and ethanol has limited influence upon the expression of genes involved in these two functional classes.

When comparing with DE COGs for squalene challenge (Fig 4.3), greater numbers of genes in general function prediction only (R), and function unknown (S) were up-regulated for both treatments, indicating there is likely to be a common global response to ethanol and squalene. This response remains uncharacterised in *S. aureus*. Both treatments resulted in greater numbers of down-regulated genes in energy production and conversion (C), amino acid transport and metabolism (E), carbohydrate transport and metabolism (G), and coenzyme transport and metabolism (H), suggesting challenge with both ethanol and squalene lowers the metabolism level of *S. aureus*.

To compare the effects between two treatments on each COG class, the percentage of the DE genes per COG class was calculated (Fig 6.6). For up-regulated DE genes, squalene challenge resulted in more DE genes than ethanol challenge in almost all COG classes except L (replication, recombination and repair) and T (Signal transduction mechanisms). On the contrary, ethanol challenge resulted in more down regulated DE genes than squalene challenge in most COG class except K (transcription) and L. The differences in the number of DE genes in COG class of replication, recombination and repair and signal transduction mechanisms between two treatments may suggest the sensing pathways in *S. aureus* in response to ethanol and squalene are different.

(a)

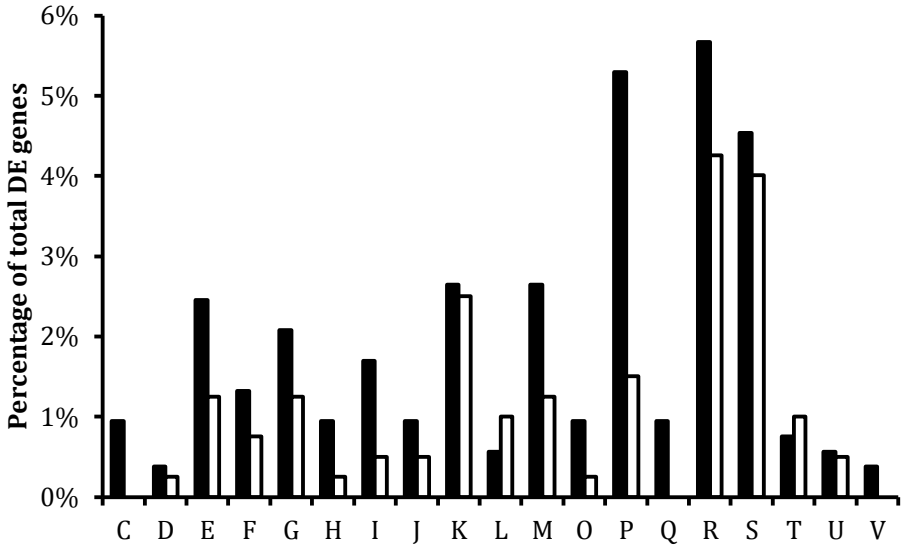

(b)

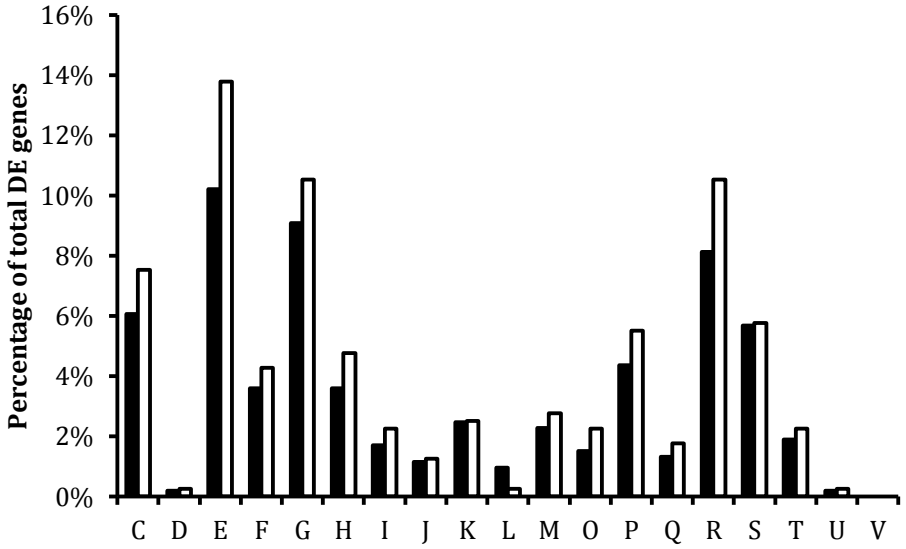

Figure 6.6 Comparison of the percentage of the DE genes in response to squalene (black bars) or ethanol challenge (white bars) per COG class for up-regulated DE genes (a) and down-regulated DE genes (b). Genes were assigned to a COG class using WebMGA, the number of DE genes in each class were then calculated using a bespoke Perl script. C: Energy production and conversion; D: Cell cycle control, cell division, chromosome partitioning; E: Amino acid transport and metabolism; F: Nucleotide transport and metabolism; G: Carbohydrate transport and metabolism; H: Coenzyme transport and metabolism; I: Lipid transport and metabolism; J: Translation, ribosomal structure and biogenesis; K: Transcription; L: Replication, recombination and repair; M: Cell wall/membrane/envelope biogenesis; O: Posttranslational modification,

protein turnover, chaperones; P: Inorganic ion transport and metabolism; Q: Secondary metabolites biosynthesis, transport and catabolism; R: General function prediction only; S: Function unknown; T: Signal transduction mechanisms; U: Intracellular trafficking, secretion, and vesicular transport; V: Defence mechanisms.

6.3.5 Comparison of DE metabolic pathways

KEGG mapper (version 2.1) search & colour was also applied to the ethanol challenge transcriptome data. This program was executed using the lists of DE genes produced by the CGR. From the analysis, 238 DE genes (54.6 %) of *S. aureus* Newman were not assigned into any pathways. This is due to incomplete pathway annotation for staphylococci to date, together with unknown functions of genes. The annotated metabolic pathway genes within the ethanol challenge transcriptome were compared with those of the squalene challenge transcriptome generated in chapter 4. The hypothesis was that analysis of these DE genes and pathways that contribute to known metabolic processes would reveal speculative mechanisms for the effect of ethanol on *S. aureus* metabolism.

Both treatments exhibited great consistency of down-regulation of genes involved in energy production (Table 6.2). This consistency is not only reflected in the directional trend of regulation, but also the extent (fold-level) of differential expression. The clear stand out pathways and trends with this overlap include: reduced level of glycolysis (*glcA, tpi, gapA, pgk, gpmA, pckA* and *aldA*); decreased pentose, fructose, mannose, and galactose metabolism (*gntK*, *NWMN_0083*, *mtlF, mtlA, mtlD, fruB, fruA,* and *malA*), and declined pyruvate, propanoate, and butanoate metabolism (*NWMN_2459*, *poxB, fumC, alsD, ilvB, sdhA, sdhB, sucA,* and *sucB*). Overall, a trend in regulation is observed that reveals decreased energy production in response to both ethanol and squalene challenge.

Table 6.2 Ethanol and squalene regulated DE genes involved in energy production pathways in *S. aureus* Newman.

DE genes highlighted by KEGG mapper analysis and their level of $\log_2$ fold change in *S. aureus* Newman are shown. Genes that were not DE in one treatment are indicated by a dash in the relevant fold change column. KEGG mapper output pathways relevant to this table were glycolysis/gluconeogenesis, pentose phosphate pathway, fructose and mannose metabolism, galactose metabolism, amino sugar and nucleotide sugar metabolism, pyruvate metabolism, propanoate metabolism, and butanoate metabolism.

Gene name	Fold change (log2)	
	Ethanol challenge	Squalene challenge
Glycolysis		
glcA	-0.72	-1.35
ptsG	-	-1.37
tpi	-0.85	-1.07
gapA	-1.21	-1.08
pgk	-1.55	-0.89
gpmA	-1.52	-1.83
pckA	-1.11	-1.41
aldA	-1.52	-1.28
Pentose, fructose, mannose, and galactose metabolism		
gntK	-1.21	-1.53
NWMN_0083	-1.09	-1.01
mtlF	-1.38	-1.58
mtlA	-1.90	-1.56
mtlD	-1.45	-1.43
fruB	-2.07	-2.19
fruA	-2.05	-2.64

malA	-1.16	-1.33
lacA	-1.33	-1.89
mnaA	-1.05	-0.87
Pyruvate, propanoate, and butanoate metabolism		
NWMN_2459	-0.99	-
poxB	-1.63	-1.43
fumC	-0.75	-0.94
alsD	-2.19	-2.13
ilvB	-1.71	-0.99
sdhA	-1.14	-1.55
sdhB	-0.65	-2.04
sucA	-1.59	-1.57
sucB	-1.07	-1.24

Overall, the expression of genes involved in ammonia production was down-regulated in both treatments, and it was more pronounced with ethanol challenge (Table 6.3). In the ethanol challenge transcriptome, down-regulation of the *nrdG, narI*, *purF, purD, purN, purQ, purL, purM,* and *purH* genes associated with purine biosynthesis is indicative that *S .aureus* cells reduced their production of purine and ammonia. This response together with the down-regulation of genes that would reduce the pool of ammonia, including argininosuccinate synthase (*argG*) and argininosuccinate lyase (*argH*) suggest a homeostatic mechanism due to reduced ammonia production, which was also observed in the squalene challenge transcriptomic data (Table 4.3).

Table 6.3 Ethanol and squalene regulated DE genes involved in ammonia production pathways in *S. aureus* Newman.

DE genes highlighted by KEGG mapper analysis and the level of log_2 fold change in *S. aureus* Newman are shown. Genes that were not DE in one treatment are indicated by a dash in the relevant fold change column. KEGG mapper output pathways relevant to this table were purine metabolism, arginine and proline metabolism, and nitrogen metabolism.

Gene name	Fold change (log2)	
	Ethanol	Squalene
nrdG	-1.98	-2.09
narI	-2.47	-2.27
narJ	-4.10	-4.33
narH	-4.22	-4.67
purF	-2.20	-0.92
purD	-1.39	-
purN	-1.51	-
purQ	-1.45	-0.72
purL	-1.84	-0.94
purM	-1.78	-
purH	-1.38	-
nrdD	-1.28	-1.62
NWMN_2454	-1.36	-1.04
putA	-2.58	-2.82
argH	-2.19	-2.14
argG	-2.28	-2.52

Table 6.4 Ethanol and squalene regulated DE genes involved in amino acids metabolism pathways in *S. aureus* Newman.

DE genes highlighted by KEGG mapper analysis and the level of log_2 fold change in *S. aureus* Newman are shown. Genes that were not DE in one treatment are indicated by a dash in the relevant fold change column. KEGG mapper output pathways relevant to this table were histidine metabolism, glycine, serine and threonine metabolism, cysteine and methionine metabolism, lysine biosynthesis, valine, leucine and isoleucine biosynthesis and alanine, aspartate and glutamate metabolism.

Gene name	Fold change (log2)	
	Ethanol	Squalene
hisIE	-1.16	-
hisH	-1.57	-
hisB	-1.35	-
hisD	-1.10	-
hutG	-0.92	-1.52
sdhA	-1.14	-1.55
sdhB	-0.65	-2.04
leuD	-1.34	-
leuC	-1.12	-
leuB	-1.35	-
leuA	-1.55	-
ilvA	-0.98	-
trpB	-1.93	-
metB	0.78	0.90
metL	-1.36	-0.79
thrA	-1.75	-1.40

thrB	-1.39	-
thrC	-1.08	-0.88
lysC	-2.87	-
asd	-2.42	-1.02
cysM	1.23	1.64
dapA	-2.45	-
dapB	-1.98	-
dapD	-1.82	-
pyrAA	-2.21	-2.47
pyrB	-2.21	-2.54
argH	-2.14	-2.19
argG	-2.52	-2.28
gltB	-0.98	-
NWMN_2454	-1.36	-1.04

The overall expression of genes involved in amino acid metabolism was down-regulated, but with the exceptions of *metB* and *cysM* (Table 6.4). Both genes are associated with cysteine biosynthesis, which indicates that challenge with either ethanol or squalene elevates cysteine/sulphur metabolism. A reduction in transcription of biosynthetic genes of other amino acids was more apparent in the ethanol challenge dataset. Down-regulated expression of genes involved in production of histidine (*hisIE, hisH, hisB, hisD*), leucine (*leuD, leuC, leuB, leuA*), isoleucine and valine (*ilvA*), lysine (*dapA, dapB, dapD*) and glutamate (*gltB*) was only determined after ethanol challenge. Furthermore, although no up-regulated genes associated with serine biosynthesis were identified, genes facilitating serine degradation (*sdhA, sdhB*) were down-regulated, indicating potential for conservation of serine levels in *S. aureus* cells.

The overlap of both stimuli was also observed with expression of virulence genes, whereby ethanol challenge exhibited the same trend as squalene challenge, although it was more pronounced after squalene challenge (Table 6.5). The majority of DE virulence factor genes were up-regulated after both challenges, including: *isdA* that has been described to increase cell hydrophobicity independent of its role in haem iron acquisition (Clarke *et al*., 2007); those encoding enzymes that specifically target leukocytes, such as *lukS*, *lukF*, *hlgB*, and *hlgC*; and *fnbB* encoding a cell surface-associated protein with a role in tissue adhesion specificity,. plus a series of genes encoding or predicted to encode immune evasion determinants including *ssl2nm, ssl3nm, ssl4nm, ssl5nm, ssl9nm, ssl6* (Omoe *et al*., 2004; Orwin *et al*., 2001; Niedergang *et al*., 1995). This suggests that both ethanol and squalene challenges induce survival/invasion responses of *S. aureus*.

Table 6.5 Ethanol and squalene regulated DE virulence factor genes involved in amino acids metabolism pathways in *S. aureus* Newman. DE genes highlighted by KEGG mapper analysis and the level of log_2 fold change in *S. aureus* Newman are shown. Genes that were not DE in one treatment are indicated by a dash in the relevant fold change column. KEGG mapper output pathways relevant to this table was *S. aureus* infection.

Gene name	Fold change (log2)	
	Ethanol	Squalene
clfA	-1.14	-1.17
sbi	1.19	1.00
sdrC	-	0.90
sdrD	-	1.51
lukS	1.07	1.82
lukF	-	1.54
hlgB	1.02	1.81
hlgC	1.00	1.74
NWMN_1503	-	1.44
ssl2nm	2.09	1.52
ssl3nm	2.11	1.35
ssl4nm	1.88	1.35
ssl5nm	1.60	1.27
ssl9nm	1.31	1.25
ssl6	1.33	1.09
isdA	-	1.61
NWMN_0165	1.23	-
fnbB	1.42	1.91

6.3.6 Ethanol transcriptome and *S. aureus* pigmentation

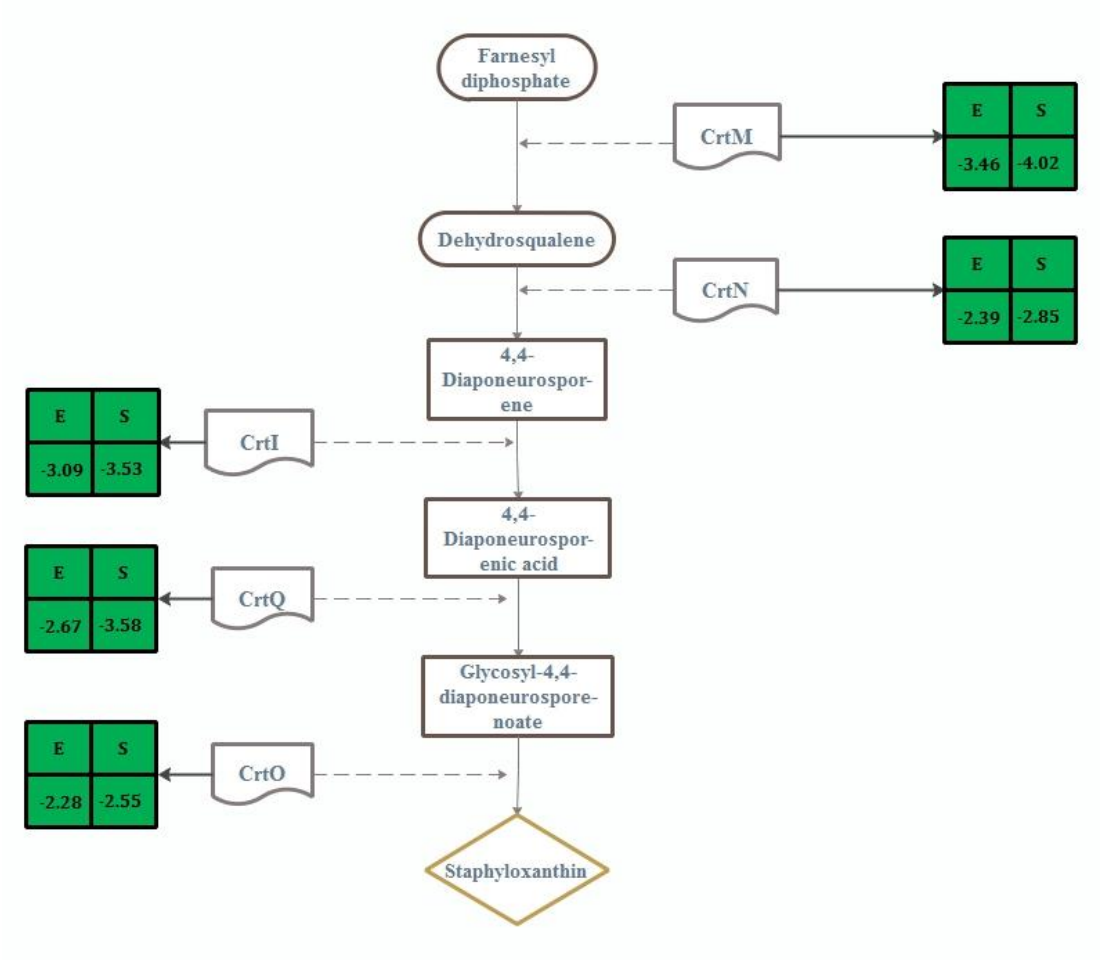

Figure 6.7 DE genes of the staphyloxanthin biosynthetic pathway in response to squalene or ethanol challenge in *S. aureus* Newman. In each box linked to the respective enzymes, the transcription changes relative to the control are shown as fold number. Green boxes represent the respective transcript was significantly down-regulated. Ethanol transcriptome data values are labelled E with S for the squalene transcriptome data. CrtO, NWMN_2465; CrtI, NWMN_2464; CrtQ, NWMN_2463; CrtM, NWMN_2462; CrtN, NWMN_2461.

In this chapter, it was confirmed that ethanol has a negative effect on pigment expression of *S. aureus* (Fig 6.1). And further investigation determined that this reduced level of pigmentation resulted in increased susceptibility of *S. aureus* to H_2O_2 (Fig 6.2). Since staphyloxanthin (STX) is produced via the *crt* operon in most staphylococci, the decreased expression of *crt* genes was expected to be evident in the transcriptomic data of *S. aureus* cells challenged with squalene.

As predicted, five genes in *crt* operon encoding enzymes in staphyloxanthin biosynthesis, *crtM, crtN, crtI, crtQ, and crtO* exhibited a decreased level of expression with the same trend as that observed after squalene challenge (Fig 6.7). This decline of expression explains the reduced cell pigmentation. Just as observed with squalene challenge, the gene expression of *sigB* remains unchanged, such that expression changes must either reflect changes to the activity of the RsbU, RsbV and RsbW modulators and anti-sigma factors that control the ability of SigmaB to direct transcription or it indicates there is another regulatory pathway modulating *crt* expression.

6.3.7 Quantitative PCR validation

Validation of the RNA-Seq data was performed by transcript quantification using qPCR for selected DE genes in the ethanol challenge RNA-Seq dataset. For each selected gene, the fold-changes in relative transcript abundance between control and ethanol challenge samples were determined and then compared with RNA-Seq data. At least three biological and two technical qPCR replicates were used for each gene. RNA integrity was assessed by gel electrophoresis prior to conversion to cDNA for qPCR.

The *S. aureus crtM*, *crtI*, *lytR*, and *fnbB* transcript levels were assessed for comparison. Collectively these genes are representative of carotenoid biosynthesis, autolysin regulation and virulence factors. All primers chosen were determined to have amplification efficiency values above 90 % and gave products of approximately 150 bp. The primers and their efficiency values are shown in Table 6.6.

Table 6.6 Primers for qPCR

Gene name	Primer sequences	Efficiency (%)	Reference
crtI	F- CCGGCAAGCTCAGGATATGT	92.2	This study
	R-TACTGGCGCTTGTGTGTGAT		
crtM	F- CGTAGAATCATGATGGCGCTTC	91.3	This study
	R- CCGAATAATTCAGCGTCCGT		
fnbB	F- CTCATGGTATCTCAACACTGC	90.4	This study
	R- TGCGTCACTGTTGTAGGATC		
lytR	F- GCAACTGCACATGACCAATAC	90.2	This study
	R- TCGCCGACATATCATTCGC		

The fold changes determined from the qPCR data showed good agreement with RNA-Seq (Fig 6.8), where the down-regulation of *crtM* and *crtI* and up-regulation of *fnbB* and *lytR* were both observed in qPCR results. All fold changes showed broadly similar values as those determined in RNA-Seq data. However, values of qPCR data were consistently lower than the fold changes from RNA-Seq. This phenomenon may reflect the different methods of testing between the two technologies and underestimation of gene expression by qPCR. Overall, the data from qPCR supports the differential expression changes in the RNAseq dataset.

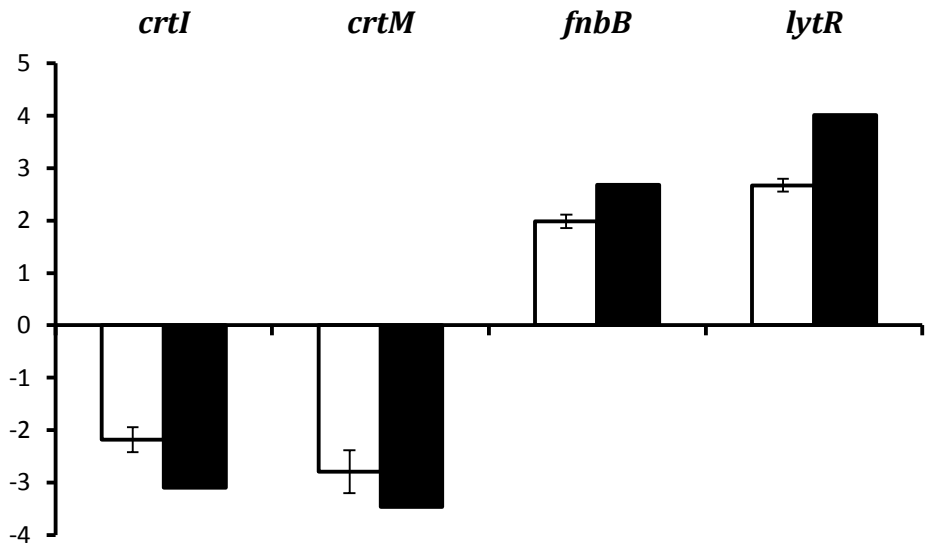

Figure 6.8 Differential expression of *crtI, crtM*, *fnbB* and *lytR* in *S. aureus* after challenge with ethanol, assessed by qPCR. Black bars indicate the fold change in gene expression from RNA-Seq data while white bars indicate fold change in gene expression from qPCR data. Error bars were determined from three replicate experiments.

6.3.8 Experimental evolution of *S. aureus* with ethanol selection

The selection of genetic mutations that confer an increased resistance of *S. aureus* to ethanol was achieved through passage in broth containing 6 % (v/v) ethanol as this concentration of ethanol induced a sub-bactericidal effect on *S. aureus* allowing limited growth. Use of pooled samples containing the genomes from selected isolates with increased resistance was applied in this study. The pool and their parental strain were sequenced to identify Single Nucleotide Polymorphisms (SNPs) and Insertions and Deletions (INDELs) associated with the increased resistance. Sequencing of pools enables more isolates to be sequenced without additional costs, and may reveal more SNPs and INDELs. In addition, high frequency of a SNP in multiple isolates within the pool is identified by a high proportion of variance at a particular position and this indicates the SNP is more likely to be involved in resistance.

The wild-type strain, *S. aureus* Newman was passaged by repeated incubations in broth containing 6 % (v/v) ethanol in 24 h batch cultures for 14 d. From the second day forward, cells that were cultured for 24 h with ethanol were diluted to OD_{600} reading of 0.02 and added into fresh broth with the same concentration of ethanol. A control culture was also conducted using the same method with passage of the parental stain for 14 days in broth without ethanol. Any genetic variance, such as SNPs in the control culture would help to rule out any mutations selected during continuous culture in the broth over 14 d. The passages were performed in duplicate experiments. By the end of the 14 passages, 6 isolates (3 from squalene passage, 3 from broth passage) from each duplicate experiment were picked and their genomic DNA was extracted and equal amounts of each clone was added to make a DNA pool for sequencing.

6.3.9 Susceptibility of experimentally evolved isolates to ethanol

At the end of the passages, the growth curves of selected isolates were measured to verify that resistance to ethanol was elevated after experimental evolution. To achieve this, 3 isolates from the ethanol passage and 3 isolates of control passage (no ethanol) were selected from each duplicate and these isolates together with a parental Newman control were cultured in BHI with 6 % (v/v) ethanol and their growth was recorded by absorbance measurement (Fig 6.9).

(a)

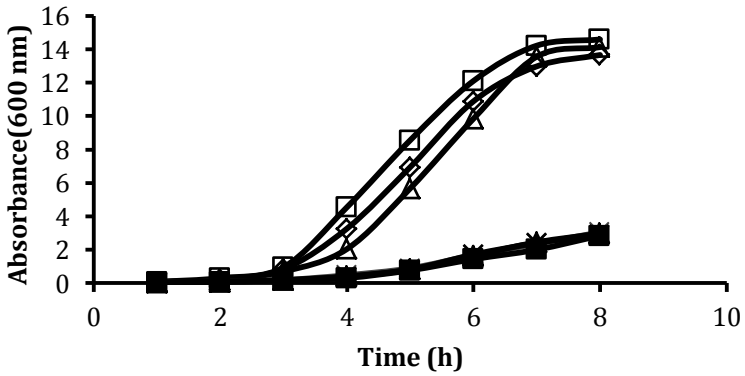

(b)

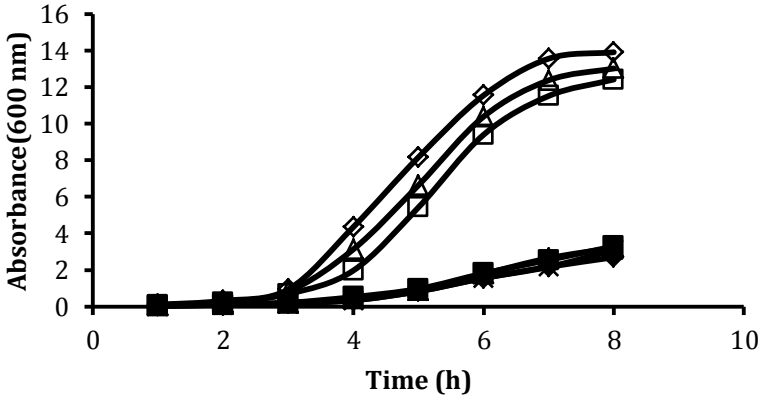

Figure 6.9 Growth curves of selected isolates cultured in BHI with 6 % (v/v) ethanol for first (a) and second (b) duplicate experiments. Open diamond, square and triangle: three isolates from ethanol passage. Closed diamond, square and triangle: three isolates of control passage (no ethanol). Cross: parental *S. aureus* Newman strain that has not undergone any passages.

The growth curve data confirmed that the isolates from ethanol selection cultures exhibited greatly increased growth rates and yield compared with isolates chosen from cultures without ethanol selection. The growth yield values of ethanol selection isolates (open diamond, square and triangle) after 8 h of culture was over four times greater than broth only control isolates (closed diamond, square and triangle) and the parental strain. These differences in growth support that increased resistance was due to evolution of fixed genetic changes in response to sub-bactericidal ethanol and not caused by selection to the BHI broth.

6.3.10 Sequencing QC and alignment

Sequencing of selected isolates was performed to determine SNPs and INDELs that account for changes in growth in the presence of ethanol. Prior to sequencing, DNA samples were assessed to ensure these were of sufficient quality and quantity for sequencing. All genome DNA samples used for sequencing should have minimal protein, salt and solvent contamination, and sufficient purity was indicated by 260/280 & 260/230 ratios greater than 1.8 (Table 6.7). DNA samples were also visualised by gel electrophoresis to confirm the integrity of the DNA was suitable (Fig 6.10).

DNA from the chosen isolates was sequenced and the reads were aligned to the reference Newman genome. After alignment, SNPs and INDELs were called and filtered using a bespoke perl script, which utilised the SNPEff version 3.4e open source software. SNPs and INDELs that were synonymous or intergenic and more than 200 bp upstream of a transcriptional start site were filtered out. A second bespoke perl script was used to filter SNPs or INDELs identical to any found in either of the controls of the parental strain or the pool of no ethanol passage isolates. After filtering twice, the remaining SNPs and INDELs were considered candidates for loci affecting resistance.

Table 6.7 Quality control analysis results for DNA samples of *S. aureus* Newman submitted for sequencing.

Data of the quality checks performed prior to DNA sequencing. Concentrations and 260/280 and 260/230 absorbance reading were assessed by Qubit and Nanodrop, respectively. C0: parental *S. aureus* Newman strain without passage; C1: passage without ethanol; E: passage with ethanol. C1 and E were made as pools consisting of 6 genomes from selected isolates with the same amount of DNA.

Strain	Sample	Nanodrop 260/280	Nanodrop 260/230	Concentration ng µl-1	Sample volume (µl)
***S. aureus* Newman**	C0	1.9	2.3	102.6	19.5
	C1	1.9	2.2	83.9	23.8
	E	2.1	2.3	99.5	20.0

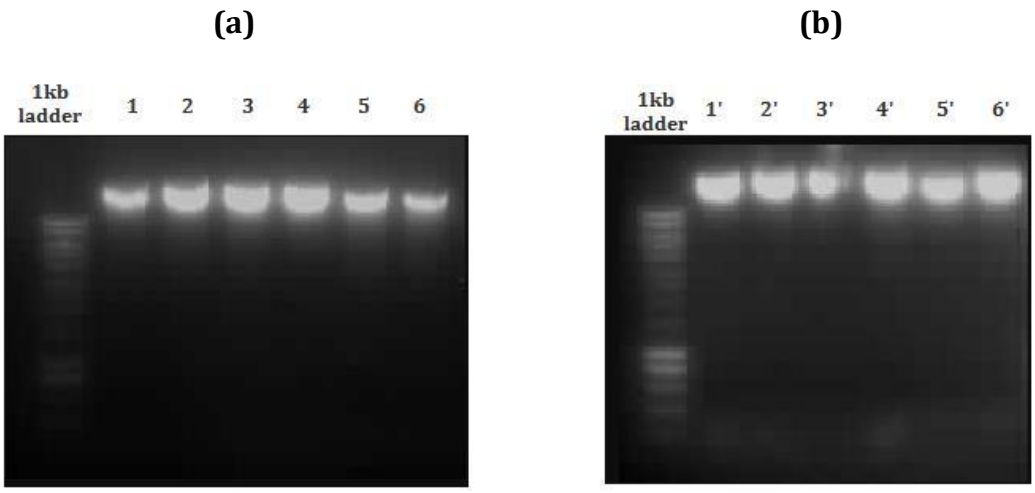

Figure 6.10 Gel electrophoresis of purified genome DNA of selected isolates from the first (a) and replicate (b) passage.

Isolates 1-3 (a) and isolates 1'-3' (b) selected from ethanol passage. Isolates 4-6 (and isolates 4'-6') were picked from broth only passage (without ethanol). No apparent sign of degradation was observed, indicating the genomes of these isolates were intact.

6.3.11 *S. aureus* Newman ethanol selected SNPs

As described above, *S. aureus* Newman isolates experimentally evolved with ethanol exhibited increase ability to grow at elevated ethanol concentration compared with isolates cultured in the absence of ethanol or the parental isolate. Filtering was done that would remove any DNA sequences identified by SNPEff that were synonymous or intergenic (more than 200 bp upstream of a transcriptional start site), or identical to the parental strain or no ethanol isolates. As a result, it revealed three non-synonymous SNPs that includes one coding SNP, and two SNPs within the upstream regulatory region of a gene (Table 6.8). The SNP in *dapD* presents in all the reads of the pool, while the other two intergenic SNPs present approximately 83 % of the reads of the pool, indicating approximately 5 of the 6 pooled isolates had these SNPs.

The genic SNP is located in *dapD* (DapD A219E), leading to the non-conservative amino acid replacement of the non-polar aliphatic alanine with the acidic, polar glutamic acid. DapD is a tetrahydrodipicolinate acetyltransferase that catalyses L-2,3,4,5-tetrahydrodipcolinate into N-Acetyl-L-2-amino-6-oxopimelate during L-lysine biosynthesis. This amino acid serves a wide variety of functions in the bacterial cell and lysine has a crucial role in biosynthesis of cell wall peptidoglycan (Jang *et al*., 2008).

Table 6.8 Non-synonymous SNPs from *S. aureus* Newman ethanol evolved isolates.

SNPs from ethanol selection of *S. aureus* Newman isolates were identified using a bespoke perl script. All mutations were confirmed by at least 6x coverage. Intergenic SNPs were included if they were less than 200 bases upstream of the predicted translational start site.

Gene name	Gene function	Position of change	Base change	Change	Position in protein
dapD	tetrahydrodipicolinate acetyltransferase	1441331	C->A	Substitution A/E	219/239 aa
NWMN_1774	conserved hypothetical protein	1986628	C->T	Upstream substitution	-10bp
NWMN_1774	conserved hypothetical protein	1986634	T->G	Upstream substitution	-16bp

Since DapD A219E potentially contributes to enhanced growth in the presence of ethanol resistance, protein modelling was attempted to examine the influence of the amino acid substitution. However, the structure of this protein is poorly understood. Only the first 87 residues have been assigned into secondary structure and the remainder of the residues remain uncharacterised. Since the SNP alters the protein sequence near the carboxyl end the amino acid substitution cannot be shown in a 3D model. Therefore it is very difficult to predict if DapD A219E lies within a domain and the effects it might cause. Should the substitution alter the catalytic efficiency of the enzyme this might alter pathway flux to counteract effects of ethanol on the cell.

If the amino acid substitution DapD A219E does not facilitate the increased growth of isolates in the presence of ethanol, the two intergenic SNPs upstream of *NWMN_1774* would be the sole explanation. These two SNPs are 10 bp and 16 bp upstream of the translational start site. Protein NWMN_1774 is annotated as being of unknown function containing the domain DUF2951 and has 99 amino acids. The protein appears to be specific to *S. aureus* and is phage-derived. NWMN_1774 is annotated as a transmembrane protein because of the presence of both alpha-helical transmembrane region and a membrane spanning region.

6.4 Discussion

Previous unpublished studies from the Horsburgh laboratory at Liverpool indicated that ethanol treatment caused a reduction in *S. aureus* pigmentation. Since a similar phenotype was revealed as a phenomenon caused by squalene treatment in this study, comparative investigation of the effects of ethanol and squalene on *S. aureus* was performed using transcriptomics. Firstly, in this chapter, pigment was extracted from *S. aureus* cells cultured in the presence or absence of ethanol. This experiment revealed that there was a negative relationship between ethanol treatment and bacterial pigmentation, and confirmed this correlation was concentration dependent. Like the experiment conducted on squalene, *S. aureus* cells cultured in the presence of ethanol showed susceptibility to H_2O_2 challenge was increased. These data matched the observation with squalene in chapter 3 and similarly fits with the hypothesis that staphyloxanthin contributes to resistance from oxidative stressors, such as H_2O_2, by scavenging free radicals with its conjugated double bonds (Liu *et al*., 2008; Götz *et al*., 2006).

Having established the similar effects of ethanol and squalene on *S. aureus* pigmentation, the transcriptional responses of *S. aureus* Newman to ethanol were determined and the results were compared with the squalene challenge transcriptional data obtained in chapter 4. The main aims were to compare the DE genes of *S. aureus* between ethanol and squalene challenge datasets to find potential clues for whether squalene and ethanol cause common transcriptional responses and what the mechanisms are in *S. aureus*.

Overall, it was revealed that there were more overlaps than divergence in transcriptional responses between ethanol and squalene. Approximately 80 % of DE genes found in ethanol challenge data were also DE in squalene challenge results, and the majority of them (90 %) also showed the same trend of regulation. This suggests ethanol and squalene, despite having different molecular structure and properties, is recognised as having underlying stimulus similarities which result in an analogous response from the bacteria.

The similarities of transcriptional response between ethanol and squalene challenge of *S. aureus* were revealed by analysis of both COG and KEGG metabolic pathways. Both treatments up-regulated more genes in general function prediction only, and function unknown categories, indicating there may be global responses that remaining uncharacterised in *S. aureus,* at least at the stimulus level. Both treatments down-regulated more genes in energy production and conversion, carbohydrate transport and metabolism, and coenzyme transport and metabolism, suggesting challenge with either ethanol or squalene induces decreased metabolism in *S. aureus*.

Analysis of the ethanol challenge transcription data overlaid to KEGG pathways revealed that the expression of DE genes ascribed to energy production, ammonia production, amino acid metabolism, and virulence factors all showed remarkable consistency with the expression profile of the squalene challenge transcriptome. These overlaps suggests that ethanol and squalene may largely trigger a common stimulus response of *S. aureus,* and this mechanism acts to manage bacterial energy levels. Neither stimulus appears to cause DNA or cell membrane damage, at least at the concentration used, since these processes almost remain unchanged.

Although most of the DE genes exhibited a consistent trend of regulation, there were still some differences, most likely due to the distinct molecular properties of ethanol and squalene. The largest difference in gene expression profile between ethanol and squalene challenge is the regulation of genes involved in iron acquisition. In chapter 4 and 5, both transcriptional data and *in vitro* experiments revealed that squalene caused iron starvation in *S. aureus* and *S. epidermidis* as determined by reduced intracellular iron concentration, leading to up-regulation of the numerous genes associated with iron uptake. However, such a large-scale trigger of derepression of iron uptake genes was absent in the ethanol transcriptome (Table 6.9). Among all the 28 DE genes identified in squalene transcriptional data, only two (*isdG* and *sdhB*) were DE with the same direction of regulation after ethanol challenge. This suggests that the cellular iron availability was not likely affected by ethanol treatment and distinguishes the cellular responses .

Table 6.9 Genes associated with iron metabolism revealed by the transcriptional data of squalene challenge and ethanol challenge. Among all the 28 DE genes identified in squalene transcriptional data, only 2 (*isdG* and *sdhB*) were DE with the same direction of regulation after ethanol challenge, indicating the intracellular iron availability was not affected by ethanol treatment.

Gene name	Description	Fold change in squalene transcriptome	Fold change in ethanol transcriptome
Genes involved in iron acquisition			
isdG	cytoplasmic heme-iron binding protein	4.08	2.05
NWMN_2081	biosynthesis of staphyloferrin A	3.81	Not DE
sbnD	membrane transporter protein	3.58	Not DE
isdC	iron-regulated cell surface protein	3.48	Not DE
sbnI	SbnI protein	3.41	Not DE
sbnH	diaminopimelate decarboxylase	3.36	Not DE
sirA	siderophore compound ABC transporter	3.20	Not DE
srtB	NPQTN-specific sortase B	3.12	Not DE
isdF	iron/heme permease	3.07	Not DE
isdA	iron-regulated heme-iron binding protein	3.05	Not DE
NWMN_2076	FecCD iron compound ABC transporter	3.03	Not DE
sbnG	2-dehydro-3-deoxyglucarate aldolase	2.97	Not DE
NWMN_2185	iron compound ABC transporter	2.83	Not DE
NWMN_0703	iron compound ABC transporter *sstB*	2.81	Not DE
sbnE	siderophore biosynthesis	2.81	Not DE
fhuB	ferrichrome transport permease	2.77	Not DE
sbnC	siderophore biosynthesis	2.69	Not DE
isdE	iron compound ABC transporter	2.66	Not DE
NWMN_0702	ferrichrome ABC transporter permease *sstA*	2.58	Not DE
NWMN_2078	ferrichrome ABC transporter lipoprotein	2.51	Not DE
sbnF	siderophore biosynthesis	2.50	Not DE

NWMN_0704	Iron ABC transporter ATP-binding protein *sstC*	2.35	Not DE
sirB	siderophore compound ABC transporter	2.17	Not DE
isdB	iron-regulated heme-iron binding protein	2.14	Not DE
fhuG	ferrichrome transport permease	1.96	Not DE
NWMN_0705	ferrichrome ABC transporter lipoprotein *sstD*	1.88	-1.97
Genes involved in iron storage and utilisation			
NWMN_1831	ferritin	-2.54	Not DE
sdhB	succinate dehydrogenase iron-sulfur	-4.08	-1.51

The RNA-Seq data confirmed that the reduction in pigmentation level of *S. aureus* after ethanol treatment was likely due to decreased expression of the *crt* operon. As was observed in squalene challenge, the gene expression of *sigB,* which is the sole accessory RNA polymerase factor that regulates the *crt* operon via altered transcript levels remains unchanged. Ethanol may be perceived through the activities of RsbUVW regulator and anti-sigma factor proteins that release SigB for engagement with the RNA polymerase complex. The role of RsbU in *S. aureus* is very poorly understood compared with the many studies in the model Gram-positive bacterium, *B. subtilis*, where the protein acts as a stimulus sentinel (Voelker *et al*., 1995; Delumeau *et al*., 2004). Alternatively, ethanol may activate other regulatory pathways that influence SigB, though this is likely to exclude SrrAB, which was described to modulate pigment expression, since there was an absence of the hypoxia regulon also controlled by this two-component system (Yarwood *et al*., 2001; Mashruwala and Boyd, 2017).

Recently, Pando *et al*. (2017) published a study of the effects of ethanol-induced stress (EIS) on *S. aureus*. The transcriptional data were obtained from two unrelated clinical MRSA isolates challenged with 10 % (v/v) ethanol for 15 min using microarray hybridisation. Their study provides excellent comparative material for the study in this thesis. Although the concentration

of ethanol challenge in their study (10 % v/v) was much higher than that was used in the current study (1 % v/v) and different strains were used, identification of the DE genes showing a consistent trend of expression contributes to our understanding of the primary and fundamental responses of *S. aureus* to ethanol.

Overall, in the study by Pando *et al*., (2017),10 % EIS resulted in differential gene expression of 1091 genes. This compares with 368 DE genes identified with 1% v/v in the current study, and this large difference in number of DE genes is most likely due to the more critical survival pressure caused by 10 % (v/v) ethanol, while 1 % (v/v) ethanol was shown here to produce negligible effects on growth and survival. This large difference in stress will explain the extensive and greater expression responses in the other study. However, it was noted that 73.3 % of DE genes in the 10% ethanol study were down-regulated, comparing with 70.7 % of down-regulated DE genes observed with 1% ethanol. This suggests that regardless of the concentration, ethanol seems to consistently induce more negative responses. Similarly, genes involved in transcription, translation and nucleotide biosynthesis were down-regulated in the 10% ethanol study, matching the trend described in this chapter.

The common DE genes shown in both studies involved in amino acid metabolism, central intermediary metabolism, cofactors and secondary metabolites, nucleotide metabolism, stress response, and virulence factor are listed in Table 6.10. This comparison shows that different concentrations of ethanol modulated the expression of these common DE genes with remarkable consistency. There is no DE gene regulated in opposite direction. The reduced expression of *crt* operon was observed even with 10 % ethanol challenge, indicating a large effective range of ethanol concentration affecting pigmentation at least from 0.1 % to 10 % (v/v).

As proposed in chapter 4 and this chapter, squalene and ethanol both induced an invasion-like response with the increased expression of a suite of virulence genes such as *hlg*, *luk*, and *sbi*. One possible explanation for that was based on the inherent genetic differences in the *sae* locus possessed by strain Newman.

The *saeS* gene in Newman has several SNPs leading to activation of the TCS with increased expression level. The two-component system SaeSR regulates expression of a large amount of virulence factors. Because of that, it is not reasonable to claim the increased expression of virulence genes was solely induced by squalene or ethanol treatment. However, confirmation of the same regulation of virulent factors in 10 % ethanol study (Pando *et al.,* 2017) suggests the genetic variations in *saeS* are irrelevant as two un-related MRSA strains were used in the EIS study but obtained the same results.

Table 6.10 Comparison of 10% and 1% ethanol challenge transcriptomes. DE genes listed here are involved in amino acid metabolism, central intermediary metabolism, cofactors and secondary metabolites, nucleotide metabolism, stress response, and virulence factor.

Gene function category	Gene name	Description	UP OR DOWN REGULATED	
			10% EtOH study	1% EtOH study
Amino Acid Metabolism	*cysK*	cysteine synthase	↑	↑
	hisC	histidinol-phosphate aminotransferase	↓	↓
	dhoM	homoserine dehydrogenase	↓	↓
	dapA	dihydrodipicolinate synthase	↓	↓
	dapB	dihydrodipicolinate reductase	↓	↓
	dapD	tetrahydrodipicolinate acetyltransferase	↓	↓
	ilvA	threonine dehydratase	↓	↓
Central Intermediary Metabolism	*adh1*	alcohol dehydrogenase	↓	↓
	alsS	alpha-acetolactate synthase	↓	↓
Cofactors and Secondary Metabolites	*ribH*	riboflavin synthase, beta subunit	↓	↓
	ribA	riboflavin biosynthesis protein	↓	↓
	ribD	riboflavin specific deaminase	↓	↓
Nucleotide Metabolism	*purC*	phosphoribosylaminoimidazole-succinocarboxamide synthase	↓	↓
	purQ	phosphoribosylformylglycinamidine synthase I	↓	↓
	purL	phosphoribosylformylglycinamidine synthetase	↓	↓
	purF	phosphoribosylpyrophosphate amidotransferase	↓	↓
	purM	phosphoribosylaminoimidazole synthetase	↓	↓
	purN	phosphoribosylglycinamide formyltransferase	↓	↓
	purH	phosphoribosylaminoimidazolecarboxamide formyltransferase/IMP cyclohydrolase	↓	↓
	purD	phosphoribosylamine-glycine ligase	↓	↓
	pyrB	aspartate carbamoyltransferase catalytic subunit	↓	↓

	pyrAA	carbamoyl-phosphate synthase small subunit	↓	↓
	pyrE	orotate phosphoribosyltransferase	↓	↓
Stress Response	*mnhF*	Na+/H+ antiporter subunit	↓	↓
	mnhC	Na+/H+ antiporter subunit	↓	↓
	mnhB	Na+/H+ antiporter, MnhB component	↓	↓
	crtN	squalene synthase	↓	↓
	crtM	squalene desaturase	↓	↓
	crtQ	glycosyl transferase, group 2 family protein	↓	↓
	crtP	4,4'-diaponeurosporene oxidase	↓	↓
	ilvD	dihydroxy-acid dehydratase	↓	↓
	ilvA	threonine dehydratase	↓	↓
Virulence Factor	*sbi*	IgG-binding protein SBI	↑	↑
	hla	alpha-hemolysin precursor	↓	↓
	lukF	putative leukocidin F subunit	↑	↑
	lukS	putative leukocidin S subunit	↑	↑
	hlgA	gamma-hemolysin chain II precursor	↑	↑
	hlgB	gamma hemolysin, component B	↑	↑
	hlgC	gamma hemolysin, component C	↑	↑
	spoVG	regulatory protein SpoVG	↑	↑
	agrA	accessory gene regulator protein A	↓	↓
	agrC	accessory gene regulator C	↓	↓
	agrD	accessory gene regulator protein D	↓	↓

In chapter 4 one candidate for a regulator of SigB is the *rsbUVW-sigB* regulatory system. As the RsbUVW-mediated regulation of SigB is in protein level, it was conceivable that the expression of *sigB* could remain unchanged and thereby was not indicated in RNA-Seq data. The transcriptional data of squalene challenge revealed the expression level of *rsbV* was slightly decreased (-1.8-fold). Considering the *rsbV* gene is in an operon with *rsbUVW-sigB*, this transcript difference might not be expression level since all the other genes on the same transcript was not DE. This together with the fact that none of *rsbUVW* were DE in ethanol challenge transcriptome, suggesting a different mechanism possessed by ethanol to affect the activity of SigB.

Whole genome comparisons of antimicrobial-resistant strains and susceptible strains have been previously proven as a powerful tool to identify resistance determinants. Some of these studies have used isogenic clinical isolates (Mwangi *et al*., 2007; Howden *et al*., 2011) whilst others have used laboratory-evolved isolates (Renzoni *et al*., 2011; Song *et al*., 2013). The use of laboratory-evolved isolates has the advantage that selection for resistance is specific to the antimicrobial used. However, antimicrobial specific evolution could also be considered a disadvantage, as complex interactions of the antimicrobial with host factors may require different or multiple resistance determinants due to possible synergistic interactions. In addition, horizontal gene transfer from other members of the host microflora is a frequent and critical mechanism for clinically-evolved isolates to gain resistance determinants, whilst this cannot happen in typical experiments that generate laboratory-evolved isolates.

In this chapter, increased growth in the presence of ethanol was selected for in *S. aureus* Newman. Three SNPs were identified as the result of selective pressure from 6 % (v/v) ethanol. Considering the greatly increased growth after ethanol passage (Fig 6.9) only one non-synonymous SNP, causing the non-conservative replacement DapD A219E, was located in a coding region.

DapD is a tetrahydrodipicolinate acetyltransferase that catalyses L-2,3,4,5-tetrahydrodipcolinate into N-Acetyl-L-2-amino-6-oxopimelate which is a step in L-lysine biosynthesis. The specific step is required for biosynthesis of meso-

diaminopimelic acid which is an essential component of cell wall peptidoglycan in staphylococci and many other bacterial species. Enzymes of the meso-diaminopimelic acid/lysine pathway are potential targets for the development of antibacterial agents (Chapot-Chartier and Kulakauskas, 2014). The A219E amino acid replacement might alter catalytic activity that mediates changes in L-lysine pathway flux. It is difficult to predict the impact of the amino acid change on the C-terminal DapD domain as the structure of the protein in staphylococci is incomplete. Although tetrahydrodipicolinate acetyltransferase is widely distributed in bacteria, the closest protein YkuQ from *Bacillus subtilis* with known structure only has 60 % identity, which makes it less reliable applying this SNP into that model.

By searching for the *dapD* gene in other *S. aureus* transcriptional studies and including the squalene and ethanol transcriptomes derived in the current study, it was found that *dapD* may be regulated in response to various kinds of antimicrobials. Treatments with ethanol, vancomycin, and ortho-phenylphenol (Brackman *et al*., 2016; Jang *et al*., 2008; Pando *et al*., 2017) all caused down-regulation of *dapD,* whilst squalene did not alter transcription. Notably, there was a 5.45 fold decrease in the 1% ethanol transcriptional data in the current study and a 4.28 fold decrease revealed in the 10% ethanol challenge study (Pando *et al*., 2017). In view of the knowledge that DapD has a crucial role in biosynthesis of cell peptidoglycan (Jang *et al*., 2008), it is possible that decreased expression of this protein is part of a coordinated defence mechanisms possessed by *S. aureus* in response to certain types of antimicrobials. If so, the SNP in *dapD* is a reasonable candidate for the observed enhanced resistance in evolved isolates which may help to maintain flux in the L-Lysine pathway to maintain cell wall integrity.

The other candidates that might contribute are two SNPs in the upstream control region of *NWMN_1774*. Both SNPs, 10 bp and 16 bp upstream of the translational start site, respectively might alter the abundance of the protein, especially if these are located around the Shine-Dalgarno ribosome binding site. NWMN_1774 is a small, hypothetical protein of unknown function, that appears to be a transmembrane protein based on the presence of both alpha-helical

transmembrane region and the membrane spanning region. The potential involvement of the protein in enhancing growth in ethanol is difficult to predict and will require construction of isogenic gene inactivation and SNP variant strains together with further study in the future.

Since selection of SNPs in the genome of *S. aureus* appears facile in a laboratory, it brings into question why antimicrobials produced on human skin are still functional against *S. aureus* after thousands of years of evolution. One explanation is that it is possible that the combination of components found on the skin prevent antimicrobial lipid resistance developing to any one of these without a major loss of fitness. This is supported by studies where increasing antimicrobial lipid resistance simultaneously decreased resistance to other antimicrobials found on the skin such as the "seesaw effect" between daptomycin nonsusceptibility and beta-lactam susceptibility in *S. haemolyticus* (Sieradzki and Tomasz, 1997; Vignaroli *et al*., 2011).

Chapter 7 General discussion

7.1 Summary of this study

The aims of this thesis were to determine if squalene potentially plays a role in the colonisation and persistence of staphylococci on skin and comparatively investigate the effects of squalene upon *S. aureus* and *S. epidermidis*. To complete these aims, firstly experiments were undertaken to determine whether squalene has antimicrobial effects on staphylococci. The conclusion of its lack of toxicity in rich medium was made while quantifying that the eponymous golden colour of *S. aureus* cells was dramatically reduced by squalene. Next, taking into consideration the known relationships between pigment level and resistance to certain antimicrobials, experiments were performed to investigate if squalene treatment is capable of modulating the activities of four distinct antimicrobials, H_2O_2, nisin, sapienic acid and LL-37, with respect to *S. aureus* and *S. epidermidis*. These studies showed that pre-treatment with squalene has no effect on resistance to sapienic acid, but lowered the susceptibility of *S. aureus* but not *S. epidermidis* to H_2O_2 and nisin. However, The opposite pattern was observed for LL-37, where pre-treatment of squalene enhanced the resistance of *S. epidermidis* but did not alter the resistance of *S. aureus*. Thirdly, to gain insights into the overall gene expression profiles after squalene challenge, the transcriptional response of *S. aureus* and *S. epidermidis* was recorded by RNA-Seq and a further prolonged effects of squalene to *S. aureus* was assessed using a quantitative proteomics approach. The results of RNA-Seq analysis revealed numerous overlaps as well as significant differences between both species in their transcriptional responses to squalene, and possible genetic bases for previous experiments were also found and proposed. Of note, challenge with squalene triggered the derepression of the iron acquisition mechanisms in both *S. aureus* and *S. epidermidis*, and down-regulation of ferritin was further confirmed in proteomic data of *S. aureus*. The unexpected effect of squalene with respect to iron transport systems, lead to quantification of its effects on cellular iron level. ICP-

OES confirmed that the intracellular iron level was significantly decreased in squalene-treated cells and revealed that squalene treatment caused a pronounced growth defect in iron-limited defined growth medium. Squalene was found to have no ability to sequester iron from broth suggesting simple chelation could not explain the phenomenon.

Ethanol treatment was observed to produce a similar reduction in *S. aureus* pigment level during culture. Consequently, a transcriptomics approach was used to enable comparison with the squalene data that had been generated previously. Analysis of RNA-Seq data for ethanol challenge was compared with that for squalene challenge to determine whether squalene and ethanol might act via a common mechanism to affect staphyloxanthin production. The similar extent of *crt* operon down-regulation after ethanol challenge supports shared responses by squalene and ethanol that extended beyond staphylococcal pigment genes to metabolic and virulence pathways. Finally, the experimental evolution of *S. aureus* to sub-bactericidal concentration of ethanol was conducted to identify SNPs in genes that might act as resistance determinants to ethanol. Three SNPs were identified as the result of selective pressure from 6 % (v/v) ethanol. Two SNPs were in the leader sequence of a gene for a hypothetical protein and could not be explained. One non-synonymous SNP in a gene (*dapD,* producing DapD A219E) of the lysine biosynthesis pathway responsible for production of meso-diaminopimelic acid could affect flux in cell wall peptidoglycan biosynthesis.

7.2 Unanswered questions and future research

Although considerable progress has been made in understanding the role of squalene on colonisation and persistence of *S. aureus* and *S. epidermidis*, several questions remain unanswered. Of these, two questions with the highest importance are:

- How squalene (and ethanol) acts via transcription to reduce the pigment biosynthesis of *S. aureus*?
- What is the mechanism by which squalene lowers staphylococcal cellular iron levels?

Squalene and ethanol may employ the same or two distinct mechanisms affecting the pigmentation of *S. aureus*, but both end up with the decreased expression level of the *crt* operon. Therefore, factors that are capable of regulating the *crt* operon become the most likely susceptible targets for squalene and ethanol. Currently, it is known that the stress response alternative sigma factor SigB regulates STX production; the SigB deletion mutant is white and lacks STX (Kullik *et al*., 1998). Direct SigB regulation was proposed, and a consensus SigB DNA binding motif was identified in the *crt* promoter, but direct interaction was not confirmed (Hall *et al*., 2017). SigB activity is mediated by the upstream *sigB* operon genes encoding the RsbUVW regulatory system, where RsbU dephosphorylates the anti-anti-sigmaB factor RsbV and thus leads to the release of SigB from its inhibitory complex with RsbW (Pané-Farré *et al*., 2009). With respect to this study, the down-regulation of *rsbV* revealed in the squalene challenge transcriptome might indicate that squalene acts indirectly to lower pigment production through interfering with SigB activity. While this would require complex regulation, neither *rsbV,* nor any other genes within the *rsb* operon was DE in the ethanol challenge transcriptome, suggesting both ethanol and squalene may directly, though more likely indirectly, act via RsbU (the stimulus modulator) or there exists an alternative regulation system of the *crt* operon.

Recently, it was reported the oxygen-sensing and redox-signalling AirSR TCS transcriptionally regulates the STX-biosynthetic *crt* operon (Hall *et al*., 2017).

Overexpression of the AirR response regulator increased colony pigmentation, and the *ΔairSR* mutant exhibited an over 4.5-fold decrease in expression level of *crt* operon compared with the parental wild-type strain (Hall *et al*., 2017). Unlike the *ΔsigB* mutant, a gene knockout of *airSR* did not result in complete shutdown of STX biosynthesis, indicating that *airSR* is epistatic to *sigB*, as AirSR regulation of *crt* is dependent on the presence of SigB (Hall *et al*., 2017). Moreover, it was identified that there is a specific AirR binding region upstream of *crtOPQMN* indicating direct regulation of the biosynthetic operon via the DNA recognition motif (G/T)AA(C/A)ATNNA(C/A)AAAT, which was present in all 11 AirSR-regulated promoters (Hall *et al*., 2017). In further agreement with the current study, their microarray data revealed that two STX-biosynthetic genes, *crtM* and *crtN*, to be down-regulated 2- to 3-fold at the mid-exponential phase of growth during *airS* antisense RNA induction (Hall *et al*., 2017). This combined with the decreased expression level of the *crt* operon in an *airSR* mutant, suggests AirSR TCS could be an alternative target besides RsbUVW for the actions of squalene and ethanol.

Therefore, to answer the question of how squalene/ethanol transcriptionally reduces expression level of *crt* operon, future studies should primarily focus on a determination of whether squalene and ethanol have effects on AirSR TCS or the RsbUVW regulatory system. Firstly, although transcriptional data in this study showed the expression level of *airSR, rsbU*, and *rsbW* remained unchanged after squalene or ethanol challenge, this result can be double checked by examining the expression level of both treated and untreated samples via qPCR. If the qPCR results confirm the expressions of *airSR* and *rsbU(V)W* are not influenced by squalene or ethanol challenge, a protein activity-level interference from squalene or ethanol with AirSR and RsbUVW will be expected. Determination of whether squalene or ethanol are affecting the *crt* operon through AirSR can be conducted by assessing the pigment level of a *ΔairSR* mutant with or without squalene or ethanol treatment. As shown in the study (Hall *et al*., 2017), the expression of the *crt* operon was uninterrupted but at a lower level in *ΔairSR* mutant, meaning the pigment level should be still measurable. Consequently, if there is no difference in pigment level of an *airSR*

mutant between the two treatments, it can be confirmed that the ability of squalene or ethanol to lower *crt* expression is via impairing the function of AirSR. Otherwise, if squalene or ethanol treatment causes a further decreased level of pigmentation for an *ΔairSR* mutant, it can be concluded that AirSR is irrelevant to the squalene or ethanol-induced reduction in staphylococcal pigmentation.

A similar experiment could also be applied to determine whether activity of RsbUVW is influenced by squalene or ethanol treatment. Inactivation of RsbU activity in *S. aureus* 8325-4 shuts down the majority of pigment biosynthesis (Horsburgh *et al*., 2002), but the remaining pigment should be measurable using a more precise method. Construction of an entire *rsbUVW* knockout strain or separately inactivation of *rsbU, rsbV* and *rsbW* are both theoretically feasible, and whether there is a difference in pigment level between two treatments will be the key determinant.

Iron acquisition is a critical mechanism that is required for bacteria to colonise vertebrate hosts, and humans possess several mechanisms that minimises free iron to $<10^{-18}$ M to prevent bacterial outgrowth. In this study, challenge with squalene triggered the derepression of the iron acquisition mechanisms in both *S. aureus* and *S. epidermidis,* and further investigations revealed that this change in gene expression profile was due to a significant reduction in cellular iron. To answer the question of how this long chain lipid without functional side groups is able to lower cellular iron level, molecular tracking of both squalene and iron ions could be performed using isotope labelling method in future research studies.

Biological studies based on isotope labelling have been widely established, especially investigating metabolic fluxes and determining the structure of metabolic pathways and networks including the studies determining carbon and iron metabolisms (Dunn *et al*., 2013; Klein *et al*., 2012; Skaar *et al*, 2004). This technique is particularly powerful in biochemical pathway analysis allowing scientists to trace the conversion of one chemical to another following incorporation of heavy atoms from precursor substrates into different

metabolic products (Chokkathukalam *et al*., 2014; Fan *et al*., 2012). Usage of radioactive isotope is a common method in isotope labelling research due to its high sensitivity. But the amount of radioactive isotope used in the study should be strictly controlled within the limits of what an experimental organism can support, as excess amount of radiation could induce mutations thus affecting the results. Alternatively, usage of stable isotopes does not have the mutagenic effect. Stable isotopes have the same number of protons as common elements, and consequently share the same physicochemical properties, but differ in mass due to a difference in the number of neutrons, which enables MS-based analytical tools to easily separate isotopically labelled compounds based on mass difference. Skaar *et al* (2004) used stable isotope labelling to detect source-specific iron by mass spectrometry, and revealed that haem-iron is the preferred source of iron in the presence of both transferrin and either haem or haemoglobin during infection for *S. aureus*, which indicates using isotope labelling method to study metabolic pathway in *S. aureus* is feasible.

Therefore, to determine if squalene interferes with an iron efflux mechanism that leads to a net deficit of intracellular iron, *S. aureus* cells can be pre-cultured in an iron-deficient medium with supplement of stable iron-isotope to create a saturated heavy isotope-labelled metabolome. Then transferring the pre-cultured cells into a new medium without iron-isotope and culturing with or without squalene for several hours. By comparing the amount of iron-isotope found in the supernatant of the new media between two treatments, a squalene-induced iron efflux could be assured if observing a higher level of iron-isotope in squalene treated sample than the untreated. Moreover, if applying the radioactive isotope of iron in the above experiment, it would allow a more dynamic *in vivo* tracking to examine whether there are differences in the passage of iron through bacteria between squalene treated and untreated samples. In addition, isotope labelled iron-containing proteins such as transferrin, lactoferrin, and haem could replace isotope-iron ions to obtain the more *in vivo* like results.

Using an isotope labelling method could also facilitate our understanding of the relationship between squalene and staphylococcal pigment biosynthesis. By

treatment of staphylococci with a customised isotope-labelled squalene then tracking its flux in bacterial metabolic pathways, it will be determined whether squalene enters the cell membrane; whether bacteria consume squalene as a carbon source, and if so, which metabolic pathways squalene passes through.

Although squalene did not exhibit antimicrobial effects on staphylococci in rich media as shown in chapter 3 (Fig 3.2), a squalene-induced growth defect was observed in low iron media (chapter 5, Fig 5.3). This suggests the experimental evolution of *S. aureus* to squalene is feasible in low iron (0-0.02 μM) media as squalene induces enough survival pressure for selection of mutations. The methods for experimental evolution of *S. aureus* to ethanol (chapter 2.8) could apply to conduct the experiment by changing culture media from BHI to iron-deficient CDM.

In this study, increased growth yield of *S. aureus* Newman was achieved by selection using 6% (v/v) ethanol and experimental evolution. Three non-synonymous SNPs were identified as the result of the ethanol selective pressure. They include a non-synonymous SNP in *dapD* (producing DapD.A219E) and two intergenic SNPs in the leader sequence of *NWMN_1774*. Due to poor understanding of the functions of the latter gene, the role of these leader sequence SNPs in increased ethanol resistance was not progressed. Construction of a defined SNP variant of the leader sequence and an allelic replacement mutant of *NWMN_1774* would be valuable to conduct future investigation. The possible divergence of ethanol resistance between the wild-type and mutant strain will facilitate determining the functions of the SNPs. The DapDA219E variant protein could be studied to examine the effect it has on flux through the L-Lysine biosynthesis pathway and whether synthesis of meso-diaminopimelic acid for cell wall biosynthesis is the critical change that improves growth in ethanol by preventing the stress response limitation of this catalytic step.

7.3 Limitations of the study and relevance to skin

Over the process of this investigation, one concern that could limit the validity and impact of these data is: how do results gained *in vitro* differ from the *in vivo* scenario. For example, the squalene concentrations used in this study were 0.1 % (v/v) and 1 % (v/v), which was lower than that reported in sebum, where squalene comprises 12 % of total skin surface lipids. As sebum is unevenly distributed all over the body, it would be tempting to suggest that the effects observed in this study should be more pronounced in sebum-rich areas but less influential in sebum-lacking areas. However, this conclusion may not be always true as the ratio of sebaceous lipids to epidermal lipids differs across the body, resulting in different extents of dilution of squalene across the skin. Furthermore, the water concentration of skin is also extremely reduced compared with the assays described here. Given that squalene and some antimicrobial lipids are amphipathic molecules these differences could lead to considerable divergence for the results presented. Therefore, the use of skin models is required to obtain more valid conclusions in future research.

To overcome the perceived and known divergence between *in vitro* and *in vivo*, most staphylococcal *in vivo* experiments rely on a variety of animal models, such as inoculation of *S. aureus* in epidermal rodent skin models (Onunkwo *et al*., 2010). However, besides the considerable differences between human skin and rodent skin in both histology and immunology such as the amount of squalene, the results from studies using rodent skin models have shown a lack of consistency over extended periods of time, which complicates interpretation of data with respect to bacterial localisation and replication in the skin (Kanzaki *et al*., 1996; Abe *et al*., 1993; Kugelberg *et al*., 2005). Moreover, the majority of existing *S. aureus* animal skin models require severe mechanical disruption of the skin to compromise the initial barrier function which facilitates bacterial growth (Nippe *et al*., 2010; Cho *et al*., 2011; Inoshima *et al*., 2011). Although these experiments are useful for studying staphylococcal pathogenesis, they do not facilitate our understanding of how *S. aureus* adapts to an intact tissue or how *S. aureus* transits from asymptomatic colonization state to invasive infection (Popov *et al*., 2014).

The use of *ex vivo* human skin explants provides another method for studying the interactions between bacterial colonisers and the human skin components, regardless of limitations described in murine model. *Ex vivo* human skin explants are typically acquired from neonatal foreskin, surgical or cadaveric tissues, which can be maintained in cell culture media or on supports in an air-liquid interface and remain viable in culture for up to two weeks (Popov *et al*., 2014). The advantage of skin explants is that they contain all components of the skin tissue including all resident cell types of the epidermis and dermis as well as skin appendages. However, there are also limitations originating from genetic variations between each individual, and the relatively restricted availability of human skin (Popov *et al*., 2014).

At present, there are an increasing number of studies employing a 3-D organotropic human skin model as an *in vivo* like tool to dispel the above concern (Ridky *et al*., 2010; Groeber *et al*., 2011; Soong *et al*., 2012; Kretz *et al*, 2013; Hogk *et al*., 2013). The 3-D human skin culture models are a tractable experimental system that could contribute to investigations of the determinants of *S. aureus* interaction with the multi-layer skin tissue in future study. Organotropic 3-D skin models are developed from immortalised human keratinocytes, grown at an air-liquid interface on a supporting matrix which can be seeded with fibroblasts (Gangatirkar *et al*., 2007). In particular, fibroblasts are seeded into human dermal tissue to provide the underlying support matrix. Subsequently keratinocytes are then seeded on top of the matrix and grown for several days until the keratinocytes are fully differentiated thereby establish a basement membrane and all of the stratified epidermal layers from stratum basale to stratum corneum (Popov *et al*., 2014). As a result, the entire human skin proteins, cells and other components including the skin-derived antimicrobials are all involved in the 3-D human organotropic model, displaying the very similar thickness and the cellular architecture with the human epidermis (Fig 7.1)(Popov *et al*., 2014). However, even these models have limitations due to the absence of hair follicles and sebaceous glands, which means the sebaceous and epidermal lipids including squalene may need to be added artificially unlike the human explant skin.

The future study of staphylococci, squalene and skin awaits the development and publication of new models and on the horizon are models of human skin grated onto mice that maintain skin barrier functions for several weeks (Keira Mellican, personal communication).

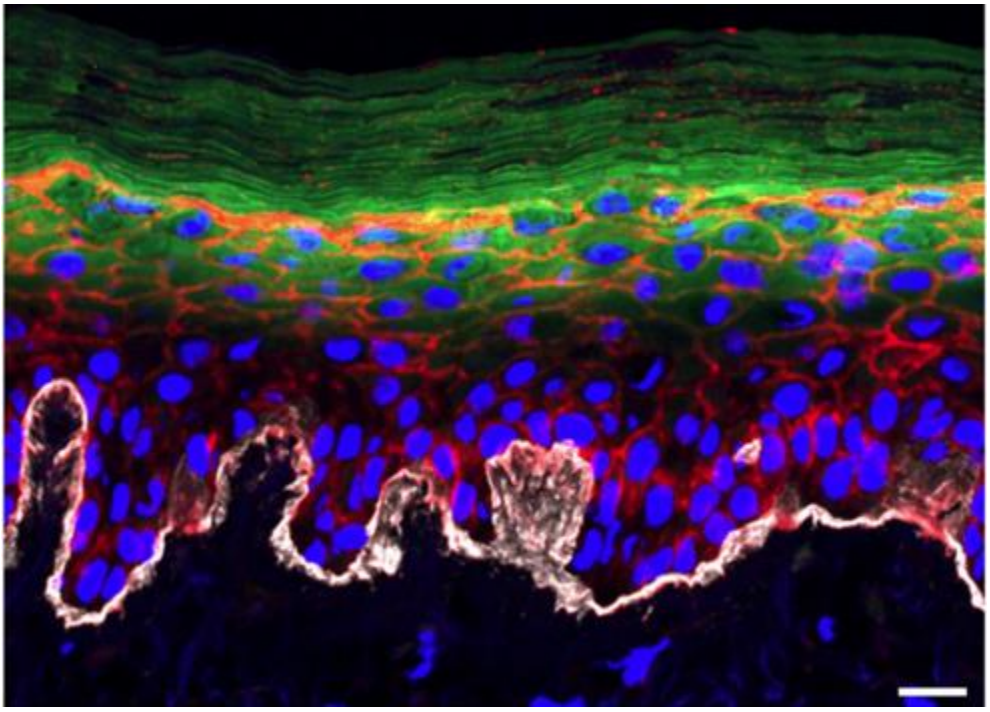

Figure 7.1 Three-dimensional organotropic human epidermal tissues recapitulate the stratified structure of the epidermis. (Popov *et al*., 2014)

Chapter 8 References

Abdelnour, A., Arvidson, S., Bremell, T., Ryden, C. & Tarkowski, A. 1993. The accessory gene regulator (agr) controls *Staphylococcus aureus* virulence in a murine arthritis model. *Infect Immun,* 61**,** 3879-85.

Abe, Y., Akiyama, H. & Arata, J. 1993. Furuncle-like lesions in mouse experimental skin infections with *Staphylococcus aureus*. *J Dermatol,* 20**,** 198-202.

Alnaseri, H., Arsic, B., Schneider, J. E., Kaiser, J. C., Scinocca, Z. C., Heinrichs, D. E. & Mcgavin, M. J. 2015. Inducible Expression of a Resistance-Nodulation-Division-Type Efflux Pump in *Staphylococcus aureus* Provides Resistance to Linoleic and Arachidonic Acids. *J Bacteriol,* 197**,** 1893-905.

Amin, U. S., Wilkinson, B. J. & Lash, T. D. 1995. Proline betaine is a highly effective osmoprotectant for *Staphylococcus aureus*. *Archives of Microbiology,* 163**,** 138-142.

Anderson, K. S., Wong, J., Polyak, K., Aronzon, D. & Enerback, C. 2009. Detection of psoriasin/S100A7 in the sera of patients with psoriasis. *Br J Dermatol,* 160**,** 325-32.

Archer, G. L. 1998. *Staphylococcus aureus*: a well-armed pathogen. *Clin Infect Dis,* 26**,** 1179-81.

Arikawa, J., Ishibashi, M., Kawashima, M., Imokawa, G., Takagi, Y. & Ichikawa, Y. 2002. Decreased levels of sphingosine, a natural antimicrobial agent, may be associated with vulnerability of the stratum corneum from patients with atopic dermatitis to colonization by *Staphylococcus aureus*. *Journal of Investigative Dermatology,* 119**,** 433-439.

Arvidson, S. & Tegmark, K. 2001. Regulation of virulence determinants in *Staphylococcus aureus*. *Int J Med Microbiol,* 291**,** 159-70.

Arya, R. & Princy, S. A. 2016. Exploration of Modulated Genetic Circuits Governing Virulence Determinants in *Staphylococcus aureus*. *Indian J Microbiol,* 56**,** 19-27.

Aswani, V., Tremblay, D. M., Moineau, S. & Shukla, S. K. 2011. *Staphylococcus epidermidis* bacteriophages from the anterior nares of humans. *Applied and Environmental Microbiology,* 77**,** 7853-7855.

Athanasopoulos, A. N., Economopoulou, M., Orlova, V. V., Sobke, A., Schneider, D., Weber, H., Augustin, H. G., Eming, S. A., Schubert, U., Linn, T., Nawroth, P. P., Hussain, M., Hammes, H. P., Herrmann, M., Preissner, K. T. & Chavakis, T. 2006. The extracellular adherence protein (Eap) of *Staphylococcus aureus* inhibits wound healing by interfering with host defense and repair mechanisms. *Blood,* 107**,** 2720-7.

Ayer, J. & Burrows, N. 2006. Acne: more than skin deep. *Postgraduate Medical Journal,* 82**,** 500-506.

Barber, M. 1961. Methicillin-resistant staphylococci. *J Clin Pathol,* 14**,** 385-93.

Barker, C. & Park, S. F. 2001. Sensitization of Listeria monocytogenes to low pH, organic acids, and osmotic stress by ethanol. *Appl Environ Microbiol,* 67**,** 1594-600.

Barns, K. J. & Weisshaar, J. C. 2013. Real-time attack of LL-37 on single *Bacillus subtilis* cells. *Biochim Biophys Acta,* 1828**,** 1511-20.

Baviera, G. et al., 2014. Microbiota in healthy skin and in atopic eczema. *BioMed research international*, 2014, p.436921.

Becker, K., Heilmann, C. & Peters, G. 2014. Coagulase-negative staphylococci. *Clin Microbiol Rev,* 27**,** 870-926.

Bera, A., Biswas, R., Herbert, S., Kulauzovic, E., Weidenmaier, C., Peschel, A. & Gotz, F. 2007. Influence of wall teichoic acid on lysozyme resistance in *Staphylococcus aureus*. *J Bacteriol,* 189**,** 280-3.

Bischoff, M., Dunman, P., Kormanec, J., Macapagal, D., Murphy, E., Mounts, W., Berger-Bachi, B. & Projan, S. 2004. Microarray-based analysis of the *Staphylococcus aureus* sigmaB regulon. *J Bacteriol,* 186**,** 4085-99.

Bore, E., Langsrud, S., Langsrud, O., Rode, T. M. & Holck, A. 2007. Acid-shock responses in *Staphylococcus aureus* investigated by global gene expression analysis. *Microbiology,* 153**,** 2289-303.

Bouwstra, J. A., Gooris, G. S., Dubbelaar, F. E., Weerheim, A. M., Ijzerman, A. P. & Ponec, M. 1998. Role of ceramide 1 in the molecular organization of the stratum corneum lipids. *J Lipid Res,* 39**,** 186-96.

Bowden, M. G., Visai, L., Longshaw, C. M., Holland, K. T., Speziale, P. & Hook, M. 2002. Is the GehD lipase from *Staphylococcus epidermidis* a collagen binding adhesin? *J Biol Chem,* 277**,** 43017-23.

Bowles, L. K. & Ellefson, W. L. 1985. Effects of butanol on Clostridium acetobutylicum. *Applied and Environmental Microbiology,* 50**,** 1165-1170.

Brackman, G., Breyne, K., De Rycke, R., Vermote, A., Van Nieuwerburgh, F., Meyer, E., Van Calenbergh, S. & Coenye, T. 2016. The Quorum Sensing Inhibitor Hamamelitannin Increases Antibiotic Susceptibility of *Staphylococcus aureus* Biofilms by Affecting Peptidoglycan Biosynthesis and eDNA Release. *Sci Rep,* 6**,** 20321.

Bronner, S., Monteil, H. & Prevost, G. 2004. Regulation of virulence determinants in *Staphylococcus aureus*: complexity and applications. *FEMS Microbiol Rev,* 28**,** 183-200.

Brooker, B. E. & Fuller, R. 1984. The adhesion of coagulase negative staphylococci to human skin and its relevance to the bacterial flora of milk. *J Appl Bacteriol,* 57**,** 325-32.

Bubeck Wardenburg, J., Williams, W. A. & Missiakas, D. 2006. Host defenses against *Staphylococcus aureus* infection require recognition of bacterial lipoproteins. *Proc Natl Acad Sci U S A,* 103**,** 13831-6.

Bunce, C., Wheeler, L., Reed, G., Musser, J. & Barg, N. 1992. Murine model of cutaneous infection with gram-positive cocci. *Infect Immun,* 60**,** 2636-40.

Burts, M. L., Dedent, A. C. & Missiakas, D. M. 2008. EsaC substrate for the ESAT-6 Secretion Pathway and its role in persistent infections of S. aureus. *Molecular microbiology,* 69**,** 736-746.

Calfee, D. P. 2011. The epidemiology, treatment, and prevention of transmission of methicillin-resistant *Staphylococcus aureus*. *J Infus Nurs,* 34**,** 359-64.

Campbell, I. M., Crozier, D. N., Pawagi, A. B. & Buivids, I. A. 1983. In vitro response of *Staphylococcus aureus* from cystic fibrosis patients to combinations of linoleic and oleic acids added to nutrient medium. *J Clin Microbiol,* 18**,** 408-15.

Campbell, J., Singh, A. K., Swoboda, J. G., Gilmore, M. S., Wilkinson, B. J. & Walker, S. 2012. An antibiotic that inhibits a late step in wall teichoic acid biosynthesis induces the cell wall stress stimulon in *Staphylococcus aureus*. *Antimicrob Agents Chemother,* 56**,** 1810-20.

Candi, E., Schmidt, R. & Melino, G. 2005. The cornified envelope: a model of cell death in the skin. *Nat Rev Mol Cell Biol,* 6**,** 328-40.

Cartron, M. L., England, S. R., Chiriac, A. I., Josten, M., Turner, R., Rauter, Y., Hurd, A., Sahl, H. G., Jones, S. & Foster, S. J. 2014. Bactericidal activity of the human skin fatty acid cis-6-hexadecanoic acid on *Staphylococcus aureus*. *Antimicrob Agents Chemother,* 58**,** 3599-609.

Chamberlain, N. R. & Brueggemann, S. A. 1997. Characterisation and expression of fatty acid modifying enzyme produced by *Staphylococcus epidermidis*. *J Med Microbiol,* 46**,** 693-7.

Chamberlain, N. R., Mehrtens, B. G., Xiong, Z., Kapral, F. A., Boardman, J. L. & Rearick, J. I. 1991. Correlation of carotenoid production, decreased membrane fluidity, and

resistance to oleic acid killing in *Staphylococcus aureus* 18Z. *Infect Immun,* 59**,** 4332-7.
Chapot-Chartier, M. P. & Kulakauskas, S. 2014. Cell wall structure and function in lactic acid bacteria. *Microb Cell Fact,* 13 Suppl 1**,** S9.
Chatterjee, I., Somerville, G. A., Heilmann, C., Sahl, H. G., Maurer, H. H. & Herrmann, M. 2006. Very low ethanol concentrations affect the viability and growth recovery in post-stationary-phase *Staphylococcus aureus* populations. *Appl Environ Microbiol,* 72**,** 2627-36.
Chavakis, T., Hussain, M., Kanse, S. M., Peters, G., Bretzel, R. G., Flock, J. I., Herrmann, M. & Preissner, K. T. 2002. *Staphylococcus aureus* extracellular adherence protein serves as anti-inflammatory factor by inhibiting the recruitment of host leukocytes. *Nat Med,* 8**,** 687-93.
Cheng, A. G., Dedent, A. C., Schneewind, O. & Missiakas, D. 2011. A play in four acts: *Staphylococcus aureus* abscess formation. *Trends in microbiology,* 19**,** 225-232.
Cheng, A. G., Kim, H. K., Burts, M. L., Krausz, T., Schneewind, O. & Missiakas, D. M. 2009. Genetic requirements for *Staphylococcus aureus* abscess formation and persistence in host tissues. *Faseb j,* 23**,** 3393-404.
Cheung, A. L., Eberhardt, K. J., Chung, E., Yeaman, M. R., Sullam, P. M., Ramos, M. & Bayer, A. S. 1994. Diminished virulence of a sar-/agr- mutant of *Staphylococcus aureus* in the rabbit model of endocarditis. *J Clin Invest,* 94**,** 1815-22.
Chiou, R. Y., Phillips, R. D., Zhao, P., Doyle, M. P. & Beuchat, L. R. 2004. Ethanol-mediated variations in cellular fatty acid composition and protein profiles of two genotypically different strains of Escherichia coli O157:H7. *Appl Environ Microbiol,* 70**,** 2204-10.
Cho, J. S., Zussman, J., Donegan, N. P., Ramos, R. I., Garcia, N. C., Uslan, D. Z., Iwakura, Y., Simon, S. I., Cheung, A. L., Modlin, R. L., Kim, J. & Miller, L. S. 2011. Noninvasive in vivo imaging to evaluate immune responses and antimicrobial therapy against *Staphylococcus aureus* and USA300 MRSA skin infections. *J Invest Dermatol,* 131**,** 907-15.
Cho, S. H., Strickland, I., Boguniewicz, M. & Leung, D. Y. 2001. Fibronectin and fibrinogen contribute to the enhanced binding of *Staphylococcus aureus* to atopic skin. *J Allergy Clin Immunol,* 108**,** 269-74.
Chokkathukalam, A., Kim, D. H., Barrett, M. P., Breitling, R. & Creek, D. J. 2014. Stable isotope-labeling studies in metabolomics: new insights into structure and dynamics of metabolic networks. *Bioanalysis,* 6**,** 511-24.
Cingolani, P., Platts, A., Wang Le, L., Coon, M., Nguyen, T., Wang, L., Land, S. J., Lu, X. & Ruden, D. M. 2012. A program for annotating and predicting the effects of single nucleotide polymorphisms, SnpEff: SNPs in the genome of Drosophila melanogaster strain w1118; iso-2; iso-3. *Fly (Austin),* 6**,** 80-92.
Clarke, S. R., Andre, G., Walsh, E. J., Dufrene, Y. F., Foster, T. J. & Foster, S. J. 2009. Iron-regulated surface determinant protein A mediates adhesion of *Staphylococcus aureus* to human corneocyte envelope proteins. *Infect Immun,* 77**,** 2408-16.
Clarke, S. R., Harris, L. G., Richards, R. G. & Foster, S. J. 2002. Analysis of Ebh, a 1.1-megadalton cell wall-associated fibronectin-binding protein of *Staphylococcus aureus*. *Infect Immun,* 70**,** 6680-7.
Clarke, S. R., Mohamed, R., Bian, L., Routh, A. F., Kokai-Kun, J. F., Mond, J. J., Tarkowski, A. & Foster, S. J. 2007. The *Staphylococcus aureus* surface protein IsdA mediates resistance to innate defenses of human skin. *Cell Host Microbe,* 1**,** 199-212.
Clarke, S. R., Wiltshire, M. D. & Foster, S. J. 2004. IsdA of *Staphylococcus aureus* is a broad spectrum, iron-regulated adhesin. *Mol Microbiol,* 51**,** 1509-19.
Coates, R., Moran, J. & Horsburgh, M. J. 2014. Staphylococci: colonizers and pathogens of human skin. *Future Microbiol,* 9**,** 75-91.
Cogen, A. L., Nizet, V. & Gallo, R. L. 2008. Skin microbiota: a source of disease or defence? *Br J Dermatol,* 158**,** 442-55.

Cogen, A. L., Yamasaki, K., Muto, J., Sanchez, K. M., Crotty Alexander, L., Tanios, J., Lai, Y., Kim, J. E., Nizet, V. & Gallo, R. L. 2010a. *Staphylococcus epidermidis* antimicrobial delta-toxin (phenol-soluble modulin-gamma) cooperates with host antimicrobial peptides to kill group A *Streptococcus*. *PLoS One,* 5**,** e8557.

Cogen, A. L., Yamasaki, K., Sanchez, K. M., Dorschner, R. A., Lai, Y., Macleod, D. T., Torpey, J. W., Otto, M., Nizet, V., Kim, J. E. & Gallo, R. L. 2010b. Selective antimicrobial action is provided by phenol-soluble modulins derived from *Staphylococcus epidermidis*, a normal resident of the skin. *J Invest Dermatol,* 130**,** 192-200.

Costello, E. K., Lauber, C. L., Hamady, M., Fierer, N., Gordon, J. I. & Knight, R. 2009. Bacterial community variation in human body habitats across space and time. *Science,* 326**,** 1694-7.

Cotter, P. D. & Hill, C. 2003. Surviving the Acid Test: Responses of Gram-Positive Bacteria to Low pH. *Microbiology and Molecular Biology Reviews,* 67**,** 429-453.

Courcol, R. J., Trivier, D., Bissinger, M. C., Martin, G. R. & Brown, M. R. 1997. Siderophore production by *Staphylococcus aureus* and identification of iron-regulated proteins. *Infect Immun,* 65**,** 1944-8.

Croucher, N. J. & Thomson, N. R. 2010. Studying bacterial transcriptomes using RNA-seq. *Curr Opin Microbiol,* 13**,** 619-24.

Cuaron, J. A., Dulal, S., Song, Y., Singh, A. K., Montelongo, C. E., Yu, W., Nagarajan, V., Jayaswal, R. K., Wilkinson, B. J. & Gustafson, J. E. 2013. Tea Tree Oil-Induced Transcriptional Alterations in *Staphylococcus aureus*. *Phytotherapy research : PTR,* 27**,** 390-396.

Davis, J. M. & Ramakrishnan, L. 2009. The role of the granuloma in expansion and dissemination of early tuberculous infection. *Cell,* 136**,** 37-49.

De Goffau, M. C., Van Dijl, J. M. & Harmsen, H. J. 2011. Microbial growth on the edge of desiccation. *Environ Microbiol,* 13**,** 2328-35.

De Goffau, M. C., Yang, X., Van Dijl, J. M. & Harmsen, H. J. 2009. Bacterial pleomorphism and competition in a relative humidity gradient. *Environ Microbiol,* 11**,** 809-22.

De Luca, C. & Valacchi, G. 2010a. Surface Lipids as Multifunctional Mediators of Skin Responses to Environmental Stimuli. *Mediators of Inflammation,* 2010.

De Luca, C. & Valacchi, G. 2010b. Surface lipids as multifunctional mediators of skin responses to environmental stimuli. *Mediators Inflamm,* 2010**,** 321494.

Delumeau, O., Dutta, S., Brigulla, M., Kuhnke, G., Hardwick, S. W., Volker, U., Yudkin, M. D. & Lewis, R. J. 2004. Functional and structural characterization of RsbU, a stress signaling protein phosphatase 2C. *J Biol Chem,* 279**,** 40927-37.

Desbois, A. P. & Smith, V. J. 2010. Antibacterial free fatty acids: activities, mechanisms of action and biotechnological potential. *Appl Microbiol Biotechnol,* 85**,** 1629-42.

Diep, B. A., Gill, S. R., Chang, R. F., Phan, T. H., Chen, J. H., Davidson, M. G., Lin, F., Lin, J., Carleton, H. A., Mongodin, E. F., Sensabaugh, G. F. & Perdreau-Remington, F. 2006. Complete genome sequence of USA300, an epidemic clone of community-acquired meticillin-resistant *Staphylococcus aureus*. *Lancet,* 367**,** 731-9.

Drabkin, D. L. 1951. Metabolism of the hemin chromoproteins. *Physiol Rev,* 31**,** 345-431.

Drake, D. R., Brogden, K. A., Dawson, D. V. & Wertz, P. W. 2008. Thematic review series: skin lipids. Antimicrobial lipids at the skin surface. *J Lipid Res,* 49**,** 4-11.

Drewe, P., Stegle, O., Hartmann, L., Kahles, A., Bohnert, R., Wachter, A., Borgwardt, K. & Ratsch, G. 2013. Accurate detection of differential RNA processing. *Nucleic Acids Res,* 41**,** 5189-98.

Dunn, W. B., Erban, A., Weber, R. J. M., Creek, D. J., Brown, M., Breitling, R., Hankemeier, T., Goodacre, R., Neumann, S., Kopka, J. & Viant, M. R. 2013. Mass appeal: metabolite identification in mass spectrometry-focused untargeted metabolomics. *Metabolomics,* 9**,** 44-66.

Durr, U. H., Sudheendra, U. S. & Ramamoorthy, A. 2006. LL-37, the only human member of the cathelicidin family of antimicrobial peptides. *Biochim Biophys Acta,* 1758**,** 1408-25.

Elias, P. M. & Feingold, K. R. 1992. Lipids and the epidermal water barrier: metabolism, regulation, and pathophysiology. *Semin Dermatol,* 11**,** 176-82.
Enright, M. C., Robinson, D. A., Randle, G., Feil, E. J., Grundmann, H. & Spratt, B. G. 2002. The evolutionary history of methicillin-resistant *Staphylococcus aureus* (MRSA). *Proc Natl Acad Sci U S A,* 99**,** 7687-92.
Ernst, C. M. & Peschel, A. 2011. Broad-spectrum antimicrobial peptide resistance by MprF-mediated aminoacylation and flipping of phospholipids. *Mol Microbiol,* 80**,** 290-9.
Fan, T. W., Lorkiewicz, P. K., Sellers, K., Moseley, H. N., Higashi, R. M. & Lane, A. N. 2012. Stable isotope-resolved metabolomics and applications for drug development. *Pharmacol Ther,* 133**,** 366-91.
Foell, D., Wittkowski, H., Vogl, T. & Roth, J. 2007. S100 proteins expressed in phagocytes: a novel group of damage-associated molecular pattern molecules. *J Leukoc Biol,* 81**,** 28-37.
Foster, T. J. 2009. Colonization and infection of the human host by staphylococci: adhesion, survival and immune evasion. *Vet Dermatol,* 20**,** 456-70.
Frank, D. N., Feazel, L. M., Bessesen, M. T., Price, C. S., Janoff, E. N. & Pace, N. R. 2010. The Human Nasal Microbiota and *Staphylococcus aureus* Carriage. *PLoS ONE,* 5**,** e10598.
Frawley, E. R. & Fang, F. C. 2014. The ins and outs of bacterial iron metabolism. *Mol Microbiol,* 93**,** 609-16.
Fried, V. A. & Novick, A. 1973. Organic solvents as probes for the structure and function of the bacterial membrane: effects of ethanol on the wild type and an ethanol-resistant mutant of Escherichia coli K-12. *J Bacteriol,* 114**,** 239-48.
Friedman, D. B., Stauff, D. L., Pishchany, G., Whitwell, C. W., Torres, V. J. & Skaar, E. P. 2006. *Staphylococcus aureus* redirects central metabolism to increase iron availability. *PLoS Pathog,* 2**,** e87.
Fu, X., Fu, N., Guo, S., Yan, Z., Xu, Y., Hu, H., Menzel, C., Chen, W., Li, Y., Zeng, R. & Khaitovich, P. 2009. Estimating accuracy of RNA-Seq and microarrays with proteomics. *BMC Genomics,* 10**,** 161.
Furubayashi, M., Li, L., Katabami, A., Saito, K. & Umeno, D. 2014. Construction of carotenoid biosynthetic pathways using squalene synthase. *FEBS Lett,* 588**,** 436-42.
Fuchs, S., Pane-Farre, J., Kohler, C., Hecker, M., Engelmann, S. 2007. Anaerobic gene expression in Staphylococcus aureus. *J Bacteriol,* 189, 4275-89.
Gamon, M. R., Moreira, E. C., De Oliveira, S. S., Teixeira, L. M. & Bastos Mdo, C. 1999. Characterization of a novel bacteriocin-encoding plasmid found in clinical isolates of *Staphylococcus aureus*. *Antonie Van Leeuwenhoek,* 75**,** 233-43.
Gangatirkar, P., Paquet-Fifield, S., Li, A., Rossi, R. & Kaur, P. 2007. Establishment of 3D organotypic cultures using human neonatal epidermal cells. *Nat Protoc,* 2**,** 178-86.
Gardete, S., Wu, S. W., Gill, S. & Tomasz, A. 2006. Role of VraSR in antibiotic resistance and antibiotic-induced stress response in *Staphylococcus aureus*. *Antimicrob Agents Chemother,* 50**,** 3424-34.
Geiger, T., Goerke, C., Mainiero, M., Kraus, D. & Wolz, C. 2008. The virulence regulator Sae of *Staphylococcus aureus*: promoter activities and response to phagocytosis-related signals. *J Bacteriol,* 190**,** 3419-28.
Giardine, B., Riemer, C., Hardison, R. C., Burhans, R., Elnitski, L., Shah, P., Zhang, Y., Blankenberg, D., Albert, I., Taylor, J., Miller, W., Kent, W. J. & Nekrutenko, A. 2005. Galaxy: a platform for interactive large-scale genome analysis. *Genome Res,* 15**,** 1451-5.
Giraudo, A. T., Calzolari, A., Cataldi, A. A., Bogni, C. & Nagel, R. 1999. The sae locus of *Staphylococcus aureus* encodes a two-component regulatory system. *FEMS Microbiol Lett,* 177**,** 15-22.

Glaser, R., Harder, J., Lange, H., Bartels, J., Christophers, E. & Schroder, J. M. 2005. Antimicrobial psoriasin (S100A7) protects human skin from Escherichia coli infection. *Nat Immunol,* 6**,** 57-64.

Goecks, J., Nekrutenko, A. & Taylor, J. 2010. Galaxy: a comprehensive approach for supporting accessible, reproducible, and transparent computational research in the life sciences. *Genome Biol,* 11**,** R86.

Goerke, C., Fluckiger, U., Steinhuber, A., Bisanzio, V., Ulrich, M., Bischoff, M., Patti, J. M. & Wolz, C. 2005. Role of *Staphylococcus aureus* Global Regulators sae and σ(B) in Virulence Gene Expression during Device-Related Infection. *Infection and Immunity,* 73**,** 3415-3421.

Gopal, S. & Divya, K. C. 2017. Can methicillin-resistant *Staphylococcus aureus* prevalence from dairy cows in India act as potential risk for community-associated infections?: A review. *Veterinary World,* 10**,** 311-318.

Gordon, Y. J., Huang, L. C., Romanowski, E. G., Yates, K. A., Proske, R. J. & Mcdermott, A. M. 2005. Human cathelicidin (LL-37), a multifunctional peptide, is expressed by ocular surface epithelia and has potent antibacterial and antiviral activity. *Curr Eye Res,* 30**,** 385-94.

Götz, F., Bannerman, T. & Schleifer, K.-H. 2006. The Genera Staphylococcus and Macrococcus. *In:* DWORKIN, M., FALKOW, S., ROSENBERG, E., SCHLEIFER, K.-H. & STACKEBRANDT, E. (eds.) *The Prokaryotes: Volume 4: Bacteria: Firmicutes, Cyanobacteria.* New York, NY: Springer US.

Grice, E. A., Kong, H. H., Conlan, S., Deming, C. B., Davis, J., Young, A. C., Program, N. C. S., Bouffard, G. G., Blakesley, R. W., Murray, P. R., Green, E. D., Turner, M. L. & Segre, J. A. 2009. Topographical and Temporal Diversity of the Human Skin Microbiome. *Science (New York, N.Y.),* 324**,** 1190-1192.

Groeber, F., Holeiter, M., Hampel, M., Hinderer, S. & Schenke-Layland, K. 2011. Skin tissue engineering--in vivo and in vitro applications. *Adv Drug Deliv Rev,* 63**,** 352-66.

Haggar, A., Ehrnfelt, C., Holgersson, J. & Flock, J.-I. 2004. The Extracellular Adherence Protein from *Staphylococcus aureus* Inhibits Neutrophil Binding to Endothelial Cells. *Infection and Immunity,* 72**,** 6164-6167.

Hall, J. W., Yang, J., Guo, H. & Ji, Y. 2017. The *Staphylococcus aureus* AirSR Two-Component System Mediates Reactive Oxygen Species Resistance via Transcriptional Regulation of Staphyloxanthin Production. *Infect Immun,* 85.

Hammer, N. D. & Skaar, E. P. 2011. Molecular mechanisms of *Staphylococcus aureus* iron acquisition. *Annu Rev Microbiol,* 65**,** 129-47.

Hanada, Y., Sekimizu, K. & Kaito, C. 2011. Silkworm apolipophorin protein inhibits *Staphylococcus aureus* virulence. *J Biol Chem,* 286**,** 39360-9.

Hantke, K. 1981. Regulation of ferric iron transport in Escherichia coli K12: isolation of a constitutive mutant. *Mol Gen Genet,* 182**,** 288-92.

Hartman, B. J. & Tomasz, A. 1984. Low-affinity penicillin-binding protein associated with beta-lactam resistance in *Staphylococcus aureus*. *J Bacteriol,* 158**,** 513-6.

Hecker, M., Pane-Farre, J. & Volker, U. 2007. SigB-dependent general stress response in *Bacillus subtilis* and related gram-positive bacteria. *Annu Rev Microbiol,* 61**,** 215-36.

Hecker, M., Schumann, W. & Volker, U. 1996. Heat-shock and general stress response in *Bacillus subtilis*. *Mol Microbiol,* 19**,** 417-28.

Heilmann, C. 2011. Adhesion mechanisms of staphylococci. *Adv Exp Med Biol,* 715**,** 105-23.

Heilmann, C., Thumm, G., Chhatwal, G. S., Hartleib, J., Uekotter, A. & Peters, G. 2003. Identification and characterization of a novel autolysin (Aae) with adhesive properties from *Staphylococcus epidermidis*. *Microbiology,* 149**,** 2769-78.

Hell, W., Meyer, H. G. & Gatermann, S. G. 1998. Cloning of aas, a gene encoding a Staphylococcus saprophyticus surface protein with adhesive and autolytic properties. *Mol Microbiol,* 29**,** 871-81.

Herbert, S., Bera, A., Nerz, C., Kraus, D., Peschel, A., Goerke, C., Meehl, M., Cheung, A. & Götz, F. 2007. Molecular Basis of Resistance to Muramidase and Cationic Antimicrobial Peptide Activity of Lysozyme in Staphylococci. *PLoS Pathogens,* 3**,** e102.

Hiron, A., Falord, M., Valle, J., Debarbouille, M. & Msadek, T. 2011. Bacitracin and nisin resistance in *Staphylococcus aureus*: a novel pathway involving the BraS/BraR two-component system (SA2417/SA2418) and both the BraD/BraE and VraD/VraE ABC transporters. *Mol Microbiol,* 81**,** 602-22.

Hogk, I., Rupp, S. & Burger-Kentischer, A. 2013. 3D-tissue model for herpes simplex virus-1 infections. *Methods Mol Biol,* 1064**,** 239-51.

Horsburgh, M. J., Aish, J. L., White, I. J., Shaw, L., Lithgow, J. K. & Foster, S. J. 2002. sigmaB modulates virulence determinant expression and stress resistance: characterization of a functional rsbU strain derived from *Staphylococcus aureus* 8325-4. *J Bacteriol,* 184**,** 5457-67.

Horsburgh, M. J., Ingham, E. & Foster, S. J. 2001. In *Staphylococcus aureus*, fur is an interactive regulator with PerR, contributes to virulence, and Is necessary for oxidative stress resistance through positive regulation of catalase and iron homeostasis. *J Bacteriol,* 183**,** 468-75.

Howard, B. E., Hu, Q., Babaoglu, A. C., Chandra, M., Borghi, M., Tan, X., He, L., Winter-Sederoff, H., Gassmann, W., Veronese, P. & Heber, S. 2013. High-throughput RNA sequencing of pseudomonas-infected Arabidopsis reveals hidden transcriptome complexity and novel splice variants. *PLoS One,* 8**,** e74183.

Howden, B. P., Mcevoy, C. R., Allen, D. L., Chua, K., Gao, W., Harrison, P. F., Bell, J., Coombs, G., Bennett-Wood, V., Porter, J. L., Robins-Browne, R., Davies, J. K., Seemann, T. & Stinear, T. P. 2011. Evolution of multidrug resistance during *Staphylococcus aureus* infection involves mutation of the essential two component regulator WalKR. *PLoS Pathog,* 7**,** e1002359.

Huang, L., Forsberg, C. W. & Gibbins, L. N. 1986. Influence of External pH and Fermentation Products on Clostridium acetobutylicum Intracellular pH and Cellular Distribution of Fermentation Products. *Applied and Environmental Microbiology,* 51**,** 1230-1234.

Huang, Y. C., Lin, Y. M., Chang, T. W., Wu, S. J., Lee, Y. S., Chang, M. D., Chen, C., Wu, S. H. & Liao, Y. D. 2007. The flexible and clustered lysine residues of human ribonuclease 7 are critical for membrane permeability and antimicrobial activity. *J Biol Chem,* 282**,** 4626-33.

Ibarra, J. A., Pérez-Rueda, E., Carroll, R. K. & Shaw, L. N. 2013. Global analysis of transcriptional regulators in *Staphylococcus aureus*. *BMC Genomics,* 14**,** 126-126.

Inoshima, I., Inoshima, N., Wilke, G. A., Powers, M. E., Frank, K. M., Wang, Y. & Bubeck Wardenburg, J. 2011. A *Staphylococcus aureus* pore-forming toxin subverts the activity of ADAM10 to cause lethal infection in mice. *Nat Med,* 17**,** 1310-4.

Ishikawa, J., Narita, H., Kondo, N., Hotta, M., Takagi, Y., Masukawa, Y., Kitahara, T., Takema, Y., Koyano, S., Yamazaki, S. & Hatamochi, A. 2010. Changes in the ceramide profile of atopic dermatitis patients. *J Invest Dermatol,* 130**,** 2511-4.

Iwase, T., Uehara, Y., Shinji, H., Tajima, A., Seo, H., Takada, K., Agata, T. & Mizunoe, Y. 2010. *Staphylococcus epidermidis* Esp inhibits *Staphylococcus aureus* biofilm formation and nasal colonization. *Nature,* 465**,** 346-9.

Jang, H.-J., Nde, C., Toghrol, F. & Bentley, W. E. 2008. Microarray analysis of toxicogenomic effects of Ortho-phenylphenol in *Staphylococcus aureus*. *BMC Genomics,* 9**,** 411-411.

Jeong, D. W., Cho, H., Jones, M. B., Shatzkes, K., Sun, F., Ji, Q., Liu, Q., Peterson, S. N., He, C. & Bae, T. 2012. The auxiliary protein complex SaePQ activates the phosphatase

activity of sensor kinase SaeS in the SaeRS two-component system of *Staphylococcus aureus*. *Mol Microbiol,* 86**,** 331-48.
Jeong, D. W., Cho, H., Lee, H., Li, C., Garza, J., Fried, M. & Bae, T. 2011. Identification of the P3 promoter and distinct roles of the two promoters of the SaeRS two-component system in *Staphylococcus aureus*. *J Bacteriol,* 193**,** 4672-84.
Jevons, M. P. 1961. "Celbenin" - resistant Staphylococci. *British Medical Journal,* 1**,** 124-125.
Johnson, M., Cockayne, A. & Morrissey, J. A. 2008. Iron-regulated biofilm formation in *Staphylococcus aureus* Newman requires ica and the secreted protein Emp. *Infect Immun,* 76**,** 1756-65.
Kabara, J. J., Swieczkowski, D. M., Conley, A. J. & Truant, J. P. 1972. Fatty Acids and Derivatives as Antimicrobial Agents. *Antimicrobial Agents and Chemotherapy,* 2**,** 23-28.
Kanehisa, M. & Goto, S. 2000. KEGG: kyoto encyclopedia of genes and genomes. *Nucleic Acids Res,* 28**,** 27-30.
Kanehisa, M., Goto, S., Sato, Y., Furumichi, M. & Tanabe, M. 2012. KEGG for integration and interpretation of large-scale molecular data sets. *Nucleic Acids Res,* 40**,** D109-14.
Kanzaki, H., Morishita, Y., Akiyama, H. & Arata, J. 1996. Adhesion of *Staphylococcus aureus* to horny layer: role of fibrinogen. *J Dermatol Sci,* 12**,** 132-9.
Kapral, F. A., Smith, S. & Lal, D. 1992. The esterification of fatty acids by *Staphylococcus aureus* fatty acid modifying enzyme (FAME) and its inhibition by glycerides. *J Med Microbiol,* 37**,** 235-7.
Katzif , S., Lee, E.-H., Law, A. B., Tzeng, Y.-L. & Shafer, W. M. 2005. CspA Regulates Pigment Production in *Staphylococcus aureus* through a SigB-Dependent Mechanism. *Journal of Bacteriology,* 187**,** 8181-8184.
Kehl-Fie, T. E., Chitayat, S., Hood, M. I., Damo, S., Restrepo, N., Garcia, C., Munro, K. A., Chazin, W. J. & Skaar, E. P. 2011. Nutrient metal sequestration by calprotectin inhibits bacterial superoxide defense, enhancing neutrophil killing of *Staphylococcus aureus*. *Cell Host Microbe,* 10**,** 158-64.
Kenny, J. G., Moran, J., Kolar, S. L., Ulanov, A., Li, Z., Shaw, L. N., Josefsson, E. & Horsburgh, M. J. 2013. Mannitol utilisation is required for protection of *Staphylococcus aureus* from human skin antimicrobial fatty acids. *PLoS One,* 8**,** e67698.
Kenny, J. G., Ward, D., Josefsson, E., Jonsson, I. M., Hinds, J., Rees, H. H., Lindsay, J. A., Tarkowski, A. & Horsburgh, M. J. 2009. The *Staphylococcus aureus* response to unsaturated long chain free fatty acids: survival mechanisms and virulence implications. *PLoS One,* 4**,** e4344.
Kim, J. E., Kim, B. J., Jeong, M. S., Seo, S. J., Kim, M. N., Hong, C. K. & Ro, B. I. 2005. Expression and Modulation of LL-37 in Normal Human Keratinocytes, HaCaT cells, and Inflammatory Skin Diseases. *Journal of Korean Medical Science,* 20**,** 649-654.
King, N. P., Beatson, S. A., Totsika, M., Ulett, G. C., Alm, R. A., Manning, P. A. & Schembri, M. A. 2011. UafB is a serine-rich repeat adhesin of Staphylococcus saprophyticus that mediates binding to fibronectin, fibrinogen and human uroepithelial cells. *Microbiology,* 157**,** 1161-75.
King, N. P., Sakinc, T., Ben Zakour, N. L., Totsika, M., Heras, B., Simerska, P., Shepherd, M., Gatermann, S. G., Beatson, S. A. & Schembri, M. A. 2012. Characterisation of a cell wall-anchored protein of Staphylococcus saprophyticus associated with linoleic acid resistance. *BMC Microbiol,* 12**,** 8.
Klein, S. & Heinzle, E. 2012. Isotope labeling experiments in metabolomics and fluxomics. *Wiley Interdiscip Rev Syst Biol Med,* 4**,** 261-72.
Kloos, W. E. & Musselwhite, M. S. 1975. Distribution and persistence of Staphylococcus and Micrococcus species and other aerobic bacteria on human skin. *Appl Microbiol,* 30**,** 381-5.

Kloos, W. E. & Schleifer, K. H. 1975. Isolation and Characterization of Staphylococci from Human Skin II. Descriptions of Four New Species: Staphylococcus warneri, Staphylococcus capitis, Staphylococcus hominis, and Staphylococcus simulans1. *International Journal of Systematic and Evolutionary Microbiology,* 25**,** 62-79.

Knapp, H. R. & Melly, M. A. 1986. Bactericidal effects of polyunsaturated fatty acids. *J Infect Dis,* 154**,** 84-94.

Kocianova, S., Vuong, C., Yao, Y., Voyich, J. M., Fischer, E. R., Deleo, F. R. & Otto, M. 2005. Key role of poly-γ-dl-glutamic acid in immune evasion and virulence of *Staphylococcus epidermidis*. *Journal of Clinical Investigation,* 115**,** 688-694.

Kohler, T., Weidenmaier, C. & Peschel, A. 2009. Wall Teichoic Acid Protects *Staphylococcus aureus* against Antimicrobial Fatty Acids from Human Skin. *Journal of Bacteriology,* 191**,** 4482-4484.

Kong, H.H. et al., 2012. Temporal shifts in the skin microbiome associated with disease flares and treatment in children with atopic dermatitis. *Genome Research*, 22(5), pp.850–859.

Kraus, D., Herbert, S., Kristian, S. A., Khosravi, A., Nizet, V., Gotz, F. & Peschel, A. 2008. The GraRS regulatory system controls *Staphylococcus aureus* susceptibility to antimicrobial host defenses. *BMC Microbiol,* 8**,** 85.

Kretz, M., Siprashvili, Z., Chu, C., Webster, D. E., Zehnder, A., Qu, K., Lee, C. S., Flockhart, R. J., Groff, A. F., Chow, J., Johnston, D., Kim, G. E., Spitale, R. C., Flynn, R. A., Zheng, G. X., Aiyer, S., Raj, A., Rinn, J. L., Chang, H. Y. & Khavari, P. A. 2013. Control of somatic tissue differentiation by the long non-coding RNA TINCR. *Nature,* 493**,** 231-5.

Kugelberg, E., Norstrom, T., Petersen, T. K., Duvold, T., Andersson, D. I. & Hughes, D. 2005. Establishment of a superficial skin infection model in mice by using *Staphylococcus aureus* and Streptococcus pyogenes. *Antimicrob Agents Chemother,* 49**,** 3435-41.

Kullik, I., Giachino, P. & Fuchs, T. 1998. Deletion of the alternative sigma factor sigmaB in *Staphylococcus aureus* reveals its function as a global regulator of virulence genes. *J Bacteriol,* 180**,** 4814-20.

Kuroda, M., Tanaka, Y., Aoki, R., Shu, D., Tsumoto, K. & Ohta, T. 2008. *Staphylococcus aureus* giant protein Ebh is involved in tolerance to transient hyperosmotic pressure. *Biochem Biophys Res Commun,* 374**,** 237-41.

Lai, Y., Cogen, A. L., Radek, K. A., Park, H. J., Macleod, D. T., Leichtle, A., Ryan, A. F., Di Nardo, A. & Gallo, R. L. 2010. Activation of TLR2 by a small molecule produced by *Staphylococcus epidermidis* increases antimicrobial defense against bacterial skin infections. *J Invest Dermatol,* 130**,** 2211-21.

Lai, Y., Di Nardo, A., Nakatsuji, T., Leichtle, A., Yang, Y., Cogen, A. L., Wu, Z.-R., Hooper, L. V., Von Aulock, S., Radek, K. A., Huang, C.-M., Ryan, A. F. & Gallo, R. L. 2009. Commensal bacteria regulate TLR3-dependent inflammation following skin injury. *Nature medicine,* 15**,** 1377-1382.

Lai, Y., Villaruz, A. E., Li, M., Cha, D. J., Sturdevant, D. E. & Otto, M. 2007. The human anionic antimicrobial peptide dermcidin induces proteolytic defence mechanisms in staphylococci. *Mol Microbiol,* 63**,** 497-506.

Langmead, B., Trapnell, C., Pop, M. & Salzberg, S. L. 2009. Ultrafast and memory-efficient alignment of short DNA sequences to the human genome. *Genome Biol,* 10**,** R25.

Lee, H. S., Lee, D. H., Cho, S. & Chung, J. H. 2006. Minimal heating dose: a novel biological unit to measure infrared irradiation. *Photodermatol Photoimmunol Photomed,* 22**,** 148-52.

Li, H. & Durbin, R. 2009. Fast and accurate short read alignment with Burrows-Wheeler transform. *Bioinformatics,* 25**,** 1754-60.

Li, H., Handsaker, B., Wysoker, A., Fennell, T., Ruan, J., Homer, N., Marth, G., Abecasis, G. & Durbin, R. 2009. The Sequence Alignment/Map format and SAMtools. *Bioinformatics,* 25**,** 2078-9.

Libberton, B., Coates, R. E., Brockhurst, M. A. & Horsburgh, M. J. 2014. Evidence that intraspecific trait variation among nasal bacteria shapes the distribution of *Staphylococcus aureus*. *Infect Immun,* 82**,** 3811-5.
Lindsay, J. A. & Riley, T. V. 1994. Staphylococcal iron requirements, siderophore production, and iron-regulated protein expression. *Infect Immun,* 62**,** 2309-14.
Liu, G. Y. & Nizet, V. 2009. Color me bad: microbial pigments as virulence factors. *Trends Microbiol,* 17**,** 406-13.
Liu, Q., Yeo, W.-S. & Bae, T. 2016. The SaeRS Two-Component System of *Staphylococcus aureus*. *Genes,* 7**,** 81.
Long, J. P., Hart, J., Albers, W. & Kapral, F. A. 1992. The production of fatty acid modifying enzyme (FAME) and lipase by various staphylococcal species. *J Med Microbiol,* 37**,** 232-4.
Lowy, F. D. 1998. *Staphylococcus aureus* infections. *N Engl J Med,* 339**,** 520-32.
Lowy, F. D. 2003. Antimicrobial resistance: the example of *Staphylococcus aureus*. *J Clin Invest,* 111**,** 1265-73.
Lu, T., Park, J. Y., Parnell, K., Fox, L. K. & Mcguire, M. A. 2012. Characterization of fatty acid modifying enzyme activity in staphylococcal mastitis isolates and other bacteria. *BMC Res Notes,* 5**,** 323.
Madison, K. C. 2003. Barrier function of the skin: "la raison d'etre" of the epidermis. *J Invest Dermatol,* 121**,** 231-41.
Mainiero, M., Goerke, C., Geiger, T., Gonser, C., Herbert, S. & Wolz, C. 2010. Differential target gene activation by the *Staphylococcus aureus* two-component system saeRS. *J Bacteriol,* 192**,** 613-23.
Mantione, K. J., Kream, R. M., Kuzelova, H., Ptacek, R., Raboch, J., Samuel, J. M. & Stefano, G. B. 2014. Comparing Bioinformatic Gene Expression Profiling Methods: Microarray and RNA-Seq. *Medical Science Monitor Basic Research,* 20**,** 138-141.
Marguerat, S. & Bahler, J. 2010. RNA-seq: from technology to biology. *Cell Mol Life Sci,* 67**,** 569-79.
Marioni, J. C., Mason, C. E., Mane, S. M., Stephens, M. & Gilad, Y. 2008. RNA-seq: an assessment of technical reproducibility and comparison with gene expression arrays. *Genome Res,* 18**,** 1509-17.
Martin, M. 2011. Cutadapt removes adapter sequences from high-throughput sequencing reads. *2011,* 17.
Mashruwala, A. A. & Boyd, J. M. 2017. The *Staphylococcus aureus* SrrAB Regulatory System Modulates Hydrogen Peroxide Resistance Factors, Which Imparts Protection to Aconitase during Aerobic Growth. *PLoS One,* 12**,** e0170283.
Massey, R. C., Horsburgh, M. J., Lina, G., Hook, M. & Recker, M. 2006. The evolution and maintenance of virulence in *Staphylococcus aureus*: a role for host-to-host transmission? *Nat Rev Microbiol,* 4**,** 953-8.
Matousek, J. L. & Campbell, K. L. 2002. A comparative review of cutaneous pH. *Vet Dermatol,* 13**,** 293-300.
Mazmanian, S. K., Skaar, E. P., Gaspar, A. H., Humayun, M., Gornicki, P., Jelenska, J., Joachmiak, A., Missiakas, D. M. & Schneewind, O. 2003. Passage of heme-iron across the envelope of *Staphylococcus aureus*. *Science,* 299**,** 906-9.
Mcdevitt, D., Francois, P., Vaudaux, P. & Foster, T. J. 1994. Molecular characterization of the clumping factor (fibrinogen receptor) of *Staphylococcus aureus*. *Mol Microbiol,* 11**,** 237-48.
Mcewan, N. A., Mellor, D. & Kalna, G. 2006. Adherence by Staphylococcus intermedius to canine corneocytes: a preliminary study comparing noninflamed and inflamed atopic canine skin. *Vet Dermatol,* 17**,** 151-4.
Mckenney, D., Hubner, J., Muller, E., Wang, Y., Goldmann, D. A. & Pier, G. B. 1998. The ica locus of *Staphylococcus epidermidis* encodes production of the capsular polysaccharide/adhesin. *Infect Immun,* 66**,** 4711-20.

Melnik, B. 2006. Disturbances of antimicrobial lipids in atopic dermatitis. *JDDG: Journal der Deutschen Dermatologischen Gesellschaft,* 4**,** 114-123.
Messenger, A. J. M. & Barclay, R. 1983. Bacteria, iron and pathogenicity. *Biochemical Education,* 11**,** 54-63.
Mishra, N. N., Liu, G. Y., Yeaman, M. R., Nast, C. C., Proctor, R. A., Mckinnell, J. & Bayer, A. S. 2011. Carotenoid-related alteration of cell membrane fluidity impacts *Staphylococcus aureus* susceptibility to host defense peptides. *Antimicrob Agents Chemother,* 55**,** 526-31.
Moreillon, P., Entenza, J. M., Francioli, P., Mcdevitt, D., Foster, T. J., Francois, P. & Vaudaux, P. 1995. Role of *Staphylococcus aureus* coagulase and clumping factor in pathogenesis of experimental endocarditis. *Infect Immun,* 63**,** 4738-43.
Mulcahy, M. E., Geoghegan, J. A., Monk, I. R., O'keeffe, K. M., Walsh, E. J., Foster, T. J. & Mcloughlin, R. M. 2012. Nasal colonisation by *Staphylococcus aureus* depends upon clumping factor B binding to the squamous epithelial cell envelope protein loricrin. *PLoS Pathog,* 8**,** e1003092.
Muthaiyan, A., Silverman, J. A., Jayaswal, R. K. & Wilkinson, B. J. 2008. Transcriptional Profiling Reveals that Daptomycin Induces the *Staphylococcus aureus* Cell Wall Stress Stimulon and Genes Responsive to Membrane Depolarization. *Antimicrobial Agents and Chemotherapy,* 52**,** 980-990.
Mwangi, M. M., Wu, S. W., Zhou, Y., Sieradzki, K., De Lencastre, H., Richardson, P., Bruce, D., Rubin, E., Myers, E., Siggia, E. D. & Tomasz, A. 2007. Tracking the in vivo evolution of multidrug resistance in *Staphylococcus aureus* by whole-genome sequencing. *Proceedings of the National Academy of Sciences,* 104**,** 9451-9456.
Nagamachi, E., Hirai, Y., Tomochika, K. & Kanemasa, Y. 1992. Studies on osmotic stability of liposomes prepared with bacterial membrane lipids by carboxyfluorescein release. *Microbiol Immunol,* 36**,** 231-4.
Nagase, N., Sasaki, A., Yamashita, K., Shimizu, A., Wakita, Y., Kitai, S. & Kawano, J. 2002. Isolation and species distribution of staphylococci from animal and human skin. *J Vet Med Sci,* 64**,** 245-50.
Netzer, R., Stafsnes, M. H., Andreassen, T., Goksoyr, A., Bruheim, P. & Brautaset, T. 2010a. Biosynthetic pathway for gamma-cyclic sarcinaxanthin in Micrococcus luteus: heterologous expression and evidence for diverse and multiple catalytic functions of C(50) carotenoid cyclases. *J Bacteriol,* 192**,** 5688-99.
Netzer, R., Stafsnes, M. H., Andreassen, T., Goksøyr, A., Bruheim, P. & Brautaset, T. 2010b. Biosynthetic Pathway for γ-Cyclic Sarcinaxanthin in Micrococcus luteus: Heterologous Expression and Evidence for Diverse and Multiple Catalytic Functions of C50 Carotenoid Cyclases. *Journal of Bacteriology,* 192**,** 5688-5699.
Neuhaus, F. C. & Baddiley, J. 2003. A continuum of anionic charge: structures and functions of D-alanyl-teichoic acids in gram-positive bacteria. *Microbiol Mol Biol Rev,* 67**,** 686-723.
Neumann, Y., Ohlsen, K., Donat, S., Engelmann, S., Kusch, H., Albrecht, D., Cartron, M., Hurd, A. & Foster, S. J. 2015. The effect of skin fatty acids on *Staphylococcus aureus*. *Arch Microbiol,* 197**,** 245-67.
Nicholas, R. O., Li, T., Mcdevitt, D., Marra, A., Sucoloski, S., Demarsh, P. L. & Gentry, D. R. 1999. Isolation and Characterization of a sigB Deletion Mutant of *Staphylococcus aureus*. *Infection and Immunity,* 67**,** 3667-3669.
Nicolaides, N. 1974. Skin lipids: their biochemical uniqueness. *Science,* 186**,** 19-26.
Nicolaides, N. & Ansari, M. N. 1968. Fatty acids of unusual double-bond positions and chain lengths found in rat skin surface lipids. *Lipids,* 3**,** 403-10.
Niedergang, F., Hemar, A., Hewitt, C. R., Owen, M. J., Dautry-Varsat, A. & Alcover, A. 1995. The *Staphylococcus aureus* enterotoxin B superantigen induces specific T cell receptor down-regulation by increasing its internalization. *J Biol Chem,* 270**,** 12839-45.

Nippe, N., Varga, G., Holzinger, D., Loffler, B., Medina, E., Becker, K., Roth, J., Ehrchen, J. M. & Sunderkotter, C. 2011. Subcutaneous infection with S. aureus in mice reveals association of resistance with influx of neutrophils and Th2 response. *J Invest Dermatol,* 131**,** 125-32.

Niyonsaba, F. & Ogawa, H. 2005. Protective roles of the skin against infection: implication of naturally occurring human antimicrobial agents beta-defensins, cathelicidin LL-37 and lysozyme. *J Dermatol Sci,* 40**,** 157-68.

Nizet, V. 2007. Understanding how leading bacterial pathogens subvert innate immunity to reveal novel therapeutic targets. *J Allergy Clin Immunol,* 120**,** 13-22.

Nolan, T., Hands, R. E. & Bustin, S. A. 2006. Quantification of mRNA using real-time RT-PCR. *Nat Protoc,* 1**,** 1559-82.

Novick, R. P. 2003. Autoinduction and signal transduction in the regulation of staphylococcal virulence. *Mol Microbiol,* 48**,** 1429-49.

Novick, R. P. & Geisinger, E. 2008. Quorum sensing in staphylococci. *Annu Rev Genet,* 42**,** 541-64.

Novick, R. P. & Jiang, D. 2003. The staphylococcal saeRS system coordinates environmental signals with agr quorum sensing. *Microbiology,* 149**,** 2709-17.

Ohniwa, R. L., Kitabayashi, K. & Morikawa, K. 2013. Alternative cardiolipin synthase Cls1 compensates for stalled Cls2 function in *Staphylococcus aureus* under conditions of acute acid stress. *FEMS Microbiol Lett,* 338**,** 141-6.

Ohsawa, K., Watanabe, T., Matsukawa, R., Yoshimura, Y. & Imaeda, K. 1984. The possible role of squalene and its peroxide of the sebum in the occurrence of sunburn and protection from the damage caused by U.V. irradiation. *J Toxicol Sci,* 9**,** 151-9.

Olson, M. E., Nygaard, T. K., Ackermann, L., Watkins, R. L., Zurek, O. W., Pallister, K. B., Griffith, S., Kiedrowski, M. R., Flack, C. E., Kavanaugh, J. S., Kreiswirth, B. N., Horswill, A. R. & Voyich, J. M. 2013. *Staphylococcus aureus* nuclease is an SaeRS-dependent virulence factor. *Infect Immun,* 81**,** 1316-24.

Omoe, K., Imanishi, K., Hu, D. L., Kato, H., Takahashi-Omoe, H., Nakane, A., Uchiyama, T. & Shinagawa, K. 2004. Biological properties of staphylococcal enterotoxin-like toxin type R. *Infect Immun,* 72**,** 3664-7.

Ong, P. Y., Ohtake, T., Brandt, C., Strickland, I., Boguniewicz, M., Ganz, T., Gallo, R. L. & Leung, D. Y. 2002. Endogenous antimicrobial peptides and skin infections in atopic dermatitis. *N Engl J Med,* 347**,** 1151-60.

Onunkwo, C. C., Hahn, B. L. & Sohnle, P. G. 2010. Clearance of experimental cutaneous *Staphylococcus aureus* infections in mice. *Arch Dermatol Res,* 302**,** 375-82.

Orwin, P. M., Leung, D. Y., Donahue, H. L., Novick, R. P. & Schlievert, P. M. 2001. Biochemical and biological properties of Staphylococcal enterotoxin K. *Infect Immun,* 69**,** 360-6.

Oshlack, A. & Wakefield, M. J. 2009. Transcript length bias in RNA-seq data confounds systems biology. *Biol Direct,* 4**,** 14.

Ottesen, E. A., Young, C. R., Eppley, J. M., Ryan, J. P., Chavez, F. P., Scholin, C. A. & Delong, E. F. 2013. Pattern and synchrony of gene expression among sympatric marine microbial populations. *Proc Natl Acad Sci U S A,* 110**,** E488-97.

Otto, M. 2012. Molecular basis of *Staphylococcus epidermidis* infections. *Semin Immunopathol,* 34**,** 201-14.

Palmqvist, N., Patti, J. M., Tarkowski, A. & Josefsson, E. 2004. Expression of staphylococcal clumping factor A impedes macrophage phagocytosis. *Microbes Infect,* 6**,** 188-95.

Paget, M. 2015. Bacterial Sigma Factors and Anti-Sigma Factors: Structure, Function and Distribution. *Biomolecules*, 5, 1245-1265.

Pando, J. M., Pfeltz, R. F., Cuaron, J. A., Nagarajan, V., Mishra, M. N., Torres, N. J., Elasri, M. O., Wilkinson, B. J. & Gustafson, J. E. 2017. Ethanol-induced stress response of *Staphylococcus aureus*. *Can J Microbiol,* 63**,** 745-757.

Pane-Farre, J., Jonas, B., Forstner, K., Engelmann, S. & Hecker, M. 2006. The sigmaB regulon in *Staphylococcus aureus* and its regulation. *Int J Med Microbiol,* 296**,** 237-58.
Pane-Farre, J., Jonas, B., Hardwick, S. W., Gronau, K., Lewis, R. J., Hecker, M. & Engelmann, S. 2009. Role of RsbU in controlling SigB activity in *Staphylococcus aureus* following alkaline stress. *J Bacteriol,* 191**,** 2561-73.
Pappas, A. 2009. Epidermal surface lipids. *Dermato-endocrinology,* 1**,** 72-76.
Park, B., Iwase, T. & Liu, G. Y. 2011. Intranasal application of S. epidermidis prevents colonization by methicillin-resistant *Staphylococcus aureus* in mice. *PLoS One,* 6**,** e25880.
Park, S., You, X. & Imlay, J. A. 2005. Substantial DNA damage from submicromolar intracellular hydrogen peroxide detected in Hpx- mutants of Escherichia coli. *Proc Natl Acad Sci U S A,* 102**,** 9317-22.
Patel, R. K. & Jain, M. 2012. NGS QC Toolkit: A Toolkit for Quality Control of Next Generation Sequencing Data. *PLoS ONE,* 7**,** e30619.
Peacock, S. J., De Silva, I. & Lowy, F. D. 2001. What determines nasal carriage of *Staphylococcus aureus*? *Trends Microbiol,* 9**,** 605-10.
Peacock, S. J. & Paterson, G. K. 2015. Mechanisms of Methicillin Resistance in *Staphylococcus aureus*. *Annu Rev Biochem,* 84**,** 577-601.
Pelz, A., Wieland, K. P., Putzbach, K., Hentschel, P., Albert, K. & Gotz, F. 2005. Structure and biosynthesis of staphyloxanthin from *Staphylococcus aureus*. *J Biol Chem,* 280**,** 32493-8.
Periasamy, S., Chatterjee, S. S., Cheung, G. Y. C. & Otto, M. 2012. Phenol-soluble modulins in staphylococci: What are they originally for? *Communicative & Integrative Biology,* 5**,** 275-277.
Perkins, T. T., Kingsley, R. A., Fookes, M. C., Gardner, P. P., James, K. D., Yu, L., Assefa, S. A., He, M., Croucher, N. J., Pickard, D. J., Maskell, D. J., Parkhill, J., Choudhary, J., Thomson, N. R. & Dougan, G. 2009. A strand-specific RNA-Seq analysis of the transcriptome of the typhoid bacillus Salmonella typhi. *PLoS Genet,* 5**,** e1000569.
Peschel, A., Jack, R. W., Otto, M., Collins, L. V., Staubitz, P., Nicholson, G., Kalbacher, H., Nieuwenhuizen, W. F., Jung, G., Tarkowski, A., Van Kessel, K. P. & Van Strijp, J. A. 2001. *Staphylococcus aureus* resistance to human defensins and evasion of neutrophil killing via the novel virulence factor MprF is based on modification of membrane lipids with l-lysine. *J Exp Med,* 193**,** 1067-76.
Peschel, A., Otto, M., Jack, R. W., Kalbacher, H., Jung, G. & Gotz, F. 1999. Inactivation of the dlt operon in *Staphylococcus aureus* confers sensitivity to defensins, protegrins, and other antimicrobial peptides. *J Biol Chem,* 274**,** 8405-10.
Picardo, M., Ottaviani, M., Camera, E. & Mastrofrancesco, A. 2009. Sebaceous gland lipids. *Dermatoendocrinol,* 1**,** 68-71.
Pietiainen, M., Francois, P., Hyyrylainen, H. L., Tangomo, M., Sass, V., Sahl, H. G., Schrenzel, J. & Kontinen, V. P. 2009. Transcriptome analysis of the responses of *Staphylococcus aureus* to antimicrobial peptides and characterization of the roles of vraDE and vraSR in antimicrobial resistance. *BMC Genomics,* 10**,** 429.
Popov, L., Kovalski, J., Grandi, G., Bagnoli, F. & Amieva, M. R. 2014. Three-Dimensional Human Skin Models to Understand *Staphylococcus aureus* Skin Colonization and Infection. *Front Immunol,* 5**,** 41.
Potter, A., Ceotto, H., Coelho, M. L., Guimaraes, A. J. & Bastos Mdo, C. 2014. The gene cluster of aureocyclicin 4185: the first cyclic bacteriocin of *Staphylococcus aureus*. *Microbiology,* 160**,** 917-28.
Potts, M. 1994. Desiccation tolerance of prokaryotes. *Microbiol Rev,* 58**,** 755-805.
Proksch, E., Brandner, J. M. & Jensen, J. M. 2008. The skin: an indispensable barrier. *Exp Dermatol,* 17**,** 1063-72.
Punyauppa-Path S, P. P., Rattanachaikunsopon P 2015. NISIN: PRODUCTION AND MECHANISM OF ANTIMICROBIAL ACTION. *IJCRR,* 7**,** 47-53.

Ramundo, M. S., Beltrame, C. O., Botelho, A. M., Coelho, L. R., Silva-Carvalho, M. C., Ferreira-Carvalho, B. T., Nicolas, M. F., Guedes, I. A., Dardenne, L. E., O'gara, J. & Figueiredo, A. M. 2016. A unique SaeS allele overrides cell-density dependent expression of saeR and lukSF-PV in the ST30-SCCmecIV lineage of CA-MRSA. *Int J Med Microbiol,* 306**,** 367-80.

Ratledge, C. & Dover, L. G. 2000. Iron metabolism in pathogenic bacteria. *Annu Rev Microbiol,* 54**,** 881-941.

Renzoni, A., Andrey, D. O., Jousselin, A., Barras, C., Monod, A., Vaudaux, P., Lew, D. & Kelley, W. L. 2011. Whole genome sequencing and complete genetic analysis reveals novel pathways to glycopeptide resistance in *Staphylococcus aureus*. *PLoS One,* 6**,** e21577.

Ridky, T. W., Chow, J. M., Wong, D. J. & Khavari, P. A. 2010. Invasive three-dimensional organotypic neoplasia from multiple normal human epithelia. *Nat Med,* 16**,** 1450-5.

Rieg, S., Steffen, H., Seeber, S., Humeny, A., Kalbacher, H., Dietz, K., Garbe, C. & Schittek, B. 2005. Deficiency of dermcidin-derived antimicrobial peptides in sweat of patients with atopic dermatitis correlates with an impaired innate defense of human skin in vivo. *J Immunol,* 174**,** 8003-10.

Rippke, F., Schreiner, V. & Schwanitz, H. J. 2002. The acidic milieu of the horny layer: new findings on the physiology and pathophysiology of skin pH. *Am J Clin Dermatol,* 3**,** 261-72.

Roberson, E. B. & Firestone, M. K. 1992. Relationship between Desiccation and Exopolysaccharide Production in a Soil Pseudomonas sp. *Applied and Environmental Microbiology,* 58**,** 1284-1291.

Robinson, M. D., Mccarthy, D. J. & Smyth, G. K. 2010. edgeR: a Bioconductor package for differential expression analysis of digital gene expression data. *Bioinformatics,* 26**,** 139-40.

Robinson, M. D. & Oshlack, A. 2010. A scaling normalization method for differential expression analysis of RNA-seq data. *Genome Biology,* 11**,** 1-9.

Rogasch, K., Ruhmling, V., Pane-Farre, J., Hoper, D., Weinberg, C., Fuchs, S., Schmudde, M., Broker, B. M., Wolz, C., Hecker, M. & Engelmann, S. 2006. Influence of the two-component system SaeRS on global gene expression in two different *Staphylococcus aureus* strains. *J Bacteriol,* 188**,** 7742-58.

Rohmer, M., Bouvier, P. & Ourisson, G. 1979. Molecular evolution of biomembranes: structural equivalents and phylogenetic precursors of sterols. *Proc Natl Acad Sci U S A,* 76**,** 847-51.

Romantsov, T., Guan, Z. & Wood, J. M. 2009. Cardiolipin and the osmotic stress responses of bacteria. *Biochim Biophys Acta,* 1788**,** 2092-100.

Roth, R. R. & James, W. D. 1988. Microbial ecology of the skin. *Annu Rev Microbiol,* 42**,** 441-64.

Ryu, S., Song, P. I., Seo, C. H., Cheong, H. & Park, Y. 2014. Colonization and Infection of the Skin by S. aureus: Immune System Evasion and the Response to Cationic Antimicrobial Peptides. *International Journal of Molecular Sciences,* 15**,** 8753-8772.

Sahl, H. G., Kordel, M. & Benz, R. 1987. Voltage-dependent depolarization of bacterial membranes and artificial lipid bilayers by the peptide antibiotic nisin. *Arch Microbiol,* 149**,** 120-4.

Sakinc, T., Kleine, B., Michalski, N., Kaase, M. & Gatermann, S. G. 2009. SdrI of Staphylococcus saprophyticus is a multifunctional protein: localization of the fibronectin-binding site. *FEMS Microbiol Lett,* 301**,** 28-34.

Schaible, U. E. & Kaufmann, S. H. 2004. Iron and microbial infection. *Nat Rev Microbiol,* 2**,** 946-53.

Schielke, S., Schmitt, C., Spatz, C., Frosch, M., Schubert-Unkmeir, A. & Kurzai, O. 2010. The transcriptional repressor FarR is not involved in meningococcal fatty acid

resistance mediated by the FarAB efflux pump and dependent on lipopolysaccharide structure. *Appl Environ Microbiol,* 76**,** 3160-9.
Schmid-Wendtner, M. H. & Korting, H. C. 2006. The pH of the skin surface and its impact on the barrier function. *Skin Pharmacol Physiol,* 19**,** 296-302.
Schroder, J. M. & Harder, J. 2006. Antimicrobial skin peptides and proteins. *Cell Mol Life Sci,* 63**,** 469-86.
Scriba, T. J., Sierro, S., Brown, E. L., Phillips, R. E., Sewell, A. K. & Massey, R. C. 2008. The Staphyloccous aureus Eap protein activates expression of proinflammatory cytokines. *Infect Immun,* 76**,** 2164-8.
Senyurek, I., Paulmann, M., Sinnberg, T., Kalbacher, H., Deeg, M., Gutsmann, T., Hermes, M., Kohler, T., Gotz, F., Wolz, C., Peschel, A. & Schittek, B. 2009. Dermcidin-derived peptides show a different mode of action than the cathelicidin LL-37 against *Staphylococcus aureus*. *Antimicrob Agents Chemother,* 53**,** 2499-509.
Shin, S. Y., Bajpai, V. K., Kim, H. R. & Kang, S. C. 2007. Antibacterial activity of bioconverted eicosapentaenoic (EPA) and docosahexaenoic acid (DHA) against foodborne pathogenic bacteria. *Int J Food Microbiol,* 113**,** 233-6.
Shore, A. C. & Coleman, D. C. 2013. Staphylococcal cassette chromosome mec: recent advances and new insights. *Int J Med Microbiol,* 303**,** 350-9.
Shubbar, E., Vegfors, J., Carlstrom, M., Petersson, S. & Enerback, C. 2012. Psoriasin (S100A7) increases the expression of ROS and VEGF and acts through RAGE to promote endothelial cell proliferation. *Breast Cancer Res Treat,* 134**,** 71-80.
Sieradzki, K. & Tomasz, A. 1997. Inhibition of cell wall turnover and autolysis by vancomycin in a highly vancomycin-resistant mutant of *Staphylococcus aureus*. *Journal of Bacteriology,* 179**,** 2557-2566.
Silveira, M. G., Baumgärtner, M., Rombouts, F. M. & Abee, T. 2004. Effect of Adaptation to Ethanol on Cytoplasmic and Membrane Protein Profiles of Oenococcus oeni. *Applied and Environmental Microbiology,* 70**,** 2748-2755.
Simanski, M., Koten, B., Schroder, J. M., Glaser, R. & Harder, J. 2012. Antimicrobial RNases in cutaneous defense. *J Innate Immun,* 4**,** 241-7.
Skaar, E. P. 2010. The Battle for Iron between Bacterial Pathogens and Their Vertebrate Hosts. *PLoS Pathogens,* 6**,** e1000949.
Skaar, E. P., Gaspar, A. H. & Schneewind, O. 2004a. IsdG and IsdI, heme-degrading enzymes in the cytoplasm of *Staphylococcus aureus*. *J Biol Chem,* 279**,** 436-43.
Skaar, E. P., Humayun, M., Bae, T., Debord, K. L. & Schneewind, O. 2004b. Iron-source preference of *Staphylococcus aureus* infections. *Science,* 305**,** 1626-8.
Smith, K. R. & Thiboutot, D. M. 2008. Thematic review series: skin lipids. Sebaceous gland lipids: friend or foe? *J Lipid Res,* 49**,** 271-81.
Song, C., Weichbrodt, C., Salnikov, E. S., Dynowski, M., Forsberg, B. O., Bechinger, B., Steinem, C., De Groot, B. L., Zachariae, U. & Zeth, K. 2013. Crystal structure and functional mechanism of a human antimicrobial membrane channel. *Proceedings of the National Academy of Sciences of the United States of America,* 110**,** 4586-4591.
Soong, G., Chun, J., Parker, D. & Prince, A. 2012. *Staphylococcus aureus* activation of caspase 1/calpain signaling mediates invasion through human keratinocytes. *J Infect Dis,* 205**,** 1571-9.
Sri Charan Bindu, B., Mishra, D. P. & Narayan, B. 2015. Inhibition of virulence of *Staphylococcus aureus* – a food borne pathogen – by squalene, a functional lipid. *Journal of Functional Foods,* 18**,** 224-234.
Steinhuber, A., Goerke, C., Bayer, M. G., Doring, G. & Wolz, C. 2003. Molecular architecture of the regulatory Locus sae of *Staphylococcus aureus* and its impact on expression of virulence factors. *J Bacteriol,* 185**,** 6278-86.
Stewart, M. E. & Downing, D. T. 1991. Chemistry and function of mammalian sebaceous lipids. *Adv Lipid Res,* 24**,** 263-301.

Sun, F., Li, C., Jeong, D., Sohn, C., He, C. & Bae, T. 2010. In the *Staphylococcus aureus* two-component system sae, the response regulator SaeR binds to a direct repeat sequence and DNA binding requires phosphorylation by the sensor kinase SaeS. *J Bacteriol,* 192**,** 2111-27.

Takigawa, H., Nakagawa, H., Kuzukawa, M., Mori, H. & Imokawa, G. 2005. Deficient production of hexadecenoic acid in the skin is associated in part with the vulnerability of atopic dermatitis patients to colonization by *Staphylococcus aureus*. *Dermatology,* 211**,** 240-8.

Taylor, D., Daulby, A., Grimshaw, S., James, G., Mercer, J. & Vaziri, S. 2003. Characterization of the microflora of the human axilla. *Int J Cosmet Sci,* 25**,** 137-45.

Terracciano, J. S. & Kashket, E. R. 1986. Intracellular Conditions Required for Initiation of Solvent Production by Clostridium acetobutylicum. *Applied and Environmental Microbiology,* 52**,** 86-91.

Thiboutot, D. 2004. Regulation of human sebaceous glands. *J Invest Dermatol,* 123**,** 1-12.

Thiel, M., Caldwell, C. C. & Sitkovsky, M. V. 2003. The critical role of adenosine A2A receptors in downregulation of inflammation and immunity in the pathogenesis of infectious diseases. *Microbes Infect,* 5**,** 515-26.

Torres, V. J., Attia, A. S., Mason, W. J., Hood, M. I., Corbin, B. D., Beasley, F. C., Anderson, K. L., Stauff, D. L., Mcdonald, W. H., Zimmerman, L. J., Friedman, D. B., Heinrichs, D. E., Dunman, P. M. & Skaar, E. P. 2010. *Staphylococcus aureus* fur regulates the expression of virulence factors that contribute to the pathogenesis of pneumonia. *Infect Immun,* 78**,** 1618-28.

Torres, V. J., Pishchany, G., Humayun, M., Schneewind, O. & Skaar, E. P. 2006. *Staphylococcus aureus* IsdB is a hemoglobin receptor required for heme iron utilization. *J Bacteriol,* 188**,** 8421-9.

Torres, V. J., Stauff, D. L., Pishchany, G., Bezbradica, J. S., Gordy, L. E., Iturregui, J., Anderson, K. L., Dunman, P. M., Joyce, S. & Skaar, E. P. 2007. A *Staphylococcus aureus* regulatory system that responds to host heme and modulates virulence. *Cell Host Microbe,* 1**,** 109-19.

Trapnell, C., Roberts, A., Goff, L., Pertea, G., Kim, D., Kelley, D. R., Pimentel, H., Salzberg, S. L., Rinn, J. L. & Pachter, L. 2012. Differential gene and transcript expression analysis of RNA-seq experiments with TopHat and Cufflinks. *Nat Protoc,* 7**,** 562-78.

Truong-Bolduc, Q. C., Dunman, P. M., Eidem, T. & Hooper, D. C. 2011. Transcriptional profiling analysis of the global regulator NorG, a GntR-like protein of *Staphylococcus aureus*. *J Bacteriol,* 193**,** 6207-14.

Truong-Bolduc, Q. C., Villet, R. A., Estabrooks, Z. A. & Hooper, D. C. 2014. Native efflux pumps contribute resistance to antimicrobials of skin and the ability of *Staphylococcus aureus* to colonize skin. *J Infect Dis,* 209**,** 1485-93.

Tsai, M., Ohniwa, R. L., Kato, Y., Takeshita, S. L., Ohta, T., Saito, S., Hayashi, H. & Morikawa, K. 2011. *Staphylococcus aureus* requires cardiolipin for survival under conditions of high salinity. *BMC Microbiol,* 11**,** 13.

Uniprot 2014. Activities at the Universal Protein Resource (UniProt). *Nucleic Acids Res,* 42**,** D191-8.

Utsui, Y. & Yokota, T. 1985. Role of an altered penicillin-binding protein in methicillin- and cephem-resistant *Staphylococcus aureus*. *Antimicrob Agents Chemother,* 28**,** 397-403.

Van Smeden, J., Janssens, M., Gooris, G. S. & Bouwstra, J. A. 2014. The important role of stratum corneum lipids for the cutaneous barrier function. *Biochim Biophys Acta,* 1841**,** 295-313.

Vanderwal, A. R., Makthal, N., Pinochet-Barros, A., Helmann, J. D., Olsen, R. J. & Kumaraswami, M. 2017. Iron Efflux by PmtA Is Critical for Oxidative Stress

Resistance and Contributes Significantly to Group A Streptococcus Virulence. *Infect Immun,* 85.
Varghese, S., Wu, A., Park, S., Imlay, K. R. & Imlay, J. A. 2007. Submicromolar hydrogen peroxide disrupts the ability of Fur protein to control free-iron levels in Escherichia coli. *Mol Microbiol,* 64**,** 822-30.
Vasireddy, V., Uchida, Y., Salem, N., Kim, S. Y., Mandal, M. N. A., Reddy, G. B., Bodepudi, R., Alderson, N. L., Brown, J. C., Hama, H., Dlugosz, A., Elias, P. M., Holleran, W. M. & Ayyagari, R. 2007. Loss of functional ELOVL4 depletes very long-chain fatty acids (≥C28) and the unique ω-O-acylceramides in skin leading to neonatal death. *Human molecular genetics,* 16**,** 471-482.
Vignaroli, C., Rinaldi, C. & Varaldo, P. E. 2011. Striking "seesaw effect" between daptomycin nonsusceptibility and beta-lactam susceptibility in Staphylococcus haemolyticus. *Antimicrob Agents Chemother,* 55**,** 2495-6; author reply 296-7.
Vijay, K., Brody, M. S., Fredlund, E. & Price, C. W. 2000. A PP2C phosphatase containing a PAS domain is required to convey signals of energy stress to the sigmaB transcription factor of *Bacillus subtilis*. *Mol Microbiol,* 35**,** 180-8.
Voelker, U., Dufour, A. & Haldenwang, W. G. 1995a. The *Bacillus subtilis* rsbU gene product is necessary for RsbX-dependent regulation of sigma B. *Journal of Bacteriology,* 177**,** 114-122.
Voelker, U., Luo, T., Smirnova, N. & Haldenwang, W. 1997. Stress activation of *Bacillus subtilis* sigma B can occur in the absence of the sigma B negative regulator RsbX. *J Bacteriol,* 179**,** 1980-4.
Voelker, U., Voelker, A. & Haldenwang, W. G. 1996a. Reactivation of the *Bacillus subtilis* anti-sigma B antagonist, RsbV, by stress- or starvation-induced phosphatase activities. *J Bacteriol,* 178**,** 5456-63.
Voelker, U., Voelker, A. & Haldenwang, W. G. 1996b. The yeast two-hybrid system detects interactions between *Bacillus subtilis* sigmaB regulators. *J Bacteriol,* 178**,** 7020-3.
Voelker, U., Voelker, A., Maul, B., Hecker, M., Dufour, A. & Haldenwang, W. G. 1995b. Separate mechanisms activate sigma B of *Bacillus subtilis* in response to environmental and metabolic stresses. *J Bacteriol,* 177**,** 3771-80.
Voyich, J. M., Braughton, K. R., Sturdevant, D. E., Whitney, A. R., Said-Salim, B., Porcella, S. F., Long, R. D., Dorward, D. W., Gardner, D. J., Kreiswirth, B. N., Musser, J. M. & Deleo, F. R. 2005. Insights into mechanisms used by *Staphylococcus aureus* to avoid destruction by human neutrophils. *J Immunol,* 175**,** 3907-19.
Vuong, C., Gotz, F. & Otto, M. 2000. Construction and characterization of an agr deletion mutant of *Staphylococcus epidermidis*. *Infect Immun,* 68**,** 1048-53.
Walkenhorst, W. F., Klein, J. W., Vo, P. & Wimley, W. C. 2013. pH Dependence of microbe sterilization by cationic antimicrobial peptides. *Antimicrob Agents Chemother,* 57**,** 3312-20.
Weinrick, B., Dunman, P. M., Mcaleese, F., Murphy, E., Projan, S. J., Fang, Y. & Novick, R. P. 2004. Effect of mild acid on gene expression in *Staphylococcus aureus*. *J Bacteriol,* 186**,** 8407-23.
Wos-Oxley, M. L., Plumeier, I., Von Eiff, C., Taudien, S., Platzer, M., Vilchez-Vargas, R., Becker, K. & Pieper, D. H. 2010. A poke into the diversity and associations within human anterior nare microbial communities. *Isme j,* 4**,** 839-51.
Wu, S., Piscitelli, C., De Lencastre, H. & Tomasz, A. 1996. Tracking the evolutionary origin of the methicillin resistance gene: cloning and sequencing of a homologue of mecA from a methicillin susceptible strain of Staphylococcus sciuri. *Microb Drug Resist,* 2**,** 435-41.
Wu, S., Zhu, Z., Fu, L., Niu, B. & Li, W. 2011. WebMGA: a customizable web server for fast metagenomic sequence analysis. *BMC Genomics,* 12**,** 444.

Xiong, A., Singh, V. K., Cabrera, G. & Jayaswal, R. K. 2000. Molecular characterization of the ferric-uptake regulator, fur, from *Staphylococcus aureus*. *Microbiology,* 146 (Pt 3)**,** 659-68.

Xu, R., Fazio, G. C. & Matsuda, S. P. 2004. On the origins of triterpenoid skeletal diversity. *Phytochemistry,* 65**,** 261-91.

Yang, S. J., Bayer, A. S., Mishra, N. N., Meehl, M., Ledala, N., Yeaman, M. R., Xiong, Y. Q. & Cheung, A. L. 2012. The *Staphylococcus aureus* two-component regulatory system, GraRS, senses and confers resistance to selected cationic antimicrobial peptides. *Infect Immun,* 80**,** 74-81.

Yarwood, J. M. & Schlievert, P. M. 2003. Quorum sensing in Staphylococcus infections. *Journal of Clinical Investigation,* 112**,** 1620-1625.

Ye, J., Coulouris, G., Zaretskaya, I., Cutcutache, I., Rozen, S. & Madden, T. L. 2012. Primer-BLAST: a tool to design target-specific primers for polymerase chain reaction. *BMC Bioinformatics,* 13**,** 134.

Zeeuwen, P. L., Boekhorst, J., Van Den Bogaard, E. H., De Koning, H. D., Van De Kerkhof, P. M., Saulnier, D. M., Van, S., Ii, Van Hijum, S. A., Kleerebezem, M., Schalkwijk, J. & Timmerman, H. M. 2012. Microbiome dynamics of human epidermis following skin barrier disruption. *Genome Biol,* 13**,** R101.

Zerbino, D. R. & Birney, E. 2008. Velvet: algorithms for de novo short read assembly using de Bruijn graphs. *Genome Res,* 18**,** 821-9.

Zhao, W., He, X., Hoadley, K. A., Parker, J. S., Hayes, D. N. & Perou, C. M. 2014. Comparison of RNA-Seq by poly (A) capture, ribosomal RNA depletion, and DNA microarray for expression profiling. *BMC Genomics,* 15**,** 419.

Zouboulis, C. C. 2004. Acne and sebaceous gland function. *Clin Dermatol,* 22**,** 360-6.

Zurek, O. W., Nygaard, T. K., Watkins, R. L., Pallister, K. B., Torres, V. J., Horswill, A. R. & Voyich, J. M. 2014. The role of innate immunity in promoting SaeR/S-mediated virulence in *Staphylococcus aureus*. *J Innate Immun,* 6**,** 21-30.

Appendix

Appendix Table 1 DE genes of *S. aureus* in response to 1 % (v/v) squalene challenge. The level of fold change **(logFC)** is based on $\log_2$. All DE genes have **FDR** (false discovery rate) ≤ 0.05. DE genes that discussed in this thesis were highlighted.

Gene	Gene description	logFC	FDR
NWMN_tRNA17	tRNA-Glu	4.391714365	0.004260181
NWMN_2304	conserved hypothetical protein	2.618022746	0.000170352
NWMN_1077	conserved hypothetical protein	2.373553493	2.86E-11
NWMN_1076	conserved hypothetical protein	2.102404332	9.93E-09
isdG	cytoplasmic heme-iron binding protein	2.037769355	2.92E-05
NWMN_1075	conserved hypothetical protein	1.946814265	3.99E-07
NWMN_2081	conserved hypothetical protein	1.939721459	3.28E-06
fnbB	fibronectin binding protein B precursor	1.909883684	0.000803488
NWMN_1312	conserved hypothetical protein	1.900268288	0.001216333
NWMN_0118	conserved hypothetical protein	1.860157425	1.46E-05
sbnD	membrane transporter protein	1.845657617	0.003739599
glpD	aerobic glycerol-3-phosphate dehydrogenase	1.833967598	6.51E-06
lukS	leukocidin/hemolysin toxin family S subunit	1.818740226	0.00076537
hlgB	gamma hemolysin, component B	1.81185194	6.23E-06
isdC	iron-regulated cell surface protein	1.799175171	0.002372492
NWMN_2077	iron compound ABC transporter, permease protein	1.797097422	1.72E-06
NWMN_2069	conserved hypothetical protein	1.793441637	0.000230585
sbnI	SbnI protein	1.773132477	4.13E-06
sbnH	diaminopimelate decarboxylase	1.757325348	2.13E-06
hlgC	gamma-hemolysin component C	1.739768742	7.00E-06
NWMN_0429	N-acetylmuramoyl-L-alanine amidase aaa precursor	1.731374712	6.36E-06
NWMN_0834	conserved hypothetical protein	1.730799388	8.17E-05

NWMN_1224	conserved hypothetical protein	1.727076942	0.043338336
sirA	siderophore compound ABC transporter binding protein	1.686526318	0.004260181
NWMN_0339	conserved hypothetical protein	1.686109726	0.000988679
NWMN_2215	conserved hypothetical protein	1.653855457	0.001861831
srtB	NPQTN-specific sortase B	1.647542957	0.001618872
cysM	cysteine synthase	1.64122432	1.58E-05
NWMN_0117	conserved hypothetical protein	1.636898517	0.001169907
isdF	iron/heme permease	1.62096962	0.001676354
isdA	iron-regulated heme-iron binding protein IsdA	1.613074365	0.000373984
NWMN_2076	FecCD iron compound ABC transporter, permease family protein	1.599974347	6.66E-05
NWMN_1522	hypothetical protein	1.589735706	0.025741491
sbnG	2-dehydro-3-deoxyglucarate aldolase	1.575776824	0.000643012
NWMN_1674	CrcB-like protein	1.572478032	0.021562261
NWMN_tRNA34	tRNA-Met	1.568784472	0.008740502
NWMN_0027	conserved hypothetical protein	1.56609009	0.000154633
NWMN_0116	conserved hypothetical protein	1.542858789	0.001151533
lukF	leukocidin/hemolysin toxin family F subunit	1.537358233	0.01298427
NWMN_tRNA23	tRNA-Met	1.535625333	0.007633599
ssl2nm	staphylococcal enterotoxin-like toxin	1.520953011	1.22E-05
sdrD	Ser-Asp rich fibrinogen/bone sialoprotein-binding protein sdrD	1.510877499	0.000191935
lipA	lipase/esterase LipA	1.502486288	0.001311868
NWMN_2185	iron compound ABC transporter, iron compound-binding protein	1.501910669	0.001966684
NWMN_0703	iron compound ABC transporter, permease protein	1.495454085	0.003213835
ssp	extracellular matrix and plasma binding protein	1.491811753	0.000745931
sbnE	siderophore biosynthesis IucA family protein	1.490842566	0.007181175
gatC	glutamyl-tRNA amidotransferase subunit C	1.481465721	0.049474771
fhuB	ferrichrome transport permease fhuB	1.477806145	0.000275902
NWMN_0755	conserved hypothetical protein	1.473235181	3.67E-05

NWMN_2273	acetyltransferase, GNAT family protein	1.458763544	0.000698424
NWMN_1503	enterotoxin family protein	1.439145707	0.014526254
sbnC	siderophore biosynthesis IucC family protein	1.433731695	0.022464997
isdE	iron compound ABC transporter	1.418604072	0.003837888
NWMN_0188	conserved hypothetical protein	1.416044417	0.000335064
tatA	twin-arginine translocation protein TatA	1.41121221	0.021562261
NWMN_0434	conserved hypothetical protein	1.410512536	0.00019783
NWMN_0423	sodium-dependent symporter protein	1.410425263	0.002496427
NWMN_0764	conserved hypothetical protein	1.407957134	0.00063892
hisC	histidinol-phosphate aminotransferase	1.397222632	0.001446274
NWMN_0907	conserved hypothetical protein	1.378123716	0.001221613
NWMN_0702	ferrichrome ABC transporter permease	1.376380666	0.003629908
NWMN_0370	conserved hypothetical protein	1.36933798	0.040337837
NWMN_2396	C-terminal part of fibronectin binding protein B	1.362213163	0.049914616
ssl3nm	staphylococcal enterotoxin-like toxin	1.35186464	0.000308804
ssl4nm	staphylococcal enterotoxin-like toxin	1.351587362	0.00011058
rimJ	ribosomal-protein-alanine N-acetyltransferase	1.350559232	0.002084534
NWMN_1999	conserved hypothetical protein	1.338577629	0.003466992
NWMN_2078	ferrichrome ABC transporter lipoprotein	1.330969337	0.001677384
NWMN_0231	conserved hypothetical protein	1.32886099	0.000486682
NWMN_2259	conserved hypothetical protein	1.324491797	0.003429144
sbnF	siderophore biosynthesis IucC family protein	1.323620399	0.01224487
NWMN_0341	conserved hypothetical protein	1.299596117	0.015677591
NWMN_2223	conserved hypothetical protein	1.2746435	0.005218439
ssl5nm	staphylococcal enterotoxin-like toxin	1.269335306	0.001390424
NWMN_0784	conserved hypothetical protein	1.264700366	0.000602344
NWMN_0115	conserved hypothetical protein	1.260064119	0.002891125
NWMN_0208	conserved hypothetical protein	1.256511578	0.000689824

NWMN_2254	conserved hypothetical protein	1.253603332	0.017315124
ssl9nm	staphylococcal enterotoxin-like toxin	1.245407586	0.001675356
NWMN_2253	drug resistance transporter EmrB/QacA subfamily protein	1.241263981	0.030982684
NWMN_0704	ABC transporter ATP-binding protein	1.231132968	0.005117015
spsA	type-I signal peptidase A component	1.225833525	0.008186324
ssl10	staphylococcal enterotoxin-like toxin	1.225330243	0.001435413
NWMN_1210	hydrolase	1.213092643	0.001157292
lytM	peptidoglycan hydrolase	1.20831528	0.004177294
NWMN_0006	conserved hypothetical protein	1.182095903	0.001153031
NWMN_0028	metallo-beta-lactamase superfamily protein	1.162206966	0.001264841
NWMN_2467	O-acetyltransferase OatA	1.1589439	0.006615849
NWMN_0662	conserved hypothetical protein	1.158407355	0.010904473
NWMN_2316	cation efflux family protein	1.145545991	0.011122739
nhaC	Na?? antiporter NhaC	1.139581368	0.032277029
NWMN_0378	xanthine phosphoribosyltransferase	1.13481228	0.049983752
NWMN_0636	AraC family regulatory protein	1.134410771	0.026538061
NWMN_0997	conserved hypothetical protein	1.126973538	0.039640464
sirB	siderophore compound ABC transporter permease protein SirB	1.125725368	0.041929831
NWMN_0826	NADH-dependent flavin oxidoreductase	1.121950449	0.003925964
NWMN_0853	3-oxoacyl-(acyl-carrier-protein) synthase III	1.121152058	0.009144271
isdB	iron-regulated heme-iron binding protein IsdB	1.103608496	0.004666203
potA	spermidine/putrescine ABC transporter, ATP-binding protein	1.088866855	0.011598491
ssl6nm	staphylococcal enterotoxin-like toxin	1.08695326	0.020999208
NWMN_0026	conserved hypothetical protein	1.083918511	0.006197105
NWMN_0964	conserved hypothetical protein	1.081836462	0.026889022
NWMN_2374	conserved hypothetical protein	1.076666957	0.016134957
NWMN_0230	conserved hypothetical protein	1.075434887	0.048721384
trmU	tRNA (5-methylaminomethyl-2-thiouridylate)-methyltransferase	1.074801549	0.019883136

NWMN_2255	transcriptional regulator TetR family protein	1.074408184	0.032365366
NWMN_2271	acetyltransferase, GNAT family protein	1.068362047	0.049474771
tagA	teichoic acid biosynthesis protein A	1.067987378	0.013923834
NWMN_0038	conserved hypothetical protein	1.06428277	0.009285357
pbuX	xanthine/uracil permease	1.046172027	0.027082488
NWMN_0768	conserved hypothetical protein	1.043079883	0.021995218
NWMN_0356	conserved hypothetical protein	1.040169777	0.0464606
NWMN_1664	arsenical resistance operon repressor	1.03634975	0.027834257
NWMN_0849	conserved hypothetical protein	1.03385013	0.048804158
NWMN_2274	pyridine nucleotide-disulfide oxidoreductase family protein	1.017399281	0.008397784
NWMN_1667	mannosyl-glycoprotein endo-beta-N-acetylglucosamidase	1.012592943	0.019105916
NWMN_2341	NAD dependent epimerase/dehydratase family protein	1.011112905	0.009166342
NWMN_0693	conserved hypothetical protein	1.006752239	0.00674109
ssl8nm	staphylococcal enterotoxin-like toxin	1.000814929	0.012178034
NWMN_2070	conserved hypothetical protein	0.994037764	0.010047927
NWMN_0535	conserved hypothetical protein	0.989378763	0.030203328
NWMN_0119	conserved hypothetical protein	0.984420452	0.033416926
moaE	molybdopterin synthase large subunit	0.969922359	0.032657042
fhuG	ferrichrome transport permease fhuG	0.969351318	0.018740855
NWMN_1064	conserved hypothetical protein	0.961656036	0.017308553
pabA	para-aminobenzoate synthase component II	0.948707698	0.039640464
NWMN_0766	conserved hypothetical protein	0.942370621	0.048965994
NWMN_0189	conserved hypothetical protein	0.935086775	0.013358702
NWMN_0245	conserved hypothetical protein	0.929775452	0.046219101
NWMN_1760	A/G-specific adenine glycosylase	0.927418981	0.018213724
NWMN_0025	conserved hypothetical protein	0.926381005	0.017567592
NWMN_2159	conserved hypothetical protein	0.921753931	0.024479656
NWMN_1865	conserved hypothetical protein	0.914643411	0.015677591

NWMN_1534	N-acetylmuramoyl-L-alanine amidase, family 3	0.914268756	0.038778203
NWMN_0374	sodium:dicarboxylate symporter family protein	0.906987071	0.023963343
porA	pyruvate flavodoxin ferredoxin oxidoreductase, alpha subunit	0.906870202	0.039640464
sdrC	Ser-Asp rich fibrinogen/bone sialoprotein-binding protein SdrC	0.904721942	0.042555138
metB	cystathionine gamma-synthase	0.90316923	0.015900184
NWMN_0150	conserved hypothetical protein	0.896462718	0.029534647
NWMN_0920	conserved hypothetical protein	0.887581397	0.04455717
NWMN_1824	conserved hypothetical protein	0.886086239	0.017433034
NWMN_0954	conserved hypothetical protein	0.870790774	0.034524729
NWMN_2079	conserved hypothetical protein	0.863468143	0.025469897
NWMN_1621	conserved hypothetical protein	0.838386113	0.03027165
NWMN_0320	lipoate-protein ligase A family protein	0.836374471	0.018821644
NWMN_0582	iron compound ABC transporter, permease protein	0.833668003	0.033416926
tagG	teichoic acid ABC transporter permease protein	0.828950591	0.028045142
NWMN_0970	conserved hypothetical protein	0.828124023	0.039304655
NWMN_0978	cell division protein	0.815797794	0.039931332
NWMN_0691	ABC transporter permease protein	0.814450931	0.04080052
NWMN_2451	MmpL efflux pump	0.807733405	0.04126105
NWMN_0143	oligopeptide ABC transporter, ATP-binding protein	0.765887296	0.049474771
NWMN_2408	conserved hypothetical protein	-0.767583415	0.048965994
NWMN_1471	cytidine deaminase, homotetrameric	-0.818324714	0.04455717
modB	molybdenum ABC transporter, permease protein	-0.819779415	0.042904756
NWMN_0140	conserved hypothetical protein	-0.819976897	0.046838779
modC	molybdenum ABC transporter, ATP-binding protein ModC	-0.82840755	0.048223458
rbsR	ribose transcriptional repressor RbsR	-0.877828041	0.029285497
NWMN_2026	aldehyde dehydrogenase family protein	-0.89104504	0.021812136
rsbV	anti-sigma B factor antagonist	-0.896540693	0.036574974
NWMN_2089	osmoprotectant transporter	-0.904841818	0.01933896

purF	amidophosphoribosyltransferase precursor	-0.915886383	0.044496604
atpG	ATP synthase, gamma subunit	-0.923512623	0.048804158
deoC	deoxyribose-phosphate aldolase	-0.930082651	0.015176575
NWMN_1645	conserved hypothetical protein	-0.931146164	0.013362456
fumC	fumarate hydratase, class II	-0.944615907	0.047119649
NWMN_1072	conserved hypothetical protein	-0.955345013	0.030903811
NWMN_2202	conserved hypothetical protein	-0.960875918	0.032277029
NWMN_2212	inositol monophosphatase family protein	-0.967152853	0.046641003
NWMN_0672	aldo/keto reductase family protein	-0.968802384	0.025518882
NWMN_0673	conserved hypothetical protein	-0.978104098	0.019424705
NWMN_0155	conserved hypothetical protein	-0.978201068	0.0464606
NWMN_2479	amidohydrolase family protein	-0.982746081	0.007968853
NWMN_1352	conserved hypothetical protein	-0.98839559	0.01322002
NWMN_2480	hydrolase	-0.989761286	0.025671538
treR	trehalose operon repressor	-0.991075082	0.01398011
sarH1	staphylococcal accessory regulator A homolog	-0.997863167	0.04126105
NWMN_0753	conserved hypothetical protein	-1.001310114	0.039640464
NWMN_0083	phosphopentomutase	-1.005230335	0.024827903
NWMN_0321	oxidoreductase family protein	-1.007029859	0.01398011
NWMN_1820	conserved hypothetical protein	-1.018554457	0.011168768
NWMN_1275	4-oxalocrotonate tautomerase	-1.033733018	0.019105916
NWMN_0482	conserved hypothetical protein	-1.040971951	0.003813409
NWMN_0782	ABC transporter, substrate-binding protein	-1.041829342	0.006809057
NWMN_1819	low molecular weight phosphotyrosine protein phosphatase	-1.05665713	0.011220097
NWMN_1767	ThiJ/PfpI family protein	-1.059913304	0.007858775
oppC	oligopeptide ABC transporter, permease protein	-1.068490901	0.037256536
katA	catalase	-1.069271884	0.010242254
tpi	triosephosphate isomerase	-1.074946695	0.047694905

NWMN_0973	inositol-1-monophosphatase family protein	-1.090966746	0.014325508
ald1	alanine dehydrogenase 1	-1.091697463	0.006943523
NWMN_0649	conserved hypothetical protein	-1.10589775	0.01293585
NWMN_1074	conserved hypothetical protein	-1.109347115	0.038249752
rpsU	30S ribosomal protein S21	-1.131760378	0.003546585
NWMN_0286	conserved hypothetical protein	-1.136189433	0.007881096
clfA	clumping factor A	-1.168357011	0.00384788
NWMN_0047	conserved hypothetical protein	-1.183808176	0.005729119
NWMN_1038	phage holin	-1.191576812	0.044342298
NWMN_0289	phage terminase large subunit	-1.198356207	0.008100091
NWMN_1688	conserved hypothetical protein	-1.203453656	0.000596259
NWMN_2417	conserved hypothetical protein	-1.210368917	0.042555138
bsaG	lantibiotic ABC transporter protein	-1.211687481	0.027795832
NWMN_0460	conserved hypothetical protein	-1.216968484	0.00892544
NWMN_1689	conserved hypothetical protein	-1.217607098	0.000949032
NWMN_1631	conserved hypothetical protein	-1.218147686	0.000920521
NWMN_2075	conserved hypothetical protein	-1.220841125	0.021534821
NWMN_2594	conserved hypothetical protein	-1.231597632	0.008475979
NWMN_0737	conserved hypothetical protein	-1.231628922	0.00125063
NWMN_2270	conserved hypothetical protein	-1.232171882	0.001885155
NWMN_2217	phosphosugar-binding transcriptional regulator RpiR family protein	-1.235868365	0.000785597
sucB	dihydrolipoamide succinyltransferase E2 component of 2-oxoglutarate dehydrogenase complex	-1.241262015	0.001342878
NWMN_0250	ABC transporter, permease protein	-1.242121692	0.000596918
NWMN_0251	ABC transporter ATP-binding protein	-1.251793928	0.000578823
NWMN_1059	hypothetical protein	-1.258672252	0.01579016
NWMN_1821	ribonuclease BN	-1.261264898	0.001676354
srrA	DNA-binding response regulator SrrA	-1.27091017	0.010803254
NWMN_0547	conserved hypothetical protein	-1.272232738	0.011862374

aldA	aldehyde dehydrogenase homolog	-1.276864757	0.016384269
NWMN_0601	conserved hypothetical protein	-1.28359699	0.039427602
NWMN_2330	conserved hypothetical protein	-1.289935306	0.014072465
qoxA	quinol oxidase polypeptide II QoxA	-1.299811326	0.009270761
NWMN_2353	ABC transporter, ATP-binding protein	-1.309722712	0.002918126
NWMN_0650	conserved hypothetical protein	-1.312263499	0.001311868
NWMN_1632	general stress protein-like protein	-1.315279613	0.001047098
NWMN_1746	conserved hypothetical protein	-1.324636718	0.000269303
malA	alpha-D-1,4-glucosidase	-1.327595221	0.010568249
NWMN_0219	conserved hypothetical protein	-1.332445675	0.007020509
NWMN_0603	ABC transporter ATP-binding protein	-1.34137692	0.001879748
NWMN_1831	ferritin	-1.343125123	0.000830872
NWMN_0053	conserved hypothetical protein	-1.344645886	0.000164285
bsaE	lantibiotic ABC transporter protein	-1.34728546	0.034984162
NWMN_2465 crtO	conserved hypothetical protein	-1.353324593	0.013720801
glcA	glucose-specific PTS transporter protein IIABC component	-1.353697866	0.002301503
NWMN_0587	conserved hypothetical protein	-1.356405362	0.000345402
ptsG	PTS system, glucose-specific IIABC component	-1.369964474	0.000293668
NWMN_0288	conserved hypothetical protein	-1.37459303	0.000477792
NWMN_0290	phage portal protein	-1.378010196	0.001550749
NWMN_2350	para-nitrobenzyl esterase chain A	-1.391709838	0.001096582
bsaP	lantibiotic leader peptide processing serine protease	-1.392294145	0.000200322
NWMN_0856	oligopeptide transport system permease protein	-1.394267694	0.012152613
NWMN_0310	phage tail fiber	-1.39730765	0.004185379
NWMN_0291	conserved hypothetical protein	-1.399689293	0.000366213
treC	alpha,alpha-phosphotrehalase	-1.403606343	0.00202554
arcA	arginine deiminase	-1.410235925	0.045888079
pckA	phosphoenolpyruvate carboxykinase	-1.413206543	0.003282012

tnp1	transposase for IS1181	-1.417192718	0.003727185
cidB	holin-like protein CidB	-1.419709376	0.000200322
NWMN_0299	conserved hypothetical protein	-1.424594155	0.000789478
hla	alpha-hemolysin precursor	-1.426526711	0.041041611
mtlD	mannitol-1-phosphate 5-dehydrogenase	-1.426611973	0.000235897
poxB	pyruvate oxidase	-1.430850621	0.000117337
NWMN_2444	conserved hypothetical protein	-1.439396126	0.04568425
NWMN_1861	conserved hypothetical protein	-1.440394291	0.019105916
serS	seryl-tRNA synthetase	-1.442192501	0.011245842
NWMN_1601	metallo-beta-lactamase superfamily protein	-1.443632497	0.004708024
qoxB	quinol oxidase polypeptide I QoxB	-1.460081127	0.003422458
NWMN_0285	conserved hypothetical protein	-1.463969938	0.001120834
NWMN_0293	conserved hypothetical protein	-1.468065948	0.000569633
NWMN_0050	67 kDa Myosin-crossreactive streptococcal antigen homolog	-1.485128575	0.016695602
ribA	riboflavin biosynthesis protein	-1.485881222	0.043039003
NWMN_0173	ABC transporter, substrate-binding protein	-1.488557371	0.011771823
crtN	squalene synthase	-1.51362285	0.000383827
NWMN_2229	oxidoreductase, short chain dehydrogenase/reductase family protein	-1.51451763	3.36E-05
NWMN_2356	conserved hypothetical protein	-1.515861208	0.000359118
hutG	formiminoglutamase	-1.516716748	0.000120711
ilvD	dihydroxy-acid dehydratase	-1.525215538	0.018670554
NWMN_2487	fructosamine kinase family protein	-1.52580299	0.010255107
gntK	gluconate kinase	-1.526785948	0.002309274
NWMN_2369	short chain dehydrogenase	-1.535682979	8.55E-05
pyrE	orotate phosphoribosyltransferase	-1.540463885	7.64E-05
NWMN_0602	conserved hypothetical protein	-1.541760999	0.016559644
sdhA	succinate dehydrogenase flavoprotein subunit	-1.551299422	8.20E-05
mtlA	mannitol-specific IIA component	-1.562402284	0.000154633

sucA	2-oxoglutarate dehydrogenase E1 component	-1.568777644	0.001136177
NWMN_2209	conserved hypothetical protein	-1.568980601	3.35E-05
pryF	orotidine 5'-phosphate decarboxylase	-1.57492933	0.000335064
NWMN_1989	conserved hypothetical protein	-1.579031698	1.64E-05
mtlF	PTS system, mannitol-specific IIBC component	-1.581150174	2.69E-05
qoxC	quinol oxidase polypeptide III	-1.588247449	0.000198597
NWMN_0767	conserved hypothetical protein	-1.593792357	0.000120711
NWMN_0300	conserved hypothetical protein	-1.595966377	0.000184327
NWMN_1730	conserved hypothetical protein	-1.619833188	1.46E-05
NWMN_2419	acetyltransferase, GNAT family protein	-1.619928643	0.016559644
nrdD	anaerobic ribonucleoside-triphosphate reductase	-1.621304953	0.041237103
NWMN_1600	universal stress protein family protein	-1.643233388	0.006864013
NWMN_2210	formate dehydrogenase homolog	-1.645647927	1.69E-05
NWMN_0306	conserved hypothetical protein	-1.651356271	2.18E-05
NWMN_2275	conserved hypothetical protein	-1.654057221	0.001342878
NWMN_0303	conserved hypothetical protein	-1.6555396	0.000109974
NWMN_1298	phosphate ABC transporter, permease protein	-1.662822391	0.048561295
NWMN_0137	RpiR family transcriptional regulator	-1.663047395	0.003540924
NWMN_1124	conserved hypothetical protein	-1.663917268	0.002515842
NWMN_0896	conserved hypothetical protein	-1.674011077	0.01672517
NWMN_0302	phage tape measure protein	-1.67992967	0.000410558
NWMN_0297	conserved hypothetical protein	-1.680750913	0.00051392
NWMN_0366	conserved hypothetical protein	-1.692731099	0.000999683
NWMN_0667	fructose operon transcriptional regulator	-1.695870549	0.006809057
NWMN_0695	conserved hypothetical protein	-1.706147889	3.30E-06
spoVG	stage V sporulation protein G homolog	-1.710639782	3.07E-06
NWMN_1750	extracellular glutamine-binding protein	-1.711584118	0.003546585
NWMN_0294	phage major head protein	-1.712126103	9.13E-05

pnp	purine nucleoside phosphorylase	-1.71302074	0.007386273
NWMN_0304	phage minor structural protein	-1.716879516	0.000109311
NWMN_2058	transcriptional antiterminator BglG family protein	-1.717837161	2.13E-06
ribH	riboflavin synthase, beta subunit	-1.718287414	0.015068407
NWMN_0295	conserved hypothetical protein	-1.729203283	1.28E-05
treP	PTS system, trehalose-specific IIBC component	-1.730083571	0.002152744
NWMN_0136	sucrose-specific PTS transporter IIBC component protein	-1.745995645	0.005218439
NWMN_0948	conserved hypothetical protein	-1.747510801	0.00892652
NWMN_0305	conserved hypothetical protein	-1.757961623	5.17E-05
NWMN_0364	conserved hypothetical protein	-1.758794739	6.70E-06
NWMN_2591	conserved hypothetical protein	-1.779955967	3.73E-05
NWMN_0585	conserved hypothetical protein	-1.787301175	0.003335764
NWMN_rRNA12	23S ribosomal RNA	-1.796735315	0.014748844
NWMN_1299	phosphate ABC transporter, permease protein	-1.815399927	0.030903811
crtI	phytoene dehydrogenase	-1.81784514	3.25E-07
NWMN_0771	OsmC-like protein	-1.823846103	2.44E-06
NWMN_0377	conserved hypothetical protein	-1.829245782	1.28E-06
gpmA	2,3-bisphosphoglycerate-dependent phosphoglycerate mutase	-1.829624939	6.73E-05
NWMN_2463 crtQ	glycosyl transferase, group 2 family protein	-1.836278635	1.29E-05
NWMN_rRNA15	23S ribosomal RNA	-1.85179186	0.005052173
NWMN_0296	conserved hypothetical protein	-1.852887404	2.87E-05
bsaF	lantibiotic immunity protein F	-1.856893678	1.54E-05
pyrAB	carbamoyl-phosphate synthase, pyrimidine-specific, large chain	-1.864114305	2.24E-06
NWMN_0298	conserved hypothetical protein	-1.877776557	1.23E-05
lacA	galactose-6-phosphate isomerase LacA subunit	-1.888521425	0.026915502
NWMN_1749	glutamine transport ATP-binding protein	-1.888790695	8.20E-05
NWMN_0301	conserved hypothetical protein	-1.899831791	1.42E-05
NWMN_0125	conserved hypothetical protein	-1.932851738	0.006229133

lrgB	antiholin-like protein LrgB	-1.955615897	0.00843734
NWMN_2368	conserved hypothetical protein	-1.967329979	2.76E-06
NWMN_1527	conserved hypothetical protein	-1.969317656	4.52E-05
NWMN_1604	universal stress protein family protein	-1.987339779	0.000663965
NWMN_2282	conserved hypothetical protein	-1.991792992	8.65E-06
NWMN_2352	conserved hypothetical protein	-1.992833412	2.45E-06
crtM	squalene desaturase	-2.014282558	0.000329079
scdA	cell wall metabolism protein	-2.020168979	0.001092088
lacD	tagatose 1,6-diphosphate aldolase	-2.021269167	0.030982684
NWMN_2087	conserved hypothetical protein	-2.025111086	9.30E-07
NWMN_2371	alkylhydroperoxidase AhpD family protein	-2.025417197	7.31E-06
NWMN_2502	conserved hypothetical protein	-2.029333151	0.001524848
sdhB	succinate dehydrogenase iron-sulfur protein	-2.039064459	2.23E-08
NWMN_2442	conserved hypothetical protein	-2.064592907	0.000228957
NWMN_2557	conserved hypothetical protein	-2.066296651	3.14E-06
thiM	hydroxyethylthiazole kinase	-2.072183059	0.002742565
NWMN_2086	alkaline shock protein 23	-2.073915939	3.78E-06
nrdG	anaerobic ribonucleotide reductase, small subunit	-2.091118199	0.018737372
NWMN_0041	conserved hypothetical protein	-2.09789887	0.010024104
NWMN_2088	conserved hypothetical protein	-2.099267381	7.21E-07
cidA	holin-like protein CidA	-2.105353836	0.004185379
NWMN_1998	transcriptional regulator TenA family protein	-2.105904124	0.012331396
pstS	phosphate ABC transporter, phosphate-binding protein PstS	-2.115650483	0.008522657
qoxD	quinol oxidase polypeptide IV	-2.122198187	3.30E-06
alsD	alpha-acetolactate decarboxylase	-2.133285669	0.000684584
argH	argininosuccinate lyase	-2.139712868	0.000449823
NWMN_0651	conserved hypothetical protein	-2.186101106	9.05E-06
fruB	fructose 1-phosphate kinase	-2.189272564	0.000341088

NWMN_2048	conserved hypothetical protein	-2.195718847	4.90E-07
lip	lipase precursor	-2.209128171	0.003787795
NWMN_0247	formate/nitrite transporter family protein	-2.210263199	0.031170158
narI	respiratory nitrate reductase, gamma subunit	-2.265144815	0.010134274
NWMN_1526	hypothetical protein	-2.304341594	2.23E-08
NWMN_2507	conserved hypothetical protein	-2.306586164	1.84E-10
NWMN_0135	conserved hypothetical protein	-2.313626238	0.012993982
thiD1	phosphomethylpyrimidine kinase	-2.319759035	0.000410259
NWMN_0944	conserved hypothetical protein	-2.376941967	0.000308804
gntR	gluconate operon transcriptional repressor	-2.383994781	0.000718315
thiE	thiamine-phosphate pyrophosphorylase	-2.385986995	0.001542734
NWMN_0945	conserved hypothetical protein	-2.38610841	0.000260283
NWMN_rRNA02	23S ribosomal RNA	-2.445567144	0.031238834
pyrAA	carbamoyl-phosphate synthase, pyrimidine-specific, small chain	-2.465465401	3.68E-06
NWMN_2597	conserved hypothetical protein	-2.472911779	0.000490694
pyrP	uracil permease	-2.48357913	8.65E-06
pyrC	dihydroorotase multifunctional complex type	-2.487631207	6.13E-07
argG	argininosuccinate synthase	-2.516203038	0.00032862
pyrB	aspartate carbamoyltransferase catalytic subunit	-2.536274264	7.80E-06
alsS	alpha-acetolactate synthase	-2.53830195	0.0004116
NWMN_0943	conserved hypothetical protein	-2.577047175	3.76E-05
NWMN_0783	CsbD-like superfamily protein	-2.598835133	1.33E-07
NWMN_0078	conserved hypothetical protein	-2.6379771	2.63E-09
fruA	fructose specific permease	-2.642488034	6.26E-05
NWMN_2074	conserved hypothetical protein	-2.734211938	8.55E-05
NWMN_0175	flavohemoprotein	-2.815939113	0.001157292
putA	proline dehydrogenase	-2.818989005	0.000334049
NWMN_0134	conserved hypothetical protein	-2.974493212	0.000373326

NWMN_2377	conserved hypothetical protein	-3.089043829	0.003230466
ald	alanine dehydrogenase 2	-3.164464926	0.008561475
NWMN_0721	sigma 54 modulation protein	-3.178060333	0.000191978
agrA	staphylococcal accessory gene regulator A	-3.17967839	1.35E-05
NWMN_1346	conserved hypothetical protein	-3.191143403	0.000442002
NWMN_rRNA01	16S ribosomal RNA	-3.257403918	0.007881096
adhE	iron-containing alcohol dehydrogenase	-3.30235649	0.001311868
NWMN_2268	L-lactate permease 2	-3.487800488	0.000216958
agrB	staphylococcal accessory gene regulator protein B	-3.509905208	8.17E-05
agrC	staphylococcal accessory gene regulator protein C	-3.602753557	1.15E-05
NWMN_1347	amino acid permease	-3.666890342	0.000373984
ilvA	threonine dehydratase II	-3.99231362	0.000294381
agrD	staphylococcal accessory gene regulator protein D	-4.017818192	7.83E-08
NWMN_2620	phenol-soluble modulin beta 2	-4.133611445	0.000629443
narJ	respiratory nitrate reductase, delta subunit	-4.326965147	0.000284867
ldh1	L-lactate dehydrogenase	-4.471711918	0.000452466
adh1	alcohol dehydrogenase	-4.60720312	0.000896027
cysG	uroporphyrin-III C-methyl transferase	-4.667737692	4.78E-05
narH	nitrate reductase beta chain	-4.675899151	5.34E-05
nirD	assimilatory nitrite reductase [NAD(P)H], small subunit	-4.833992474	0.000115345
nirR	nitrite reductase transcriptional regulator NirR	-5.308002638	6.26E-05
narG	nitrate reductase, alpha subunit	-5.446085452	8.96E-06
nirB	assimilatory nitrite reductase [NAD(P)H], large subunit	-5.487423945	1.20E-05
NWMN_1084	phenol-soluble modulin beta 1	-5.505010759	4.12E-05
hld	delta-hemolysin	-5.538554629	1.66E-05
NWMN_2288	nitrite transport protein	-6.279226177	3.50E-05
NWMN_2616	phenol-soluble modulin alpha 4	-6.29011892	3.67E-06
NWMN_0163	conserved hypothetical protein	-6.568192269	3.67E-06

Appendix Table 2 DE genes of *S. epidermidis* in response to 1 % (v/v) squalene challenge. Only the DE genes with log_2 fold change **(logFC)** ≤ -0.5 or ≥0.5 were listed. All DE genes have **FDR** (false discovery rate) ≤ 0.05. DE genes that discussed in this thesis were highlighted.

Gene	Gene_description	logFC	FDR
SETU_00201	hypothetical protein	4.040921308	0
SETU_02044	dihydrolipoamide dehydrogenase	2.721163543	0
SETU_02043	glutathione peroxidase	2.567467246	7.30E-195
SETU_01290	heat-shock protein htrA	2.423217529	2.57E-257
SETU_02045	transcriptional regulator	2.405674936	5.98E-197
clpC	endopeptidase Clp ATP-binding subunit C	2.236031485	8.06E-137
SETU_00142	ATP:guanido phosphotransferase	2.170979854	1.81E-174
SETU_01841	NAD(P)H-flavin oxidoreductase	2.080468467	1.97E-291
SETU_00141	UvrB/UvrC domain-containing protein	2.002942597	6.95E-230
SETU_01367	protein export protein PrsA	1.972651498	7.39E-198
SETU_00140	CtsR family transcriptional regulator	1.932741558	3.20E-137
SETU_02098	general stress protein 170	1.898207562	3.45E-184
SETU_01218	hypothetical protein	1.838953214	7.29E-29
SETU_00681	cytochrome d ubiquinol oxidase subunit 1-like protein	1.805068513	1.63E-184
SETU_00230	hypothetical protein	1.777323412	1.06E-32
SETU_02169	phosphotransferase mannnose-specific family component IIA	1.742524783	4.95E-173
SETU_00784	TM2 domain-containing protein	1.728625634	2.76E-67
SETU_02170	DAK2 domain-containing protein	1.715626669	1.15E-173
SETU_01442	two-component sensor histidine kinase	1.714237858	2.23E-165
SETU_00375	ribosomal subunit interface protein	1.682303961	1.33E-55
SETU_00906	threonine synthase	1.661843548	5.62E-161
clpP	ATP-dependent Clp protease proteolytic subunit	1.658846365	4.16E-119
SETU_00057	putative transmembrane protein coupled to NADH-ubiquinone	1.633548824	2.39E-159
SETU_00682	cytochrome d ubiquinol oxidase subunit II-like protein	1.556526974	1.98E-100

SETU_00905	homoserine dehydrogenase	1.54127263	3.41E-99
SETU_02143	hypothetical protein	1.517790053	1.23E-128
SETU_01654	alanine racemase domain-containing protein	1.509827127	3.00E-124
SETU_01655	aerobactin biosynthesis protein	1.491591345	8.02E-128
vraR	DNA-binding response regulator VraR	1.474196973	3.63E-129
SETU_01444	hypothetical protein	1.442875887	8.84E-66
SETU_01080	alpha-D-1,4-glucosidase	1.434391933	1.40E-138
SETU_00056	NADH dehydrogenase subunit 5	1.4277874	2.79E-122
SETU_01443	transporter associated with VraSR	1.417004893	5.56E-83
SETU_01657	aerobactin biosynthesis protein	1.397732117	1.84E-131
SETU_00894	aromatic amino acid beta-eliminating lyase	1.352898899	1.22E-113
SETU_00522	clpB protein	1.322233312	4.91E-54
SETU_01513	molecular chaperone GroEL	1.300893128	4.35E-68
cysK	cysteine synthase	1.281190216	1.09E-79
SETU_01656	transporter	1.279534214	1.19E-79
dapA	dihydrodipicolinate synthase	1.268940433	1.58E-80
SETU_00970	dihydrodipicolinate reductase	1.24698507	1.35E-69
SETU_01943	aldehyde dehydrogenase	1.235923495	3.13E-118
SETU_00953	transferrin receptor	1.234674364	4.25E-87
SETU_02128	triacylglycerol lipase	1.228833569	2.92E-80
groES	co-chaperonin GroES	1.216317159	3.69E-80
SETU_01840	hypothetical protein	1.214288817	3.19E-38
SETU_02171	dihydroxyacetone kinase subunit DhaK	1.201430012	8.83E-67
gldA	glycerol dehydrogenase	1.194185225	8.49E-91
SETU_00903	hypothetical protein	1.187950347	2.40E-26
SETU_02278	putative membrane protein	1.171470768	4.58E-14
SETU_01956	D-ribose pyranase	1.15824172	6.89E-18
tpx	thiol peroxidase	1.152045726	1.18E-59

SETU_00034	alkyl hydroperoxide reductase	1.132882131	4.22E-47
SETU_00971	tetrahydrodipicolinate acetyltransferase	1.132166552	3.65E-29
SETU_02009	L-lactate dehydrogenase	1.131093596	1.07E-63
SETU_00035	alkyl hydroperoxide reductase	1.1207805	2.40E-67
sucC	succinyl-CoA synthetase subunit beta	1.119982779	2.79E-51
SETU_00357	ferrichrome ABC transporter permease	1.105569447	1.02E-57
SETU_00919	hypothetical protein	1.102207259	1.09E-46
SETU_00989	dihydrolipoamide succinyltransferase	1.09849226	5.82E-75
SETU_00358	ferrichrome ABC transporter ATP-binding protein	1.097962476	6.31E-54
SETU_00359	ferrichrome ABC transporter	1.090693493	7.84E-62
SETU_02042	phosphoadenosine phosphosulfate reductase	1.088473959	3.69E-80
SETU_01155	heat-inducible transcriptional repressor	1.086743493	5.33E-75
SETU_01154	heat shock protein GrpE	1.076019674	2.25E-87
SETU_00250	monovalent cation/H antiporter subunit C	1.064323167	5.78E-17
SETU_00320	PTS system fructose-specific transporter subunit IIABC	1.054425284	3.29E-52
SETU_01944	NAD(P)H-flavin oxidoreductase	1.053425765	4.73E-74
SETU_00981	5-bromo-4-chloroindolyl phosphate hydrolysis protein XpaC	1.052444876	6.22E-75
SETU_02038	precorrin-2 dehydrogenase	1.045234243	5.43E-38
hisB	imidazoleglycerol-phosphate dehydratase	1.044287588	7.57E-36
dnaK	molecular chaperone DnaK	1.03328307	5.83E-32
SETU_00536	thimet oligopeptidase-like protein	1.032013674	8.23E-65
SETU_00221	oxidoreductase ion channel	1.030984189	5.80E-78
SETU_01653	ferrichrome ABC transporter	1.02591654	1.63E-75
SETU_02008	acetolactate synthase	1.025456779	1.57E-52
SETU_00584	lipoate-protein ligase-like protein	1.021998992	4.80E-47
SETU_01283	glycerophosphoryl diester phosphodiesterase	1.018162096	1.77E-48
SETU_00516	5-oxo-1,2,5-tricarboxylic-3-penten acid decarboxylase	1.013832867	2.35E-79
sucD	succinyl-CoA synthetase subunit alpha	1.011343537	7.62E-59

SETU_01539	ketol-acid reductoisomerase	1.011340142	3.84E-22
SETU_00356	ferrichrome ABC transporter permease	1.008352901	1.47E-59
SETU_01538	acetolactate synthase 1 regulatory subunit	1.006974036	0.02902264
SETU_00798	fatty acid biosynthesis transcriptional regulator	0.997654837	1.69E-59
SETU_00980	acylphosphatase	0.997492855	3.25E-32
SETU_00058	hypothetical protein	0.994751891	9.87E-62
sucA	2-oxoglutarate dehydrogenase E1	0.990918678	5.91E-48
SETU_00907	homoserine kinase	0.98046572	5.30E-48
SETU_01986	copper-transporting ATPase copA	0.969115038	2.57E-36
SETU_00314	putative membrane protein	0.961070895	1.72E-18
ycnE	Putative monooxygenase ycnE	0.946049469	3.33E-48
SETU_00968	aspartate semialdehyde dehydrogenase	0.942844664	2.22E-54
SETU_00446	OsmC/Ohr family protein	0.933656827	1.28E-43
SETU_01959	hypothetical protein	0.93215584	6.46E-05
SETU_00982	tellurite resistance protein	0.926966474	1.04E-69
SETU_00538	globin family protein	0.926151725	5.35E-19
leuD	isopropylmalate isomerase small subunit	0.924890728	2.17E-07
SETU_01874	amino acid ABC transporter-like protein	0.912232238	6.81E-52
SETU_00302	hypothetical protein	0.909922808	2.09E-62
SETU_00283	putative integral membrane protein that interacts with FtsH	0.907588572	2.80E-46
SETU_00537	YjbH-like, GTP pyrophosphokinase domain-containing protein	0.906621869	2.20E-63
mraZ	cell division protein MraZ	0.90625367	6.72E-27
SETU_00172	branched-chain amino acid aminotransferase	0.905347627	1.45E-49
SETU_00370	lipophilic protein	0.897761054	2.56E-42
SETU_00503	NADH-dependent flavin oxidoreductase	0.89107274	2.82E-61
SETU_00254	monovalent cation/H antiporter subunit G	0.883775374	7.52E-46
SETU_02039	uroporphyrin-III C-methyltransferase	0.879247542	6.11E-46
SETU_01061	hypothetical protein	0.875640451	1.90E-29

SETU_01191	luciferase	0.875534817	1.02E-47
trap	signal transduction protein	0.871292104	1.62E-29
hisG	ATP phosphoribosyltransferase	0.867197041	2.34E-07
SETU_01285	aminotransferase class V	0.865164313	4.29E-28
SETU_00531	peptide binding protein OppA	0.863201412	3.80E-34
SETU_00449	thioredoxin	0.861580004	6.80E-34
SETU_01779	hypothetical protein	0.859129752	8.21E-35
SETU_01259	citrate synthase	0.848388482	1.43E-25
isaB	immunodominant antigen B	0.846529111	2.53E-25
SETU_01870	hypothetical protein	0.843278051	8.71E-42
SETU_00458	CsbD family protein	0.841165827	8.23E-40
SETU_01078	glucose-6-phosphate 1-dehydrogenase	0.832778697	1.03E-23
SETU_01934	fructose-bisphosphatase	0.826132807	9.54E-49
SETU_00319	fructose 1-phosphate kinase	0.824234119	4.48E-21
SETU_01059	elastin binding protein	0.820951899	1.86E-32
mraW	S-adenosyl-methyltransferase MraW	0.820283432	2.48E-41
SETU_01334	hypothetical protein	0.820032454	7.17E-25
SETU_01193	Rrf2 family protein	0.81627686	1.05E-42
pgi	glucose-6-phosphate isomerase	0.814435355	3.69E-32
SETU_01540	2-isopropylmalate synthase	0.809866546	1.15E-25
SETU_01984	dehydrogenase	0.808824848	3.34E-32
SETU_01272	alanine dehydrogenase	0.808060864	3.64E-26
SETU_00252	monovalent cation/H antiporter subunit E	0.806817867	2.19E-15
SETU_00255	Na?? antiporter	0.802126496	2.76E-52
SETU_01983	1-pyrroline-5-carboxylate dehydrogenase	0.801409164	3.97E-16
SETU_01287	HAD superfamily hydrolase	0.799766459	2.20E-33
gltD	glutamate synthase subunit beta	0.798549267	3.24E-24
sodA2	superoxide dismutase	0.798275727	7.23E-28

SETU_01995	regulatory protein	0.797281189	2.72E-33
SETU_01646	hypothetical protein	0.79581828	5.09E-17
sarX	accessory regulator A-like protein	0.792634637	6.09E-20
SETU_00871	aerobic glycerol-3-phosphate dehydrogenase	0.792377892	1.98E-40
SETU_01281	GAF domain-containing protein	0.789743519	4.35E-30
SETU_00490	Na?? antiporter family protein	0.783296645	1.00E-29
SETU_01275	Adenine-specific methyltransferase	0.781272021	3.48E-40
SETU_01613	putative membrane protein	0.779164278	4.46E-12
SETU_00908	HAD superfamily hydrolase	0.778845049	1.45E-27
SETU_00318	transcription repressor of fructose operon	0.769429163	1.11E-08
SETU_00249	monovalent cation/H antiporter subunit B	0.766601872	1.56E-18
SETU_01333	translaldolase	0.761972507	1.60E-41
SETU_00448	nitroreductase	0.75782644	6.83E-39
SETU_00037	nitro/flavin reductase	0.753896623	8.50E-29
SETU_01900	endo-1,4-beta-glucanase	0.749964968	1.38E-27
SETU_00751	cell division protein	0.748069702	1.67E-35
lacG	6-phospho-beta-galactosidase	0.744578134	4.09E-35
SETU_01868	hypothetical protein	0.744018112	6.02E-22
SETU_00301	hypothetical protein	0.743462939	7.35E-26
SETU_01977	3-hydroxy-3-methylglutaryl-CoA synthase	0.740572559	6.83E-39
SETU_01610	hypothetical protein	0.740493197	1.46E-39
SETU_01837	general stress protein 26	0.739164104	5.60E-25
SETU_02007	alpha-acetolactate decarboxylase	0.737199684	7.63E-33
SETU_02041	sulfite reductase (NADPH) flavoprotein	0.733993583	5.36E-38
SETU_01041	putative metal-dependent peptidase	0.726492315	9.85E-24
SETU_00251	monovalent cation/H antiporter subunit D	0.725387735	6.00E-36
SETU_00212	heme peroxidase	0.720023973	2.11E-37
SETU_00393	hypothetical protein	0.718700584	4.39E-06

SETU_01152	molecular chaperone DnaJ	0.717455787	1.20E-27
SETU_01658	alkaline shock protein 23	0.715917916	5.52E-23
SETU_01627	lytic regulatory protein	0.708744447	4.48E-29
sat	sulfate adenylyltransferase	0.708092216	6.15E-34
SETU_00243	accessory regulator A	0.699393595	4.08E-24
SETU_00520	PaaD-like protein	0.69618227	2.01E-17
SETU_00647	acetyltransferase	0.695319554	2.23E-11
SETU_00875	glutathione peroxidase	0.694108272	4.40E-21
SETU_01668	tagatose 1,6-diphosphate aldolase	0.688416356	8.52E-19
SETU_00229	alcohol dehydrogenase	0.686576851	3.72E-30
hisH	imidazole glycerol phosphate synthase subunit HisH	0.682764027	8.33E-06
SETU_00248	monovalent cation/H antiporter subunit A	0.682146932	7.62E-38
SETU_01619	hypothetical protein	0.681963558	5.11E-17
SETU_01940	acetyltransferase	0.680810506	3.01E-20
SETU_02229	malate:quinone oxidoreductase	0.677241977	2.11E-21
SETU_02035	adenylylsulfate kinase	0.676454733	1.18E-26
SETU_01786	dehydrogenase	0.669627768	5.70E-15
SETU_01760	glycerate dehydrogenase	0.66649	8.99E-34
SETU_00972	hippurate hydrolase	0.659500524	2.23E-10
SETU_01941	glyoxalase	0.658294631	2.45E-19
SETU_00323	plant-metabolite dehydrogenase	0.657466532	5.68E-30
SETU_02135	histidinol dehydrogenase	0.656248152	3.26E-10
SETU_02103	hypothetical protein	0.65543462	1.71E-20
SETU_01015	virulence factor C	0.653699247	1.07E-21
trxA	thioredoxin	0.652036569	5.21E-29
SETU_00763	cell-divisio initiation protein	0.651840795	1.31E-30
SETU_01217	hypothetical protein	0.646903298	3.10E-14
SETU_02150	branched-chain alpha-keto acid dehydrogenase subunit E2	0.639273942	2.09E-15

SETU_01102	Xaa-Pro dipeptidase	0.637846656	5.19E-29
SETU_01271	Xaa-Pro dipeptidase	0.633462924	2.89E-24
SETU_01955	ribokinase	0.633087254	5.17E-20
prmA	ribosomal protein L11 methyltransferase	0.629085338	6.00E-29
SETU_01536	dihydroxy-acid dehydratase	0.625772157	2.62E-06
SETU_00394	cell-division inhibitor	0.623961476	1.47E-26
pflA	pyruvate formate-lyase-activating enzyme	0.623245998	1.40E-19
SETU_01933	alkaline phosphatase	0.61792155	1.64E-18
SETU_00519	HAD superfamily hydrolase	0.617907782	1.25E-23
SETU_02037	putative permease	0.617450092	3.39E-24
SETU_01216	hypothetical protein	0.615491644	5.99E-11
SETU_01537	acetolactate synthase large subunit	0.613367948	1.11E-12
thiE	thiamine-phosphate pyrophosphorylase	0.60658784	1.05E-08
SETU_00701	hypothetical protein	0.606168487	1.17E-27
SETU_00053	regulatory protein PfoR	0.605572458	2.07E-09
SETU_01611	amidase	0.605524529	9.64E-25
SETU_01541	3-isopropylmalate dehydrogenase	0.602158696	2.40E-13
SETU_01960	poly-gamma-glutamate synthesis protein PgsA	0.60112602	2.15E-12
SETU_01988	D-lactate dehydrogenase	0.60081181	1.11E-09
SETU_01337	2,5-didehydrogluconate reductase	0.598545416	7.65E-23
SETU_01306	D-alanine aminotransferase	0.598233217	1.83E-28
SETU_01286	D-3-phosphoglycerate dehydrogenase	0.596613134	1.04E-19
SETU_01667	PTS system lactose-specific transporter subunit IIA	0.59643822	0.000182405
SETU_01308	hypothetical protein	0.594839672	3.65E-28
SETU_00102	translation initiation inhibitor-like protein	0.594435778	1.97E-17
SETU_01064	riboflavin ECF transporter substrate-specific protein RibU	0.592766744	2.65E-18
SETU_00585	IDEAL domain protein	0.590575715	2.67E-09
SETU_02151	branched-chain alpha-keto acid dehydrogenase E1	0.590211726	5.40E-05

SETU_00345	histidinol-phosphate aminotransferase	0.585594314	4.96E-17
SETU_00311	anion transporter family protein	0.582892563	1.45E-18
SETU_02011	amino acid transporter	0.582727165	2.64E-08
SETU_01432	ThiJ/PfpI family protein	0.581016827	1.76E-16
fdaB	fructose-1,6-bisphosphate aldolase	0.57584036	8.94E-15
SETU_01307	dipeptidase PepV	0.575112475	6.35E-19
SETU_01641	SmrB	0.573332571	3.09E-08
SETU_01614	phosphopentomutase	0.571955174	4.89E-21
SETU_01602	aldehyde dehydrogenase	0.569858005	4.59E-21
SETU_01362	ABC transporter ecsB	0.567118504	2.31E-17
SETU_01709	hypothetical protein	0.565205535	1.66E-13
SETU_00242	esterase/lipase	0.564462185	4.52E-25
SETU_01477	6-phosphogluconolactonase	0.563459502	1.82E-23
SETU_01640	multidrug resistance protein	0.561126338	9.37E-26
SETU_00315	quinolone resistance protein	0.560810631	4.84E-10
SETU_00253	monovalent cation/H antiporter subunit F	0.560150799	4.05E-11
secA	preprotein translocase subunit SecA	0.560005953	1.58E-20
SETU_00071	poly (glycerol-phosphate) alpha-glucosyltransferase	0.556229812	1.01E-22
SETU_01544	threonine dehydratase	0.552611552	3.49E-08
SETU_01003	acetyltransferase	0.550891067	2.65E-17
SETU_00973	alanine racemase	0.549972411	1.60E-13
SETU_01669	tagatose-6-phosphate kinase	0.549949832	4.88E-12
SETU_00498	monovalent cation/H antiporter subunit B	0.549739733	2.40E-16
SETU_01005	hypothetical protein	0.549697886	6.76E-11
SETU_01007	methionine sulfoxide reductase B	0.548254316	5.12E-12
SETU_01659	hypothetical protein	0.54783104	0.001896192
SETU_01901	hypothetical protein	0.546518836	1.42E-09
SETU_01957	ribose transporter RbsU	0.545952061	3.70E-16

SETU_00525	3-oxoacyl-ACP synthase	0.545831897	1.32E-18
SETU_00245	Integral membrane protein	0.543303609	5.64E-12
SETU_00959	oligoendopeptidase	0.542243713	3.35E-23
SETU_01089	DNA repair protein	0.542165217	1.76E-18
SETU_00872	lysophospholipase	0.540063139	2.19E-22
SETU_01966	thioredoxin	0.539858098	1.99E-12
mnhC	putative monovalent cation/H antiporter subunit C	0.538124088	6.12E-16
SETU_01014	hypothetical protein	0.536688848	2.02E-14
SETU_02040	sulfite reductase subunit beta	0.53616828	1.27E-23
SETU_00324	CsbB stress response protein	0.53565646	5.11E-20
SETU_01615	pyrimidine-nucleoside phosphorylase	0.534380737	9.64E-22
SETU_01660	hypothetical protein	0.531633883	2.60E-14
SETU_00539	adenylate cyclase family protein	0.52555577	3.95E-08
SETU_00033	putative lipoprotein	0.524041487	3.29E-18
lacE	PTS system lactose-specific transporter subunit IIBC	0.523878666	4.36E-14
SETU_01996	D-serine/D-alanine/glycine transporter	0.522432536	2.73E-17
SETU_01172	Mn2?? transporter NRAMP family protein	0.521516153	5.55E-15
SETU_00312	deoxyribodipyrimidine photolyase	0.521350942	3.20E-10
SETU_01559	membrane-flanked domain-containing protein	0.520522315	5.81E-06
SETU_00074	YibE/F-like protein	0.520503718	1.34E-16
SETU_01038	tRNA CCA-pyrophosphorylase	0.520299576	4.28E-19
SETU_01360	signal transduction protein TRAP	0.517706358	2.13E-16
SETU_02017	coenzyme A disulfide reductase	0.517579519	7.01E-19
SETU_01785	putative flavoprotein oxygenase, DIM6/NTAB family protein	0.516817559	9.82E-14
SETU_00911	catalase	0.514291766	9.59E-18
SETU_00297	lipoprotein	0.512470159	2.46E-14
SETU_02096	N-acetylmuramoyl-L-alanine amidase	0.509005538	2.57E-15
SETU_01424	cysteinyl-tRNA synthetase-like protein	-0.514550027	3.80E-16

SETU_01105	lipoate-protein ligase A	-0.5166228	9.97E-16
rnpA	ribonuclease P	-0.517431888	5.08E-13
SETU_01371	transcriptional regulator	-0.518188971	6.53E-08
SETU_00795	alkaline shock protein	-0.518450631	1.74E-13
SETU_00042	xanthine phosphoribosyltransferase	-0.519723937	1.16E-12
SETU_00709	hypothetical protein	-0.520720623	2.02E-14
SETU_01156	coproporphyrinogen III oxidase	-0.521212819	7.45E-14
hisS	histidyl-tRNA synthetase	-0.52338417	1.03E-21
alaS	alanyl-tRNA synthetase	-0.52717917	3.65E-20
cbiO_1	cobalt transporter ATP-binding subunit	-0.527831237	2.58E-08
SETU_02030	choline transporter	-0.53084102	4.21E-22
SETU_01759	SMR-type multidrug efflux transporter	-0.533065873	0.035219196
tufA	elongation factor Tu	-0.533899143	2.80E-09
SETU_01482	putative membrane protein	-0.535677821	3.61E-08
SETU_01677	cobalt transport family protein	-0.535828027	1.32E-14
truA	tRNA pseudouridine synthase A	-0.536134677	8.41E-18
SETU_01490	hypothetical protein	-0.536990921	9.37E-11
SETU_01278	thiamine biosynthesis protein ThiI	-0.540690362	1.41E-18
pheS	phenylalanyl-tRNA synthetase subunit alpha	-0.547225649	1.03E-20
SETU_00281	low-affinity inorganic phosphate transporter	-0.548086662	3.99E-19
SETU_01209	ACT domain-containing protein	-0.548249644	9.09E-07
SETU_01806	hypothetical protein	-0.548415322	1.99E-12
SETU_00523	hypothetical protein	-0.555930259	8.82E-09
SETU_00805	signal recognition particle	-0.556334267	1.13E-18
SETU_01672	lactose phosphotransferase system repressor	-0.556949991	3.96E-14
SETU_00664	phosphoribosylformylglycinamidine synthase II	-0.561565183	2.41E-24
SETU_01566	hypothetical protein	-0.561800352	0.000496582
SETU_01715	hypothetical protein	-0.56288892	2.81E-05

SETU_01381	rRNA methylase	-0.566731038	7.04E-13
SETU_01185	hypothetical protein	-0.57065721	6.26E-06
pheT	phenylalanyl-tRNA synthetase subunit beta	-0.572335128	1.11E-19
SETU_01129	ABC transporter ATP-binding protein	-0.572648848	2.13E-20
obgE	GTPase ObgE	-0.573176135	8.50E-25
gmk	guanylate kinase	-0.575483078	2.11E-19
SETU_01339	S-adenosylmethionine synthetase	-0.576431237	2.34E-24
SETU_01862	ABC transporter ATP binding subunit	-0.576539891	4.26E-19
SETU_01279	iron-sulfur cofactor synthesis protein nifZ	-0.583958498	1.68E-17
pyrH	uridylate kinase	-0.591081252	6.12E-24
SETU_00434	CSD family cold shock protein	-0.593005127	1.11E-16
SETU_01474	pyrazinamidase/nicotinamidase-like protein	-0.595772709	1.03E-20
SETU_01974	hypothetical protein	-0.599671347	5.30E-09
SETU_01783	Na?? antiporter	-0.603895688	5.68E-25
rimM	16S rRNA-processing protein RimM	-0.613020228	1.84E-11
ureG	urease accessory protein UreG	-0.614876321	5.72E-16
SETU_01277	putative membrane protein YfcA	-0.615007532	1.58E-18
SETU_01456	lipid kinase	-0.616091219	1.74E-27
SETU_02099	hypothetical protein	-0.61682017	0.000232286
SETU_01743	urease subunit gamma	-0.619279045	1.12E-07
SETU_01836	transcription regulatory protein	-0.619285525	3.17E-26
SETU_01596	Sua5/YciO/YrdC/YwlC family protein	-0.620678102	2.50E-26
pyrB	aspartate carbamoyltransferase	-0.620993502	4.29E-13
SETU_00931	DNA topoisomerase IV subunit B	-0.621565864	8.57E-33
SETU_00455	ABC transporter permease	-0.621648572	2.40E-20
SETU_01622	mannnose-6 phospate isomelase pmi	-0.622299622	4.66E-24
SETU_00043	xanthine permease	-0.628350888	7.43E-28
SETU_00914	guanosine 5-monophosphate oxidoreductase	-0.629075956	1.74E-25

SETU_00843	polynucleotide phosphorylase	-0.632320782	1.08E-23
SETU_02363	hypothetical protein	-0.634467235	4.81E-06
SETU_02202	phage protein	-0.635565419	8.48E-14
SETU_01184	Holliday junction resolvase-like protein	-0.637796967	2.68E-20
SETU_02297	hypothetical protein	-0.639358074	1.65E-07
infB	translation initiation factor IF-2	-0.639452139	4.17E-26
aspS	aspartyl-tRNA synthetase	-0.639884213	1.10E-29
glyS	glycyl-tRNA synthetase	-0.640972704	1.15E-19
SETU_02264	rRNA large subunit methyltransferase	-0.646747185	1.53E-26
SETU_00113	RNA binding protein , contains ribosomal protein S1 domain	-0.647586069	1.29E-19
SETU_00380	hypothetical protein	-0.65070153	8.20E-07
SETU_01528	hypothetical protein	-0.655002607	9.98E-06
SETU_00369	GGDEF domain-containing protein	-0.656010389	1.45E-20
prfA	peptide chain release factor 1	-0.65742219	3.23E-31
SETU_00123	5S ribosomal RNA	-0.660938407	0.037666297
SETU_00932	DNA topoisomerase IV subunit A	-0.664285552	3.74E-26
SETU_01621	hypothetical protein	-0.666220076	6.73E-11
SETU_01757	secretory antigen SsaA	-0.666455399	1.17E-27
SETU_01465	His repressor	-0.668229923	5.72E-16
nusA	transcription elongation factor NusA	-0.669015151	6.50E-33
SETU_01597	protoporphyrinogen oxidase	-0.669211138	1.86E-27
frr	ribosome recycling factor	-0.671247714	8.85E-29
SETU_00269	membrane protein	-0.673414036	6.71E-25
epiB	epidermin biosynthesis protein EpiB	-0.674664631	1.15E-20
SETU_01545	hypothetical protein	-0.675450808	1.97E-06
SETU_00667	phosphoribosylglycinamide formyltransferase	-0.67708521	3.38E-23
SETU_01626	phosphodiesterase	-0.677351336	1.93E-22
guaB	inositol-monophosphate dehydrogenase	-0.678573591	1.22E-30

SETU_00834	clustered with transcriptiontermination protein NusA	-0.678822927	1.69E-30
SETU_00856	phosphodiesterase	-0.679046183	1.06E-18
SETU_01016	preQ0 transporter	-0.679676743	2.57E-23
SETU_02189	branched-chain amino acid transport system carrier protein	-0.680346243	3.61E-36
SETU_01879	integral membrane efflux protein	-0.681163688	2.66E-27
SETU_02282	seryl-tRNA synthetase	-0.683349883	4.27E-32
sdhA	succinate dehydrogenase flavoprotein subunit	-0.685039685	5.54E-34
qoxC	quinol oxidase subunit III	-0.68593681	2.08E-28
SETU_01790	hypothetical protein	-0.688741955	1.24E-05
SETU_01164	iojap-related protein	-0.694892884	1.60E-26
thrS	threonyl-tRNA synthetase	-0.699410569	3.04E-30
SETU_00372	DegV family protein	-0.70589375	2.39E-40
SETU_01789	abortive infection family protein	-0.709458389	5.36E-36
SETU_01555	PemK family protein	-0.713293259	3.04E-20
SETU_01221	folylpolyglutamate synthase	-0.714300235	8.29E-29
SETU_00200	major facilitator family transporter	-0.715383148	4.14E-21
SETU_02358	lantibiotic biosynthesis protein	-0.715434201	3.20E-27
SETU_00836	hypothetical protein	-0.718366412	7.98E-14
sdhB_1	succinate dehydrogenase iron-sulfur subunit	-0.7195976	2.09E-31
SETU_00930	acyl-phosphate:glycerol-3-phosphateO- acyltransferase PlsY	-0.71986152	3.75E-24
SETU_01183	hypothetical protein	-0.722014632	1.19E-26
SETU_01525	probabale ammonium transporter	-0.725654403	9.00E-31
SETU_01433	hypothetical protein	-0.734246636	6.54E-25
qoxA	quinol oxidase subunit I	-0.736156111	9.08E-25
purS	phosphoribosylformylglycinamidine synthase, PurS protein	-0.737061777	1.98E-06
SETU_00570	permease	-0.746397996	1.88E-39
SETU_00236	iron-binding protein	-0.747478648	8.77E-33
SETU_00484	YuzD-like protein	-0.748247621	3.48E-13

SETU_01251	Phage-related replication protein	-0.754468678	2.36E-36
SETU_00966	ABC transporter ATP-binding protein	-0.755195008	2.22E-40
SETU_01417	tRNA-Ala	-0.762027011	3.17E-08
SETU_00179	deoxypurine kinase	-0.763855806	7.40E-29
SETU_01556	programmed cell death antitoxin YdcD	-0.765042054	2.43E-05
SETU_00139	pyrimidine nucleoside transport protein	-0.771593103	1.49E-37
ureE	urease accessory protein UreE	-0.778270159	3.72E-09
SETU_01606	DNA-directed RNA polymerase subunit delta	-0.77836141	6.11E-42
SETU_01595	phosphatase	-0.78084587	3.19E-26
SETU_00488	NADH dehydrogenase	-0.781089506	2.48E-33
SETU_00837	ribosomal protein L7AE family protein	-0.781677493	3.48E-17
SETU_00656	quinol oxidase polypeptide II QoxA	-0.781858439	2.17E-23
purF	amidophosphoribosyltransferase	-0.791569113	6.81E-27
rpsT	30S ribosomal protein S20	-0.792784782	4.94E-30
SETU_00280	phosphate transport regulator	-0.794149597	1.15E-35
SETU_01633	tRNA-Lys	-0.79742966	0.000119561
SETU_02228	Putative protein-S-isoprenylcysteine methyltransferase	-0.805458505	7.60E-33
SETU_01171	5-methylthioadenosine nucleosidase	-0.806612071	1.38E-24
SETU_00278	ABC transporter ATP-binding protein vraF	-0.816247281	3.38E-26
SETU_00279	ABC transporter permease vraG	-0.818748439	2.33E-54
SETU_00099	Veg protein	-0.821970926	7.05E-45
SETU_02176	hypothetical protein	-0.828877258	1.58E-25
guaA	GMP synthase	-0.829209175	9.24E-46
tsf	elongation factor Ts	-0.83091321	3.31E-31
SETU_02298	AcrR family transcriptional regulator	-0.834260799	6.59E-13
SETU_01756	hypothetical protein	-0.837420573	3.53E-38
SETU_00736	succinate dehydrogenase cytochrome b-558	-0.838890664	2.52E-28
SETU_00929	HesB/YadR/YfhF-family protein	-0.84177354	5.44E-20

SETU_00180	deoxypurine kinase	-0.850035111	2.76E-34
trmD	tRNA (guanine-N(1)-)-methyltransferase	-0.851946942	3.82E-36
SETU_02000	hypothetical protein	-0.85471345	2.20E-31
rpsU	30S ribosomal protein S21	-0.856874963	1.15E-12
rplQ	50S ribosomal protein L17	-0.858653952	3.48E-33
galU	UTP-glucose-1-phosphate uridylyltransferase	-0.861463244	6.92E-44
SETU_00819	DNA topoisomerase I	-0.862553837	1.00E-49
SETU_01182	caffeoyl-CoA O-methyltransferase	-0.869499836	7.33E-37
SETU_01181	protease	-0.873719664	2.79E-50
SETU_00915	SCP family extracellular protein	-0.878906178	2.15E-35
SETU_00137	pyridoxal biosynthesis lyase PdxS	-0.883381055	2.80E-42
ureB	urease subunit beta	-0.886761301	1.07E-12
SETU_01106	rhodanese-like domain-containing protein	-0.896751003	1.18E-31
SETU_01601	hypothetical protein	-0.897449328	1.24E-59
purH	bifunctional phosphoribosylaminoimidazolecarboxamide formyltransferase/IMP cyclohydrolase	-0.904476987	6.00E-56
SETU_01165	HAD family hydrolase, YqeK	-0.914189113	8.33E-34
SETU_01338	hypothetical protein	-0.922299812	6.84E-42
SETU_01168	shikimate dehydrogenease	-0.924387073	3.46E-47
SETU_01170	HAD superfamily hydrolase	-0.92547821	1.75E-40
SETU_00138	glutamine amidotransferase subunit PdxT	-0.927824033	2.03E-57
SETU_00316	hypothetical protein	-0.937066922	1.23E-33
SETU_00454	ABC transporter ATP-binding protein	-0.939129022	3.90E-55
purD	phosphoribosylamine--glycine ligase	-0.941505315	5.46E-47
SETU_00666	phosphoribosylaminoimidazole synthetase	-0.944349891	8.62E-42
SETU_00983	branched-chain amino acid carrier protein	-0.947849621	5.00E-66
SETU_01466	adenylosuccinate lyase	-0.948379148	4.50E-62
SETU_01166	nicotinate-nucleotide adenylyltransferase	-0.953387661	8.32E-50
SETU_01180	protease	-0.95715389	2.05E-60

SETU_00921	hypothetical protein	-0.965846943	6.00E-36
SETU_00939	4-oxalocrotonate tautomerase	-0.967778854	3.01E-37
SETU_02019	lipoprotein	-0.97338347	4.79E-58
gid	tRNA (uracil-5-)-methyltransferase Gid	-0.982925844	8.42E-60
rpmB	50S ribosomal protein L28	-1.009156272	3.48E-65
SETU_00445	lactococcal prophage ps3 protein 05	-1.013144135	1.28E-29
rpmF	50S ribosomal protein L32	-1.014087308	4.80E-23
rpsM	30S ribosomal protein S13	-1.024108891	1.79E-66
greA	transcription elongation factor GreA	-1.026302115	1.11E-70
SETU_01179	uridine kinase	-1.028771982	1.66E-57
SETU_01169	GTP-binding protein YqeH	-1.036223367	8.18E-63
SETU_00770	uracil permease	-1.037670701	2.93E-15
SETU_01167	RNA binding protein	-1.04897284	4.61E-24
rpsK	30S ribosomal protein S11	-1.049739197	2.45E-75
rpoA	DNA-directed RNA polymerase subunit alpha	-1.050945161	2.78E-53
SETU_01372	hypothetical protein	-1.056774561	6.51E-48
typA	GTP-binding protein TypA	-1.078046208	2.19E-71
SETU_02085	zinc metalloproteinase aureolysin aur	-1.081674979	1.80E-76
SETU_00106	50S ribosomal protein L25	-1.108007403	1.39E-49
SETU_00723	protein in cluster with ribosomal protein L32p	-1.111548966	5.76E-67
SETU_00646	N-acetylmuramoyl-L-alanine amidase	-1.119232183	1.90E-55
SETU_00978	CSD family cold shock protein	-1.121440263	1.51E-24
fbaA	fructose-bisphosphate aldolase	-1.127575751	9.56E-49
rpsO	30S ribosomal protein S15	-1.132719191	1.75E-71
SETU_00268	pyrimidine nucleoside transporter	-1.135263092	7.26E-78
SETU_00159	16S rRNA methyltransferase	-1.136911455	3.08E-43
SETU_00936	oxacillin resistance-related FmtC protein	-1.13851983	1.36E-102
rpmA	50S ribosomal protein L27	-1.148391044	1.21E-58

SETU_00282	secretory antigen SsaA-like protein	-1.150110165	3.29E-87
rpmJ	50S ribosomal protein L36	-1.152235579	1.53E-97
secY_1	preprotein translocase subunit SecY	-1.171212012	7.58E-77
rplO	50S ribosomal protein L15	-1.182629757	9.67E-80
infA	translation initiation factor IF-1	-1.185412293	2.79E-95
rplS	50S ribosomal protein L19	-1.191798868	2.81E-75
SETU_00165	elongation factor G	-1.199376539	2.07E-46
SETU_01913	poly (glycerol-phosphate) alpha-glucosyltransferase	-1.218612547	1.55E-83
SETU_00925	Large-conductance mechanosensitive channel	-1.220080985	2.83E-87
rpsR	30S ribosomal protein S18	-1.230189513	7.81E-68
rpsG	30S ribosomal protein S7	-1.230592007	4.64E-66
SETU_01710	xanthine/uracil permease	-1.245378533	3.72E-96
SETU_00825	30S ribosomal protein S2p (SAe)	-1.248416367	4.36E-73
SETU_00456	ABC transporter substrate-binding protein	-1.249640562	5.47E-64
rpmE2	50S ribosomal protein L31 type B	-1.25006402	4.97E-63
SETU_01839	proton/sodium-glutamate symport protein	-1.254363825	2.96E-98
SETU_00926	glycine betaine transporter	-1.272930431	1.57E-90
rpsP	30S ribosomal protein S16	-1.27401071	6.57E-78
SETU_01990	ssaA protein	-1.2780742	1.92E-79
sarV	accessory regulator V	-1.284266738	8.28E-60
rplW	50S ribosomal protein L23	-1.285448254	3.17E-76
SETU_01110	shikimate kinase	-1.291826327	1.72E-64
SETU_00769	bifunctional pyrimidine regulatory protein PyrR uracil phosphoribosyltransferase	-1.301610095	8.26E-57
SETU_01823	L-lactate permease lctP-like protein	-1.306427861	1.67E-95
adk	adenylate kinase	-1.314787809	8.55E-103
SETU_00272	membrane protein , putative	-1.318968897	8.86E-97
rplB	50S ribosomal protein L2	-1.327105527	3.55E-91
pyrG	CTP synthetase	-1.335917099	7.81E-110

rplK	50S ribosomal protein L11	-1.336927071	3.26E-76
SETU_00878	glutamine synthetase repressor	-1.339549049	6.04E-95
rpsF	30S ribosomal protein S6	-1.346515968	2.79E-116
glnA	glutamine synthetase	-1.35134612	2.48E-96
rplR	50S ribosomal protein L18	-1.359034025	4.89E-68
rpsS	30S ribosomal protein S19	-1.360018668	1.57E-93
SETU_01373	transcriptional regulator	-1.379432916	7.26E-69
rplX	50S ribosomal protein L24	-1.381652747	7.77E-79
rplF	50S ribosomal protein L6	-1.381671892	2.50E-73
rpmD	50S ribosomal protein L30	-1.394733487	3.29E-87
rplD	50S ribosomal protein L4	-1.400120595	1.89E-116
rplJ	50S ribosomal protein L10	-1.401783334	3.82E-82
rplC	50S ribosomal protein L3	-1.403908913	1.67E-100
rplE	50S ribosomal protein L5	-1.423938929	4.14E-97
rplP	50S ribosomal protein L16	-1.424834088	3.42E-148
rpsJ	30S ribosomal protein S10	-1.424869722	1.42E-104
rpsC	30S ribosomal protein S3	-1.434180747	1.97E-127
rplM	50S ribosomal protein L13	-1.437060793	1.50E-111
SETU_01212	ribosomal protein YsxB	-1.43812083	3.32E-113
SETU_00026	ssDNA-binding protein	-1.439275766	1.27E-122
rplN	50S ribosomal protein L14	-1.44118898	7.58E-95
rplL	50S ribosomal protein L7/L12	-1.444099511	2.52E-61
rpsL	30S ribosomal protein S12	-1.447102556	4.72E-84
rpsQ	30S ribosomal protein S17	-1.450602922	3.25E-109
rplV	50S ribosomal protein L22	-1.455435903	1.23E-140
rpsN_2	30S ribosomal protein S14	-1.459568288	2.29E-107
SETU_01891	amino acid transporter	-1.459941042	1.45E-129
rpsI	30S ribosomal protein S9	-1.461785575	1.07E-80

SETU_00162	ribosomal protein L7Ae-like protein	-1.465839273	1.55E-118
rpmC	50S ribosomal protein L29	-1.472600002	7.70E-82
rpsH	30S ribosomal protein S8	-1.478120566	4.09E-108
rpsE	30S ribosomal protein S5	-1.507386964	4.83E-91
rplA	50S ribosomal protein L1	-1.508668203	3.39E-82
isaA	immunodominant antigen A	-1.516821658	1.92E-107
rpmH	50S ribosomal protein L34	-1.530874318	3.87E-108
SETU_01562	ATP-dependent RNA helicase	-1.532086472	1.11E-130
rpsD	30S ribosomal protein S4	-1.580314316	1.70E-101
SETU_01842	transcriptional regulator	-1.619006092	1.06E-160
rplU	50S ribosomal protein L21	-1.653364113	6.12E-102
rpmI	50S ribosomal protein L35	-1.702738163	3.19E-139
rplT	50S ribosomal protein L20	-1.717312369	1.12E-93
SETU_01975	secretory antigen SsaA	-1.730221491	1.25E-113
infC	translation initiation factor IF-3	-1.784440433	1.84E-174
SETU_00466	hypothetical protein	-1.834984719	1.89E-154
SETU_00070	autolysin (N-acetylmuramoyl-L-alanine amidase	-2.027264232	9.36E-208
SETU_00325	histidine protein kinase saeS	-2.094124501	6.70E-152
SETU_00326	response regulator saeR	-2.099735516	1.86E-185
SETU_00327	DoxX family protein	-2.15956713	1.25E-203
SETU_00328	lipoprotein	-2.23398693	1.34E-235
SETU_00482	poly(glycerophosphate chain) D-alanine transfer protein	-2.394369248	2.12E-254
SETU_00480	DltB membrane protein	-2.43795197	0
dltC	D-alanine--poly(phosphoribitol) ligase subunit 2	-2.717241101	1.35E-151
SETU_00479	D-alanine--poly(phosphoribitol) ligase subunit 1	-2.751652683	0
dltX	D-Ala-teichoic acid biosynthesis protein	-2.7954962	3.97E-253

Appendix Table 3 DE genes of *S. aureus* in response to 1 % (v/v) ethanol challenge. The level of fold change **(logFC)** is based on $\log_2$. All DE genes have **FDR** (false discovery rate) ≤ 0.05. DE genes that discussed in this thesis were highlighted.

Gene	Gene_description	logFC	FDR
NWMN_2304	conserved hypothetical protein	3.102706418	6.28E-08
NWMN_1224	conserved hypothetical protein	2.72192875	1.49E-05
NWMN_1077	conserved hypothetical protein	2.397187795	4.14E-15
NWMN_0265	conserved hypothetical protein	2.11429059	8.03E-06
ssl3nm	staphylococcal enterotoxin-like toxin	2.113070988	1.13E-11
ssl2nm	staphylococcal enterotoxin-like toxin	2.08567587	9.72E-13
NWMN_1075	conserved hypothetical protein	2.068180248	9.15E-11
NWMN_1076	conserved hypothetical protein	2.018335972	4.41E-11
lytR	autolysin two-component response regulator	2.003392836	1.44E-07
ssl4nm	staphylococcal enterotoxin-like toxin	1.878247595	9.18E-11
gatC	glutamyl-tRNA amidotransferase subunit C	1.868116982	0.000586103
NWMN_0116	conserved hypothetical protein	1.866612313	1.13E-06
NWMN_0356	conserved hypothetical protein	1.838976847	1.34E-06
NWMN_1083	DNA-binding protein	1.838384405	0.004204336
NWMN_2000	hypothetical protein	1.825173505	0.00442656
ssl10	staphylococcal enterotoxin-like toxin	1.787660796	9.68E-09
ssp	extracellular matrix and plasma binding protein	1.778664304	7.62E-07
NWMN_2396	C-terminal part of fibronectin binding protein B	1.742822997	0.000484395
NWMN_2160	conserved hypothetical protein	1.714378261	0.00327232
NWMN_1312	conserved hypothetical protein	1.692622602	0.000298143
NWMN_2215	conserved hypothetical protein	1.609619668	0.000135876
ssl5nm	staphylococcal enterotoxin-like toxin	1.597223738	5.86E-07
NWMN_1225	conserved hypothetical protein	1.564449484	8.52E-06
NWMN_2259	conserved hypothetical protein	1.56313504	1.17E-05

NWMN_0907	conserved hypothetical protein	1.561996406	5.15E-06
NWMN_1811	phage anti-repressor	1.535402157	6.24E-05
NWMN_1828	conserved hypothetical protein	1.534412103	0.000365805
NWMN_2203	secretory antigen precursor SsaA	1.5318344	0.000307249
NWMN_0115	conserved hypothetical protein	1.524989066	5.28E-06
NWMN_2316	cation efflux family protein	1.492572421	1.52E-05
NWMN_1012	conserved hypothetical protein	1.479444094	0.000177515
nupC	pyrimidine nucleoside transport protein	1.47833266	6.61E-06
ssl11nm	staphylococcal enterotoxin-like toxin	1.466827226	0.001433362
NWMN_2260	truncated transposase for IS1272	1.457704875	0.004375022
NWMN_0118	conserved hypothetical protein	1.455084948	3.48E-05
NWMN_0374	sodium:dicarboxylate symporter family protein	1.451430983	1.30E-06
NWMN_0834	conserved hypothetical protein	1.439721481	5.45E-05
NWMN_tRNA23	tRNA-Met	1.434063591	0.001155099
fnbB	fibronectin binding protein B precursor	1.419969753	0.001693579
NWMN_0401	conserved hypothetical protein	1.407089774	0.004109273
NWMN_0429	N-acetylmuramoyl-L-alanine amidase aaa precursor	1.407001024	7.57E-06
pryR	pyrimidine operon regulatory protein	1.388373415	2.59E-06
NWMN_1276	ImpB/MucB/SamB family DNA-damage repair protein	1.387940284	0.001758848
NWMN_0766	conserved hypothetical protein	1.373271561	6.52E-05
NWMN_1673	conserved hypothetical protein	1.368009423	0.002109237
NWMN_0964	conserved hypothetical protein	1.367439413	0.000151945
NWMN_2467	O-acetyltransferase OatA	1.365337409	3.63E-05
NWMN_0022	conserved hypothetical protein	1.36424801	2.82E-05
isdG	cytoplasmic heme-iron binding protein	1.362954079	0.000582833
NWMN_1860	conserved hypothetical protein	1.360473226	0.000628632
tcaA	teicoplanin resistance associated protein A	1.354751897	0.004585478
NWMN_2469	immunodominant antigen A	1.340665366	0.000395471

NWMN_0117	conserved hypothetical protein	1.338499752	0.000852524
NWMN_0995	phage anti-repressor protein	1.335421637	0.000411344
ssl6nm	staphylococcal enterotoxin-like toxin	1.329708966	0.000155455
NWMN_0157	conserved hypothetical protein	1.324644414	0.000345662
NWMN_0266	conserved hypothetical protein	1.322521692	4.18E-06
pabA	para-aminobenzoate synthase component II	1.314217304	8.42E-05
ssl9nm	staphylococcal enterotoxin-like toxin	1.310127102	3.42E-05
ssl8nm	staphylococcal enterotoxin-like toxin	1.299124086	1.88E-05
NWMN_0416	conserved hypothetical protein	1.297430405	0.000929049
NWMN_0006	conserved hypothetical protein	1.287630095	1.03E-05
NWMN_1921	phage cI-like repressor	1.282134748	0.000280098
NWMN_1343	conserved hypothetical protein	1.273239086	0.005795289
spsA	type-I signal peptidase A component	1.267138777	0.000362864
NWMN_1739	conserved hypothetical protein	1.263576562	0.001101372
NWMN_0997	conserved hypothetical protein	1.254707613	0.001500101
cysM	cysteine synthase	1.232199417	7.77E-05
NWMN_0165	conserved hypothetical protein	1.22548222	0.001597512
sbi	immunoglobulin G-binding protein Sbi	1.19333474	0.004308893
NWMN_0725	conserved hypothetical protein	1.190183736	2.10E-05
NWMN_2246	sodium/glutamate symporter	1.083278296	0.004184942
NWMN_0849	conserved hypothetical protein	1.079620391	0.00393837
potA	spermidine/putrescine ABC transporter, ATP-binding protein	1.074653717	0.001001675
oatA	secretory antigen precursor SsaA homolog	1.072450253	0.00464117
lukS	leukocidin/hemolysin toxin family S subunit	1.070578307	0.012185339
NWMN_1636	conserved hypothetical protein	1.044190404	0.003694685
NWMN_0249	5'-nucleotidase, lipoprotein e(P4) family protein	1.033365308	0.003066422
NWMN_0714	conserved hypothetical protein	1.03325113	0.003891235
NWMN_1865	conserved hypothetical protein	1.026372137	0.00031247

hlgB	gamma hemolysin, component B	1.02242267	0.001648931
NWMN_1674	CrcB-like protein	1.013997822	0.04457468
NWMN_2273	acetyltransferase, GNAT family protein	1.010213753	0.003451285
NWMN_1342	conserved hypothetical protein	1.009893304	0.003108872
hlgC	gamma-hemolysin component C	1.001448617	0.001452626
rimJ	ribosomal-protein-alanine N-acetyltransferase	0.992959102	0.004149538
arsC	arsenate reductase	0.980464334	0.004891006
NWMN_2587	conserved hypothetical protein	0.973126021	0.00536495
NWMN_1812	phage repressor	0.961478682	0.002230475
lytS	autolysin sensor histidine kinase protein	0.944435185	0.000914738
hsdS	type I restriction modification system, site specificity determination subunit	0.942518043	0.002970029
NWMN_1623	glycosyl transferase, family 51	0.931621407	0.003347848
NWMN_0622	conserved hypothetical protein	0.909737422	0.002363459
NWMN_2236	abortive infection protein family protein	0.86088258	0.005537797
NWMN_0143	oligopeptide ABC transporter, ATP-binding protein	0.848250028	0.002286138
NWMN_0434	conserved hypothetical protein	0.608112411	0.045856979
tagG	teichoic acid ABC transporter permease protein	0.601208325	0.029164456
NWMN_1689	conserved hypothetical protein	-0.57745596	0.048268046
NWMN_0635	conserved hypothetical protein	-0.592618958	0.037297398
NWMN_0587	conserved hypothetical protein	-0.617819476	0.041847509
sdhB	succinate dehydrogenase iron-sulfur protein	-0.64720583	0.028337905
katA	catalase	-0.65420436	0.037565297
NWMN_2545	conserved hypothetical protein	-0.655471877	0.046588838
atpG	ATP synthase, gamma subunit	-0.670675857	0.043840467
NWMN_0467	conserved hypothetical protein	-0.675625023	0.011776538
NWMN_1471	cytidine deaminase, homotetrameric	-0.690307966	0.017757981
NWMN_0296	conserved hypothetical protein	-0.701259166	0.047891918
msrB	methionine sulfoxide reductase B	-0.719918253	0.035690871

glcA	glucose-specific PTS transporter protein IIABC component	-0.72470482	0.036742215
NWMN_0251	ABC transporter ATP-binding protein	-0.7364494	0.011319894
NWMN_0295	conserved hypothetical protein	-0.74726141	0.019566202
spoVG	stage V sporulation protein G homolog	-0.751325061	0.011394321
fumC	fumarate hydratase, class II	-0.752621331	0.02626678
NWMN_1767	ThiJ/PfpI family protein	-0.760251484	0.01241162
NWMN_2253	drug resistance transporter EmrB/QacA subfamily protein	-0.818734402	0.049010633
NWMN_2548	conserved hypothetical protein	-0.824482574	0.004025891
atpB	ATP synthase subunit a	-0.837716945	0.004961709
NWMN_1477	conserved hypothetical protein	-0.838927434	0.005166506
NWMN_2480	hydrolase	-0.84063864	0.009813954
tpi	triosephosphate isomerase	-0.845680465	0.028324519
NWMN_1038	phage holin	-0.860172168	0.041163732
NWMN_0250	ABC transporter, permease protein	-0.869523911	0.002716795
NWMN_2417	conserved hypothetical protein	-0.871633722	0.040182749
mnhC1	Na?? antiporter subunit	-0.872137334	0.003710961
NWMN_0029	conserved hypothetical protein	-0.875910669	0.001104369
srrA	DNA-binding response regulator SrrA	-0.878310954	0.019324862
NWMN_0285	conserved hypothetical protein	-0.898226994	0.011401438
NWMN_2202	conserved hypothetical protein	-0.902796079	0.005652482
NWMN_2314	drug resistance transporter EmrB/QacA subfamily protein	-0.903411394	0.002806745
hutG	formiminoglutamase	-0.921748775	0.003753688
qoxC	quinol oxidase polypeptide III	-0.924600728	0.006924014
NWMN_1688	conserved hypothetical protein	-0.929659924	0.000955664
treR	trehalose operon repressor	-0.93427235	0.002109621
NWMN_2460	aminotransferase, class I	-0.93564036	0.005154791
NWMN_2026	aldehyde dehydrogenase family protein	-0.936571171	0.00115695
NWMN_1730	conserved hypothetical protein	-0.937602855	0.002048212

serS	seryl-tRNA synthetase	-0.959803877	0.024457678
NWMN_1472	diacylglycerol kinase	-0.959947833	0.002974531
gltB	glutamate synthase, large subunit	-0.979423904	0.005165572
ilvA1	threonine dehydratase	-0.979993692	0.020593868
NWMN_0705	ferrichrome ABC transporter lipoprotein	-0.980831919	0.004134269
modB	molybdenum ABC transporter, permease protein	-0.985214531	0.000730577
rplP	50S ribosomal protein L16	-0.98572401	0.001764223
hslU	ATP-dependent protease ATP-binding subunit	-0.987356118	0.00167422
NWMN_2459	D-isomer specific 2-hydroxyacid dehydrogenase family protein	-0.99182	0.001805982
ipdC	indole-3-pyruvate decarboxylase	-0.992912713	0.000514872
NWMN_2275	conserved hypothetical protein	-1.01461124	0.012374602
qoxB	quinol oxidase polypeptide I QoxB	-1.019872126	0.008357485
NWMN_0737	conserved hypothetical protein	-1.025165696	0.000743823
NWMN_1124	conserved hypothetical protein	-1.025664055	0.016474718
NWMN_2557	conserved hypothetical protein	-1.032367809	0.003665352
entB	isochorismatase	-1.035069188	0.000974365
NWMN_0673	conserved hypothetical protein	-1.035375558	0.000922122
NWMN_1989	conserved hypothetical protein	-1.03810591	0.000518303
mnaA	UDP-GlcNAc 2-epimerase	-1.0456847	0.001047525
NWMN_2018	conserved hypothetical protein	-1.052747471	0.003116038
NWMN_1746	conserved hypothetical protein	-1.06113212	0.000307703
NWMN_1631	conserved hypothetical protein	-1.061265209	0.00031225
sucB	dihydrolipoamide succinyltransferase E2 component of 2-oxoglutarate dehydrogenase complex	-1.068025172	0.000531332
NWMN_0973	inositol-1-monophosphatase family protein	-1.070368793	0.001428956
NWMN_2254	conserved hypothetical protein	-1.072324339	0.006406326
NWMN_2444	conserved hypothetical protein	-1.075253838	0.035154096
thrC	threonine synthase	-1.08005808	0.00100889
NWMN_0779	conserved hypothetical protein	-1.082104718	0.003554141

NWMN_1645	conserved hypothetical protein	-1.082275751	0.00014753
atpE	ATP synthase subunit c	-1.087383969	0.001890503
NWMN_0083	phosphopentomutase	-1.08801947	0.001000076
NWMN_0482	conserved hypothetical protein	-1.094986252	0.000101295
hisD	histidinol dehydrogenase HisD	-1.102620822	0.001778838
pckA	phosphoenolpyruvate carboxykinase	-1.107701136	0.003067709
leuC	3-isopropylmalate dehydratase, large subunit	-1.11674044	0.006590703
NWMN_1819	low molecular weight phosphotyrosine protein phosphatase	-1.117213085	0.000412484
NWMN_0650	conserved hypothetical protein	-1.118994698	0.000576157
NWMN_1230	phospholipase	-1.128006525	0.002369866
sdhA	succinate dehydrogenase flavoprotein subunit	-1.137450824	0.000366372
NWMN_0048	conserved hypothetical protein	-1.140349572	0.00035003
NWMN_2350	para-nitrobenzyl esterase chain A	-1.140644156	0.000780289
clfA	clumping factor A	-1.141023788	0.000303571
NWMN_2353	ABC transporter, ATP-binding protein	-1.141925515	0.00092749
NWMN_0321	oxidoreductase family protein	-1.154014987	0.000196959
malA	alpha-D-1,4-glucosidase	-1.156373076	0.0032609
ald1	alanine dehydrogenase 1	-1.164439652	0.000190445
hisIE	histidine biosynthesis bifunctional protein HisIE	-1.164581208	0.002062534
NWMN_2205	D-isomer specific 2-hydroxyacid dehydrogenase family protein	-1.182765093	0.003858385
NWMN_0621	conserved hypothetical protein	-1.183974756	0.004668218
bsaP	lantibiotic leader peptide processing serine protease	-1.18811376	9.17E-05
NWMN_2465 crtO	conserved hypothetical protein	-1.189217454	0.003992611
NWMN_1820	conserved hypothetical protein	-1.19368005	9.36E-05
NWMN_2210	formate dehydrogenase homolog	-1.195796764	0.000132344
NWMN_1505	conserved hypothetical protein	-1.198232846	0.001037402
NWMN_2330	conserved hypothetical protein	-1.207805793	0.002269296
gapA	glyceraldehyde 3-phosphate dehydrogenase 1	-1.209669534	0.003738249

cidB	holin-like protein CidB	-1.212821277	8.94E-05
gntK	gluconate kinase	-1.212909656	0.002037738
NWMN_0377	conserved hypothetical protein	-1.233785918	5.97E-05
mnhB1	Na?? antiporter subunit	-1.240201861	0.000427257
NWMN_1601	metallo-beta-lactamase superfamily protein	-1.245273976	0.001619485
NWMN_2369	short chain dehydrogenase	-1.2557302	7.75E-05
crtN	squalene synthase	-1.257872443	0.000255219
NWMN_1259	conserved hypothetical protein	-1.261278999	0.030177572
NWMN_2456	conserved hypothetical protein	-1.270347624	6.65E-05
NWMN_1298	phosphate ABC transporter, permease protein	-1.27228017	0.032234776
NWMN_1527	conserved hypothetical protein	-1.277419148	0.0010079
NWMN_1749	glutamine transport ATP-binding protein	-1.278024362	0.000913657
NWMN_1821	ribonuclease BN	-1.283567944	6.05E-05
nrdD	anaerobic ribonucleoside-triphosphate reductase	-1.283991983	0.023202247
NWMN_0771	OsmC-like protein	-1.286430611	4.45E-05
NWMN_2212	inositol monophosphatase family protein	-1.295997042	0.000214195
NWMN_0136	sucrose-specific PTS transporter IIBC component protein	-1.304918224	0.00638549
NWMN_1059	hypothetical protein	-1.305761555	0.00087228
NWMN_2039	conserved hypothetical protein	-1.318856876	0.000756058
NWMN_0780	ABC transporter ATP-binding protein	-1.322806852	6.25E-05
NWMN_0695	conserved hypothetical protein	-1.323900495	1.08E-05
lacA	galactose-6-phosphate isomerase LacA subunit	-1.328836905	0.030267144
NWMN_0053	conserved hypothetical protein	-1.331279159	4.72E-06
NWMN_2591	conserved hypothetical protein	-1.331787407	0.000142746
leuD	3-isopropylmalate dehydratase, small subunit	-1.335660064	0.008522584
NWMN_0173	ABC transporter, substrate-binding protein	-1.340926046	0.002621312
treP	PTS system, trehalose-specific IIBC component	-1.34368647	0.002372615
hisB	imidazole glycerol phosphate dehydratase HisB	-1.345719029	0.004992592

bsaG	lantibiotic ABC transporter protein	-1.347080567	0.000884716
leuB	3-isopropylmalate dehydrogenase	-1.347403201	0.00164158
NWMN_2487	fructosamine kinase family protein	-1.349279692	0.002719852
metL	homoserine dehydrogenase	-1.355495573	0.000161797
NWMN_2454	delta-1-pyrroline-5-carboxylate dehydrogenase	-1.35601388	0.002850203
pgm	2,3-bisphosphoglycerate-independent phosphoglycerate mutase	-1.357800016	0.00060372
NWMN_0137	RpiR family transcriptional regulator	-1.358107329	0.002146592
hisC1	histidinol-phosphate aminotransferase	-1.358949999	0.000272713
scdA	cell wall metabolism protein	-1.362866778	0.005014654
treC	alpha,alpha-phosphotrehalase	-1.364375754	0.000154062
NWMN_0860	conserved hypothetical protein	-1.370215153	3.20E-06
purH	bifunctional purine biosynthesis protein	-1.376584649	4.03E-05
mtlF	PTS system, mannitol-specific IIBC component	-1.383084281	7.31E-06
purD	phosphoribosylamine-glycine ligase	-1.385076686	3.70E-06
thrB	homoserine kinase	-1.391985703	2.61E-05
NWMN_2229	oxidoreductase, short chain dehydrogenase/reductase family protein	-1.412587892	2.46E-06
NWMN_2463 crtQ	glycosyl transferase, group 2 family protein	-1.415975286	3.79E-05
NWMN_1750	extracellular glutamine-binding protein	-1.418390791	0.00185543
NWMN_2422	D-isomer specific 2-hydroxyacid dehydrogenase family protein	-1.423130619	0.003760843
NWMN_2270	conserved hypothetical protein	-1.432197257	6.15E-06
accC1	acetyl-CoA biotin carboxylase	-1.439034457	0.000617644
mtlD	mannitol-1-phosphate 5-dehydrogenase	-1.453235571	4.34E-06
purQ	phosphoribosylformylglycinamidine synthase I	-1.45378777	2.45E-05
NWMN_1632	general stress protein-like protein	-1.457220268	6.37E-06
NWMN_1509	urea amidolyase-related protein	-1.462439191	0.001149505
trpD	anthranilate phosphoribosyltransferase	-1.482148431	0.000842975
NWMN_2089	osmoprotectant transporter	-1.503868473	2.73E-07
purN	phosphoribosylglycinamide formyltransferase	-1.507840627	1.03E-05

NWMN_2479	amidohydrolase family protein	-1.51631052	1.41E-07
aldA	aldehyde dehydrogenase homolog	-1.517124896	0.00015831
gpmA	2,3-bisphosphoglycerate-dependent phosphoglycerate mutase	-1.518788379	4.57E-05
NWMN_0078	conserved hypothetical protein	-1.545932647	1.70E-05
pgk	phosphoglycerate kinase	-1.548511472	0.000168984
leuA	2-isopropylmalate synthase	-1.549427815	5.84E-05
hisH	imidazole glycerol phosphate synthase, subunit H	-1.573793282	0.000947982
ldh	L-lactate dehydrogenase 2	-1.585869463	0.004231775
sucA	2-oxoglutarate dehydrogenase E1 component	-1.587979277	3.92E-05
NWMN_0364	conserved hypothetical protein	-1.588920647	7.74E-07
ilvC	ketol-acid reductoisomerase	-1.592944513	0.000758414
NWMN_2086	alkaline shock protein 23	-1.608807862	1.19E-05
NWMN_2368	conserved hypothetical protein	-1.623128063	2.32E-06
poxB	pyruvate oxidase	-1.628207649	9.75E-08
crtI	phytoene dehydrogenase	-1.63436426	2.40E-08
NWMN_0125	conserved hypothetical protein	-1.635125372	0.00245518
NWMN_1600	universal stress protein family protein	-1.64120673	0.000454448
NWMN_2500	amino acid permease family protein	-1.651161002	0.000411866
NWMN_0247	formate/nitrite transporter family protein	-1.653687014	0.024135727
NWMN_0667	fructose operon transcriptional regulator	-1.654543514	0.000599733
pryF	orotidine 5'-phosphate decarboxylase	-1.657265138	3.61E-06
oppD	oligopeptide transport ATP-binding protein	-1.663075187	1.05E-05
pyrE	orotate phosphoribosyltransferase	-1.676402185	1.66E-07
NWMN_2442	conserved hypothetical protein	-1.69293587	0.000173163
NWMN_1604	universal stress protein family protein	-1.707377783	0.000255921
ilvB	acetolactate synthase, large subunit, biosynthetic type	-1.712881806	9.66E-05
NWMN_2371	alkylhydroperoxidase AhpD family protein	-1.73838802	2.74E-06
thrA	aspartate kinase	-1.751819663	0.001180336

pyrAB	carbamoyl-phosphate synthase, pyrimidine-specific, large chain	-1.757400218	6.19E-08
accB1	acetyl-CoA carboxylase, biotin carboxyl carrier protein	-1.759943423	0.000330955
NWMN_0651	conserved hypothetical protein	-1.782531726	9.41E-06
purM	phosphoribosylformylglycinamidine cyclo-ligase	-1.783231368	4.67E-09
agrA	staphylococcal accessory gene regulator A	-1.785173008	0.001815813
crtM	squalene desaturase	-1.791258451	7.44E-05
NWMN_2074	conserved hypothetical protein	-1.799324658	0.001071496
NWMN_2419	acetyltransferase, GNAT family protein	-1.806449776	0.000408182
bsaF	lantibiotic immunity protein F	-1.809207258	3.56E-07
NWMN_0041	conserved hypothetical protein	-1.816609177	0.003102767
dapD	tetrahydrodipicolinate acetyltransferase	-1.82076467	0.000341357
purL	phosphoribosylformylglycinamidine synthase II	-1.841888681	3.70E-07
NWMN_2087	conserved hypothetical protein	-1.846756053	5.03E-08
NWMN_0782	ABC transporter, substrate-binding protein	-1.874909469	6.99E-10
NWMN_0366	conserved hypothetical protein	-1.893651874	5.17E-06
mtlA	mannitol-specific IIA component	-1.897421781	2.56E-08
oppC	oligopeptide ABC transporter, permease protein	-1.905169318	6.05E-07
pyrP	uracil permease	-1.915224093	2.32E-05
NWMN_0542	conserved hypothetical protein	-1.918092232	2.19E-05
trpB	tryptophan synthase, beta subunit	-1.931193955	2.60E-05
ilvD	dihydroxy-acid dehydratase	-1.94553129	7.42E-05
pyrC	dihydroorotase multifunctional complex type	-1.97385491	1.04E-06
nrdG	anaerobic ribonucleotide reductase, small subunit	-1.978253283	0.002765895
NWMN_1531	conserved hypothetical protein	-1.980681121	0.000240284
bsaE	lantibiotic ABC transporter protein	-1.981559033	2.80E-05
dapB	dihydrodipicolinate reductase	-1.984949316	3.96E-06
gntR	gluconate operon transcriptional repressor	-1.990002715	0.000382079
NWMN_0781	ABC transporter permease protein	-2.022973716	1.47E-06

NWMN_1526	hypothetical protein	-2.023651568	3.07E-09
NWMN_0856	oligopeptide transport system permease protein	-2.033456005	2.34E-06
NWMN_2088	conserved hypothetical protein	-2.039438011	5.05E-09
fruA	fructose specific permease	-2.051474127	0.0001044
lip	lipase precursor	-2.069585594	0.000489429
fruB	fructose 1-phosphate kinase	-2.070218725	2.84E-05
NWMN_0603	ABC transporter ATP-binding protein	-2.076279049	3.67E-09
thiM	hydroxyethylthiazole kinase	-2.109538007	0.000112812
trpF	N-(5'phosphoribosyl)anthranilate isomerase	-2.121818982	2.33E-06
NWMN_1346	conserved hypothetical protein	-2.149536789	0.002310932
NWMN_2048	conserved hypothetical protein	-2.154564836	2.29E-09
NWMN_0134	conserved hypothetical protein	-2.180411145	0.0008999
argH	argininosuccinate lyase	-2.18849859	9.85E-06
alsD	alpha-acetolactate decarboxylase	-2.188704192	1.64E-05
ribD	riboflavin biosynthesis protein RibD	-2.195737152	4.33E-06
purF	amidophosphoribosyltransferase precursor	-2.197870507	8.98E-11
pyrB	aspartate carbamoyltransferase catalytic subunit	-2.21297817	1.87E-06
pyrAA	carbamoyl-phosphate synthase, pyrimidine-specific, small chain	-2.214599589	4.34E-07
NWMN_2502	conserved hypothetical protein	-2.215517197	1.70E-05
NWMN_0175	flavohemoprotein	-2.221583234	0.001049404
oppF	oligopeptide ABC transporter, ATP-binding protein	-2.223006211	4.40E-09
NWMN_1998	transcriptional regulator TenA family protein	-2.248094501	0.000453209
argG	argininosuccinate synthase	-2.2828285	5.12E-05
NWMN_2377	conserved hypothetical protein	-2.285549159	0.00409883
NWMN_1347	amino acid permease	-2.297103014	0.003633173
NWMN_0896	conserved hypothetical protein	-2.334072317	1.37E-05
NWMN_2597	conserved hypothetical protein	-2.363224893	3.62E-05
agrC	staphylococcal accessory gene regulator protein C	-2.416666813	0.000178072

asd	aspartate-semialdehyde dehydrogenase	-2.416914824	4.17E-06
ald	alanine dehydrogenase 2	-2.418933942	0.006765065
NWMN_2268	L-lactate permease 2	-2.435281338	0.000919785
ribA	riboflavin biosynthesis protein	-2.437071897	7.41E-06
dapA	dihydrodipicolinate synthase	-2.447829364	1.76E-06
trpC	indole-3-glycerol phosphate synthase	-2.458007547	2.26E-06
narI	respiratory nitrate reductase, gamma subunit	-2.469668759	0.000258796
thiD1	phosphomethylpyrimidine kinase	-2.496432407	3.35E-06
NWMN_0163	conserved hypothetical protein	-2.506268785	0.010189532
thiE	thiamine-phosphate pyrophosphorylase	-2.561010324	2.39E-05
putA	proline dehydrogenase	-2.583472572	4.36E-05
NWMN_0602	conserved hypothetical protein	-2.596651393	2.35E-07
ribH	riboflavin synthase, beta subunit	-2.60219292	2.19E-06
ribB	riboflavin synthase, alpha subunit	-2.603676542	3.11E-06
NWMN_0943	conserved hypothetical protein	-2.636779722	3.16E-07
agrD	staphylococcal accessory gene regulator protein D	-2.69651701	4.73E-06
alsS	alpha-acetolactate synthase	-2.732019261	3.34E-06
ldh1	L-lactate dehydrogenase	-2.74287702	0.004075409
ilvA	threonine dehydratase II	-2.75058395	0.001177457
agrB	staphylococcal accessory gene regulator protein B	-2.824509884	6.55E-05
adhE	iron-containing alcohol dehydrogenase	-2.840542572	0.000419628
NWMN_0944	conserved hypothetical protein	-2.864396841	1.55E-07
lysC	aspartokinase II	-2.865536217	2.20E-06
NWMN_0945	conserved hypothetical protein	-2.870176536	1.19E-07
NWMN_0721	sigma 54 modulation protein	-3.023380113	1.17E-05
adh1	alcohol dehydrogenase	-3.203644942	0.002151334
NWMN_2620	phenol-soluble modulin beta 2	-3.38727687	0.000324066
cidA	holin-like protein CidA	-3.399602135	2.55E-08

hld	delta-hemolysin	-3.607432124	0.0002027
pflB	formate acetyltransferase	-3.687382755	0.000554865
narJ	respiratory nitrate reductase, delta subunit	-4.104988919	1.89E-05
NWMN_1084	phenol-soluble modulin beta 1	-4.20471231	4.98E-05
narH	nitrate reductase beta chain	-4.227760678	5.45E-06
cysG	uroporphyrin-III C-methyl transferase	-4.228474397	4.54E-06
NWMN_2616	phenol-soluble modulin alpha 4	-4.573754093	9.02E-06
NWMN_2102	conserved hypothetical protein	-4.904640643	0.001514021